Understanding the Formation, Function and Inhibition of Multinucleated Giant Cells in Giant Cell Arteritis.

Annie Peacock
MSc

Submitted in fulfilment of the requirements for the degree of Doctor of Philosophy

College of Medical, Veterinary, and Life Sciences School of Infection & Immunity University of Glasgow

October 2025

Abstract.

Giant cell arteritis (GCA) is the most common form of vasculitis in patients over 50 which can lead to irreversible blindness and strokes if not properly treated. GCA is characterised by immune mediated destruction of the medial layer of small blood vessels followed by aberrant repair leading to intimal hyperplasia and narrowing of the vessel. Multinucleated giant cells (MGCs) are a hallmark of disease pathology. Despite these cells being observed close to sites of both media destruction and intimal hyperplasia, their role and formation in GCA pathogenesis have not yet been fully explored. Furthermore, reliable models to investigate the early stages of GCA pathogenesis, particularly the migration of circulating monocyte precursors and the generation of MGCs, remain scarce. Accordingly, this thesis seeks to elucidate the mechanisms underlying the development and functional roles of MGCs and their precursors.

To address this gap in knowledge, this thesis employed spatial transcriptomics to characterise macrophages and MGCs within distinct vascular layers and to elucidate the mechanisms underlying their development and functional roles. The results showed that macrophages in the intima of GCA vessels were transcriptionally similar to MGCs. Furthermore, cell deconvolution analysis of MGCs showed that these cells were transcriptionally akin to an undifferentiated macrophage suggesting they could be both pro- and anti-inflammatory in nature.

Furthermore, it was important to understand the mechanisms involved in MGC formation. This thesis showed that GCA like MGCs could be generated by stimulating monocytes with GM-CSF+IFNγ. This culture produced both Langhans, and foreign body giant cells as observed in GCA tissue. These cultured cells produced markers observed in the tissue such as MMP9 and CTSD.

Differences in MGC formation by cultured monocytes from healthy controls and GCA patients suggested that there are differences in circulating monocyte precursors of MGCs. Flow cytometric analysis, RNA sequencing and

epigenetic profile analysis of these monocytes revealed that GCA monocytes express high CCR5 and GM-CSF receptor on their surface. Analysis also showed differences in H3K427me3 and H3K4me3 profiles in GCA monocytes compared to healthy controls.

Lastly, as CCR5 was shown to be highly expressed on GCA monocytes, it was assessed in the context of MGC formation. CCR5 and its ligands CCL3, and 5 could be observed in GCA tissue localized to and surrounding MGCs. CCR5 modulation by small molecules and monoclonal antibodies (such as maraviroc and Leronlimab respectively) were added to the previously described culture. This inhibition led to a large reduction in the number of MGCs observed in culture suggesting a role for this chemokine receptor in the formation of MGCs.

In summary, this thesis established a role of MGCs in GCA pathogenesis. It presented the first in vitro model of GCA MGC formation from enriched monocytes, enabling investigation of their initiation and modulation. It also identified differences in protein expression and epigenetic modifications between healthy and GCA monocytes and implicates the chemokine receptor CCR5 in MGC formation, highlighting CCR5 modulators such as Maraviroc and Leronlimab as potential therapies. Future work should explore GCA monocyte co-culture systems and develop 3D models to extend these findings.

Table of Contents

Abstract. *2*

List of Tables *7*

List of Figures *8*

Acknowledgements. *10*

Author's Declaration *12*

Definitions/Abbreviations *13*

Chapter 1 Introduction. *16*

1.1 Giant Cell Arteritis. **16**
1.1.1 Diagnosis of GCA. 16
1.1.2 Risk factors for GCA development. 18

1.2 Immunopathology of GCA. **19**
1.2.1 Innate immunity in GCA. 20
1.2.2 Adaptive immunity in GCA, ... 26
1.2.3 The role of vascular cells in GCA. 28
1.2.4 Inflammaging. 28

1.3 Treatment strategies. **29**
1.3.1 Glucocorticoids. 29
1.3.2 DMARDs and biologics. 31

1.4 Models of GCA pathology. **32**
1.4.1 Animal models. 33

1.5 Multinucleated giant cells. **34**
1.5.1 In health and diseases. 34
1.5.2 The presence and role of MGCs in GCA. 36

1.6 Chemokines and Chemokine receptors. **36**
1.6.1 The chemokine receptor CCR5. 37
1.6.2 The role of CCR5 in immune-mediated inflammatory diseases. 38
1.6.3 Inhibitors of CCR5 signalling. 39

1.7 Unmet need in GCA research. **39**

1.8 Hypothesis and aims. **41**

Chapter 2 Methods and materials. *43*

2.1 Patient and control samples. **43**
2.1.1 GCA and control peripheral blood. 43
2.1.2 GCA tissue 43
2.1.3 TARDIS study. 44
2.1.4 UKBiobank. 44

2.2 Human cell isolation. **45**
2.2.1 PBMC isolation 45
2.2.2 Monocyte purification. 45
2.2.3 Preparation of monocytes for RNA seq. 46
2.2.4 Monocyte preparation for epigenetic analysis. 47

2.3 Flow cytometry. **49**
2.3.1 Isolated PBMCs. 50
2.3.2 TARDIS Flow cytometry. 51

2.4 Culture of Multinucleated giant cells. **52**
2.4.1 Addition of chemokines. 52

2.4.2 Addition of CCR5 inhibitors. 53
2.4.3 Staining and visualisation. 53

2.5 Processing of GCA tissue. 54
2.5.1 Immunohistochemistry. 55
2.5.2 Immunofluorescence staining. 56
2.5.3 Staining for Geomx spatial transcriptomics. 56

2.6 Bioinformatic analysis. 57
2.6.1 Bulk RNA-Seq. 57
2.6.2 CUT&Tag histone modification profiling. 57
2.6.3 Geomx spatial transcriptomics. 58

2.7 UKBiobank analysis of SNPs. 58
2.7.1 Analysis 58

2.8 Statistical analysis. 59

Chapter 3 Using Spatial Transcriptomics to understand MGCs in GCA. 60

3.1 Introduction. 60

3.2 Results 63
3.2.1 Macrophages and MGCs have differences in expression profiles in GCA tissue. 63
3.2.2 Intimal macrophages are potential precursors to MGCs. 66
3.2.3 Linking Gene Expression to potential MGC Function. 70
3.2.4 Protein-Level Validation of MGC Spatial Transcriptomics. 73

3.3 Discussion 77

Chapter 4 Using an in vitro culture model of MGCs to understand their formation in GCA. 83

4.1 Introduction 83

4.2 Results 86
4.2.1 Patient information. 86
4.2.2 Optimising an *in vitro* culture model of MGC formation. 87
4.2.3 Validation of the in vitro model for the study of MGCs in GCA. 92
4.2.4 Application of the *In Vitro* Model to Compare MGC Formation in GCA and Healthy Controls. 98

4.3 Discussion. 101

Chapter 5 Investigating the circulating monocyte population. 107

5.1 Introduction 107

5.2 Results 110
5.2.1 GCA monocytes have higher expression of chemokine and growth factor receptors than healthy monocytes. 110
5.2.2 Patient characteristics of samples used for transcriptomic and epigenetic profiling. 116
5.2.3 Expression profile differences between healthy and GCA monocytes. 118
5.2.4 Epigenetic modifications in GCA monocytes. 122

5.3 Discussion 131

Chapter 6 The role of CCR5 in MGC formation and GCA. 137

6.1 Introduction. 137

6.2 Results. 140
6.2.1 Presence of CCR5 in GCA tissue. 140
6.2.2 CCR5 binding inhibition alters MGC formation. 146
6.2.3 Clinical significance of CCR5 in GCA. 154

6.3 Discussion. 157

Chapter 7 General discussion..... 162

7.1 General discussion. 162

7.2 Multinucleated giant cells as key players in GCA pathology. 162

7.3 Monocytes in circulation are primed to become MGCs. 166

7.4 CCR5 is a key molecule in GCA. 169

7.5 Summary. 170

Appendix 173

List of References 178

List of Tables

Table 1.1 : ACR/EULAR GCA diagnosis criteria.....17
Table 2.1: Table of antibodies used to stain PBMCs for flow cytometry.....51
Table 2.2: Table of antibodies used to stain TARDIS PBMCs for flow cytometry.....52
Table 4.1: GCA patient information 86
Table 4.2: Healthy control patient information 87
Table 5.1: TARDIS control patient information. 116
Table 5.2 : TARDIS GCA positive patient information..... 117
Table 5.3: FastQC report summary of reads..... 124
Table 5.4: Summary of peaks in each sample..... 124
Table 6.1: UK biobank cohort statistics. 156
Table 6.2: Results from generalized linear model of SNP association with GCA incidence..... 156

List of Figures

Figure 1.1: Representative images of a healthy and GCA TAB sample. 18
Figure 1.2:Immunopathology of GCA. 20
Figure 1.3: Myeloid development from progenitors. 22
Figure 1.5: ACR/ Vasculitis Foundation guidelines for GCA management. 30
Figure 1.6: Outcomes and adverse outcomes of Glucocorticoid treatment in GCA. 31
Figure 1.7: Multinucleated Giant Cell subtypes.....35
Figure 1.8: The functions of chemokines in health and disease.....37
Figure 1.9: CCR5 structure and ligands. 38
Figure 1.10: Proposed Mechanism of Maraviroc action. 39
Figure 3.1: representative images of spatial transcriptomic ROI selection. ..64
Figure 3.2: Macrophages and Giant cells have differences in transcriptional outputs. 65
Figure 3.3: Macrophages separate based on area. 67
Figure 3.4: MGCs are phenotypically comparable to M0 macrophages. 70
Figure 3.5: M0 signature genes highly expressed in MGCs and intima.....71
Figure 3.6: Potential function of MGC in GCA. GO pathway analysis was carried out on significantly upregulated genes associated with MGCs. 72
Figure 3.7: Genes associated with pathways. 72
Figure 3.8 : Both TRAP positive and TRAP negative MGC's can be observed in TAB samples. 75
Figure 3.9: MGC's highly express proteins related to matrix remodeling.....76
Figure 4.1: MGCs can be generated in vitro from GM-CSF+ IFNγ and MCSF+IL-4. 88
Figure 4.2: Maximal giant cell numbers were reached by day 7 of culture. ..91
Figure 4.3: Increasing the concentration of cytokines a small effect on MGC formation. 93
Figure 4.4: Monocytes from GCA patients fuse to form multinucleated giant cells. 95
Figure 4.5: Increase in giant cell numbers when cultured with MCSF then GMCSF but not the other way around. 95
Figure 4.6: Cultured MGCs express the same markers found in GCA tissue MGCs 96
Figure 4.7: TRAP staining of MGCs cultured from GCA monocytes.....97
Figure 4.8: Both FBGCs and LHGCs can be seen in GCA tissue and in vitro cultured MGCs. 98
Figure 4.9: Monocytes from GCA patients fuse to form both subsets of MGCs. 98
Figure 4.10: MGCs are more likely to fuse under different stimulation between healthy and GCA. 99
Figure 4.11: GCA MGCs are more likely to be both LHGC and FBGC than healthy. 100
Figure 5.1 : Representative gating strategy of surface marker expression in monocytes. 111
Figure 5.2 : GCA monocytes express different cell surface markers. 112
Figure 5.3 : No differences in monocyte subset numbers between GCA and healthy monocytes. 113
Figure 5.4 : Difference in surface markers is subset dependent. 114
Figure 5.5 : Minimal differences in transcription profiles between GCA and control. 119

Figure 5.6: Upregulated GCA genes are associated with cell cycle processes. 121
Figure 5.7: Differential expression of genes of interest. 121
Figure 5.8: CUT&Tag quality control data of H3K4Me3 and H3K27Me3. 123
Figure 5.9: Epigenetic changes on the histone H3K27Me3 between control and GCA monocytes. 127
Figure 5.10: Gene set enrichment analysis of H3K27Me3 peaks. 128
Figure 5.11 Increased repression of MGC related genes in control monocytes. 129
Figure 5.12 Minimal epigenetic changes on the histone H3K4Me3 between control and GCA monocytes. 130
Figure 6.1: Expression of CCR5 and its ligands in TAB tissue. 141
Figure 6.2: CCR5 ligands CCL3 and CCL5 are expressed in GCA tissue. 142
Figure 6.3: CCR5 and its ligands co-localize with CD68. 143
Figure 6.4: CCR5 and its ligands are expressed in cultured MGCs. 145
Figure 6.5: Maraviroc treatment significantly reduces MGC formation in healthy macrophage cultures. 147
Figure 6.6: In vitro cultured MGCs from GCA peripheral blood do not respond the same to maraviroc. 149
Figure 6.7: Culture of classical monocytes alone leads to more MGC formation than all monocyte subsets together. 150
Figure 6.8: Increased inhibition of CD14+ derived MGCs by Maraviroc. 151
Figure 6.9: Dose dependent reduction of MGCs with Leronlimab. 152
Figure 6.10: CCR5 ligands influence MGC formation in culture. 153
Figure 6.11: CCR5 expression changes between baseline and relapse. 155
Figure 7.1: Graphical summary of key findings. 172
Figure 7.2: Healthy donor recruitment poster. 175
Figure 7.3: Healthy donor consent form. 176
Figure 7.4: Patient information sheet example. 177

Acknowledgements.

Firstly, I would like to thank my supervisors, Carl Goodyear, Cecilia Ansalone and Neil Basu for their constant support and encouragement over these past four years. Cecilia, having you as both a supervisor and mentor has been one of the greatest privileges of this journey. Your thoughtful advice, and genuine care (especially your reminders to take care of myself) have meant more than I can say. Working alongside you has been an incredible and formative experience. Thank you. Carl, your scientific insight and unwavering belief in my abilities has been invaluable throughout this project. I am deeply grateful for your guidance and quiet support along the way. Lastly, Neil, thank you, not only for offering me the opportunity to pursue this PhD, but for your belief in me from the very beginning. For encouraging me to become the best scientist I can be.

A huge thank you to The Lauren Currie Twilight Foundation, especially Adrienne and Grant. Thank you for funding this research and for giving me the chance to speak directly with vasculitis patients and their families. Those conversations at the coffee mornings reminded me why this work really matters and they have kept me motivated when I needed it most.

The research presented in this thesis would not have been at all possible without the following people: thank you to the nurses and staff at Gartnavel General Hospital; and Glasgow Royal Infirmary for making blood sample collection such a smooth process, and for the kind chats in the waiting rooms. Kieran, Andy, and Sam, I'd probably still be staring hopelessly at a blank RStudio screen if not for your help. Thank you for your patience, the coding tips, and for keeping me sane when the scripts just wouldn't run. Aysin, Dianne, and Alana, my flow cytometry gurus, thank you for always being so generous with your time

and expertise. Lastly, Yuriko, thank you for always being there when I needed blood.
A massive thank you to the Goodyear lab, past and present. I've been so fortunate to work among such a kind, supportive, and fun group of people. Whether I needed help, advice or just a good laugh, you were always there. It's a rare environment and I'll never take it for granted. Andrew, Emily, and Lauren (aka PPPP), I honestly don't know how I would have survived these years without your friendship. You've been there for every vent, every laugh, and every ridiculous moment (we are single handedly keeping The Craft Pottery open).

Matt, thank you for your love, patience, and unwavering support over these last few years. Your belief in me, even when I doubt myself, means more than words can express. Thank you for listening to me yap about my research, even if you have no idea what I'm on about.

Thank you to my Gran and Granda, your support and encouragement mean the world to me. I am so grateful to have you both in my life. Lastly, Mum and Dad, I wouldn't be where I am without you. Your constant love, encouragement, and practical support (from proof-reading and printing, to dinners, lifts, and post-meltdown hot chocolates) made this whole thing possible. I'm so incredibly lucky to have you both, not only as parents but as best friends.

Author's Declaration

I declare that this thesis is the result of my own work. No part of this thesis has been submitted or is pending submission for any other degree at The University of Glasgow, or any other institution. Appropriate acknowledgements have been made where any necessary support has been provided by another individual.

……

Annie Peacock

Definitions/Abbreviations

α-MEM alpha minimum essential media.

ACR American College of Rheumatology.

C-GCA Cranial Giant Cell Arteritis.

CCR C-C motif chemokine receptor.

CCL C-C motif chemokine ligand.

CD Cluster of differentiation.

CRP C-reactive protein.

CSB Cell separation buffer.

CTS Cathepsin.

CXC C-X-C chemokine.

CXCR C-X-C chemokine receptor

DAMP Danger associated molecular pattern

DCs Dendritic cells

DMARDS disease modifying anti-rheumatic drugs

EC endothelial cell

EDTA Ethylenediamine tetra-acetic acid

ESR Erythrocyte sedimentation rate

EULAR European Alliance of Associations for Rheumatology

FBGC Foreign body giant cell

FBS Fetal bovine serum

FDG-PET Fluorodeoxyglucose Positron Emission Tomography

GCA Giant Cell Arteritis

GCs Glucocorticoids

GM-CSF Granulocyte-macrophage colony-stimulating factor

GPCRs G-protein coupled receptors

HCs Healthy controls

HLA-DR Human Leukocyte antigen – DR

HLD High Linkage disequilibrium

IFN Interferon

IgG Immunoglobulin

IL Interleukin

JAK Janus kinase

lcRNA long non-coding ribonuclease acid

LDRs Leukocyte reduction cones

LHGC Langhans giant cell

LV-GCA large vessel giant cell arteritis

MAPK Mitogen-Activated Protein Kinase

MCSF macrophage colony-stimulating factor

MCP Monocyte chemotactic protein

MDMs monocyte derived macrophages

MHC Major Histocompatibility Complex

MGCs Multinucleated giant cells

MMPs Matrix metalloproteinases

mRNA messenger ribonuclease acid

M.tb Mycobacterium Tuberculosis

MV Maraviroc

N Number of donors

NF-κB nuclear factor – kappa B

iNOS inducible nitrous oxide

OC Osteoclast

PAMP Pathogen associated molecular pattern

PBMCs Peripheral blood mononuclear cells

PBS Phosphate buffered saline

PDGF Platelet-derived growth factor

RA Rheumatoid arthritis

RANK receptor activator of nuclear factor – kappa B

RANKL receptor activator of nuclear factor – kappa B ligand

ROS Reactive oxygen species

RT Room temperature

SASP Senescence associated secretory phenotype

SD Standard deviation

SNP Single nucleotide polymorphism

SSC side-scatter

TAB Temporal artery biopsy

TLR Toll-like receptor

TNF Tumour necrosis factor

TNFR Tumour necrosis factor receptor

TRAP Tartrate-resistant acid phosphatase

TRM Tissue resident macrophage

VSMC Vascular smooth muscle cell

VEGF Vascular endothelial growth factor.

Chapter 1 Introduction.

1.1 Giant Cell Arteritis.

Giant cell arteritis (GCA) is the most common form of granulomatous vasculitis in Europe, affecting those over the age of 50 (Nordborg and Nordborg, 2003). This form of vasculitis affects medium and large sized arteries and is more prevalent in women than men. GCA affects roughly 10-50 in every 100,000 people in Europe (Li *et al.*, 2021) and around 3 million people globally are expected to have GCA by 2050 (De Smit, Palmer and Hewitt, 2015). There are two main subtypes of GCA, cranial-GCA (C-GCA) which affects the temporal artery and can lead to irreversible vision loss, jaw claudication and ischemic strokes. The other subtype of GCA is known as large vessel-GCA (LV-GCA) which can affect the aorta and its branches causing arterial stenosis, limb claudication and aortic aneurisms. Patients can present with one or both of these manifestations (Tomelleri *et al.*, 2022). However, this thesis focuses on C-GCA.

1.1.1 Diagnosis of GCA.

Diagnosis of GCA relies on clinical presentation, histopathological evidence and abnormalities on imaging. As per the American College of Rheumatology/ European Alliance of Associations for Rheumatology scaling system (Table 1.1), patients must be ≥ 50 years of age and present with multiple of the following: stiffness of the shoulders and neck, sudden vision loss, scalp tenderness and abnormal examination of the temporal artery (defined as a diminished pulse with tenderness and or a hard appearance) (Ponte *et al.*, 2022).

Laboratory and biopsy criteria are also important for classification. Prior to treatment, an erythrocyte sedimentation rate (ESR) of ≥ 50mm per hour and a C-reactive protein volume of ≥ 10mg/litre^2 indicate GCA, when combined with a positive temporal artery biopsy (TAB). Temporal artery biopsies of around 1 to 2 cm are standard practice for C-GCA diagnosis.

Absolute requirement	Classification score
Age at diagnosis ≥ 50	
Clinical Criteria	
Morning stiffness in shoulders and neck	+2
Sudden visual loss	+3
Jaw or tongue claudication	+2
New temporal headache	+2
Scalp tenderness	+2
Abnormal examination of temporal artery*	+2
Laboratory, imaging and histology criteria	
Max ESR ≥ 50mm/ hour. Max CRP ≥ 10mg/l[2]	+3
Positive TAB or halo sign on ultrasound	+5
Bilateral axillary involvement**	+2
FED-PET activity throughout Aorta.	+2

Table 1.1 : ACR/EULAR GCA diagnosis criteria A score of ≥ 6 is needed for the classification of GCA adapted from (Ponte C. et.al. 2022)
***absent/diminished pulse, tenderness or hard 'cord-like appearance'**
****luminal damage on imaging**

There is currently no definitive histological measure of GCA. However, indicators of GCA are, the presence of Multinucleated Giant Cells (MGCs), mononuclear cell infiltration with granulomatous inflammation, fragmentation of the internal elastic lamina and a high degree of intimal hyperplasia (Figure 1.1) (Arteritis *et al.*, 2016). False negatives and positives are highly likely with this diagnostic method which could lead to inadequate treatment and permanent vision loss or unnecessary treatment with high doses of glucocorticoids and side effects, respectively. Therefore, imaging is emerging as a crucial and less invasive method of diagnosis which is particularly useful for LV-GCA (Prieto-Peña, Castañeda, *et al.*, 2021). Imaging techniques include temporal ultrasound where a halo-sign indicates the presence of C-GCA and/ or evidence of large vessel involvement. Furthermore, fluorodeoxyglucose uptake on positron emission tomography (FDG-PET) is used to identify LV-GCA.

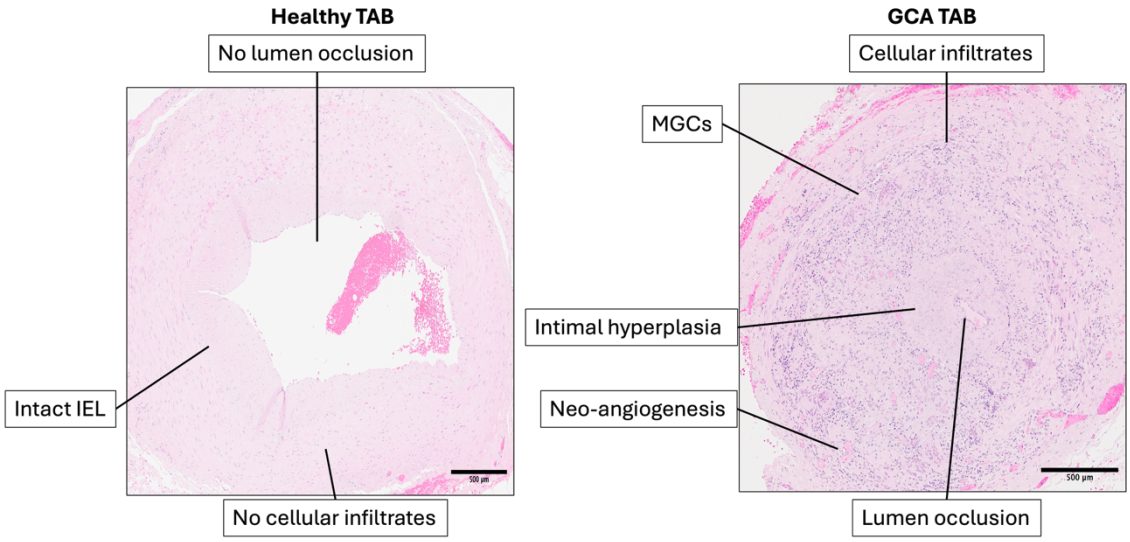

Figure 1.1: Representative images of a healthy and GCA TAB sample.H&E staining of TAB samples taken as part of the diagnostic process of GCA. IEL – internal elastic lamina.

1.1.2 Risk factors for GCA development.

Age is the most prominent risk factor for GCA. There is a large increase of incidence of the disease with increasing age. The mean age of GCA diagnosis is 75 with peak incidence between 70 to 80 years of age (Gonzalez-Gay *et al.*, 2007). Sex is another key risk factor in the development of GCA. Women are more likely to be affected than men, with a female to male ratio of 2-3:1(Gonzalez-Gay *et al.*, 2009). Despite this knowledge, the exact reason for this sex specific risk is still unknown. Furthermore, the geographic specificity of disease cases, Northern hemisphere, particularly Northern European countries such as Sweden, suggests ethnicity and genetics may be a risk factor for GCA development (González-Gay *et al.*, 2025). However, very few genetic loci have been identified in GCA, with no evidence of hereditary links. Some proposed genetic factors are, the presence of the HLA-DR B1*04 and the HLA-B*15 genes (Prieto-Peña, Remuzgo-Martínez, *et al.*, 2021). In one study, these genes were associated with risk of developing both C-GCA and LV-GCA. Interestingly, a GWAS study of GCA patients found two single nucleotide polymorphisms (SNPs) associated with GCA. These SNPs were found for the genes *PLG* (plasminogen) and *P4HA2* (alpha subunit of the collagen prolyl 4-hydroxylase*)*. These genes are involved in pathways implicated in GCA such as angiogenesis, collagen biosynthesis and lymphocyte recruitment (Samson *et al.*, 2017), suggesting these SNPs could play a role in GCA pathogenesis.

Environmental factors have also been assessed as risk factors for GCA. GCA is described as a granulomatous inflammation due to the clustering of many immune cells, including T cells and myeloid cells. Granulomatous inflammation can be linked to infectious triggers and, therefore, some viral infections have been implicated as an environmental

risk factor in GCA. (Cooper *et al.*, 2008). However, no specific infectious agent has been definitively proven to date. An association between GCA and several infectious agents have been described in the literature. These include cytomegalovirus, herpes simplex virus and Varicella-zoster virus (Cooper *et al.*, 2008).

Lastly, epigenetic modifications are emerging as potential risk factors in multiple auto-immune diseases. Epigenetics are defined as reversible changes to gene expression without alteration of the DNA sequence (Holliday, 2006). These changes are made post-translationally by DNA-methylation, histone modifications and microRNAs.
DNA methylation is the addition of a methyl group to cytosine residues on DNA. This methylation often occurs near promoter regions and leads to the repression of gene transcription. Therefore, the reduction of DNA methylation leads to an increase in gene transcription. In GCA, many hypomethylated (and therefore highly expressed) pro-inflammatory genes have been identified such as IFNγ, IL-6 and CD40 (Renauer, Coit and Sawalha, 2016).
Histone modifications include methylation or acetylation of histones. These modifications lead to changes in the structure of chromatin, which determines how well enhancer molecules can bind and, therefore, whether a gene will be transcribed or not. The most common histone modifications are Histone H3 Lysine 4 trimethylation (H3K4Me3), which is associated with an open chromatin state and the increased activation of genes, and Histone H3 Lysine 27 trimethylation (H3K27Me3), which is associated with closed chromatin and the repression of gene transcription (Andrew J Bannister & Tony Kouzarides, 2011). However, histone modifications have yet to be investigated in the context of GCA.
Furthermore, epigenetic modifications are associated with ageing. In particular, DNA methylation decreases with age, suggesting that the hypomethylation observed in GCA could be an age driven process. Additionally, there is a global remodelling of chromatin during the ageing process (Wang *et al.*, 2022a), This further implicates ageing as a risk factor in GCA.

1.2 Immunopathology of GCA.

GCA is characterised by loss of tolerance in the normally immune privileged arterial vessels. Immune privilege is the downregulation of a potentially damaging immune response in indispensable organs with limited regeneration capacity (Benhar, London and Schwartz, 2012). These vessels have a conserved structure (Mercadante and Raja, 2025) consisting of the adventitia, media and intima (Figure 1.2). A model of disease progress was proposed in which pathology occurs in three main stages (Aristizábal and

González, 2013). Initially, resident cells are activated by an, as yet, unknown initiator of GCA. This activation leads to infiltration of mononuclear cells into the adventitia. These cells migrate into the media of the vessel causing media destruction and neo-angiogenesis. In an attempt to repair this destruction, repair mechanisms become overactive. This leads to thickening of the inner vessel layer and subsequent narrowing of the lumen. This narrowing of the lumen reduces blood flow leading to the ischemic symptoms prevalent in GCA. Furthermore, granulomas are formed in GCA that are self-sustained and consist of T cells and macrophages and often have multinucleated giant cells (MGCs) surrounding them.

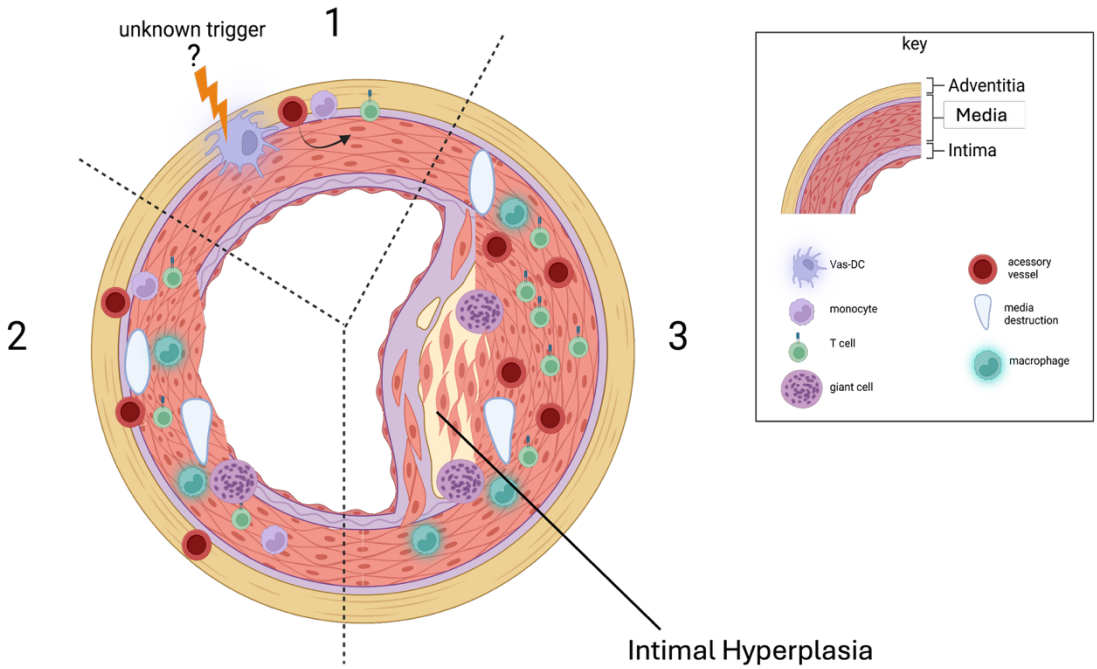

Figure 1.2:Immunopathology of GCA.Three stages of disease progression in GCA. Adapted from (Weyand and Goronzy, 2008). Made using BioRender.

1.2.1 Innate immunity in GCA.

The innate immune system is the first line of defence against invading pathogens, such as bacteria or viruses (Aristizábal and González, 2013). This arm of the immune system is largely considered to be 'non-specific' and is comprised of dendritic cells, monocytes, macrophages, neutrophils, basophils and eosinophils. Innate immune cells rely on pathogen recognition receptors, such as toll-like receptors (TLRs). To respond to conserved molecular patterns on pathogens (known as pathogen associated molecular patterns, PAMPs) and danger signals from surrounding cells (damage associated molecular patterns, DAMPS) (Turvey and Broide, 2010). Stimulation of these receptors induces a

rapid pro-inflammatory response of cytokine and chemokine production, leading to recruitment and activation of immune cells.

Innate immune cells are key players in the pathology of GCA (Akiyama, Ohtsuki, Gerald J. Berry, *et al.*, 2021), dysregulation of cytokine and chemokine production and phagocytosis drives the chronic inflammation and causes damage to the vessel and initiates the aberrant repair mechanisms leading to the intimal hyperplasia. In particular, the cells of myeloid linage have been identified as potential drivers of GCA pathology (Watanabe and Hashimoto, 2022b). Myeloid cells including monocytes and macrophages develop from a common progenitor cell in the bone marrow (Geissmann *et al.*, 2010)(Figure 1.3) and include monocytes, macrophages and dendritic cells.

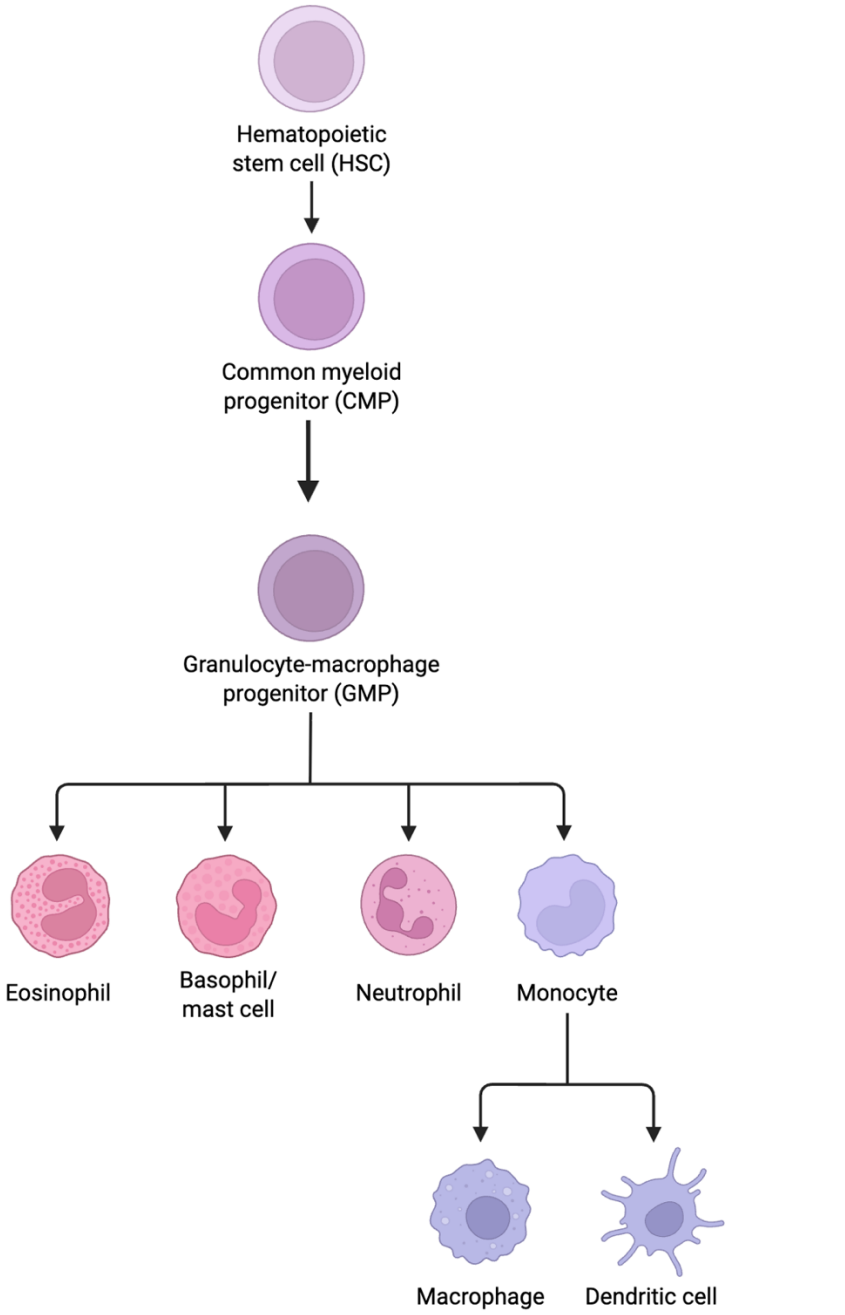

Figure 1.3: Myleoid development from progenitors.Development of monocytes, macrophages and dendritic cells from a common myeloid progenitor. Adapted from (Mouchemore and Pixley, 2012). Made using BioRender.

1.2.1.1 Monocytes.

Monocytes are some of the first responders to a pathogen (Karlmark, Tacke and Dunay, 2012). These cells migrate out of the bone marrow when chemo-attractants such as C-C motif chemokine ligand 2 (CCL2) are released in response to danger and bind with the chemokine receptor C-C motif chemokine receptor 2 (CCR2) (Serbina and Pamer, 2006). Monocytes are then released into the blood

circulation where they make up 5-10% of human leukocytes. When required, monocytes will migrate to tissues where they differentiate into macrophages. These cells are a heterogenous population defined by their cell surface expression of CD14 and CD16 and fall under three categories. Classical (CD14++CD16-), intermediate (CD14++CD16+) and non-classical monocytes (C14+CD16++). These cells vary in proportion. Classical monocytes make up the majority of this population at around 80-95%, intermediate monocytes make up 2-8% and non-classical monocytes make up 2-10% of the circulating population (Geissmann *et al.*, 2010). These subsets have differing phenotypes, surface molecule expression profiles and functions in homeostasis. Classical and intermediate monocytes are generally considered to be pro-inflammatory, whereas non-classical monocytes are described as patrolling and involved in maintenance of vascular homeostasis. However, recently these cells have been shown to have pro-inflammatory properties when activated and have been implicated in the worsening of several autoimmune diseases (Narasimhan *et al.*, 2019). Monocytes control the early phase of infections by producing pro-inflammatory cytokines such as IL-6, IL-1b, TNF-a and iNOS (Shi and Pamer, 2011). Monocytes induce cross talk with the adaptive immune system by acting as antigen presenting cells, using MHC11 to communicate with T-cells. Finally, in the tissue monocytes can differentiate into monocyte derived macrophages (MDCs) when exposed to growth factors such as macrophage-colony stimulating factor (M-CSF) or granulocyte macrophage-colony stimulating factor (GM-CSF) (Yáñez *et al.*, 2017).

In GCA, monocyte numbers are elevated compared to healthy controls. In particular, the intermediate phenotype. In the initial phases of GCA pathogenesis, monocyte derived pro-inflammatory cytokines are highly elevated such as IL-6 and IL1-ß (Watanabe and Hashimoto, 2022b). Furthermore, monocytes have been shown to have tissue invasive capacity in GCA and are thought to digest the basement membrane paving the way for their entry, and the subsequent entry of adaptive immune cells into the normally immune privileged vessel. This ability to digest the membranes of the vaso vasorum is due to their abnormally high expression of the matrix metalloprotease MMP9. When MMP9 activity was blocked by a monoclonal antibody, cellular infiltrates could not be observed, showing that this protease was needed for cells to invade

the vessel wall (Watanabe *et al.*, 2018). Crucially, monocytes which enter the vessel differentiate into MDCs (Bernaerts *et al.*, 2024).

1.2.1.2 **Macrophages.**

Macrophages have two primary sources. One group arises from embryonic yolk-sac progenitors, which migrate during development to both lymphoid and non-lymphoid tissues, where they establish long-term residence. These are the tissue-resident macrophages (TRMs), such as microglia in the brain and Langerhans cells in the epidermis (Davies *et al.*, 2013). TRMs are self-sustaining through local proliferation and persist throughout adulthood (Ginhoux and Guilliams, 2016). The second group derives from circulating monocytes that enter tissues in response to pathogens or other threats These are known as monocyte derived macrophages (MDMs).

A central role of macrophages in infection clearance is phagocytosis, mediated through pathogen recognition receptors and cytokines (Chen *et al.*, 2023). Macrophages can also present antigens to other immune cells and induce adaptive immune responses from T and B cells through cytokines and chemokines (Shapouri-Moghaddam *et al.*, 2018a).

Functionally, macrophages are often classified into two main subtypes: M1, which are pro-inflammatory and typically arise in response to GM-CSF, IFN-γ, or TNF-α, and M2, which are anti-inflammatory and induced by signals such as IL-4 and IL-13 (Strizova *et al.*, 2023). However, it has become increasingly clear in recent years that the simple M1/M2 paradigm does not reflect the complexity and plasticity of these cells, particularly in autoimmune diseases. Emerging technologies, such as single-cell RNA sequencing have shown that macrophages are highly heterogeneous between tissues and microenvironments. (Guan *et al.*, 2025)

In GCA, the main source of pathogenic macrophages has been shown to be monocyte-derived macrophages (Weinberger *et al.*, 2020). These cells are critical for both the development and maintenance of granulomas. High IFN-γ signatures in affected vessels implicate the pro-inflammatory M1 subtype as a key driver of disease (Watanabe and Hashimoto, 2022b). Distinct macrophage subtypes localize to different regions of the vessel wall (Version and Sleen, 2020), where they perform specialized roles. It is proposed that CD206+ MMP9+

macrophages reside in the adventitia/media at sites of tissue destruction whereas FRb+ macrophages reside in the intima near intimal hyperplasia (Esen *et al.*, 2021). It is thought that these monocytes are differentially regulated by exposure to MCSF or GM-CSF the source of which is not yet known (Lemaire *et al.*, 1996). Macrophages share MM9 high expression with circulating monocytes, further reinforcing their origin. At the media–intima border, macrophages contribute to fragmentation of the internal elastic lamina and drive vascular remodelling through degradation and phagocytosis of the extracellular matrix (Rittner *et al.*, 1999). This process involves the release of MMPs and reactive oxygen species (ROS) but also includes the provision of growth factors and angiogenic cytokines that promote intimal hyperplasia and narrowing of the lumen. Neovascularisation in the media and intima regions of GCA effected vessels occurs through the release of monocyte-derived vascular endothelial growth factor (Van Sleen *et al.*, 2019). In addition, macrophages can fuse to form MGCs, which not only give the disease its name but also represent a central feature of its pathology (Ahmadzadeh *et al.*, 2023). These will be, discussed in more detail, later in this introduction.

1.2.1.3 **Dendritic cells.**

Dendritic cells (DCs) are the main link between the innate and adaptive immune systems (Ardavín *et al.*, 2001). These cells present antigen to T cells and are thought to be the main initiators of T-cell driven immunity. Dendritic cells are also key in the recognition of self-antigens and the prevention of autoimmunity through auto-reactive T cell depletion (Ni and O'Neill, 1997). These cells orchestrate immune infiltrates such as T cells by producing cytokines and chemokines and induce T cell activation through antigen presentation on MHC11 (HLA-DR). They can also provide inhibitory signals to T cells to control inflammation under homeostatic conditions (Ness, Lin and Gordon, 2021). Specific tissue resident dendritic cells reside in the adventitia/media junction of the vessel to maintain immune privilege and are known as VasDCs. Under homeostatic conditions, VasDCs cells have an inactivated surface expression profile consisting of CD11c, S100 and CD68 and the lack of the activation markers CD83 or HLA-DR. This inactivation profile ensures that vascular dendritic cells cannot activate T cell responses in the immune privileged vessel (Weyand *et al.*, 2005).

In GCA, VasDCs become activated by an unknown trigger leading to a change in their functional status and a loss of tolerance to the vessel tissue. VasDCs in GCA do express the activation marker CD83 and can induce the activation of T cells. It is predicted that these tissue resident cells migrate to other areas of the vessel to present antigen to infiltrating T cells. These dendritic cells have been shown to express the co-stimulatory molecule CD86. Blocking of this molecule has been shown to reduce progression of vasculitis disease implicating this pathway in the pathogenesis of GCA (Ma-Krupa *et al.*, 2004). Interestingly, vessel remodelling, such as, intimal hyperplasia, relies on the cross linking of CD86 and its receptor CD28.
Furthermore, in GCA VasDCs lack the T cell inhibitory molecule PD-L1. During homeostasis, this molecule inhibits stimulation of T cells (Head *et al.*, 2021).

1.2.2 **Adaptive immunity in GCA,**

The adaptive immune system is a highly specific response with a 'memory' capacity that allows cells of the adaptive immune system to recognise a pathogen that they have encountered before and mount a faster, more efficient immune response to that pathogen (Bonilla and Oettgen, 2010). The main role of the adaptive immune system is to recognise no -self antigens and, in turn, mount a pathogen specific immune response and development of memory. The main cells of the adaptive immune system are T cells and B cells. These cells get their name from their tissue of origin, the thymus and the bursa of Fabricus in chickens, respectively (Zdrojewicz, Pachura and Pachura, 2016; Nandiwada, 2023). T cells express T cell receptors (TCRs) on their surface which are unique to each individual T cell. These TCRs are specific for specific foreign peptides that can initiate an immune response. T cells can be categorised into T helper cells (CD4+ T cells) and cytotoxic T cells (CD8+ T cells) which exert different functions in the immune response against pathogens. CD4 T cells do not directly kill pathogens but further mediate the adaptive response by producing cytokine and chemokine signals to call on and activate further immune cells(Constant and Bottomly, 1997). These cells also present antigens to B cells, upon which B cells can release cytokines and chemokines, become anti-body producing plasma cells, or become memory B cells (Nandiwada, 2023).

CD4 T cells are sub-characterised as Th1,2 and 17 by the type of response they induce. Th1 responses are characterised by IFNγ production and other cytokines, which induce M1 macrophages and induce opsonising antibody production by B cells. In contrast, the Th2 response is characterised by the production of IL-4 and IL-13, known to induce M2 responses and IgE antibodies from B cells as well as recruitment and activation of eosinophils and mast cells (Oliphant, Barlow and McKenzie, 2011). Lastly, Th17 cells produce IL-17 cytokines and are often associated with chronic diseases (Maddur *et al.*, 2012).
In contrast, CD8 T cells are named cytotoxic due to their direct killing of pathogen infected cells. These cells are activated by MHC 1 presentation of endogenous antigens; these cells then release soluble mediators which induce apoptosis of infected cells (Henkart, 1997).

In GCA, the dominant immune cell population within granulomatous lesions is $CD4^+$ T cells, with the adaptive immune response thought to be primarily driven by Th1 and Th17 subsets (Weyand, Younge and Goronzy, 2011). In the periphery, circulating T cells display aberrant expression of NOTCH1, which binds to JAGGED1 on endothelial cells and facilitates their migration into the vessel wall (Estupiñán-Moreno *et al.*, 2024). Once inside, Th1 cells produce IFN-γ, a cytokine highly upregulated in GCA, that drives the differentiation of monocytes into macrophages (Li, Xu and Shuai, 2021). As previously noted, the lack of PD-L1 expression in GCA results in unchecked activation of $CD4^+$ T cells, fuelling chronic inflammation. GM-CSF, expressed by both macrophages and endothelial cells and found to be elevated in GCA, further amplifies disease by acting upstream of Th1 and Th17 pathways (Terrier *et al.*, 2012). Indeed, suppression of GM-CSF in experimental models has been shown to reduce T cell infiltration, intimal thickening, and neo-angiogenesis. Importantly, T cells rely on monocytes and macrophages for successful invasion of the vessel wall, highlighting their interdependence in sustaining vascular inflammation (Wen *et al.*, 2017). Beyond $CD4^+$ T cells, $FOXP3^+$ CD8 regulatory T cells, which normally act to restrain immune activation, are defective in GCA (Watanabe *et al.*, 2017). While B cells have rarely been described in this disease and are only occasionally seen within granulomas, emerging evidence suggests that they may play a more prominent role in large-vessel GCA compared to cranial GCA (Graver *et al.*, 2019).

1.2.3 **The role of vascular cells in GCA.**

The vascular wall is composed of endothelial cells (ECs), vascular smooth muscle cells (VSMCs), and myofibroblasts, all of which play active roles in the pathogenesis of GCA. Single-cell studies have revealed that ECs not only regulate vascular integrity, but also acquire immune-related functions, including antigen presentation, phagocytosis, and recruitment of immune cells (Ly *et al.*, 2010). In the intima, myofibroblasts proliferate and deposit extracellular matrix proteins, leading to intimal thickening and ultimately vessel occlusion (Régent *et al.*, 2017). VSMCs, stimulated by macrophages, produce MMPs that contribute to tissue damage. Additionally, while IFN-γ signalling from Th1 cells induces VSMCs to secrete VEGF and PDGF, driving their proliferation, differentiation into myofibroblasts, and promoting neo-angiogenesis (Sun *et al.*, 2025).
Lastly, a subset of mesenchymal cells, collectively termed perivascular mesenchymal cells, including pericytes, adventitial fibroblasts, and mesenchymal stromal cells, has been implicated in disease (Benabid and Peduto, 2020). Normally anti-inflammatory, these cells may become dysregulated in GCA, contributing to both inflammation and fibrosis and thereby driving the tissue remodelling characteristic of the disease (Paroli, Caccavale and Accapezzato, 2024).

1.2.4 **Inflammaging.**

As age is the greatest risk factor for the development of GCA, the ageing of the immune system, often referred to as inflammaging, has been strongly implicated in disease pathogenesis (Mohan *et al.*, 2011). With advancing age, the functional capacity of the immune system progressively declines, in part due to thymic involution and the accumulation of chronic, low-grade inflammation that renders blood vessels more susceptible to immune attack (Watanabe and Hashimoto, 2022a). Senescent cells exhibiting a senescence-associated secretory phenotype (SASP) have been identified in GCA lesions, particularly among fibroblasts, macrophages, and endothelial cells (Huang *et al.*, 2022). These cells secrete high levels of IL-6, a cytokine associated with exacerbation of intimal hyperplasia, while increased oxidative stress with ageing further promotes a pro-inflammatory milieu (Veroutis *et al.*, 2023). Together, these age-related changes

create an immunological and vascular environment primed for aberrant inflammation.

Granulomatous inflammation in GCA has also been linked to the formation of tertiary lymphoid structures (TLS), a process frequently associated with immune ageing. With age, T cell receptor diversity decreases, and senescent T cells, despite being in irreversible cell-cycle arrest, adopt a SASP, releasing pro-inflammatory cytokines that perpetuate inflammation (Kloc *et al.*, 2022). In addition, loss of functional CD8 regulatory T cells represents a completely age-dependent phenomenon in healthy individuals and may occur prematurely in patients with GCA, removing a key brake on pathogenic T cell activity.
Ageing also drives dysfunction within vascular cells themselves; impaired mitochondrial biogenesis promotes senescence in endothelial cells and vascular smooth muscle cells, both of which adopt a pro-inflammatory SASP phenotype (Ong *et al.*, 2018). These processes highlight the convergence of immune and vascular ageing in fostering the chronic inflammation characteristic of GCA.

1.3 Treatment strategies.

1.3.1 Glucocorticoids.

To date, there is no effective cure for GCA, but existing therapies are able to induce remission in many patients. The current mainstay of treatment is prolonged administration of high-dose glucocorticoids (GCs) such as prednisolone or dexamethasone (Vaiopoulos *et al.*, 2023). Standard regimens typically begin with 40-60 mg/day, tapered to 15–20 mg/day within the first three months, and reduced further to around 5 mg/day by the end of the first year of treatment (Maz *et al.*, 2021) (Figure 1.5).

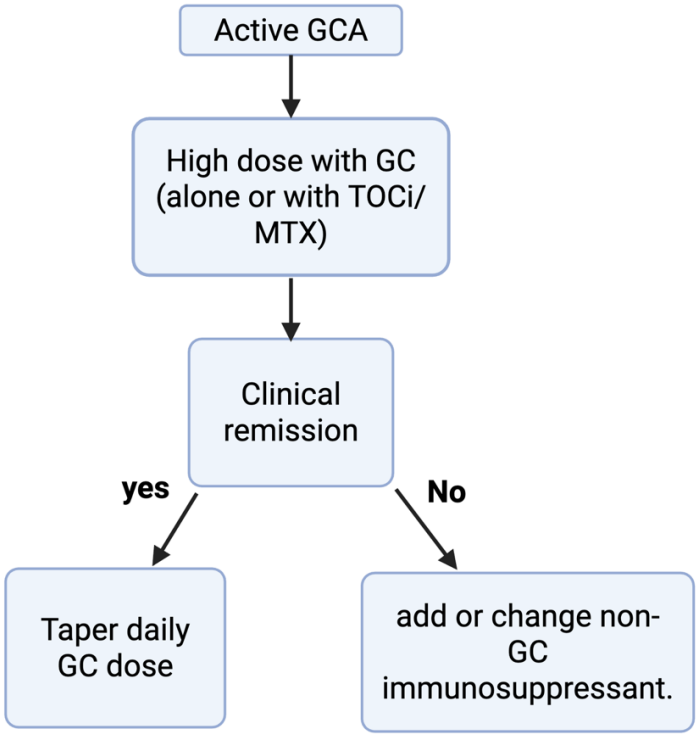

Figure 1.4: ACR/ Vasculitis Foundation guidelines for GCA management. Flow chart depicting treatment strategies for GCA. Adapted from (Maz et al., 2021). Made using BioRender.

Glucocorticoids are highly effective in preventing irreversible vision loss and act by reducing Th17-associated immune responses and lowering pro-inflammatory cytokine production. However, they do not sufficiently inhibit Th1-mediated pathways and, therefore, fail to halt vascular remodelling (Deng *et al.*, 2010). Mechanistically, glucocorticoids bind to the intracellular glucocorticoid receptor (GR), a member of the nuclear receptor family, which translocates to the nucleus and suppresses NF-κB signalling, thereby limiting pro-inflammatory cytokine production (Timmermans, Souffriau and Libert, 2019). Despite their effectiveness, treatment outcomes are suboptimal: only ~50% of patients respond fully, with relapses frequently occurring during GC tapering (Gloor *et al.*, 2025). Moreover, long-term use is associated with significant toxicity, with up to 90% of patients experiencing side effects, such as, osteoporosis, increased susceptibility to infection, insomnia, diabetes mellitus, and glaucoma (Figure 1.6). These adverse effects disproportionately affect the elderly population in which GCA arises, severely impacting quality of life (Buchman, 2001). Given their limited efficacy in controlling Th1-driven pathology and their extensive toxicity profile, there is a clear need for the development of GC-sparing therapeutic strategies.

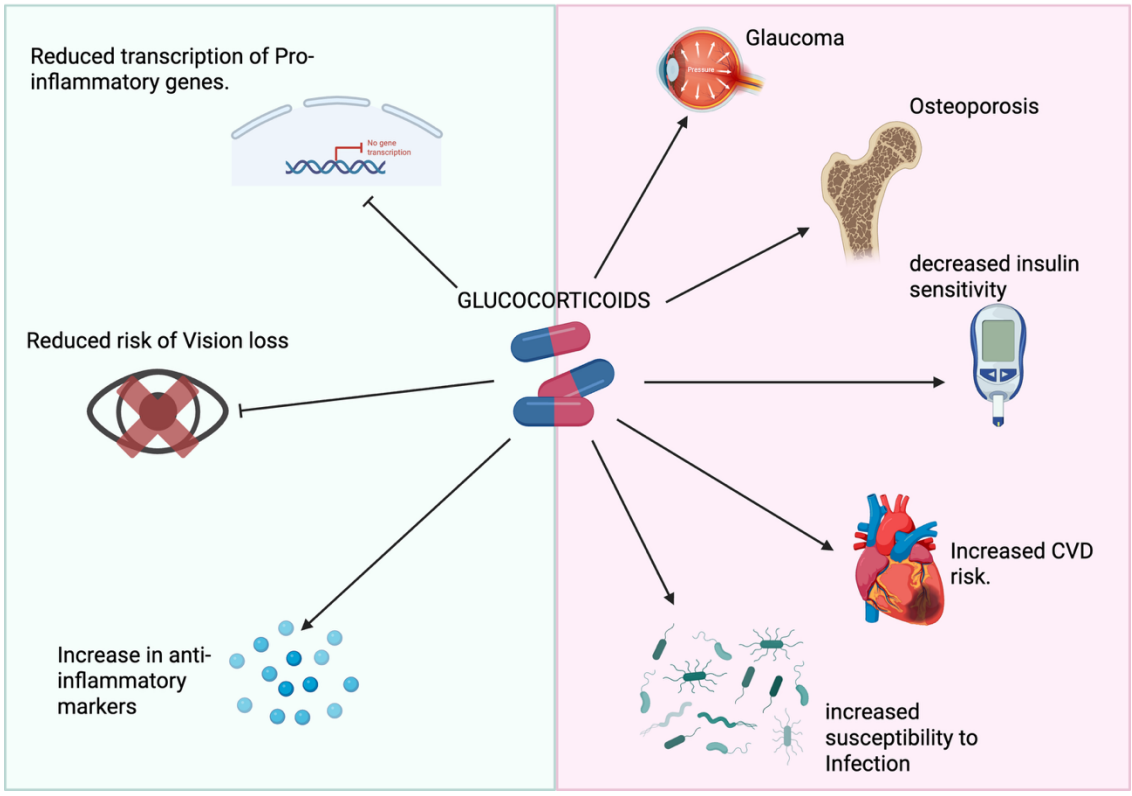

Figure 1.5: Outcomes and adverse outcomes of Glucocorticoid treatment in GCA.Positive outcomes of GC treatment in GCA (left) and adverse outcomes of GC treatment (right). Adapted from (van der Goes, Jacobs and Bijlsma, 2014). Made using BioRender.

1.3.2 DMARDs and biologics.

In recent years, Tocilizumab has emerged as a promising glucocorticoid sparring drug against GCA. Tocilizumab is a monoclonal antibody against the cytokine IL-6, which is highly implicated in the pathogenesis of GCA (Buttgereit *et al.*, 2023). This is used as a glucocorticoid sparring agent, during a clinical study of Tocilizumab the total dose of GCs used in the placebo group steroids was around 3,000 mg after 1 year whereas, patients on Tocilizumab received ~1,000mg over the year period. This sparring agent had a good benefit to risk ratio in GCA and around 60% of patients will reach clinical remission, when used with tapering steroids. However, the remaining 40% of patients fail to respond to Tocilizumab and of those who do, around 60% will experience a relapse of disease after discontinuation (Stone *et al.*, 2017). This shows the need for other biologics and treatment targets.

Some other biologics have been shown in early clinical trials to be promising treatment targets for GCA. In one, *ex vivo,* model of TABs showed a reduction in cellular infiltrates such as CD14, CD16 and CD20 when treated with Mavrilimumab, a monoclonal antibody against GM-CSF (Corbera-Bellalta *et al.*,

2022). This monoclonal antibody also was shown to reduce vascular remodelling factors such as MMP9 and iNOS. However, further clinical trials are needed to assess the benefits of Mavrilimumab in GCA. Furthermore, Jansus Kinases 1 and 2 (JAK1/2) are implicated in in GCA pathogenesis due to their activation by type 1 interferons such as IFNγ and their potential role in vascular remodelling processes in GCA. Upadacitinib, a selective JAK inhibitor which blocks the signalling of IL-6 and IFNγ, has recently been approved for treatment of GCA. A phase 3 trial of the drug, showed that this drug could be used as a glucocorticoid sparring agent (Blockmans *et al.*, 2025)

Lastly, methotrexate, a disease-modifying antirheumatic drug (DMARD), is sometimes used in the management of GCA, particularly in patients who experience adverse effects with tocilizumab or fail to respond to IL-6 blockade. While methotrexate can provide some therapeutic benefit, its mechanism as a broad immunosuppressant is associated with increased susceptibility to infections and other systemic side effects. Given these limitations, methotrexate is not an ideal long-term option for most patients (Cronstein and Aune, 2020). Instead, its use highlights the ongoing need for more targeted, patient-tailored therapies that can specifically modulate the pathogenic immune pathways of GCA without compromising host defence.

1.4 **Models of GCA pathology.**

To date, there is no reliable model for the study of the pathogenesis and initiation of GCA. Most of our understanding of GCA is from experimental studies carried out on TABs taken during the diagnostic process, as imaging is becoming increasingly used in GCA diagnosis better models are needed.
One model is the previously mention ex vivo TAB culture model by (Corbera-Bellalta *et al.*, 2014). In this model, TABs are cultured in Matrigel and can be cultured for up to 2 weeks. This model can be used to understand the modulating effects of treatments on the cells and vasculature in GCA. However, this model does not accurately depict the initiation stages of GCA and cannot be used to examine chronic, long-term inflammation. Furthermore, the Matrigel used to culture these TABs may be influencing the proliferation of vascular smooth muscle cells, leading to an upregulation of measured products and,

therefore, minimising the differences between healthy controls and GCA samples.

1.4.1 **Animal models.**

Animal models are commonly used to understand the pathogenic progression of auto-immune and inflammatory diseases. However, a reliable animal model of GCA is yet to be described.

One model is the engraftment of human GCA-temporal arteries into severe combined immuno-deficient mice (SCID). Additionally, healthy temporal arteries can be engrafted and GCA and GCA mononuclear cells added to understand the initiating events of GCA. However, chronic long-term inflammation cannot be studied due to the short life span of these mice (Chu, 2023).

One knock-out gene model in mice is the use of IL-1rn-/- mice which lack the ligand for IL-1 receptor. These mice develop an aortitis that closely resembles LV-GCA. This model has the presence of macrophages, Th1 driven immunity and vascular remodelling such as neo-angiogenesis and elastic fibre destruction. However, these mice do not develop MGCs, the hallmark of this disease (Isoda *et al.*, 2003).

Furthermore, it is believed that rodents lack the vaso-vasorum structure that humans have. This is thought to be the main source of infiltrating immune cells in GCA, meaning these models cannot fully encapsulate the physiology of this disease (WOLINSKY and GLAGOV, 1967).

Recently, bioengineered vessel models have been described for use in studying vasculitis. One model utilised a collagen type 1 matrix as a scaffold for a VSMCs and ECs lining (Shinohara *et al.*, 2013). This model was then populated with DCs, monocytes and macrophages to mimic the initiating events of vasculitis. However, this model has not yet been conducted with GCA patient cells and therefore, more studies are needed to understand whether this is a viable model for the initiation and pathogenesis of GCA.

1.5 Multinucleated giant cells.

1.5.1 In health and diseases.

Multinucleated giant cells (MGCs) are large polykaryons containing 3 or more nuclei within their cytoplasm (Anderson, 2000). These cells have been described under both homeostatic conditions as well as implicated in the pathogenesis of many auto-immune and inflammatory diseases. These cells form from a macrophage precursor, and two competing theories of formation have been put forward in previous literature. The first is that MGCs form through the fusion of macrophages in response to implanted biomaterials or infectious agents such as leishmaniasis, induced by cytokines such as IFNγ or IL-4 along with growth factors and other cell-cell communications (McNally and Anderson, 2011b; Tanneberger *et al.*, 2021). The other is that MGCs form due to incomplete cytokinesis, where daughter cells fail to separate during the cell division process (Takegahara *et al.*, 2016a). Evidence for and against both theories has been presented in the literature.

There are many types of MGCs described in both health and disease (Figure 1.7). The most well-known of which is the osteoclast. Osteoclasts are crucial in the homeostatic turnover of bone (Teitelbaum, 2007). These cells resorb bone by attaching to the surface using podosomes and releasing matrix degrading enzymes like tartrate resistant acid phosphatase (TRAP), MMP9 and cathepsin K (CTSK). Osteoclasts are induced by MCSF and the Receptor activator of nuclear factor kappa-B ligand (RANK)/ RANK receptor interaction. These MGCs have been implicated in the pathogenesis of the autoimmune disease, Rheumatoid Arthritis (RA). In RA there is an imbalance between the number of bone-forming cells (osteoblasts) and osteoclasts. Greater numbers of osteoclasts in RA lead to aberrant bone resorption and damage to the bone and cartilage (Xue *et al.*, 2020). Osteoclast-like cells have also been described in cancers, such as, osteosarcoma and giant cell tumours (Lieveld *et al.*, 2014).

Another MGC subtype is known as Langhans giant cells (LHGCs). These cells have a very specific nuclear distribution pattern within the cytoplasm. LHGCs have roughly 3 to 30 nuclei within one cytoplasm, distributed in an annular or semi-annular pattern. These cells have been found in forms of granulomatous

inflammation, such as, the inflammatory response to Mycobacterium Tuberculosis (M.*tb*) (Okamoto, Mizuno and Horio, 2003a). These cells are thought to be involved in the immune response against these pathogens and induced by macrophage exposure to GM-CSF and IFNγ(Chen *et al.*, 2022). Foreign body giant cells (FBGCs) have also been described in the literature. These are extremely large cells with anywhere from 30-300 nuclei, distributed randomly throughout the one cytoplasm (McNally and Anderson, 2011a). These cells were first identified adjacent to implanted foreign materials and are thought to be induced by anti-inflammatory cytokines such as IL-4 and IL-13, together with the growth factor M-CSF(Khan *et al.*, 2013). In other disease contexts, similar cell types have been described. For example, foam cells in atherosclerosis can develop into Touton giant cells, which are linked to IL-6 signalling. Morphologically, Touton giant cells are characterized by multiple clustered nuclei surrounded by a foamy cytoplasm enriched with accumulated lipids. While their function is not yet fully defined, they are thought to participate in the clearance of extracellular lipids and may contribute to tissue remodelling in chronic inflammatory settings (Hazra *et al.*, 2023). Understanding these parallels may provide insight into the mechanisms underlying giant cell formation in GCA.

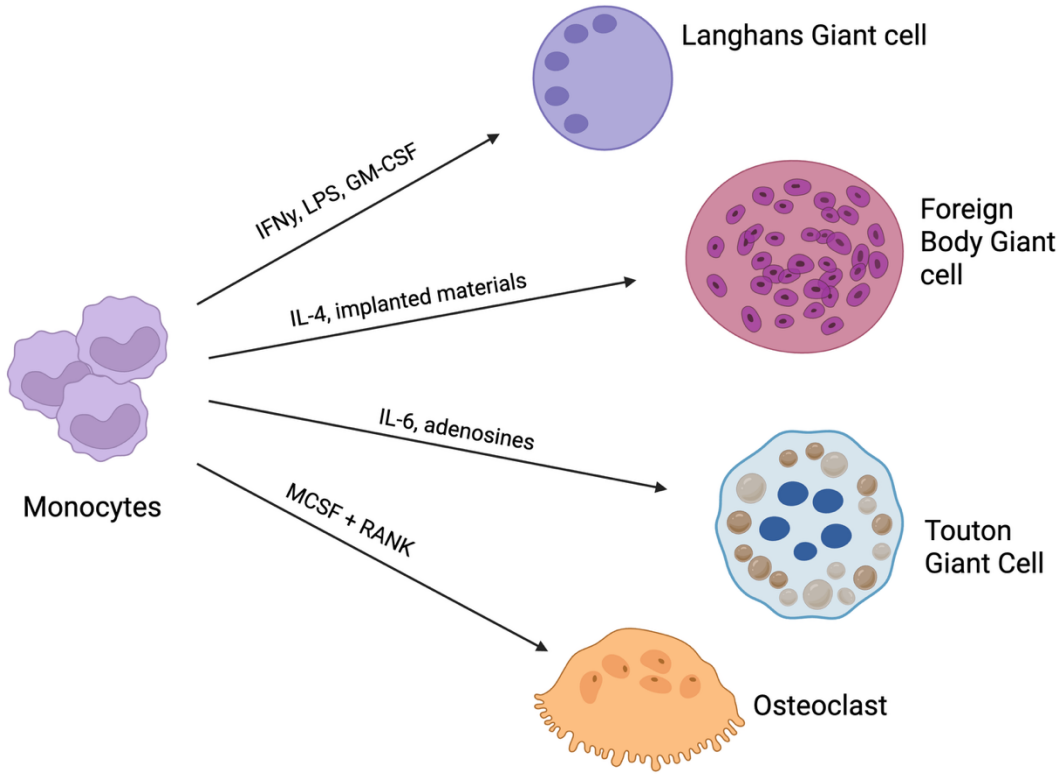

Figure 1.6: Multinucleated Giant Cell subtypes. MGC subtypes and the factors thought to be involved in their formation. Adapted from (Brooks, Glogauer and McCulloch, 2019). Made in BioRender.

1.5.2 The presence and role of MGCs in GCA.

MGCs are the namesake cells of GCA, yet their formation, function, and therapeutic potential remain poorly understood. They are detected in approximately 50–60% of patients, typically localized along the media–intima border of affected vessels (Muratore *et al.*, 2016). The predominant subtype is thought to be Langhans giant cells, although there is also evidence supporting the presence of foreign body-type giant cells within lesions (Nordborg *et al.*, 1997). MGCs have been proposed to contribute to vascular pathology through media destruction and promotion of neo-angiogenesis due to their production of MMPs, ROS and YKL40, a marker of angiogenesis (Johansen *et al.*, 1999). Their numbers appear to decrease following glucocorticoid therapy. Furthermore, several studies have reported associations between higher MGC burden and more severe clinical manifestations (Armstrong *et al.*, 2008). Moreover, increased MGC presence has also been linked to a greater risk of disease relapse (Restuccia *et al.*, 2016). Furthermore, the development of MGCs has been associated with the ageing immune system, the main risk of GCA development (Kloc *et al.*, 2022). Together, this underscores their potential importance in GCA pathogenesis and highlighting the need for further investigation into their biology and role as possible treatment targets.

1.6 Chemokines and Chemokine receptors.

Chemokines are a group of cytokines involved in numerous biological processes (Figure 1.8) such as homeostasis, organ development, chemotaxis (the directed movement of a cell towards chemokines) and angiogenesis (Bernardini *et al.*, 2003). These cytokines signal through 7 transmembrane G-protein coupled receptors and many chemokines can bind to one receptor with high affinity. Chemokines and their receptors are named based on the number of amino acids between two Cytosine residues. Where CC chemokines have two adjacent Cytosine residues, CXC chemokines have on amino acid between the residues and CX3C chemokines have 3 amino acids between the two residues (Proudfoot, 2002).

Chemokines and their receptors can also be involved in inflammatory and disease process in immune mediated inflammatory diseases. One particular

chemokine receptor that has been implicated in the pathogenesis of multiple these diseases is CCR5.

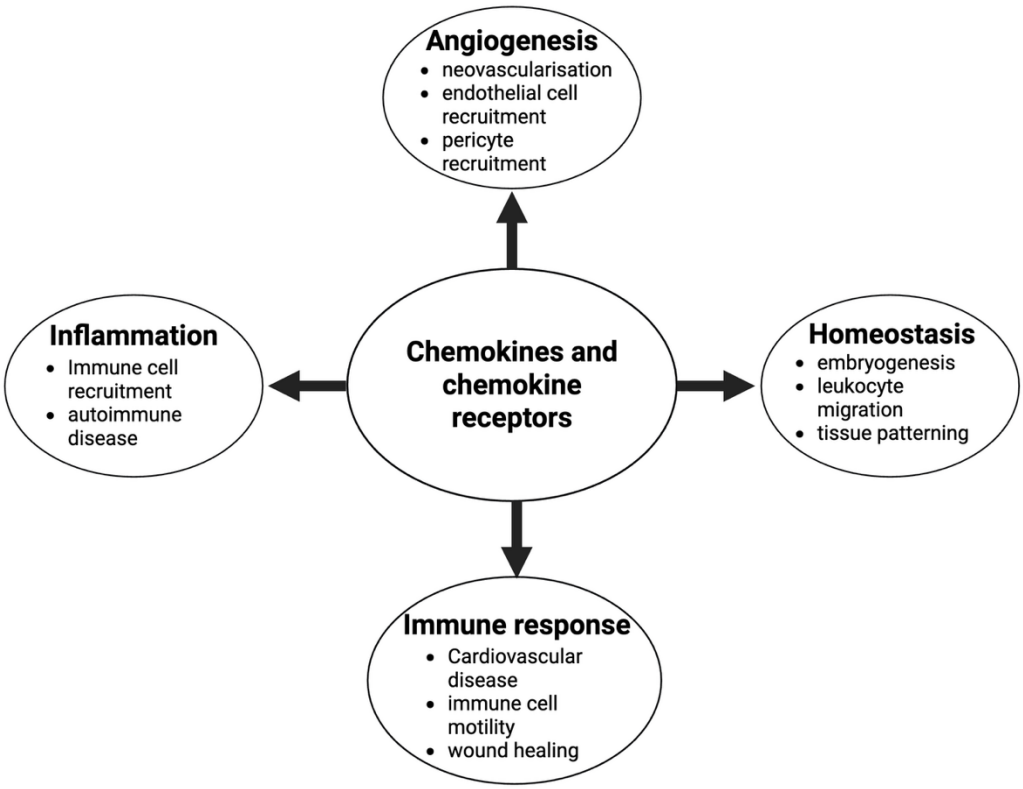

Figure 1.7: The functions of chemokines in health and disease.Mind map adapted from (Tang and Wang, 2018). Made using BioRender.

1.6.1 The chemokine receptor CCR5.

CCR5 is a member of the chemokine receptor family, a group of seven-transmembrane receptors that couple to and signal through G-proteins (Murphy, 2023)(Figure 1.9). Like other chemokine receptors, CCR5 possesses a cytoplasmic C-terminus and an extracellular N-terminus, and its transcription is regulated by the transcription factor CREB-1 (Rutger J. Wierda *et al.*, 2012). CCR5 is considered a promiscuous receptor, as it binds several chemokines with high affinity, including CCL3, CCL4, and CCL5 (Balistreri *et al.*, 2007). Ligand binding triggers receptor internalisation and activates downstream signalling cascades. Notably, CCL5 binding leads to activation of the STAT3 pathway, which can drive the production of the IL-6 receptor and amplify inflammatory responses (Tang, Hsu and Fong, 2010). CCR5 is expressed on a range of immune cells, including T cells, monocytes, macrophages, and immature dendritic cells, positioning it as

an important regulator of leukocyte trafficking and activation in inflammatory disease (Oppermann *et al.*, 1999).

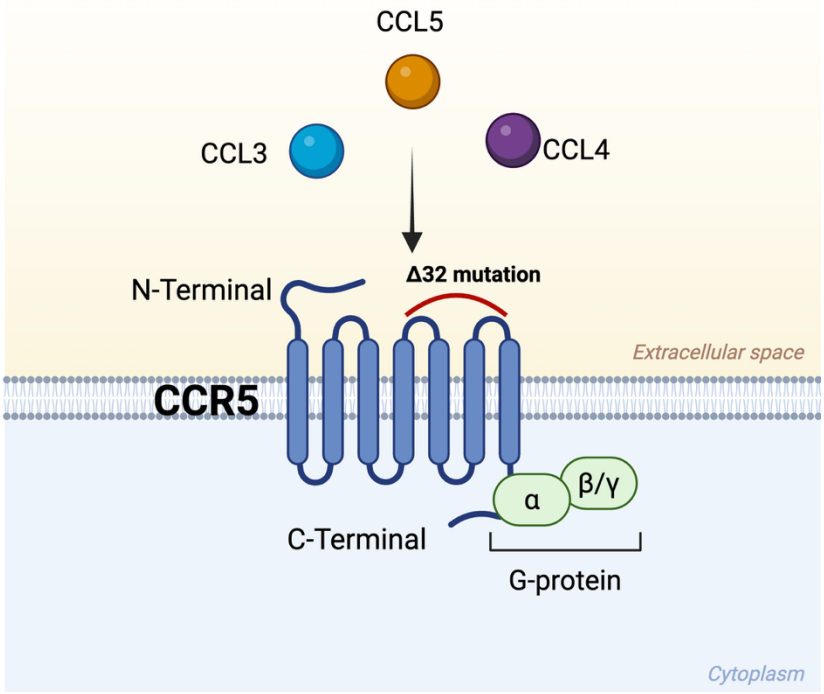

Figure 1.8: CCR5 structure and ligands. Structure of the 7-transmembrane CCR5 receptor. Red line indicates predicted region affected by the delta32 mutation. Adapted from (Hemmatazad and Berger, 2021). Made using BioRender.

1.6.2 The role of CCR5 in immune-mediated inflammatory diseases.

CCR5 has been extensively studied in the context of human immunodeficiency virus (HIV) infection, where it functions as a co-receptor with CD4 to facilitate viral binding, entry, and replication within macrophages (An *et al.*, 2011). A naturally occurring 32 base pair deletion in the CCR5 gene, known as the Δ32 mutation, results in the absence of CCR5 expression on the cell surface. Individuals heterozygous for this mutation exhibit reduced susceptibility to HIV infection, while homozygous individuals are highly protected against infection (Galvani and Novembre, 2005). Beyond its role in viral disease, CCR5 has been implicated in a range of autoimmune and vascular pathologies. In atherosclerosis, CCR5 knockout mice show reduced macrophage infiltration and plaque development during both early and late stages of disease, and the Δ32 mutation appears similarly protective in humans (Tacke *et al.*, 2007; Maguire *et al.*, 2014). CCR5 has also been linked to rheumatoid arthritis, particularly in the regulation of osteoclast formation and function, where pharmacological

inhibition of CCR5 reduces osteoclast migration and bone resorption capacity (Oba *et al.*, 2005; Lee *et al.*, 2017). Together, these findings highlight CCR5 as a central mediator of immune cell trafficking and inflammation across diverse disease contexts.

1.6.3 Inhibitors of CCR5 signalling.

Numerous CCR5 inhibitors have been developed for the treatment of HIV and are now being investigated in a variety of inflammatory and malignant conditions. Maraviroc, a small-molecule inhibitor of CCR5 (Figure 1.10), acts by inducing allosteric changes in the receptor that prevent ligand binding and downstream signalling (Dorr *et al.*, 2005). Importantly, it does not bind directly to the ligand-binding site, distinguishing it from competitive antagonists (Carter and Keating, 2007). In contrast, Leronlimab is a monoclonal antibody that binds CCR5 directly, blocking ligand engagement and subsequent signalling (Rusconi *et al.*, 2022). While both drugs were initially developed for HIV therapy, Leronlimab is also under investigation for its potential in metastatic cancers and COVID-19 (Agresti *et al.*, 2021), highlighting the broader therapeutic relevance of CCR5 inhibition beyond viral infection.

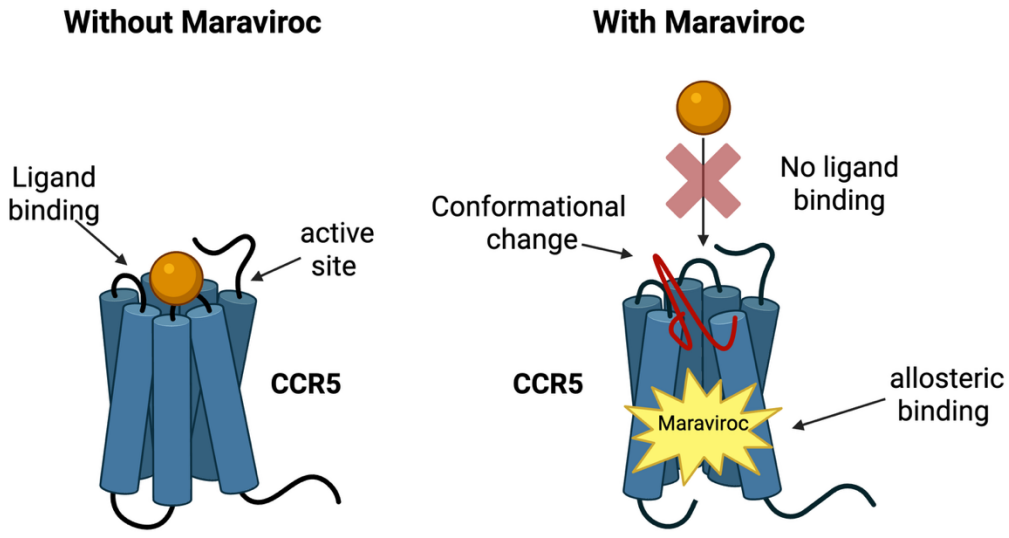

Figure 1.9: Proposed Mechanism of Maraviroc action.Schematic of maraviroc action leading to CCR5 signalling inhibition. Adapted from (Olga St. Latinovic et al., 2009). Made in BioRender.

1.7 Unmet need in GCA research.

Despite significant advances in our understanding of GCA, several key knowledge gaps remain. A major limitation is the absence of a reliable experimental model

to study the initiating events of the disease, which restricts our ability to dissect early pathogenic mechanisms. In particular, the biology of MGCs such as, their formation, function, and cellular precursors, remains poorly understood. It is also unclear whether MGCs themselves represent viable therapeutic targets. Addressing these gaps will require deeper insight into the fundamental immunology of GCA, which may ultimately reveal strategies to modulate or prevent MGC formation and open new avenues for treatment.

1.8 Hypothesis and aims.

The current mainstay treatment for giant cell arteritis (GCA) is high doses of corticosteroids which cause many side effects which reduce the patient's quality of life. The innate immune response in GCA is evidently key in the pathogenesis of this disease, in particular, monocytes, macrophages and multinucleated giant cells (MGCs). Despite being the namesake of this disease, not much is known about the formation and function of the latter in GCA. It can, therefore, be hypothesised that understanding the formation and function of these cells may lead to the identification of potential treatment targets.

MGCs are derived from the fusion or incomplete division of monocytic precursor cells. However, few studies have sought to elucidate the differences in the circulating monocyte population of GCA patients versus monocytes from 'healthy' controls over 50. It can be hypothesised that, circulating monocytes from GCA patients are markedly different from circulating monocytes of those over 50 without GCA.

Additionally, very little is known about the role that these cells play in the pathogenesis of GCA. Transcriptomic techniques such as GeoMx spatial profiling could help to elucidate the genetic expression profile of macrophages and MGCs in distinct areas of the affected vessel.

Furthermore, there are currently limited models of GCA that can be used to study the initiating events of the disease such as, the *ex vivo* temporal artery biopsy (TAB) culture model (Corbera-Bellalta M. et.al. 2014). This model uses TABs from patients with GCA. These patients already have established disease and MGC presence meaning the formation of these cells cannot be investigated. Therefore, it was hypothesised that an *in vitro* model of MGC formation, that mimic those found in GCA, could be developed by circulating monocytes from GCA patients with numerous chemokines thought to involved in disease progression.

Finally, chemokines and chemokine receptors have rarely been investigated in the formation of multinucleated giant cells in GCA, despite multiple studies of osteoclastogenesis, which suggest that the chemokine CCR5 may play a role in

the formation of these cells. Therefore, it can be hypothesised that CCR5 may play a role in the formation of MGCs in GCA and that using available CCR5 antagonists in culture, will reduce the number of MGCs formed *in vitro*.

Therefore, the work of this thesis aimed to test these hypotheses by addressing the following key aims and objectives:

Understand the formation and function of MGCs in GCA through spatial transcriptomics.
Investigate monocyte pre-cursors of MGCs.
Develop an in vitro model of MGCs for further investigation into their formation and potential modulators.

Chapter 2 Methods and materials.

2.1 Patient and control samples.

This study incorporated several cohorts to examine the molecular and immunological features of GCA across diverse biological contexts. Peripheral blood, TAB tissue samples, and genetic data were collected from different sources to provide a comprehensive view of the disease.

2.1.1 GCA and control peripheral blood.

Peripheral blood from patients with Giant Cell Arteritis (GCA) was collected from the NHS Greater Glasgow and Clyde Vasculitis service, from both Gartnavel General Hospital and The Royal Infirmary, under the ethical approval: 'NHS GG&C additional biopsies, blood, urine and/ or stool samples' application (19/WS/0111). GCA was classified using updated ACR/EULAR criteria (Ponte *et al.*, 2022). Both active and remission cases were included. Cranial-GCA was defined by clinical features and a histologically positive biopsy.
Healthy controls, over 50 years of age, were recruited from Glasgow University staff by poster advertisement. It was ensured that controls had no rheumatic disorders. From preliminary *in vitro* studies, leukocyte reduction cones (LDRs) were used for PBMC isolation. LDRs were obtained from the National Health Service Blood Transfusion (NHSBT) service in Newcastle.
Informed consent was given from all participants by clinicians during appointments, and blood was taken under the appropriate ethical approval. All donor information was anonymised after collection.

2.1.2 GCA tissue

Temporal artery biopsies are taken as part of the diagnostic process for GCA. Excess tissue is stored by the NHS Research GGC Biorepository where they were section and formalin fixed, and paraffin embedded (FFPE). These tissue sections were selected for immunofluorescence staining based on the presence of multinucleated giant cells, seen in histological staining (biorepository application number: 852).

2.1.3 **TARDIS study.**

Target Identification for Drug Discovery in Giant Cell Arteritis (TARDIS) is an ongoing clinical study under the IRAS ID 312996. Patients suspected of GCA, after informed consent, undergo routine temporal artery biopsy (TAB) for diagnostic purposes. Excess tissue and peripheral blood are brought to the lab for processing. Samples are taken again at 6 months after initial biopsy or when relapse of disease occurs. The cohort includes, GCA+ve patients and controls, which were deemed to be GCA-ve after investigation. PBMCs were isolated from peripheral blood samples using standard operating procedures (SOPs). Sample processing was carried out by trained clinical trial technicians for PBMCs were either analysed immediately by flow cytometry or cryopreserved in Bam Banker (NIPPON Genetis) for later experiments. The candidate contributed to processing on an ad hoc basis, depending on availability and timing of patient recruitment at the point of clinical presentation.

2.1.4 **UKBiobank.**

The UK Biobank is a large-scale biomedical database established to improve understanding of the determinants of human health and disease. It contains data from over 500,000 participants aged 40–69 years at recruitment, collected from 22 centres across the UK between 2006 and 2010. At baseline, participants provided detailed lifestyle and health questionnaires, physical measurements, and biological samples. These data are complemented by genetic analyses and longitudinal follow-up through linkage to medical and health records, enabling comprehensive investigation of disease risk and progression.

For this thesis, genetic, medical and phenotypic data were accessed under project ID 71392, *"Investigating complex relationships between genetics, exposures, biomarkers, endophenotypes and cardiometabolic, inflammatory, immune and brain-related health outcomes."* The UK Biobank provides a unique resource for investigating genetic and immunological contributions to disease within a large cohort.

2.2 Human cell isolation.

Peripheral blood mononuclear cells (PBMCs) were isolated from GCA and control blood for Flow Cytometric analysis. Furthermore, to enable downstream molecular and functional analyses, monocytes were purified from PBMCs, using magnetic cell separation. These cells were then prepared for transcriptomic and epigenetic assays, providing material for the characterisation of both gene expression patterns and chromatin states in health and disease.

2.2.1 PBMC isolation

Whole blood (~40ml) was collected in EDTA vacutainers tubes (BD Vacutainer) and diluted 1:1(1:3 for leukocyte cones) in room temperature DPBS. 40ml of diluted blood was added to a SepMate tube (STEMCELL Technologies) that contained 15ml of Ficoll-Paque PLUS density gradient media (Sigma-Aldritch) in the bottom section. It was then centrifuged at 1200g for 10 minutes at room temperature, with the break applied. The resulting PBMC layer was removed by a pasture pipette.

The PBMC fraction was then washed twice in DPBS (without Ca2+ and Mg2+; Gibco.), initially at 400g for 10 minutes then at 400g for 5 minutes, before being counted using trypan blue and a haemocytometer under a brightfield microscope. To count, DPBS was mixed with 10uL of trypan and 10uL of cell suspension to give a final dilution of 1:10. 10uL of this dilution was added to the haemocytometer and observed under a brightfield microscope.

Total cell number was calculated by the average number of cells in two squares multiplied by the magnification (10,000) and the dilution factor (10) and, finally, by the volume at which the cells were resuspended in.

Counted cells were then either resuspended at $1x10^6$ cells/mL in DPBS for flow cytometry, or at $5x10^7$ cell/mL in cell separation buffer (CSB, see Appendix) for monocyte isolation.

2.2.2 Monocyte purification.

Monocytes were isolated from PBMCs using EasySep™ kits (STEMCELL Technologies) based on magnetic selection, following manufacturer's

instructions. Specifically, $CD14^{++}CD16^{-}$ (classical), $CD14^{+}CD16^{+}$ (intermediate) and $CD14^{low}CD16^{++}$ (non-classical) monocytes were enriched from human PBMCs using the EasySep™ Human Monocyte Enrichment Kit without CD16 depletion (Cat: # 19058). Monocyte purity was assessed by flow cytometry after magnetic cell sorting and was shown to be 81, 10.7 and 6.8% for Classical, intermediate and non-classical monocytes respectively. Otherwise, total $CD14^{+}$ monocytes were negatively selected using the Human monocyte enrichment kit (Cat: # 19059RF). Briefly, PBMCs were resuspended to give a concentration of $5x10^{7}$ cells/mL in CSB (see Appendix) and added to a 5 mL polystyrene round-bottom tube (Corning). 50µL per mL of the antibody cocktail was added to the cells and left to incubate on ice for 10 minutes. Isolation beads were then added at 50µL/mL and incubated again on ice for 5 minutes. The FACS tube was then added to the EasySep™ magnet and incubated for 2.5 minutes at room temperature. After the incubation, the cell fraction was poured into a 15mL falcon tube (Fisher Scientific). Isolated monocytes were counted in the same way as PBMCS. Cells were washed and resuspended to 1x10^7 cells/mL in complete αMEM media (see Appendix).

2.2.3 **Preparation of monocytes for RNA seq.**

Frozen PBMCs from the TARDIS cohort were removed from storage at -150C˚ on dry ice. Vials were thawed slowly in a water bath at 37 C˚ until the sample was almost fully thawed. 1ml of the sample was slowly added to a 15ml Falcon tube containing 1ml of warmed media. The vial was washed with 1mL warmed media and added to the Falcon tube. The volume was made up to 10mL. PBMCs were counted by haemocytometer before being centrifuged at 600xg for 5 minutes. Cell viability was assessed by trypan blue staining (Gibco). Cells were resuspended to $5x10^{7}$ cells/mL for monocyte isolation, using the EasySep™ Human Monocyte Enrichment kit without CD16 depletion (STEMCELL Technologies).

Monocytes were counted, as previously described, and resuspended to $1x10^{6}$ cells/mL. $1x10^{5}$ monocytes were added to a 1.5mL RNase-free Eppendorf tube (Fisher Scientific) and centrifuged for 5 minutes at 600xg. All supernatant was removed ensuring the pellet was completely dry. 350µL of RLT lysis buffer (QIAGEN) +1% b-mercaptoethanol (Sigma Aldrich) was added and the sample,

which was vortexed until no cell pellet was visible. Lysed cells were stored at -80°C until RNA extraction using a RNAeasy micro-kit (QIAGEN). Following the manufacturer's instruction. Briefly, lysed cells were defrosted on ice and 350µL of 70% ethanol (Merk) was added and mixed by pipetting. Samples were then added to RNA elute columns and spun for 15 seconds at 8000xg. Flowthrough was discarded, 50µl of buffer RW1 was added to the column and spun at 8000xg, flow-through was discarded. 80µl of DNase I (diluted in buffer RDD) was added directly to the centre of the spin column. Spin columns were incubated at room temperature for 15 minutes before a further 350µL of buffer RW1 was added and columns spun at 8000xg for 15seconds. The flow-through was discarded. The column was then washed with 500µL buffer RPE and centrifuged at 8000xg for 15 seconds. This was followed by a wash with 500µL of 80% ethanol. Spin columns were centrifuged for 2 minutes at 8000xg, both the flow-through and collection tube were discarded. The lid of the spin column was opened, and columns centrifuged for 5 minutes at full speed to dry the column membrane. Lastly, the spin column was added to a new 1.5mL collection tube. 14µL of RNase-free water was added directly to the spin column membrane. Columns were centrifuged at full speed for minute to elute RNA. RNA was quantified using a Nanodrop Spectrophotometer. RNA was stored at -80°C until shipping for downstream library preparation and sequencing by Novogene Europe.

After RNA extraction, RNA was shipped to Novogene Europe for library preparation, sequencing and data quality control. Libraries were prepared by PolyA enrichment for Illumina sequencing. The mRNA was then sequenced using the Illumina NovaSeq X Plus Series (PE150).

2.2.4 **Monocyte preparation for epigenetic analysis.**

To assess the epigenetic landscape of circulating monocytes, the Cleavage Under Targets and Tagmentation (CUT&Tag) technology (Active Motif) was used. Samples from the TARDIS cohort, 6 controls and 6 GCA positive, were processed. Monocytes were prepared using the CUT&Tag-IT™ Assay Kit (Active Motif), according to the kit's protocol. On the first day, $8x10^6$ monocytes were separated into 4x 2mL low-bind micro-centrifuge tubes. Cells were centrifuged for 3 minutes at 600xg at room temperature. Cells were then resuspended in 1ml

of Wash Buffer and then centrifuged for a further 3 minutes at 600xg. The supernatant was removed and 1.5ml of wash buffer was added and the pellet resuspended. Cells were kept on ice until Concanavalin A beads were prepared. 20µL per sample of beads were mixed with 1.6 ml of 1x binding buffer in 4x 2ml low-bind microcentrifuge tubes and placed on a magnetic stand until clear (~2 minutes). Liquid was completely removed, making sure not to remove any beads. Beads were washed again with 1.5ml binding buffer and placed back on the magnetic stand to clear. Finally, beads were resuspended in 20µl of binding buffer for each sample. This bead slurry was slowly added to the tubes containing the cells. Tubes were placed on an end over end rotator for ten minutes to mix.

Primary antibodies for H3K4Me3 and H3K27Me3 (all diluted 1:50) were rabbit antibodies from Active Motif and were all suitable for CUT&Tag. Antibody buffer was prepared by adding 10µl of both protease inhibitor cocktail (PIC) and 5% digitonin were added for every 1mL and kept on ice. Cell tubes were added to the magnetic stand for 2 minutes to clear, supernatant was removed, and tubes were removed from the stand. Cells were resuspended in 49µL of antibody buffer and 1µL of the appropriate primary antibody. Cells were incubated overnight at 4°C in an orbital mixer.

The next day, Dig-wash buffer was prepared by adding 10µL of PIC and digitonin per mL and kept on ice. Cell tubes were placed on the magnetic stand for 2 minutes to clear and supernatant removed with a pipette. Guinea pig anti-rabbit secondary antibody was diluted 1:100 in dig-wash buffer. 100µL of diluted antibody was added to each sample. Tubes were placed in an orbital rotator at room temperature for 1 hour. Tubes were put back on the magnetic stand to clear and supernatant was removed. Cells were washed 3 times with 900µL of dig-wash buffer. Next, dig-300 buffer was prepared by adding 10µL of PIC and 2µL of digitonin per ml and placed on ice. CUT&Tag-IT™ Assembled pA-Tn5 Transposomes were diluted 1:100 in dig-300 buffer; 99µL of the transposome solution was added to the cells. Cells were incubated at room temperature on an orbital rotator for a further 1 hour. After cells were cleared on the magnetic stand for 2 minutes and the supernatant removed, they were washed 3 times with 1mL of dig-300 buffer. Cells were tagmented with 125µL of tagmentation buffer (prepared by adding 10µL of PIC and 2µL of digitonin) and incubated at 37°C for 60 minutes. Later, tagmentation was stopped and DNA fragments were

solubilised by adding 4.2 µL 0.5 M EDTA; 1.25 µL 10% SDS; 1.1 µL Proteinase K (10 µg/µL) to each sample and incubated at 55°C for 60 minutes.
To elute tagmented DNA, tubes were placed on a magnetic stand, and the supernatant was added to a new 1.5mL centrifuge tube. 625µL of DNA purification buffer was added to each sample and then transferred to a DNA purification column. Columns were centrifuged at 17000xg for 1 minute. The flow-through was discarded. Next, 750mL of DNA purification wash buffer (containing 40mL of ethanol) was added to the column, before another 1-minute spin at 17000xg. The flow-through was discarded and the empty column was centrifuged for a further 2 minutes to dry the membrane. Finally, 35µL of DNA purification elution buffer was added directly to the column membrane and incubated at room temperature for 1 minute. Columns were centrifuged at full speed for 1 minute to elute the DNA. Purified DNA was stored at -20°C until the library preparation.

2.2.4.1 Library Preparation.

DNA fragments extracted previously were amplified by PCR for library preparation. 30uL of tagmented DNA was added to a PCR master-mix containing 1uL of 10mM dNTPs, 10uL of 5x Q5 reaction buffer, 3.5uL nuclease free water and 0.5uL of Q5 polymerase per sample (Active Motif kit). Next, 2.5uL of one i7 index primer and 2.5uL of one i5 indexed primer were added to make a unique primer combination to identify each sample. DNA fragments were amplified by thermal cycler at 72°C for 5 minutes, 98°C for 30 seconds, 14 cycles of 98°C for 10 seconds, 63°C for 10 seconds and finally, 72°C for 1 minute. This was followed by an SPRI bead clean-up to ensure the DNA was clean and free of contaminants. A total of 48 samples were pooled for sequencing. As there were only 16 unique primer combinations, a total of 3 pools were sent to Novogene Europe for QC and sequencing. Libraries were sequenced using the NovaSeq X Plus Series (PE150).

2.3 Flow cytometry.

Flow cytometry was performed on PBMCs from both GCA and control blood samples to characterise monocyte populations in the context of disease. In

addition, flow cytometry data generated from blood samples collected in the TARDIS study were re-analysed as part of this thesis.

2.3.1 **Isolated PBMCs.**

Isolated PBMCs, from control and GCA peripheral blood, were resuspended in DPBS to 1x10^6 cells/mL. Approximately, 2.5x10^5 cells were kept as an unstained control, while all other samples were stained with 1µL eBioscience™ Fixable Viability Dye (Invitrogen), Live/dead stain. Cells were incubated in the tissue culture hood for 30 minutes in the dark. Samples were topped up with 1mL of FACS buffer (see Appendix) and centrifuges at 400xg for 5 minutes to wash. Next, cells were stained with the test antibody mix and 1µL of Fc block (antibodies and their concentrations listed in Table 2.1). One sample was fully stained while fluorescence minus-one (FMO) controls were set up for; CCR5, CCR2, CD116, CD115, CX3CR1 and CXCR2. After which, cells were incubated in the dark for a further 30 minutes before another wash in FACS buffer. Finally, 25µl of BD fixation buffer was added to samples and incubated for a further 15 minutes. Cells were washed again and resuspended in 1mL of FACs buffer before being stored at 4c until analysis (no longer than 72hr post staining). Flow cytometry data was collected on a BD Fortessa flow cytometer after compensation set up with UltraComp eBeads™ compensation beads (Invitrogen) single stained with each antibody.

Marker	fluorochrome	Volume for 1 test (uL)	clone
CCR5 (CD195)	BV421	5	J418F1
CD206	BV510	5	15-2
CD16	BV605	5	3G8
CD11c	BV711	1	N418
CD116	FITC	5	4H1
CXCR2	PerCP-eFluor 710	5	E8-C7-F10
lineage - (CD3, CD19, CD56, CD15)	PE	5*	UCHT1,HIB19,HCD56,W6 D3
CD115	PE-Cy7	5	9-4D2-1E4
CD68	PE-eFluor 610	5	Y1/82A
CX3CR1	APC	5	2A9-1
HLA-DR	AF 700	4	L243
live/dead	APC-eFluor 780	1	65-0865-14
CD14	BUV395	5	MϕP9
CD192 (CCR2)	BUV805	5	LS132.1D9

Table 2.1: Table of antibodies used to stain PBMCs for flow cytometry.1 test = volume needed to stain 1x10^6 cells in 100µL of FACs buffer. *In Vitro* Cell Culture.

2.3.2 TARDIS Flow cytometry.

PBMCs from blood samples collected under the TARDIS cohort were primarily processed and analysed by trained clinical trial technicians following standard operating procedures. The candidate contributed to sample handling and processing as needed, depending on availability at the time of recruitment. PBMCs were pelleted by centrifugation at 400xg for 5 minutes then resuspended in 2mL of 1x lysis buffer. Cells were incubated for 2 minutes before being washed at 200xg for 5 minutes. Cells were then resuspended to 1x10^6 cells in 50µL. An unstained control and FMOs were used as controls. 1µL of FC block was also added to cells with the antibody cocktail. Tubes were incubated in the dark for 20 minutes before washing with 2mL of FACS buffer at 400xg for 5 minutes. Cells were resuspended in 300µL of FACS buffer for acquisition. Data was collected using an Attune NxT flow cytometer (Thermofisher Scientific). Data analysis was done in FlowJo software.

Marker	Fluorochrome	Panel volume for 1 test (µl)	Clone
CD3	PE	1	UCHT1
CD56	PE	1	CMSSB
CD15	PE	1	HI98
CD19	PE	1	HIB19
CD14	APC-eFluor 780	1	61D3
CD141	APC	1	JAA17
CD1c	BV711	1	L161
CD16	eFluor 450	2	eBioCB16
HLA DR	PE-Cy7	2	L243
CD97	FITC	2	VIM3b
CCR5	AF700	3	J418F1
CD303a	PerCP.Cy5.5	3	201A
CXCR1	BV605	3	5A12
CCR2	BV510	3	K036C2
CD206	PE-CF594	2	19.2

Table 2.2: Table of antibodies used to stain TARDIS PBMCs for flow cytometry.1 test = volume needed to stain 1x10^6 cells in 100µL of FACs buffer. In Vitro Cell Culture.

2.4 Culture of Multinucleated giant cells.

To develop an in vitro model of MGCs, isolated monocytes from leukocyte cone PBMCs were resuspended at $2x10^6$ cells/mL with warmed α-mem media (see Appendix; Gibco). To induce giant cell formation in vitro, 50mL of suspended monocytes were plated at 1x10^5 cells per well on a 96 well plate (Corning Life Sciences). 100ng/ml of either human recombinant GM-CSF or M-CSF (PeproTech) were added alone or alongside IL-4 (10-80ng/ml), IFNγ (10-80ng/ml) (PeproTech) or both to differentiate macrophages and induce multinucleation. Plates were placed in an incubator at 37°C with 5% CO_2. On day 3, the media was partially changed, 50µL of media was removed and replaced with 50µL of fresh media containing the appropriate cytokine combination. Cells were incubated for a further 4 days before staining.

2.4.1 Addition of chemokines.

Cells were plated with GM-CSF alone, or GM-CSF and IFNγ. In some wells the human recombinant CCL5 (100ng/mL) and/or CCL3 (100ng/mL) (PeproTech) were additionally added on day 0. Cells were incubated, as previously described, with media replaced on day 3, followed by staining and visualisation.

Simultaneously, other cells were plated with only GM-CSF+ IFNγ on day 0. Then, after 3 days of incubation, CCL5 and/or CCL3 were added. Cells were incubated for a further 4 days until stained and visualised.

2.4.2 **Addition of CCR5 inhibitors.**

Cells were plated with GM-CSF+ IFNγ. In some wells, the CCR5 antagonist Maraviroc (Tocris, Biotechne) was added at 1μM and 10μM on day 0. The media was changed and 1 or 10 μM of Maraviroc was added every 3 days to ensure receptor occupancy. Additionally, some wells were treated with the anti-CCR5 antibody Leronlimab (Selleckchem) at the same concentrations (1-100uM). Similarly, the media was partially changed and fresh Leronlimab was added every 3 days. On the final day of incubation, cells were stained and visualised as described below. 0.2% DMSO (Invitrogen) was added to cells as a vehicle control.

2.4.3 **Staining and visualisation.**

2.4.3.1 **Haemacolour staining.**

After 7 days incubation, plates were stained for visualisation using a haemacolour staining kit (Sigma-Aldrich), following manufacturer's instructions. Briefly, media was removed from the plates and 50μL of methanol was added for 5-10 seconds to fix the cells. The methanol was then removed and followed by 50μL of stain 1, then 50μL of stain 2. Finally, plates were washed twice with the buffer solution (pH 7.2). Excess liquid was removed by tapping the plate. Plates were left to dry before visualisation.

Plates were visualised on an EVOS® FL Auto Cell Imaging System (Thermofisher Scientific), at 10x magnification using the automated acquisition feature, which stitched multiple fields of view to reconstruct the entire well. Images were then loaded into the FIJI- ImageJ software for analysis. MGCs were defined as cells with >3 nuclei, and quantification was performed with ImageJ's built-in cell counter plugin. MGCs were counted as either LHGCs or FBGCs based on cell morphology and positioning of nuclei within the cell's cytoplasm.

2.4.3.2 Tartrate-resistant acid phosphatase staining.

TRAP staining was done by removing the media from the plates before fixing cells with fixative solution (Sigma-Aldritch kit; see Appendix) for one minute, at room temperature. The plates were then washed 3 times with dH2O before being tapped dry. Cells were then incubated with TRAP staining solution (Sigma-Aldritch; see Appendix), according to the kit protocol, for 20 minutes at 37°C while protected from light. Cells were washed again 3 times with distilled water before being tapped and left to dry. Plates were visualised and cell numbers analysed, as previously described.

2.4.3.3 Immunofluorescence staining.

Cells were plated, as previously described, on 18 well glass bottom chamber μ-slides (Ibidi). Cells were incubated for 7 days with a half-media change on day 3. After incubation, cells were stained with DAPI, phalloidin-AF488 (Invitrogen), Anti-Osteopontin (SPP1) antibody (Abcam ab8448) CTSD, MMP9, FTH1 and CCR5 (Abcam ab7346). Furthermore, rabbit IgG (Invitrogen) antibody was used as isotype control. Cells were incubated with the primary antibody or isotype control overnight at 4°C, before the secondary antibody and DAPI (Invitrogen) were added. In some wells, only the secondary antibody (anti-rabbit AF467; Invitrogen) was added as a control. Slides were stored with 100μL per well of PBS at 4°C. Cells were imaged using the EVOS microscope and images were analysed using ImageJ. Using the Count and Confirm macro from, the total number of nuclei in 3 randomly selected fields of view (FOV) and the number of nuclei within the cytoplasm of an MGC in the FOV. To calculate the Percentage fusion index, the nuclei within the MGCs were divided by the total number of nuclei multiplied by 100.

2.5 Processing of GCA tissue.

Surplus TAB tissue, obtained from diagnostic procedures, was accessed through the Biobank and the TARDIS study, as previously described (section and 2.1.3). Samples were selected based on the presence of MGCs and used for immunohistochemistry and immunofluorescence staining. Additional TAB specimens were also obtained for spatial transcriptomic analysis.

2.5.1 **Immunohistochemistry.**

Samples were selected for IHC based on the presence of MGCs in H&E staining. TAB tissue from the biorepository was cut to 3µm onto Leica bond slides and backed overnight at 37˚C by the Glasgow Tissue Research Facility. Slides were kept at 4˚C until used. Prior to IHC staining, cells were baked at 60˚C for 1 hour. Slides were then dewaxed and rehydrated by submersion, twice, in Xylene for 5 minutes. This was followed by decreasing concentrations of ethanol (100%-70%) for 5 or 3 minutes. Slides were rinsed in dH2O briefly before being washed in1X TBST (100ml 10x Tris-buffered saline + 900ml dH2O + 500ul of Tween-20 (0.05%)). Simultaneously, dH2O and antigen retrieval buffer (see Appendix) was warmed to 99˚C in a steamer.

After dewaxing, slides were dipped in warmed dH2O and then left in the antigen retrieval buffer for 20 minutes. When the slides were cool, they were transferred to room temperature TBST for 5 minutes. A hydrophobic barrier was drawn around the samples and endogenous peptides were blocked with Bloxall (VectorLabs) for 10 minutes. Slides were then washed 3 times in fresh TBST. A blocking buffer with 5% horse and 10% human serum was added to the slides to block for 30 minutes. Following this, either a rabbit IgG isotype antibody (1:2200), polyclonal rabbit CCL5 (1:200) or polyclonal rabbit CCL3 (1:200), diluted in blocking buffer, were added to the slides and incubated for 1 hour, at room temperature.

After the incubation, slides were washed 3 times in fresh TBST before ImmPRESS® HRP Horse Anti-Rabbit IgG was added to the slides for 30 minutes. Next, 1 drop of DAB chromogen was added to 1mL of DAB dilutant before the solution was added to the slides for 30 seconds, until the desired staining intensity.

Lastly, to counterstain the samples, slides were dipped twice into haematoxylin stain and rinsed. Slides were dehydrated in ethanol and xylene before glass coverslips were mounted with DPX mounting medium. Slides were imaged with a Leica brightfield slide scanner.

2.5.2 **Immunofluorescence staining.**

Slides were dewaxed, rehydrated and antigens were retrieved, as previously described. Background and non-specific staining were blocked with 2.5% goat, 2.5% human and 2.5% horse serum for 30 minutes. Slides were then incubated with either MMP9, FTH1, CTSD (Thermofisher) or CCR5 (Abcam) rabbit primary antibodies for 1 hour, at room temperature. After incubation, slides were incubated with an anti-rabbit secondary antibody conjugated to AF647 (1:400) and incubated for 30 minutes, protected from the light. Next, slides were blocked with blocking serum again before CD68 conjugated to AF594 was incubated for a further 1 hour, protected from the light. Slides were washed a final 3 times before coverslips were mounted with Vectashield with antifade and DAPI (Vector Laboratories) to stain nuclei.
Slides were imaged using the Zeiss Axioimager, a widefield immunofluorescence upright microscope. Images were processed in Fiji for ImageJ.

2.5.3 **Staining for Geomx spatial transcriptomics.**

Geomx spatial transcriptomics allows for bulk RNA sequencing of tissues with spatial resolution. This method uses RNA probes that are labelled with a unique oligonucleotide barcode that are cleaved when exposed to UV, to allow for mapping of the gene to the spatial niche. Regions of interest are selected, based on fluorescent morphology staining, on the Geomx DSP software and UV light is applied to those specific regions to cleave the nucleotides. These barcodes are then collected and processed for downstream analysis.

Tissue sections 6 control and 12 GCA TABs were retrieved from the NHS Research GGC Biorepository. TABs were sliced at 5µm and mounted onto Superfrost Plus slides and baked at 60˚C for 1h by the Glasgow Tissue Research Facility (GTRF) team. Antigen retrieval and In Situ Hybridisation was carried out using the Leica Bond Rx automatic staining system.
Tissue sections were then immune-fluorescently stained for morphology markers of interest. SYTO13 green nucleic acid stain (1:10 Thermofisher), Alexa Fluor 532 CD45 (1:100, clone 2B11 + PD7/26, Novus), Alexa Fluor® 594 CD68 (1:200, clone KP1, Santa Cruz Bio), Alexa Fluor® 647 CD31 (1:200, clone JC/70A, abcam).
Slides were then loaded into the GeoMx DSP instrument.

Tissue sections were analysed with the whole transcriptome atlas on the Nanostring Digital Spatial Profiler. Specific regions of interest (ROI) were defined in the adventitia, media, and intima layers. Within these ROI, CD68 positive cells such as macrophages and MGCs were selected for using the masking function in the Geomx software. MGCs were identified manually based on morphology, including a markedly enlarged cytoplasmic area and the presence of multiple nuclei clustered in close spatial proximity within a single cellular boundary. From CD68+ve cells in each ROI, indexing oligonucleotides were collected and processed for library preparation and NGS sequencing.

2.6 Bioinformatic analysis.

2.6.1 Bulk RNA-Seq.

Raw data files were downloaded from the customer service system. Data was aligned to the human genome reference GRCh38.p13 (Ensemble) using the Spliced Transcripts Alignment to a Reference software (STAR) version 3 (Dobin *et al.*, 2013). Next read counts were normalised, and differential gene expression was analysed using the R package DeSeq2 (Love, Huber and Anders, 2014). An initial analysis was completed using the online sequencing analysis tool searchlight2 (Cole *et al.*, 2021). For further differential gene analysis and data visualisation, packages such as “ggplot”, “amap” and “tidyverse” were used in R studio (version: 2024.09.0+375).

2.6.2 CUT&Tag histone modification profiling.

The reads returned from Novogene were aligned to the human reference genome GRCh38.p13 using the default settings of Bowtie2 (V2.4.1(Langmead and Salzberg, 2012)). Enriched regions in each individual sample were then identified by calling peaks with the software GoPeaks (Yashar *et al.*, 2022). The default settings were used for all histone modifications except from H3K27ac which was called using the “--broad” function. Next, to allow comparison of histone modifications in control versus GCA samples, peaks were merged into consensus peaks. Peaks were annotated to human genes using HOMER (v5.1, http://homer.ucsd.edu/homer/).

Deseq2 was then used to normalise the count data and identify differentially expressed modifications. Data was then analysed and visualised as previously described.

2.6.3 **Geomx spatial transcriptomics.**

FASTQ files were processed using the GeoMx NGS pipeline and normalised by Sam McCallister, a bioinformatician in the lab group. Differential gene expression was analysed using Deseq2 in RStudio. Cell deconvolution was performed using CibersortX (Newman *et al.*, 2015a) and the LM22 dataset (leukocyte gene signature matrix to distinguish 22 immune subsets). Graphs and analysis were generated using R studio and previously described R packages.

2.7 **UKBiobank analysis of SNPs.**

The delta-32 mutation SNPs were extracted from the UKBiobank by Rona Strawbridge using the rsIDs rs113010081 and rs62625034. These IDs were used as proxy mutations as the delta-32 mutation is not available in the UKBiobank. All non-European ancestry was excluded from the data set. Cohorts were built in the UKBiobank DNAnexus software. The control cohort of 446,773 individuals included all participants over 50 at the time of baseline visit, and those who did NOT have any diagnosis of the ICD10 codes M31.5 (GCA with PMA) M31.6 (other GCA). Conversely, the GCA cohort of 1,285 participants was defined as participants over 50 years of age, at baseline, who did have diagnosis of M31.5 and M31.6. Other data extracted from the DNAnexus platform included age, sex and principal gametic components for each individual.

2.7.1 **Analysis**

The Cohorts and associated phenotypic data was extracted to CSV files using the table exporter tool within the DNAnexus platform. Cohort and SNP data were loaded into RStudio for analysis. An additive genetic model was assumed for analysis and, therefore, alleles were assigned a dummy variant based on whether 1 or 2 minor alleles were altered (i.e. a change in 1 minor allele was assigned the numeric value 1 and 2 minor alleles were assigned the numeric value 0. A generalised linear regression model was used to analyse the effect of the SNPs on disease outcome. The ‘glm’ function on R was used to fit the model.

Covariates such as age, sex and principal genetic components were adjusted for in the model. A p-value of <0.05 was determined to be statistically significant.

2.8 Statistical analysis.

For data visualisation and statistical analysis of all non-bioinformatic experiments, GraphPad Prism (version 10) was used. To analyse the normality of data, a Shapiro-wilk test was used. If data was normally distributed, t-tests or one/two-way ANOVA tests (with multiple comparisons) were used. If the data was deemed non-normally distributed Mann-Whitney or Kruskal-Wallis tests (with multiple comparisons) were used. A p-value of <0.05 was considered statistically significant.

Chapter 3 Using Spatial Transcriptomics to understand MGCs in GCA.

3.1 Introduction.

The immunopathogenesis of GCA involves cells of both the innate and adaptive arms of the immune system (Akiyama, Ohtsuki, Gerald J Berry, *et al.*, 2021). However, the myeloid compartment, particularly macrophages, are key players involved in the initiation and progression of the disease (van Sleen *et al.*, 2019). Macrophages exhibit high plasticity and these cells can differentiate in response to the microenvironment in which they reside (Shapouri-Moghaddam *et al.*, 2018b). Arteries have a conserved structure of three distinct layers consisting of, the adventitia, media and intima and studies have suggested that different subsets of macrophages exist in GCA tissue based on their positioning within these three layers (Jiemy *et al.*, 2020).

Macrophages that accumulate in the adventitia contribute to the initiation and propagation of both arterial wall and systemic inflammation by producing cytokines such as IL-6, IL-1, and TNF (Ly *et al.*, 2010). Those located at the adventitia/media border release cytokines and matrix metalloproteases (MMPs) which cause degradation of the media and disruption of the elastic lamina (van Sleen *et al.*, 2021). Whereas, macrophages in the intima, are implicated in aberrant tissue remodelling mechanisms, promoting smooth muscle cell proliferation and extracellular matrix deposition, which can result in subsequent occlusion of the lumen due to intimal hyperplasia (Esen *et al.*, 2021).

Macrophages can also fuse to become MGCs. These cells are large polykaryons with anywhere between 3-300 nuclei within one cytoplasm (van Sleen *et al.*, 2019). MGCs are a hallmark of GCA and are found in 50-60% of histologically confirmed GCA TABs. Despite this, little is known about the formation and function of these cells in the disease. MGCs have been shown in histopathological studies to be mainly centred around the intima/ media border and along the internal elastic lamina (Rittner *et al.*, 1999). This positioning suggests they play a role in both the medial destruction and intimal hyperplasia. Interestingly, greater presence of MGCs in histologically confirmed GCA TABs was

linked to the increased risk of developing ischemic complications such as jaw claudication and permanent vision loss (Muratore *et al.*, 2016). The localisation of these cells and their association with ischemic complications suggest that they may contribute to the pathogenesis of disease, although their exact functional role remains to be fully elucidated.

The current mainstay therapy for GCA is high doses of corticosteroids which are tapered over time. While some patients respond well to this treatment and achieve full remission, around 50% of GCA patients do not respond and will have a relapse of disease (Farina *et al.*, 2023). Studies have shown that macrophage activity in affected vessels persists even after steroid treatment (Esen *et al.*, 2021) , suggesting that these cells may contribute to ongoing vascular inflammation and play a role in disease recurrence.
Furthermore, while treatment with steroids appears to clear MGCs over a period of 6-12 months (Maleszewski *et al.*, 2017), a study of disease flares in patients found that greater presence of MGCs in TABs was significantly linked to an increased risk of disease relapse (Restuccia *et al.*, 2016). It was observed that patients in relapse had higher numbers of these cells present in TABs, at the time of diagnosis, compared to remission cases. These findings indicate that both macrophages and MGCs may contribute to disease persistence in GCA and represent potential targets for future therapeutic strategies.

Previous studies of GCA have described spatially distinct populations of macrophages in different areas of the affected vessel, although these studies have largely relied on histological analyses and in vitro experiments. Consequently, they were hypothesis-driven and limited in their ability to achieve the spatial resolution necessary to provide insight into transcriptional differences and potential functional heterogeneity across vessel regions. Furthermore, it remains unknown whether the microenvironmental context in different arterial layers promotes the formation of MGCs from macrophages. Emerging technologies such as Geomx spatial transcriptomics (Church *et al.*, 2024) allow for high-throughput mapping of gene expression to specific areas of the vessel where these cells reside. Spatial transcriptomics uses cleavable barcodes to tag RNA and map it back to the location. Fluorescent antibodies for morphology markers such as CD68, in the case of macrophages, allows for cell

type specific analysis within a region of interest. As such, this approach offers an unbiased and comprehensive profiling of gene expression across the entire tissue.

Despite the clinical significance of macrophages and MGCs in GCA, their formation and function are not fully understood. Furthermore, it is also unclear whether distinct macrophage subtypes are associated with MGC-rich regions. Therefore, this chapter aims to investigate the transcriptomic landscape of macrophages and MGCs in spatially distinct regions of GCA vessels. This approach can enable the dissection of localised gene expression profiles and pathway enrichments, offering insights into the cellular mechanisms driving tissue remodelling, inflammation, and disease progression.

3.2 Results

3.2.1 Macrophages and MGCs have differences in expression profiles in GCA tissue.

To investigate transcriptional differences between multinucleated giant cells (MGCs) and macrophages, spatial transcriptomics was employed to profile gene expression within histologically defined regions. For this body of work, the staining, in-situ hybridisation and manual selection of regions of interest were carried out by the candidate. Macrophages and MGCs were defined based on cellular morphology and CD68 immunoreactivity, using the masking functionality of the GeoMx platform (Figure 3.1a&b). Differential gene expression analysis was subsequently conducted on these regions using normalised expression data. Data normalisation was performed by bioinformaticians within the laboratory group, after which the candidate carried out downstream analysis and interpretation. Healthy controls could not be used for comparison due to the lack of cellular infiltrates (Figure 3.1c). This analysis showed a total of 17 significantly (P.adj < 0.05) different genes between MGC-rich and macrophage-rich regions, regardless of localisation within the arterial wall. Of these differentially expressed genes, 15 were upregulated in MGCs (Log2Fold > 1), as highlighted in the volcano plot in red (Figure 3.2a) and 2 were downregulated in MGCs (Log2Fold < -1), as highlighted in blue. The top 5 most significantly upregulated genes were ACP5 (aka tartrate resistant acid phosphatase (*TRAP)), RPS6KA2, PLD3, CYP27A1* and *CTSK,* (P < 0.01). Further analysis of the differentially expressed genes showed that the downregulated genes TIMP1 and CCL19 were highly expressed in most macrophage-rich regions (Figure 3.2b) and that gene expression was mostly uniform among MGC-rich regions. However, gene expression varied in macrophage rich regions. Given the limited number of differentially expressed genes between these two groups, a principal component analysis (PCA) was carried out to determine how different these samples were (Figure 3.2c). This PCA analysis, unexpectedly, showed that a group of macrophage-rich regions clustered closely to MGC rich regions, while other macrophage rich regions were very transcriptionally different to the MGC regions. Taken together, these findings suggest that a group of macrophages in the vessel act as a precursor to MGCs.

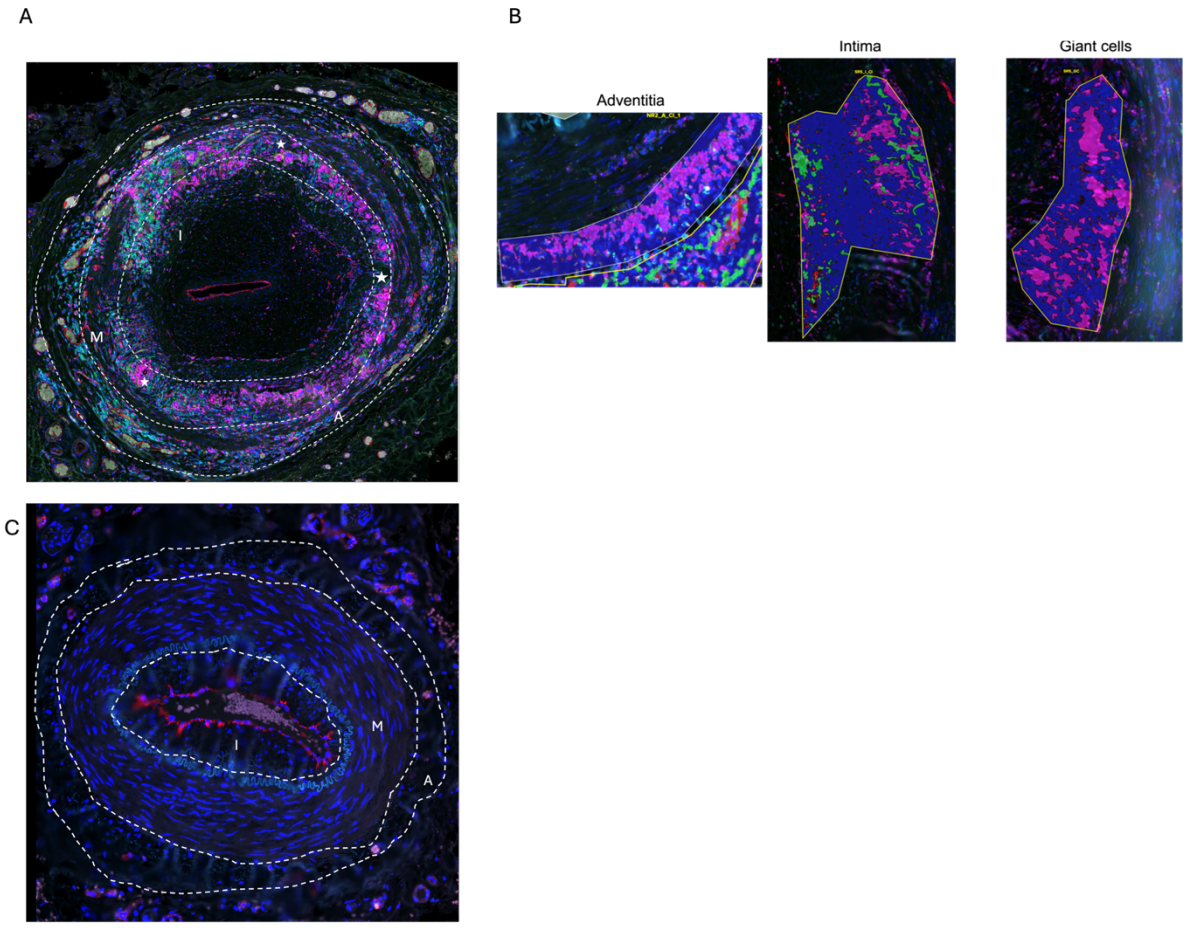

Figure 3.1: representative images of spatial transcriptomic ROI selection.(A) representative image of a GCA vessel stained with morphology markers for spatial transcriptomics. Cyan = CD45, Magenta = CD68, blue = nuclei, red = CD31. Dotted line represents distinct vessel areas adventitia (A), media (M) and intima (I). Stars denote MGCs. (B) representative images of region of interest selection with cell marker based 'masking'. (C) GCA negative control TAB with a lack of cellular infiltrates.

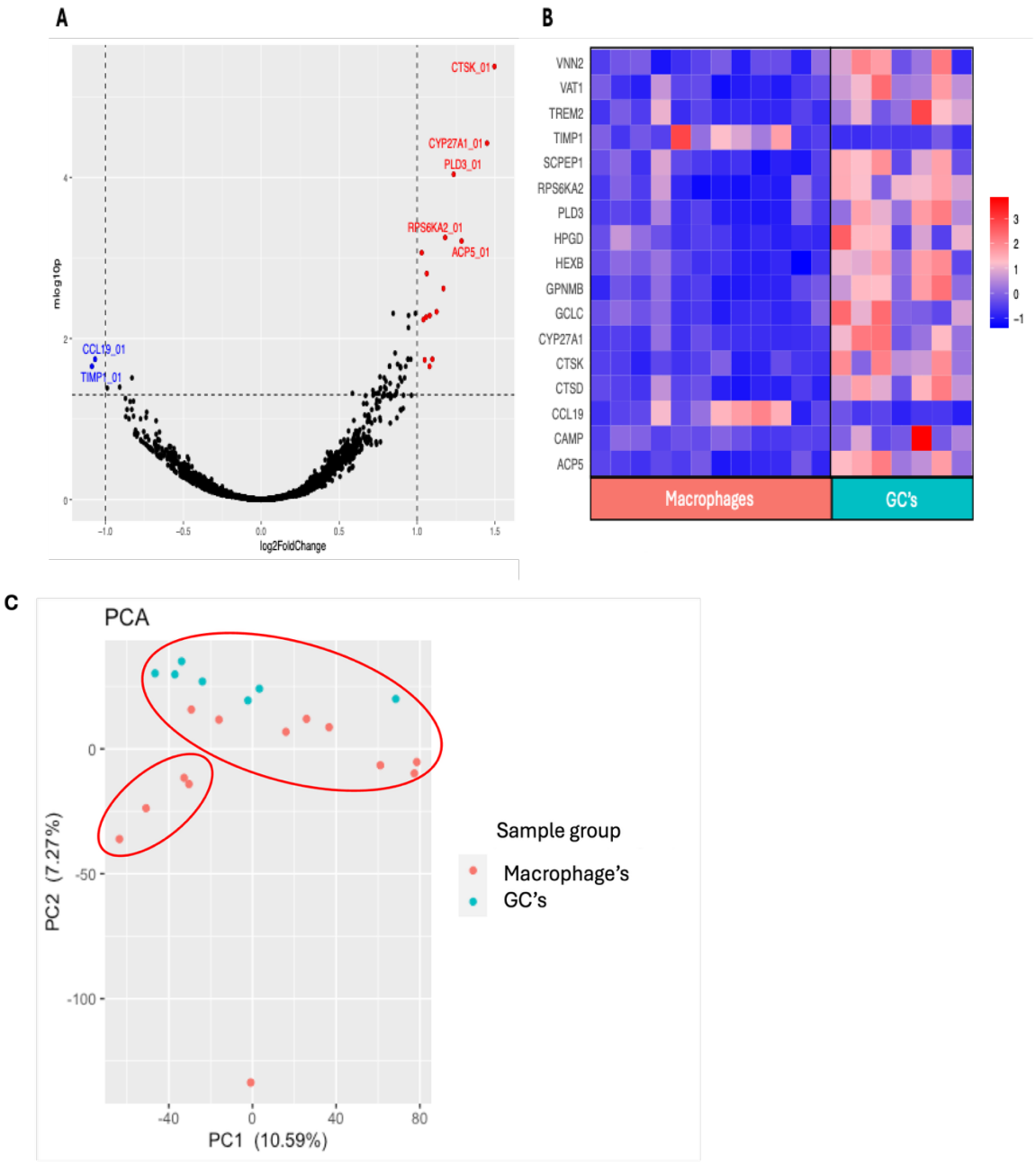

Figure 3.2: Macrophages and Giant cells have differences in transcriptional outputs.

Differentially expressed genes from spatial transcriptomics between macrophage rich regions and MGC rich regions. (A) Volcano plot showing most highly upregulated and downregulated genes. Significantly (P.adj < 0.05) upregulated in red and downregulated in blue (B) Heatmap of differentially expressed genes in macrophages vs MGCs (P.adj < 0.05). (C) Principal component analysis (PCA) scatter plot of PC1 and PC2 for macrophages and giant cells. The percentage of total variation explained by each component is given on its axis. Macrophage regions N= 12, MGC regions = 6.

3.2.2 Intimal macrophages are potential precursors to MGCs.

As previously described, several GCA studies suggest that macrophages in GCA vessels are spatially distinct. These observations, along with the data presented in this figure, led to the question of whether there is a subset of macrophages in specific areas of the vessel that are transcriptionally similar to MGCs and could, therefore, serve as precursors to MGCs. Several studies suggest that macrophage activity varies greatly in different areas of the vessel. Therefore, to examine this, macrophage regions were separated into macrophages localised in the adventitia (A) and the intima (I). Differential gene expression analysis was then re-analysed between these groups. PCA analysis (Figure 3.3a) showed that macrophages which grouped closely to MGC's were mostly from the intima region of the vessel. Whereas, macrophages which were not closely associated with MGC's, mapped to the adventitia. This prompted further investigation into the transcriptional differences between cells in distinct areas in the vessel.

Next, expression patterns of significantly different genes between the three areas were explored. This heatmap showed a clear difference in expression profiles between macrophages in the adventitia and MGCs. However, intimal macrophages had low to medium expression of all significantly different genes associated with macrophages and MGCs. This suggests that intimal macrophages are a transitional macrophage before becoming MGCs. To investigate this further, differentially upregulated genes (Log2Fold > 1) and down regulated genes (Log2Fold < -1) 1were plotted between MGCs and adventitia macrophage as well as MGCs and Intimal macrophages. There were many differentially up regulated genes in MGCs compared to adventitial macrophages such as CHI3L1, FTH1, MMP9 and SPP1. In contrast, only ACP5 was significantly different between MGCs and intimal macrophages when data was adjusted for multiple comparisons (Adj.p-value < 0.05). This further supports the hypothesis that intimal macrophages are in a transitional state to become multinucleated giant cells. To show differences in expression of these genes across the three areas, the top 15 most significantly differential genes were plotted (Figure 3.3d). Expression values were scaled before plotting to allow for visualisation. This figure illustrates that genes highly upregulated in MGC rich regions show low or downregulated expression in adventitial macrophages, while displaying

intermediate expression levels in intimal macrophages. Two genes were upregulated in adventitial macrophages were VCAN and F13A1.

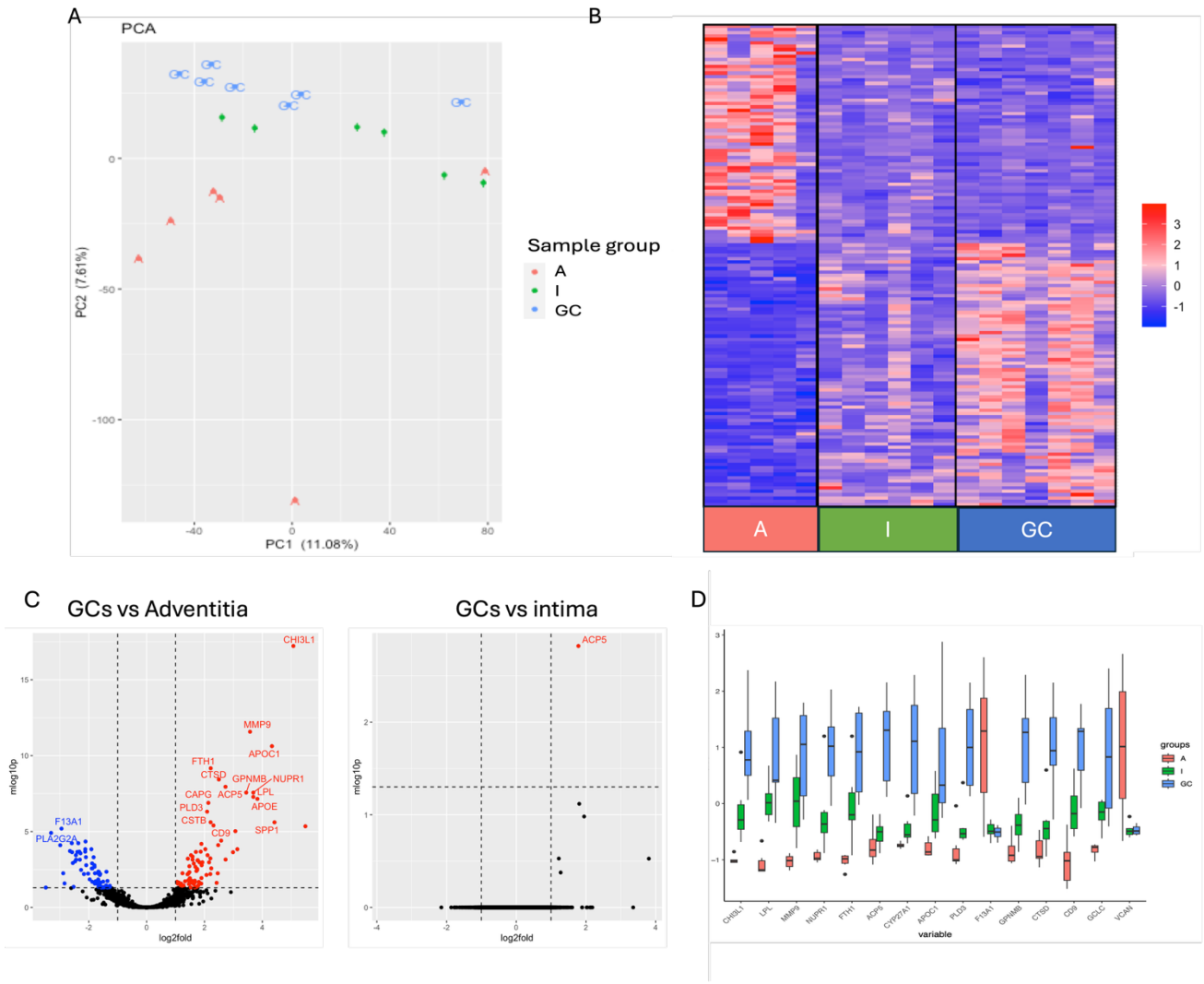

Figure 3.3: Macrophages separate based on area. Spatial transcriptomic analysis of differentially expressed genes of macrophages in the adventitia (A), intima (I) and MGC (GC) rich regions. (A) PCA plot showing adventitial vs intimal macrophages vs MGC rich regions. (B) Heatmap of differentially expressed genes between A, I and GCs (P.adj < 0.05). (C) Volcano plots showing most highly upregulated and downregulated genes. Significantly (P.adj < 0.05) upregulated in red and downregulated in blue (D) Boxplots of the top 15 most significant (P.adj< 0.05) differential genes between the regions. Value is scaled *. Adventitia N = 5, Intima N = 6, GC N = 7.

Differences in gene expression between macrophages in the adventitia, intima and MGCs suggested that intimal macrophages could act as a precursor cell to MGCs or are in a transitional state to becoming MGCs. To further transcriptionally characterise MGCs, and elucidate MGC specific markers, cell deconvolution was carried out on each area. In Geomx spatial profiling, areas of interest are selected based on cell marker expression and masking is used to collect data from specific cells e.g. CD68 positive cells (figure 3.1b). However, this can lead to bleed through from other cells in the selected area, particularly in tissue with high numbers of immune infiltrates where cells are found in close proximity to each other, such as, GCA. Therefore, to ensure this did not explain variations in gene expression, cell-types present (based on their likeness to the LM22 dataset) were plotted (figure 3.4a). This showed that most cells (10- 70%) in each area were of the monocytic or macrophage type (light orange in colour to light purple).

In previous literature, macrophages have been categorised into functionally distinct subtypes. M0 macrophages are described as an undifferentiated and non-active cell, M1 macrophage are described as pro-inflammatory due to their release of pro-inflammatory cytokines such as IL-23 etc. Finally, M2 macrophages are described as anti-inflammatory and wound healing due to their release of IL-4 etc (Isali *et al.*, 2022). Therefore, to better understand the presence and enrichment of macrophage subtypes in each area of interest, the percentage of monocytes, M0, M1 and M2 macrophages were plotted for each area (Figure 3.4b). As expected, the highest percentage of monocytes was found in the adventitia (~ 20%) whereas little to none were observed in the MGC rich regions. Interestingly, the highest percentage (55-60%) of macrophages found in MGC rich areas were the M0 or the ‘undifferentiated’ subtype. Furthermore, the M0 phenotype can also be observed in the intima region to a lesser extent than MGC rich regions but more than the adventitia (5-35%). This supports the hypothesis that intimal macrophages could be a potential precursor to MGCs.

Next, to investigate the M0 phenotype in further detail and to begin to characterise MGCs and distinguish them from their macrophage precursors, M0 related gene expression in each area was assessed using the LM22 data set to identify M0 specific genes in the adventitia and intima macrophages as well as

MGCs. These genes were then plotted on a heat map (Figure 3.5a). This heatmap showed the lack of M0 related gene expression in adventitial macrophages and high expression of these genes in MGC rich areas. Similarly, there was intermediate expression of M0 related genes in intimal macrophages. This data further supports the idea that intimal macrophages could be precursors to MGCs. To ensure that the M0 signature was specific to MGCs and not a product of the intima/media niche, M0 gene expression was assessed in the adventitia, intima and MGC rich regions. This showed the highest expression of 10 out of the 15 topmost expressed genes were expressed most highly in MGCs. Furthermore, expression analysis of selected genes revealed functional enrichment in MGCs. Firstly, FTH1, encoding the ferritin heavy chain and linked to the inhibition of ferroptosis, showed the highest expression in MGCs, compared with other groups. Additionally, CTSD, a cathepsin enzyme with roles in both matrix degradation and fibroblast-driven fibrosis, was also elevated in MGCs. Similarly, CD74, which contributes to MHC class II presentation and fibrosis, was strongly expressed in this group. Lastly, C1QB, a complement pathway component, and MMP9, associated with extracellular matrix degradation and intimal hyperplasia, showed increased expression in MGCs. Notably, expression profiles in the MGC group displayed substantial variability across donors, suggesting transcriptional heterogeneity within this cell population. Although the precise function of MGCs in pathogenesis is not yet defined, their distinct gene expression profile suggests potential functional specialisations.

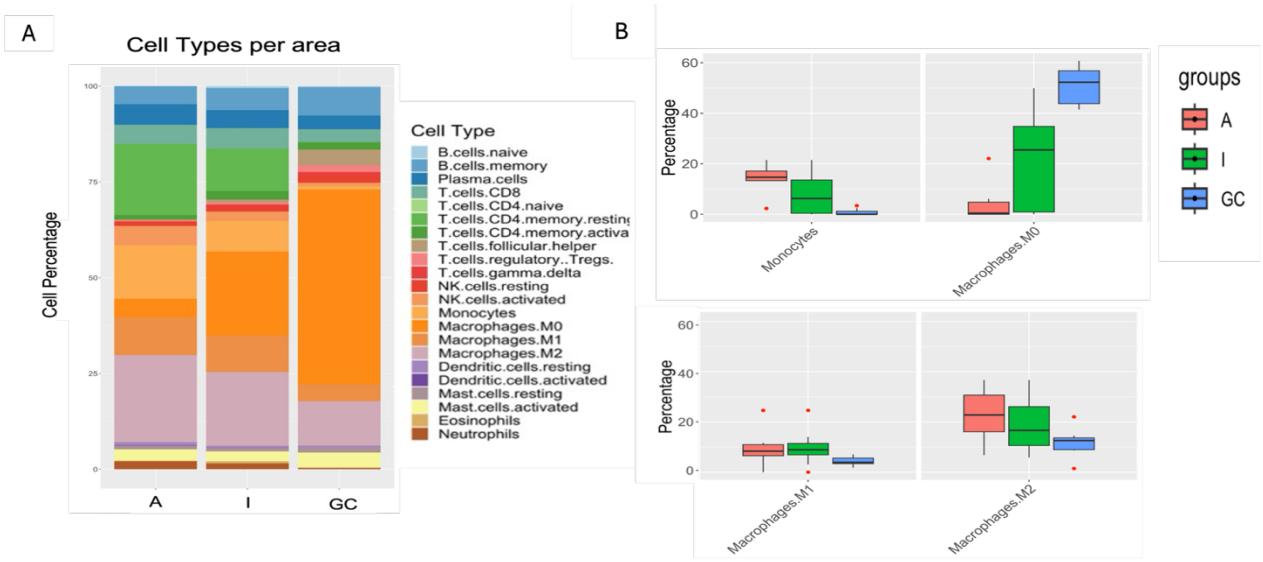

Figure 3.4: MGCs are phenotypically comparable to M0 macrophages. Cell deconvolution analysis of cell types in each region of interest. Based on the LM22 dataset for immune cells using CIBERSORTx. (A) Bar graph showing the percentage of each cell type in the A, I and GC rich regions. Each color represents a cell type and subset. Based on gene expression. (B) Boxplots showing percentage macrophage subset presence in A, I and GC rich regions. (C) Heatmap of most expressed M0 genes in each area (P.adj < 0.05). A = 6, I = 6, GC= 6.

3.2.3 Linking Gene Expression to potential MGC Function.

To begin to elucidate the function of MGCs in GCA, over-representation analysis was conducted using the genes differentially upregulated between macrophages in the adventitia and intima and MGC rich regions. First, the enriched biological processes were analysed (Figure 3.6a). There were 32 significantly enriched pathways (FDR < 0.05) in the gene set. As expected, the most enriched pathway (high gene count and low false discovery rate) was immune response given the nature of macrophages. Interestingly, as well as media destruction related pathways, positive regulation of angiogenesis was upregulated, suggesting a role for MGCs in the neovascularisation seen in GCA tissue. Furthermore, both collagen synthesis and catabolism pathways were upregulated in MGCs suggesting the function of these cells spans both destruction and repair processes. To further unpack the role that these cells play in disease, the molecular function of gene sets was analysed (Figure 3.6b). Integrin binding and fibronectin binding were two of the most enriched pathways and re-enforced the role that MGCs may play in matrix remodelling in GCA. Additionally, several pathways related to atherosclerosis development were upregulated, such as proteoglycan binding and lipoprotein particle binding.

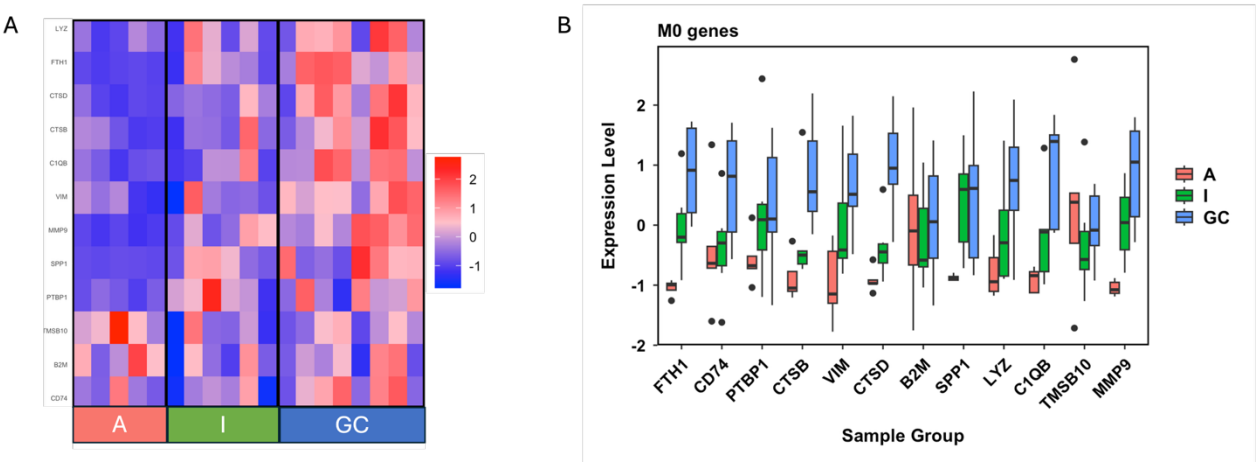

Figure 3.5: M0 signature genes highly expressed in MGCs and intima (A) Heatmap of most expressed M0 genes in each area (P.adj < 0.05). A = 6, I = 6, GC= 6. (B) Boxplots of the top 15 most significant (P.adj< 0.05) differential genes between the regions. Value is scaled *. Adventitia N = 5, Intima N = 6, GC N = 7.

To better understand the involvement of these pathways, the expression of genes associated with these pathways were evaluated (Figure 3.7). Collagen catabolism genes (e.g., *CTSK, CTSB and MMP9*) were most highly expressed in GC-rich regions, whereas collagen biosynthesis genes (*COL1A1, COL5A1* and *SERPINH1*) were elevated in the adventitia, suggesting regional differences in extracellular matrix turnover. Interestingly, genes associated with foam cell differentiation (a macrophage subtype commonly found in atherosclerosis) showed strong upregulation in GCs, including *MSR1* and *LPL*, consistent with lipid uptake and foam cell formation suggesting MGCs in GCA are transcriptionally similar to foam cells. Furthermore, ALOX15B (linked to cholesterol homeostasis in macrophages) was also enriched in GC samples.

Pathways related to cell adhesion showed widespread activity across groups, particularly in MGCs. However, certain genes (ITGA4, THBS1) were particularly upregulated in the adventitia. Similarly, positive regulation of angiogenesis was enriched in MGCs, with genes such as *CHI3L1* and *SERPINE1* showing high expression, supporting a role for MGCs in neovascularization. Finally, genes in the ERK1/2 cascade, including *MARCO, CCL3*, and *CHI3L1*, were significantly upregulated in MGCs, indicating activation of osteoclastogenesis associated signalling pathways in these regions.

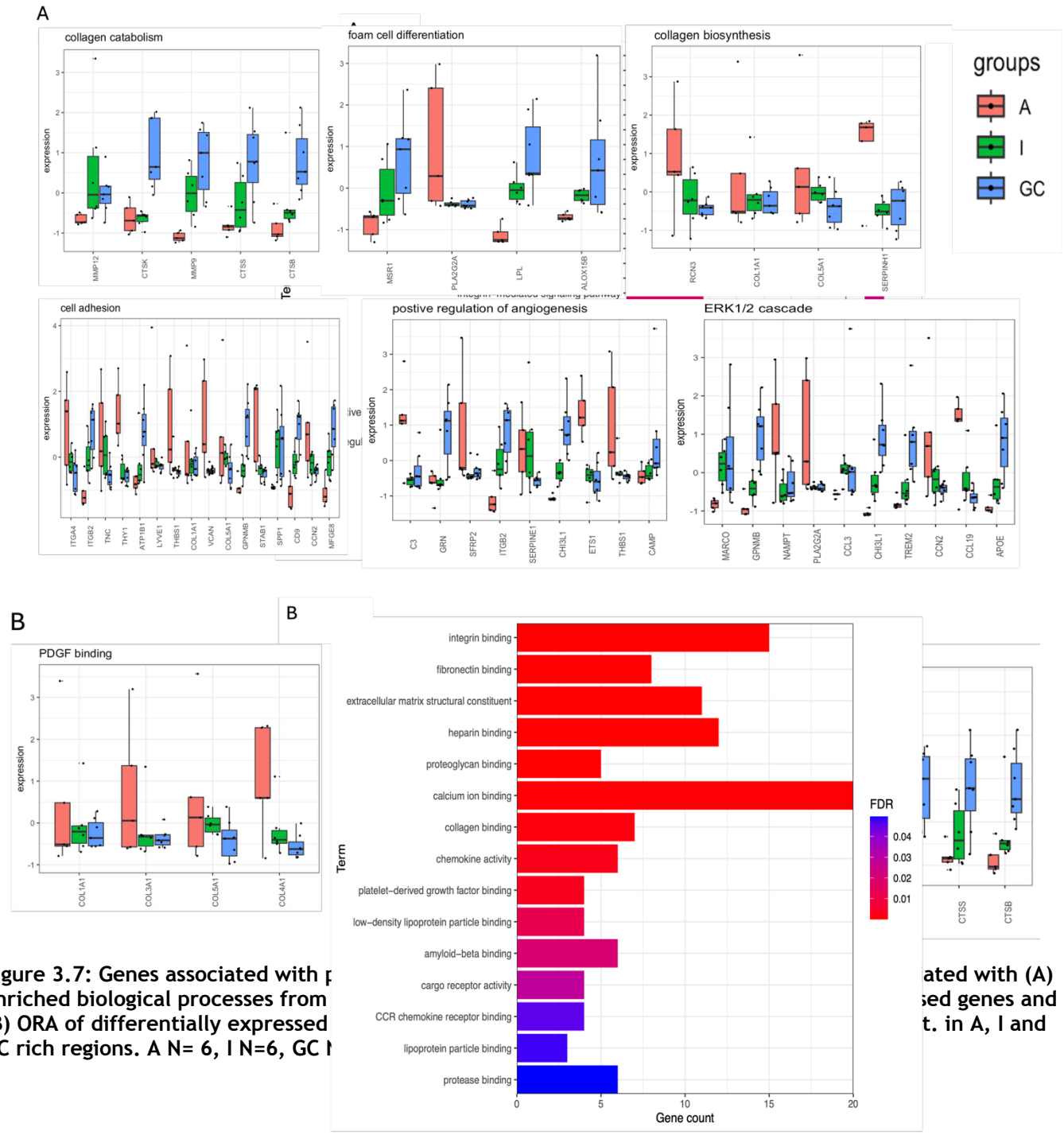

Figure 3.7: Genes associated with p ated with (A) enriched biological processes from sed genes and (B) ORA of differentially expressed t. in A, I and GC rich regions. A N= 6, I N=6, GC

Figure 3.6: Potential function of MGC in GCA. GO pathway analysis was carried out on significantly upregulated genes associated with MGCs. (A) Over representation analysis (ORA) of differentially expressed genes. Biological function. false discovery rate (FDR) < 0.05. (B) ORA of differentially expressed genes showing molecular functions associated with gene list. (FDR P.adj < 0.05). A N= 6. I N=6. GC N=6.

3.2.4 **Protein-Level Validation of MGC Spatial Transcriptomics.**

As spatial transcriptomics is an RNA sequencing technique, it was important to determine protein expression of genes which may be involved in the function of MGCs as mRNA expression does not always correlate to protein expression. Therefore, immunohistochemical and immunofluorescence staining of TAB tissues were performed to validate the transcriptional findings at the protein level.

The selected markers were chosen based on their strong upregulation in MGCs compared to macrophages and their representation of potential functional roles. MMP9 staining was included as it is a well-established mediator of tissue destruction and has been implicated in the initiating events of GCA pathogenesis and MGCs in particular. In contrast, CTSD reflects fibrotic activity driven by fibroblasts, while FTH1, the most highly upregulated M0-associated gene, may indicate a role for ferroptosis in the formation or function of these cells. In addition, ACP5 was included as it was the only differentially expressed gene between pre-MGCs and mature MGCs, making it a useful marker for assessing MGC differentiation in situ. Confirming expression of these factors at the protein level was critical to ensure that they are specifically expressed by MGCs rather than the surrounding microenvironment.

ACP5 was expressed 10 times higher in MGC rich regions than in adventitia macrophages and 3 times more than intimal macrophages and was the only significantly different gene by *adj. p* between intimal macrophages and MGCs. (Figure 3.8a) TRAP positive MGCs have not yet been described in GCA. However, osteoclasts (giant cells of the bone) are known to be TRAP positive and TRAP contributes to the resorption of the bone matrix and collagen turnover (Kular *et al.*, 2012). Therefore, to determine whether TRAP was expressed at the protein level, TAB tissue was stained for TRAP as well as with haematoxylin staining for cell and nuclei visibility. A representative image of stained tissue (Figure 3.8b) showed that TRAP positive MGCs could be seen in GCA tissue. Interestingly, not all MGCs present in the TAB tissue were TRAP positive in the same tissue sample (Figure 3.8b-c). Across four serial sections the number of TRAP positive and negative cells was comparable (ranging from 5 to 8 positive and 7-9 negative MGCs per section). This suggests, not only a potential role for TRAP in the matrix

degradation in GCA but also functional heterogeneity among MGCs in the disease. However, as this analysis was limited to a single donor, further investigation is needed to validate these findings.

Finally, to validate the suggestion that MGCs are phenotypically comparable with M0 macrophages, some of the topmost up-regulated M0 genes from Figure 3.5b were stained for by immunofluorescence staining. FTH1, CTSD and MMP9 were all highly upregulated in MGC rich areas compared to both adventitial and intima macrophages (Figure 3.9a). FTH1 was expressed 4 times higher in MGC rich regions than macrophages in the adventitia and twice as high compared to intimal macrophages. Similarly, CTSD was expressed 4-fold and 2-fold higher, respectively. Lastly, MMP9 was expressed 10 times more in MGC rich regions compared to adventitial macrophages but only around twice as much as intimal macrophages. When stained by immunofluorescence, these markers could be seen in GCA vessels. These markers were strongly localised to the cytoplasm of MGCs with faint staining in the surrounding cells in the intima. An IgG isotype primary anti-body was used as a negative control to ensure staining wasn't due to non-specific binding (Figure 3.9b). This spatial distribution of these markers may suggest a distinct MGC phenotype which is like that of the M0 macrophage subpopulation. FTH1 is involved with ferroptosis, a specific cell death mechanism linked to iron storage, CTSD (cathepsin D) in lysosomal proteolysis, and MMP9 in extracellular matrix remodelling. These findings complement the transcriptomic data and reinforce the conclusion that MGCs in GCA are not uniformly pro- or anti-inflammatory but may represent a specialised, potentially immunoregulatory or tissue-modifying population within the inflamed vessel wall.

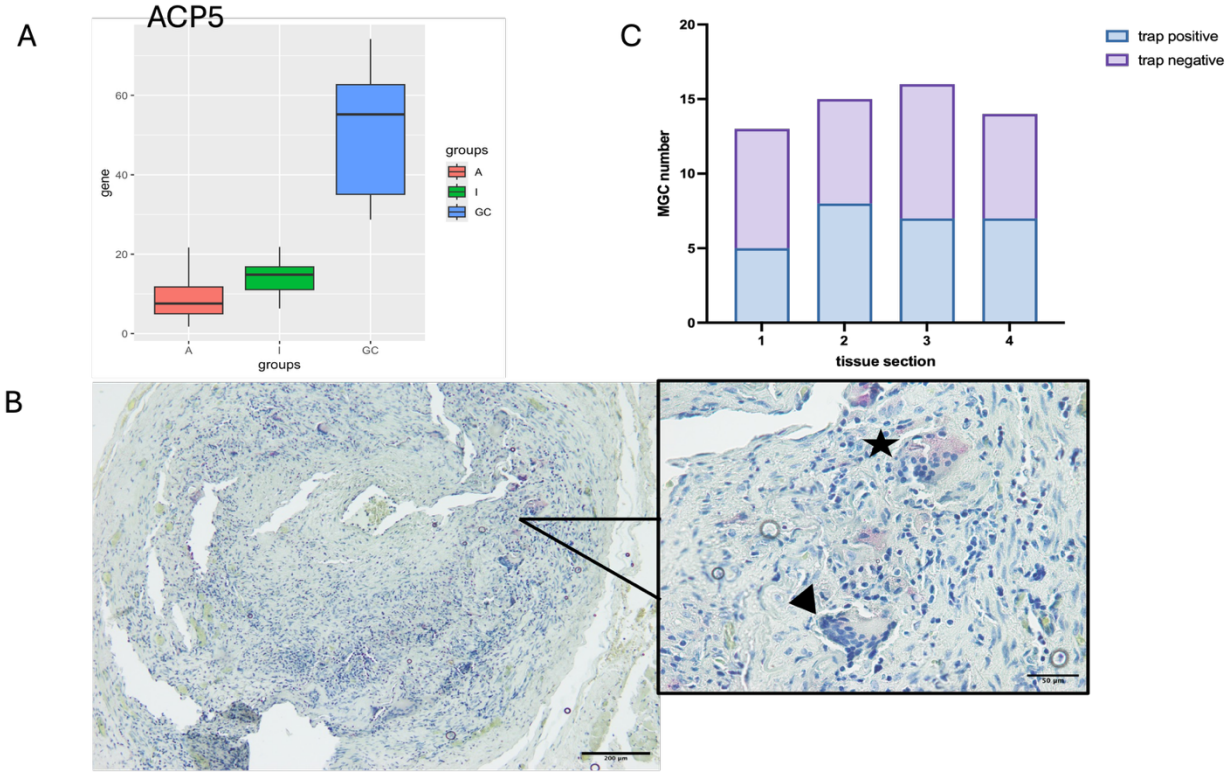

Figure 3.8 : Both TRAP positive and TRAP negative MGC's can be observed in TAB samples.(A) Boxplot of ACP5 expression in A, I and GC regions. Gene expression represented as normalized counts. (B) Representative image of TAB sample stained for TRAP expression (pink stain) and with Hematoxylin (blue) to visualise nuclei. Black arrow denotes TRAP negative MGC. Black star denotes TRAP positive MGC. (C) Quantification of trap positive vs negative MGCs in the tissue. N =1 technical replicates.

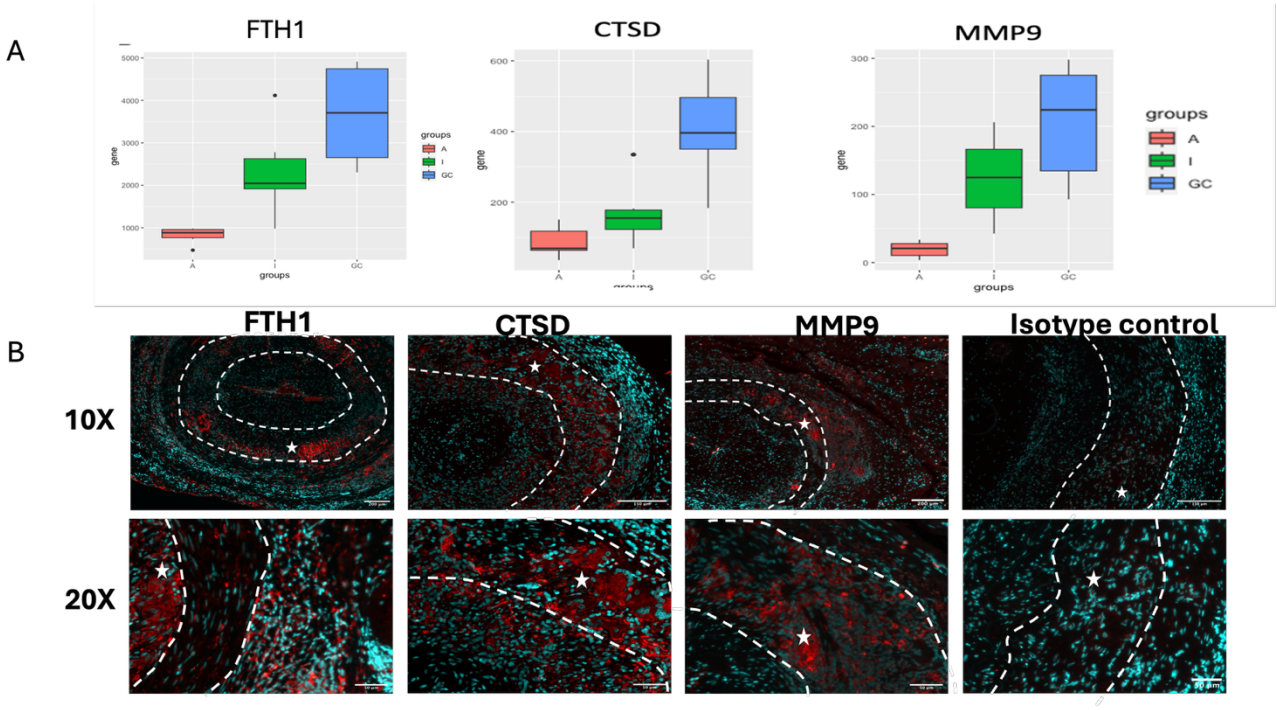

Figure 3.9: MGC's highly express proteins related to matrix remodeling. Validation of protein expression in TAB tissues (A) Box plots showing highly upregulated genes in MGC rich regions. P.Adj <0.05. (B) representative images of immunofluorescently stained TAB tissue sections. Tissues were stained overnight with primary antibodies (red) against rabbit IgG isotype, FTH1, CTSD and MMP9 then with DAPI (cyan) to visualise nuclei before being imaged on a confocal microscope. Images of the full vessel were taken at 10x, and giant cells were visualised at 20x. MGCs denoted with stars, dotted line represents distinct areas of the vessel.

3.3 Discussion

Macrophages play a key role in the pathogenesis of GCA, exhibiting functional heterogeneity depending on their localisation within the vessel wall. A subset of these macrophages undergo fusion to form MGCs, the hallmark of this disease. These cells are present in 50-60% of positive TAB tissue but their formation and functional role in disease remain poorly understood. Previous studies have linked their presence to an increased risk of cranial ischemic symptoms, including vision loss and jaw claudication. Additionally, patients who experienced disease relapse following corticosteroid treatment exhibited increased numbers of MGCs in their TAB samples. These findings suggest that MGCs could be involved in the severity of GCA as well as in the occurrence of disease relapse.

In this chapter, the transcriptional identity of multinucleated giant cells was investigated using spatial transcriptomics to distinguish them from their macrophage precursors. This was followed by downstream analyses to explore the biological pathways associated with their transcriptional expression, with further validation through marker staining to begin to better understand these cells and unpack their potential function in the disease.

To uncover their function in disease and distinguish them from their macrophage precursors, spatial transcriptomic data from the group was re-analysed to compare macrophage-rich regions and MGC-rich regions. A small number of differentially expressed genes were observed between these cell types. Among the significantly upregulated genes there were genes associated with osteoclastogenesis such as *TREM2, CTSK and ACP5*. Osteoclasts are MGCs specifically localised to the bone and are involved in the homeostatic process of bone remodelling and have been implicated in the pathogenesis of disease such as rheumatoid arthritis and osteoporosis (Ahmadzadeh *et al.*, 2022). This overlap in gene expression could suggest that these genes are not exclusively Osteoclast markers but markers defining MGCs as a whole. It also points to the function of these cells as *CTSK* and *ACP5* (TRAP) are involved in bone matrix degradation and may, therefore, play a role in GCA tissue destruction. Furthermore, TRAP has been shown to have other immunomodulatory roles in the literature. One such role is the dephosphorylation of Osteopontin (encoded by the gene SPP1, also upregulated in MGCs). This dephosphorylation has been linked to increased calcification and fibrosis by Osteopontin in diseases such as atherosclerosis

(Sainger *et al.*, 2012). This supports the hypothesis that MGCs are involved in both the media destruction and intimal hyperplasia processes in GCA. Lastly, TRAP could also be leading to the production of reactive oxygen species from MGCs. These reactive oxygen species have been linked to the activation of matrix metalloproteinases such as MMP9 which plays a crucial role in GCA pathogenesis (Hayman, 2008).

As *ACP5* was shown to be upregulated in MGCs compared to macrophages, histological staining was carried out on GCA tissue, showing the presence of both TRAP positive and negative cells in the same sample. This heterogeneity might be reflected by the presence two distinct morphologies of MGCs, Langhans (LHGC) and Foreign body (FBGC), in GCA (Nordborg, Nordborg and Petursdottir, 2000). While previous studies in RA synovium suggested TRAP positive MGCs were of the foreign body subtype while negative were of the Langhans type based on nuclear position and shape in histological analysis (Prieto-Potin *et al.*, 2015) this relationship was not clearly recapitulated in GCA tissue (figure 3.8b). This suggests that nuclear arrangement may not strictly define function in GCA-associated MGCs, and that TRAP expression could reflect additional layers of heterogeneity. However, staining and quantification was only completed on serial sections of the same donor sample, and it is, therefore, difficult to draw definite conclusions without further analysis.

Due to studies describing multiple different subtypes of macrophages described in GCA, it was expected that PCA analysis of macrophage rich regions vs MGCs would show large variation between these cells based on transcription. However, the clustering of a group of macrophage samples close to the MGCs suggested a subset of macrophages which were transcriptionally related to MGCs. When DEGs were analysed again based on the area in which the macrophages were located, it was determined that intimal macrophages were transcriptionally similar to MGCs. This could be due to their positioning along the media/ intima border and, therefore the same environmental niche. Interestingly, when DEGs between intimal macrophages and MGCs were analysed, only ACP5 (TRAP) was differentially expressed by adjusted p-value, as several genes highly expressed in MGCs were also expressed, to a lesser extent in intima macrophages. It could be possible that these cells represent a precursor, or a population of

macrophages primed to form MGCs. Functionally, the expression of TRAP in MGCs and not intimal macrophages could suggest a functional transition from MGC precursors to mature MGCs. However, this could be a shared expression profile due to their proximity and influence from local signals in the intima. One other explanation of the similarity in transcriptional activity between intimal macrophages and MGCs is the potential fusion of MGCs. In osteoclast studies, a distinct cell type known as osteomorphs have been described. These cells occur through fission of osteoclasts and can be recycled into osteoclasts later. These cells were distinct from macrophages and osteoclasts but shared a similar transcriptional profile with osteoclasts (McDonald *et al.*, 2021)
To address this question, single-cell spatial transcriptomic technologies could be employed to assess differences in intimal macrophages versus MGCs, enabling the identification of transitional or intermediate cell states, mapping of local signalling cues within their microenvironment, and clarification of whether the observed similarity reflects a true differentiation trajectory or merely convergent activation by shared stimuli.
Furthermore, due to the small number of samples, this study did not stratify patients by known confounders such as gender, age and steroid dose / response. This would be important to study in the future to better understand the transcriptional profiles of macrophages and MGCs in GCA.

It is important to note that the samples used for spatial transcriptomics had high intimal hyperplasia and media destruction meaning media residing macrophages could not be captured.

Intimal macrophages may represent a distinct subset, or a transitional population of macrophages primed for MGC formation. To further understand this, cell deconvolution was carried out using the LM22 reference matrix which can accurately categorise cells based on their transcriptional profile (Newman *et al.*, 2015b) . This analysis showed a high proportion of M0 in both the intima macrophage regions and MGC rich regions. Interestingly, M0 related genes showed low-to-moderate upregulation in the intimal region. This gradient in gene expression could suggest a model in which macrophages are primed within the microenvironment of the intima before fully adopting the transcriptional program observed in MGC-rich regions.

One study of MGCs in vitro described the process of multinucleation as a down-regulation of macrophage identity (Ahmadzadeh *et al.*, 2023), suggesting that MGCs could be described as an 'undifferentiated' macrophage as they lose key markers such as *CSF1* (which identify activated macrophage subtypes) meaning MGCs are primed to be both pro and anti-inflammatory. This could be investigated by CUT&Tag analysis of macrophages pre-MGC formation and MGCs to determine if there is an increase of repressive H3K427me3. However, it must be noted that the LM22 matrix is comprised of RNA sequencing data from in vitro studies of cultured immune cells which may not accurately represent the tissue specific heterogeneity of human macrophages. Therefore, future studies should aim to use databases of tissue macrophages, such as cardiac macrophages, as comparators to validate these results.

In depth analysis of differentially expressed M0 specific genes between macrophages and MGCs in distinct areas showed high expression of CD74 and PTBP1 on MGCs, both of which are involved in the polarisation of macrophages to a pro or anti-inflammatory phenotype (Zeiner *et al.*, 2014; Wang *et al.*, 2024; Wu *et al.*, 2024), supporting the hypothesis that MGCs are highly plastic and involved in multiple processes in GCA. This may also give an insight into the function of these cells, as many of these genes show a role for MGCs in the matrix degradation, neo-angiogenesis and intimal hyperplasia involved in the pathogenesis of GCA. For example, cathepsins such as CTSB and CTSD are involved in the matrix degradation associated with media destruction (Obermajer *et al.*, 2008). However, these molecules have also been shown to be released by macrophages and induce fibroblast activation (Morrone *et al.*, 2021). These cells are involved in the acceleration of intimal hyperplasia. In a histopathological study of GCA tissue, *MMP9* correlated with increased medial destruction and intimal hyperplasia (Rodríguez-Pla *et al.*, 2005). Additionally, *GPNMB* has been described as a ligand for the vascular endothelial growth factor receptor to modulate angiogenesis (Saade *et al.*, 2021) . Interestingly *VIM* (gene encoding vimentin) has been linked to the generation of multinucleated cells in cancers, whereby phosphorylation of vimentin leads to incomplete cytokinesis (Shen, 2024). Therefore, it would be interesting to investigate whether this protein is phosphorylated in GCA, leading to incomplete cytokinesis and induction of MGCs by Western blot.

It is important to note that the M1, M2 and M0 sub categorisation of macrophages has been shown to be an oversimplification of the highly plastic nature of these cells (Strizova *et al.*, 2023). Therefore, it is possible that MGCs represent a unique subset of cells, again a single cell spatial transcriptomic approach could help to better understand differences in these cell types.

Pathway analysis of enriched genes from DEG analysis of adventitial macrophages, intimal macrophages and MGCs provided further insight into the function of these cells in GCA. Some enriched pathways were to be expected such as immune response and inflammatory response given the fusion of MGCs from macrophages. However, this pathway analysis did give further insight into the potential functions of these cells. Interestingly, collagen biosynthesis pathways were enriched in MGCs compared to intimal and adventitial macrophages. Matrix metalloproteases MMP9 and MM12 were significantly upregulated in MGCs compared to adventitial macrophages. MMP12 secretion has been linked to the activation of myofibroblasts (Sun *et al.*, 2025), which have been implicated in the worsening of intimal hyperplasia (Hobeika *et al.*, 2007). Furthermore, the cathepsin family of proteins have not only been implicated in matrix degradation processes but also collagen deposition (Obermajer *et al.*, 2008; Morrone *et al.*, 2021). Further supporting a dual role for MGCs in GCA pathogenesis. Interestingly, genes associated with collagen catabolism were highly upregulated in the adventitia compared to the intima or MGCs. The presence of foam cell differentiation related genes in MGC regions could indicate that lipids and cholesterol are more involved in the pathogenesis of GCA than initially understood or that MGCs share similar transcription profiles across multiple diseases and tissue niches. Supporting this, genes in the ERK1/2 cascade were upregulated in MGCs such as MARCO, indicating a shared profile with osteoclasts.
Lastly, genes associated with molecular functions indicated a role for chemokine receptor binding in GCA. Interestingly, the only chemokine upregulated in intima macrophages and MGCs was CCL3, the ligand for the chemokine receptor CCR5.

While these transcriptomic findings highlight potential functions of MGCs in GCA, including their involvement in intimal hyperplasia, it remained essential to

validate whether key upregulated genes translated into protein expression within the tissue and could be used to differentiate MGCs and begin to piece together their potential function in GCA pathogenesis.

Interestingly, *FTH1* was highly upregulated in MGCs. This molecule is a component of Ferritin, involved in iron storage and homeostasis. Interestingly, antibodies against the ferritin peptide were found in almost all active GCA patients in one study (Baerlecken *et al.*, 2012). These could be due to previous bacterial infections as some infections increase ferritin expression in cells. However, ferritin autoantibodies have also been discovered in other autoimmune diseases such as RA, suggesting a role for ferritin autoantibodies in the initiation and pathogenesis of GCA (Lakota *et al.*, 2011). *FTH1* over expression has been described in different degenerative diseases such as Parkinson's disease. In a cell model of the disease, it was shown that overexpression of *FTH1* inhibited cell death by impairing ferroptosis. (Tian *et al.*, 2020). Furthermore, *FTH1* was associated with cancer cell survival, cultured pancreatic cancer cells had decreased viability when *FTH1* was knocked down by short hairpin RNAs (Park *et al.*, 2024). Taken together, this could suggest that MGCs are supressing cell death mechanisms by over-expression of *FTH1* and are therefore given a survival advantage in the inflamed vessel meaning this could be a target to inhibit MGC survival and reduce GCA pathogenesis. In the previously described study by (Ahmadzadeh *et al.*, 2023), iron metabolism in the lysosome was implicated in the initiation and maintenance of macrophage fusion into MGCs, suggesting a potential role of FTH1 in the formation of these cells.

In summary, this chapter highlights a transcriptional program in GCA MGCs consistent with potential roles in matrix remodelling, angiogenesis, and intimal hyperplasia which are key pathogenic features of GCA. Furthermore, spatial profiling suggests that intimal macrophages may serve as precursors to MGCs, occupying a transitional state within a shared microenvironment. However, the MGCs in TABs are already established, it is hard to determine how or why these cells form in GCA. Therefore, in the next chapter a model of in vitro MGC formation is proposed for the study of this initiation and potential mechanisms of modulating the formation of these cells.

Chapter 4 Using an *in vitro* culture model of MGCs to understand their formation in GCA.

4.1 Introduction

The previous chapter highlighted the expression profile of macrophages and MGCs in GCA tissue, suggesting that MGCs play a key role in the pathogenesis of GCA. The data in the previous chapter, along with other studies, suggests that MGCs are involved in medial destruction, intimal hyperplasia and potentially the severity of disease. Furthermore, MGCs have been implicated in disease relapse. However, analysis of established MGCs in TAB tissue does not reveal the cellular and molecular mechanism involved in the formation of MGCs. To understand why and how these cells form, this chapter aims to develop an *in vitro* model of MGC formation in giant cell arteritis which can be used to identify and potentially modulate the factors involved in their formation. To begin developing a model, it is important to understand the subtypes of MGCs in other diseases, where there is more information on the formation of these cells.

Multiple subtypes of MGCs exist in both homeostatic and pathological conditions, such as, bone re-modelling, implanted biomaterials, cancers, and granulomatous inflammation. In addition to osteoclasts, which are responsible for bone-remodelling, two other major subtypes are recognised: foreign body giant cells (FBGCs) and Langhans giant cells (LHGCs). FBGCs are large cells with anywhere from 30 to 300 nuclei, randomly distributed throughout a large cytoplasm, and often observed next to bio-implanted materials that cannot be phagocytosed (Mcnally and Anderson, 1995). In contrast, LHGCs are typically found in granulomatous inflammation, such as Mycobacterium tuberculosis (M. tb) infections. LHGCs are smaller than FBGCs, with 3 to 20 nuclei arranged in an annular or semi-annular pattern around the cytoplasm (Trout et.al., 2016). These cells are thought to play a role in the phagocytosis of *M. tb* bacteria and formation of granulomas. Numerous methods of culturing these cells, to study disease mechanisms, have been described in the literature. Studies have shown that culturing monocytes with M-CSF in combination with either IL-4 or IL-13 can generate cells resembling FBGCs (McNally and Anderson, 2011a). Furthermore,

studies investigating the formation and function of the LHGCs have shown that a combination of GM-CSF combined with IFNγ can induce the formation of these cells (Chen *et al.*, 2022).

GCA is described as a granulomatous vasculitis due to the presence of granulomas surrounding the internal elastic lamina (Robinette, Rao and Monach, 2021). These granulomas consist of myeloid cells and are populated with MGCs. Due to the granulomatous nature of GCA, it has been proposed that MGCs present resemble LHGCs. However, electron microscopic studies (Nordborg *et al.*, 2001) showed the presence of both MGC morphologies in temporal artery biopsies of patients with GCA, highlighting the complexity of these cells and their relevance in this disease. Given these existing in vitro models and their relevance to other diseases, it was important to assess whether a similar approach could be utilised for GCA.

Despite the relevance of these cells in the disease, no models exist of MGC formation in GCA. Current experimental models such as the ex vivo Matrigel model, which involves the culturing of GCA TAB tissue in a 3D matrix (Corbera-Bellalta *et al.*, 2014), focus on the investigation of soluble mediators and vascular remodelling factors. However, this model does not address the formation of MGCs as it relies on pre-established disease. Furthermore, in this model TABs cultured for longer than 2 weeks had a reduction in the number of MGCs observed. Similarly, mouse models of GCA, i.e. the SCID mouse- human TAB chimera, also uses GCA positive TABs to investigate mechanisms of disease progression (Ma-Krupa *et al.*, 2004) and cannot replicate de novo formation of MGCs or granulomas. Therefore, this model can be used to investigate existing MGCs and their modulation by current treatments for GCA but cannot be used to understand the mechanisms involved in MGC formation and how this formation can be inhibited.

Therefore, this chapter aims to develop a reliable model of MGC formation using monocytes isolated from healthy donors and GCA patients. These cells were cultured with cytokines and growth factors previously implicated in MGCs formation in other granulomatous diseases.

This model will allow for the identification of the molecules and pathways that specifically drive MGC formation in GCA. Furthermore, it may help determine whether monocytes from GCA patients are more prone to MGC formation than those from healthy controls and, if so, facilitate investigation into the underlying mechanisms and lead to the discovery of potential targets to inhibit MGC formation in GCA.

4.2 Results

4.2.1 Patient information.

The in vitro data in this chapter was generated using 13 GCA patient blood samples and 10 non -age matched healthy control blood samples. All healthy control samples were aged over 50 to account for age related differences.

The GCA samples had a mean age of 72.2 years of age with a range of 54 to 90 years of age (Table 4.1) and of the 13 patients sampled, 69% were female. Cranial involvement was defined by cranial symptoms and/ or a positive TAB sample whereas large-vessel involvement was defined by positive imaging tests such as FDG-PET (see intro 1.1.1). In terms of GCA manifestations, 6 patients had C-GCA only (47%) whereas, 4 (30%) patients had confirmed LV-GCA only and 3 patients had both manifestations of GCA (23%). Steroid doses varied from 25mg/day to 60mg/day. Furthermore, 9 patients received one or more adjunctive immunosuppressant therapy such as Tocilizumab or Methotrexate. Healthy controls were recruited through the university; all donors were over the age of 50. 70% of the healthy donors where female and the remaining 3 were male (Table 4.2)

Patient ID	Age	Sex	Cranial Involvement	large vessel involvement	diagnosis method	Steroid dose (mg)	Adjunctive immunosuppressant
3978_22	67	F	N	Y	PETCT	60	TOCi
4019_22	78	F	Y	N	Clinical alone	60	AZA, TOCi, MTX
4020_22	67	M	Y	N	Clinical alone (TAB negative).	60	MTX
4021_22	63	F	Y	Y	PETCT	60	MTX
4081_22	64	F	N	Y	PETCT	40	MMF, TOCi, MTX
4082_22	73	M	Y	N	TA US	40	None
4101_22	83	F	Y	N	Clinical alone	40	None
4102_22	54	F	N	Y	MRA aorta	40	MMF, TOCi
4211_23	90	M	Y	N	Clinical alone	60	None
4297_23	76	F	Y	N	TAB	40	TOCi
4298_23	64	F	N	Y	PETCT	60	MMF
4299_22	72	M	Y	Y	MRA aorta	25	MMF
5425_25	83	F	Y	Y	TAB	60	None

Table 4.1: GCA patient information AZA -Azathioprine, TOCi- tocilizumab, MTX - Methotrexate, MMF -Mycophenolate

Patient ID	Sex
4483_23	F
4549_23	M
4693_23	F
4694_23	M
4714_23	F
4902_24	F
5093_24	F
5098_24	F
5133_24	F
5196_24	M

Table 4.2: Healthy control patient information Patient ID number and sex for healthy controls all >50 years of age.

4.2.2 Optimising an *in vitro* culture model of MGC formation.

Previous studies have demonstrated the formation of MGCs *in vitro* using a combination of GM-CSF+ IFNγ or M-CSF+IL-4. However, this has not yet been explored in the context of GCA. To determine whether these cytokines can be used to induce GCA-like MGC formation under similar experimental conditions, monocytes from GCA patients were culture with these stimuli and assessed for their capacity to form MGCs.

Isolated monocytes were cultured with a combination of the previously mentioned cytokines before being stained and visualised (Figure 4.1a). MGCs were consistently observed when cells were treated with GM-CSF+ IFNγ, M-CSF+IL-4 and a combination of GM-CSF or M-CSF with both IL-4 and IFNγ (Figure 4.1b). No MGCs were observed in GM-CSF+IL-4 or MCSF+IFNγ stimulated conditions.

The highest numbers of MGC formation were observed in the GM-CSF+ IFNγ and M-CSF+IL-4 stimulated conditions (a mean of 276±333.9 and 225±234.6 cells per well respectively.) Unexpectedly, a high number of MGCs were also observed when cells were stimulated with GM-CSF+IL-4+IFNγ (245±190.7 cells per well) which has not previously been shown in the literature (Figure 4.1c).

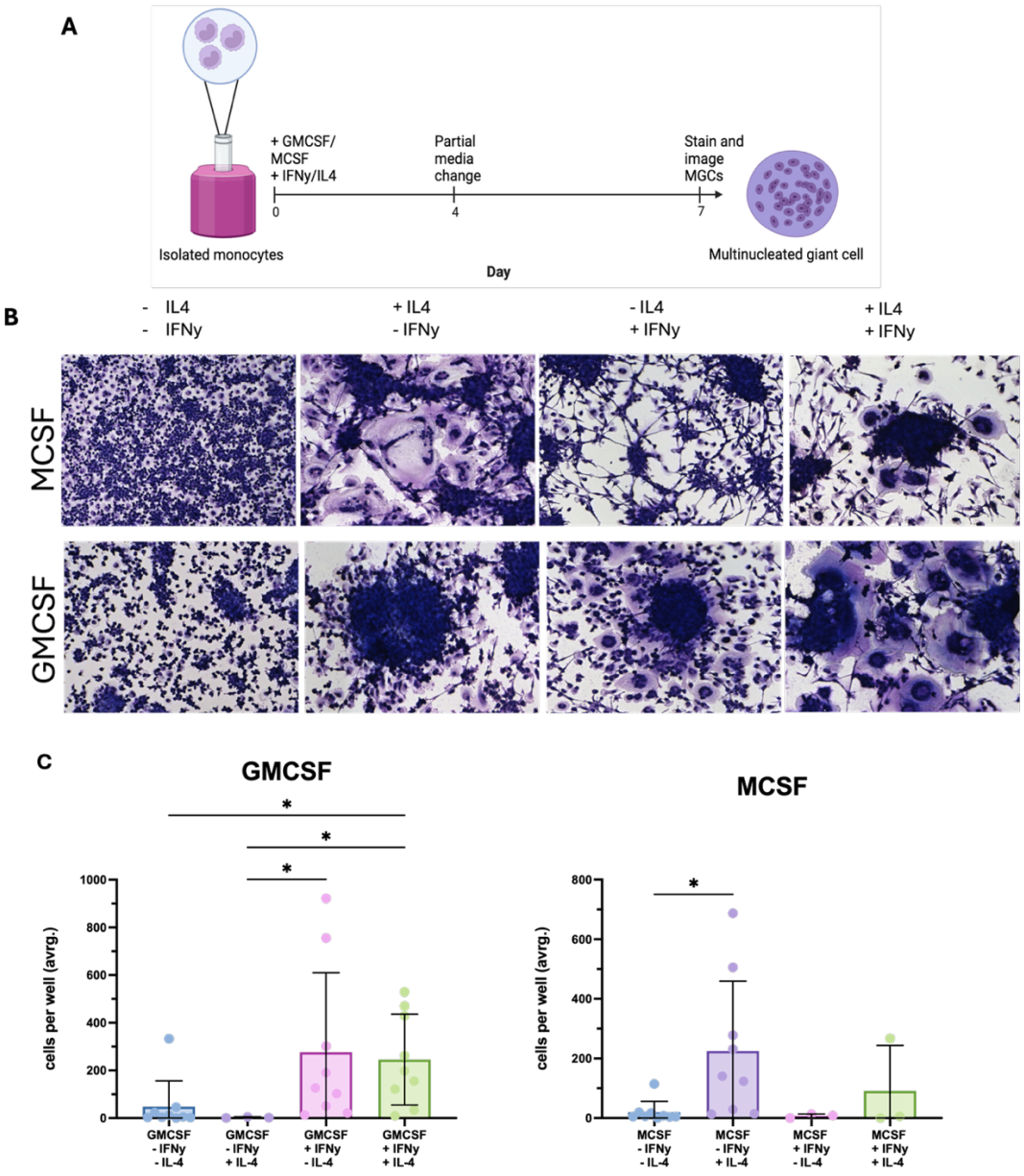

Figure 4.1: MGCs can be generated in vitro from GM-CSF+ IFNγ and MCSF+IL-4. Monocytes were isolated from leukocyte cones were stimulated with 100ng/ml of either GM-CSF or MCSF, alongside with 20ng/ml IL-4 and/ or 40ng/ml IFNγ. After 7 days incubation, cells were stained with a haemacolour staining kit and imaged. (A) Diagram of multinucleated giant cell culture protocol; made with BioRender. (B) Representative images of multinucleated giant cells under different culture conditions at 10x magnification. Multinucleated giant cells are cells with a large cytoplasm and >3 nuclei. (C) Quantification of MGC numbers. Error bars mean±SD, N=9. *P<0.05. Kruskal-Wallis test performed in GraphPad Prism.

Next, to further investigate whether the observed differences in MGC numbers between culture conditions were attributable to differences in multinucleation rather than cell number alone, isolated human monocytes were plated onto 8-well chamber slides and cultured under the indicated conditions for immunofluorescence analysis. To assess cytoplasmic morphology and actin

organization, cells were stained with phalloidin to visualize F-actin, and with DAPI to enable nuclear visualization and quantification.

When cells were cultured with GM-CSF or M-CSF alone, no multinucleated giant cells were observed. In contrast, cultures treated with GM-CSF and IFNγ gave rise to small MGCs with a rounded cytoplasm and nuclei arranged in a semi-annular pattern (Fig. 3.4a). Conversely, cells cultured with M-CSF and IL-4 formed larger MGCs containing multiple nuclei that were randomly distributed throughout the cytoplasm (Fig. 3.4b), indicating marked differences in MGC morphology between these conditions.

To quantitatively assess macrophage fusion, the multinucleation (fusion) index was calculated for each culture condition (Fig. 3.4c). Cells cultured with M-CSF and IL-4 exhibited a higher fusion percentage compared with those cultured with GM-CSF and IFNγ (50.7 ± 9.9% vs 20.1 ± 1.7%). However, this difference did not reach statistical significance. Notably, despite comparable fusion indices, MGCs generated in the presence of M-CSF and IL-4 were substantially larger and contained a greater number of nuclei per cell than those formed under GM-CSF and IFNγ conditions.

Taken together, these findings suggest that the differences in MGC numbers observed between culture conditions are likely driven by differences in MGC size and the extent of multinucleation within individual cells, rather than by differences in overall fusion frequency alone.

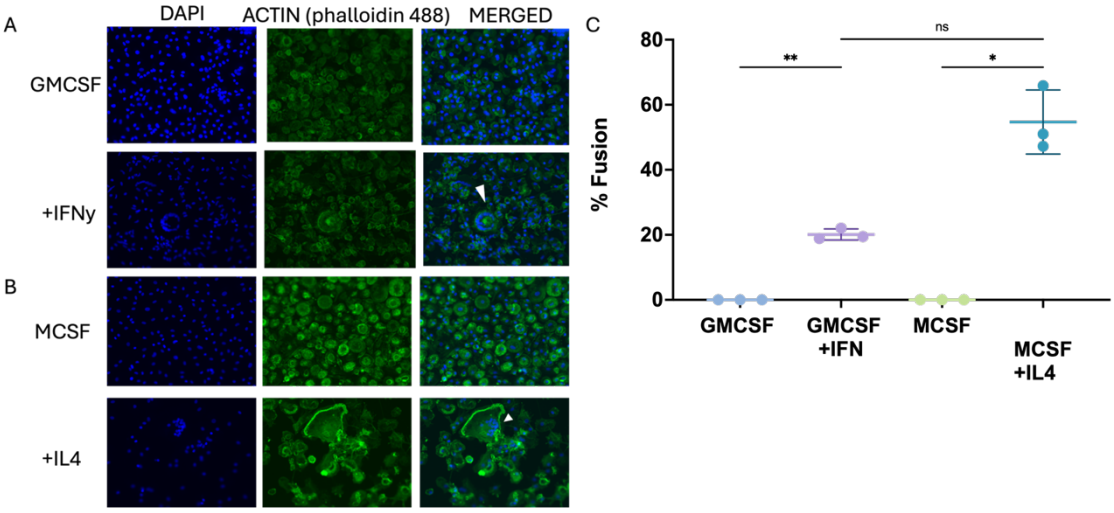

Figure 4.2: Giant cells were larger in MCSF conditions compared to GMCSF conditions. Representative images of cells cultured with GMCSF alone and GMCSF and IFNy (A), MCSF alone and MCSF with IL4 (B) White arrows indicate multinucleated giant cells. DAPI (blue) and Phalloidin 488 (green) 20x magnification are shown. (C) The rate of multinucleation was quantified using the fusion index calculation. N=3, average of three FOVs per donor. A one-way Anova was performed on Prism; *P<0.05 **P<0.01. Error bars represent the mean and standard deviation.

To determine whether the number of MGCs increases over time and to elucidate the best time point for the study of the MGCs formed, cells were stimulated for 7, 11, and 14 days. Only the stimulation conditions GM-CSF+IFNγ and M-CSF+IL-4 are shown as they produced the highest number of giant cells in previous experiments.

When cells were stimulated with GM-CSF+IFNγ, the highest number of MGCs (337±550) was observed at day 11 (Figure 4.2a). Interestingly, the numbers dropped to as low as 88±138.7 mean MGCs by day 14 when cultured with GM-CSF+ IFNγ. While there was no significant difference between the numbers, notably there was large variation between donors. For example, numbers on day 7 ranged from 11 to 755 cells per well. This is likely due to how heterogenous human samples can be and, therefore, the number of biological replicates should be increased the future experiments. Conversely, there was little to no difference in MGC numbers when cells were stimulated with M-CSF+IL-4 (Figure 4.2b). This suggests that the maximal number of MGCs is achieved by day 7 and then sustained (ranging from 189±159 to 175±38.2 mean cells per well).

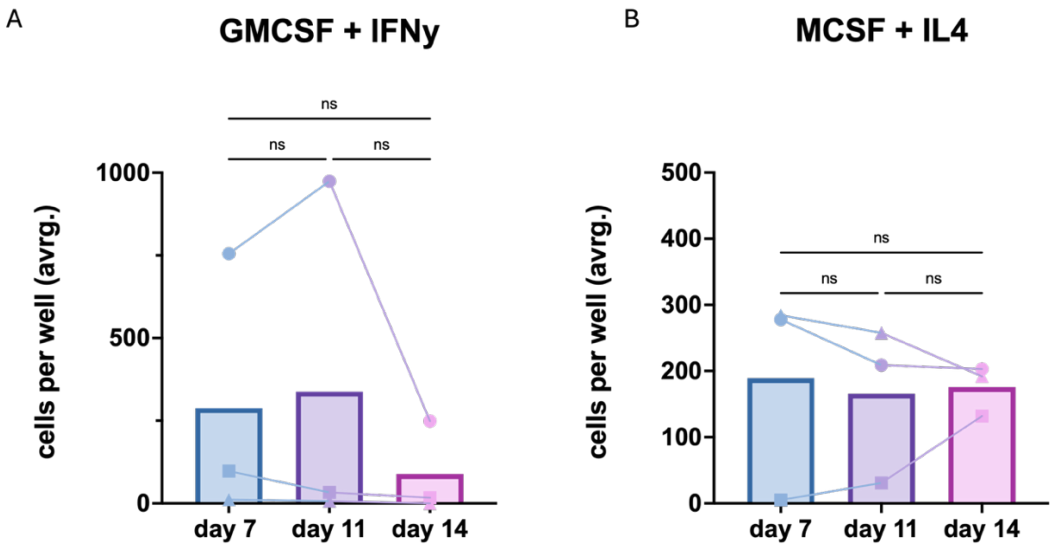

Figure 4.3: Maximal giant cell numbers were reached by day 7 of culture. Cells were cultured with GMCSF and IFNγ or MCSF and IL-4 for 7, 11 and 14 days. Cells were stained and imaged. Bar graph representing mean MGC per well. Shapes represent individual donors. Error bars mean ±SD. (A) GMCSF stimulated (B) MCSF stimulated.

In addition to assessing the timepoint with the highest number of MGCs, it was important to determine whether MGCs were formed in a dose-dependent manner.

Cells were stimulated with 10, 20, 40, and 80ng/ul of either IFNγ or IL-4 (Figure 4.3a-b). When cultured with GM-CSF and varying concentrations of IFNγ (Figure 4.3a), MGCs could be observed at all concentrations. However, cells were more likely to form clusters at higher doses of IFNγ. This was reflected in the number of MGCs observed at each concentration. Interestingly, there was a dose dependant decrease in MGC numbers with increasing concentration of IFNγ. MGC numbers were significantly reduced from a mean of 328±265 cells per well at 10ng/ul to 87±59 cells per well at 80ng/ul (Figure 4.3c).

In contrast, there was no significant difference in appearance when cells were stimulated with M-CSF+IL-4 (Figure 4.3b). This was reflected in the numbers of MGCs formed in each concentration. While there was no significant difference between the numbers of MGCs formed, but MGC numbers peaked at a mean of 250±163 cells per well when stimulated with 20ng/ul (Figure 4.3d). Similar to GM-CSF stimulated cells, the number of MGCs dropped when cultured with 80ng/ul, decreasing to 120±136 mean cells per well. This suggests that higher doses are less likely to induce MGC formation, which could be due to a negative feedback mechanism aimed at limiting inflammation. Together, this data

suggests different mechanisms of action between GM-CSF and M-CSF-mediated MGC formation.
As this data was generated using leukocyte cones, it was next important to determine whether MGCs resembling those observed in GCA tissue could be generated using isolated monocytes from GCA patients.

4.2.3 **Validation of the in vitro model for the study of MGCs in GCA.**

To determine whether this could be used as a viable model of MGC formation in GCA, circulating monocytes were isolated from peripheral blood of GCA patients and cultured as previously described.

This showed that MGCs could be generated when monocytes from GCA patients were cultured with GM-CSF+ IFNγ and GM-CSF+IL-4/ IFNγ (Figure 4.4a). Similar to previous experiments, the greatest number of MGCs (112±135) was observed in the GM-CSF+ IFNγ condition. However, GCA cells cultured with M-CSF and different combinations of IL-4 and IFNγ were less likely to form MGCs than cells from leukocyte cones (Figure 4.1c). When GCA monocytes were cultured with M-CSF+IL-4, it led to 16.5±28.5 cells per well (Figure 4.4b) compared to 225±234.6 mean cells per well from leukocyte cones (Figure 4.1c).
Interestingly, a significantly higher number of MGCs were observed in the M-CSF+ IFNγ+IL-4 conditions than in the MCSF+IL-4 condition (mean of 38±60.3 compared to a mean of 16.5±28.5). Taken together, the data suggest a prominent role for both GM-CSF and IFNγ in the formation of MGCs in the context of GCA.

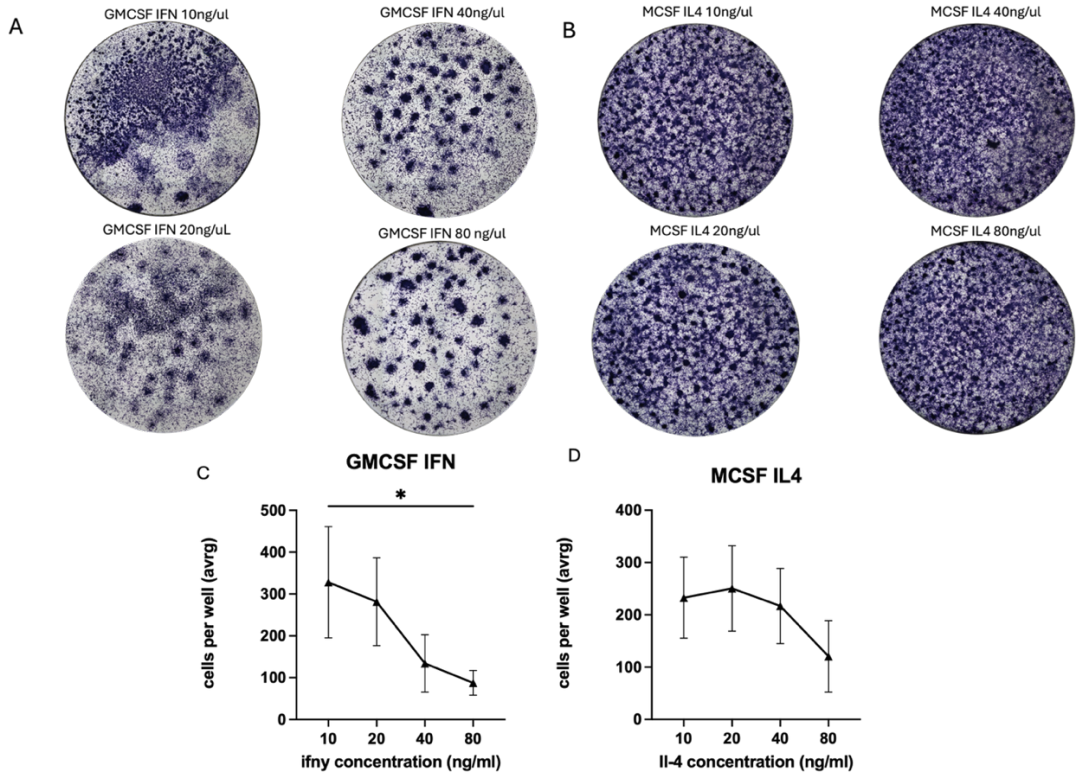

Figure 4.4: Increasing the concentration of cytokines has little effect on MGC formation.

Representative images of wells cultured with 100ng/ul of GMCSF and 10, 20, 40 or 80 ng/ul of IFNy (A) Or 100ng/ul of MCSF with 10, 20, 40 or 80ng/ul of IL4 (B) Total number of MGCs were counted for GMCSF+ IFNγ stimulated. 10x magnification. (C) and MCSF+IL-4 stimulated (D). N=3 *P<0.05 2-way ANOVA. Error bars mean ±SEM.

Previous studies have shown that both GM-CSF and M-CSF contribute to GCA pathogenesis, with macrophages encountering these growth factors in distinct regions of the vessel (Jiemy *et al.*, 2020). Accordingly, the impact of sequential stimulation with M-CSF followed by GM-CSF on MGC formation, and vice versa, was investigated. Initially, monocytes were cultured with M-CSF for 72 hours before a partial media change where GM-CSF was given to the cells (Figure 4.5a). Cells from the same donor were simultaneously cultured with M-CSF, as previously, described (Figure 4.1a). Interestingly, cells which received M-CSF for 72 hours, followed by GM-CSF, produced a significantly higher number of MGCs compared to M-CSF alone (301±338.5 and 5.5±7.3 mean MGCs respectively P= <0.05). Similarly, the number of MGCs generated when cells were cultured with MCSF+ IFNγ followed by GM-CSF was significantly greater than the number when cells were cultured with M-CSF+ IFNγ alone (262±380 mean MGCs compared to 1+1.93 MGCs respectively P=<0.05). Conversely, when cells were cultured with MCSF+IL-4 for 72 hours followed by the change to GM-CSF, there was a reduction in the number of cells compared to M-CSF+IL-4 alone (182±253 compared to

269±298 mean MGCs respectively). However, this difference was not statistically significant. There was a slight, but non-significant, increase in MGC numbers when cells were cultured with M-CSF+IL-4+ IFNγ followed by GM-CSF than with M-CSF alone. This further shows the importance of GM-CSF in the formation of MGCs from GCA monocytes but also indicates that M-CSF may also be involved in this process.

Monocytes from GCA patients were then cultured with GM-CSF and cytokines for 72hrs before it was replaced with M-CSF. It is important to note that this data was generated using only an N=2 and therefore, statistics cannot be applied. Overall, there were less MGCs generated when cells were cultured with GM-CSF followed by M-CSF compared to cells cultured with M-CSF followed by GM-CSF. Interestingly, in both donors there was a decrease in MGCs numbers when M-CSF was added at 72 hours compared to GM-CSF alone (4.8±4.75 mean MGCs compared to 12.8±2.1 MGCs). Furthermore, there was large variation between the two donors when cultured with GM-CSF+IL-4 alone and GM-CSF+IL-4 followed by M-CSF at 72hrs. However, there was a slight increase in the mean MGCs of the latter. Similarly, there was a slight increase in MGCs numbers when M-CSF was added to cells 72hrs after GM-CSF+ IFNγ compared to GM-CSF+ IFNγ alone (11.2±8.7 compared to 4±0.9 mean MGCs). Lastly, one donor saw an increase in MGCs when cells were cultured with GM-CSF and both IL-4+IFNγ followed by MCSF at 72hrs compared to cells cultured without M-CSF, whereas one donor had the opposite. Taken together, this data suggests that both M-CSF and GM-CSF are involved in the formation of MGCs by GCA monocytes particularly, when cells see M-CSF before GM-CSF. However, the donor numbers need to be increased to increase the reliability of this data.

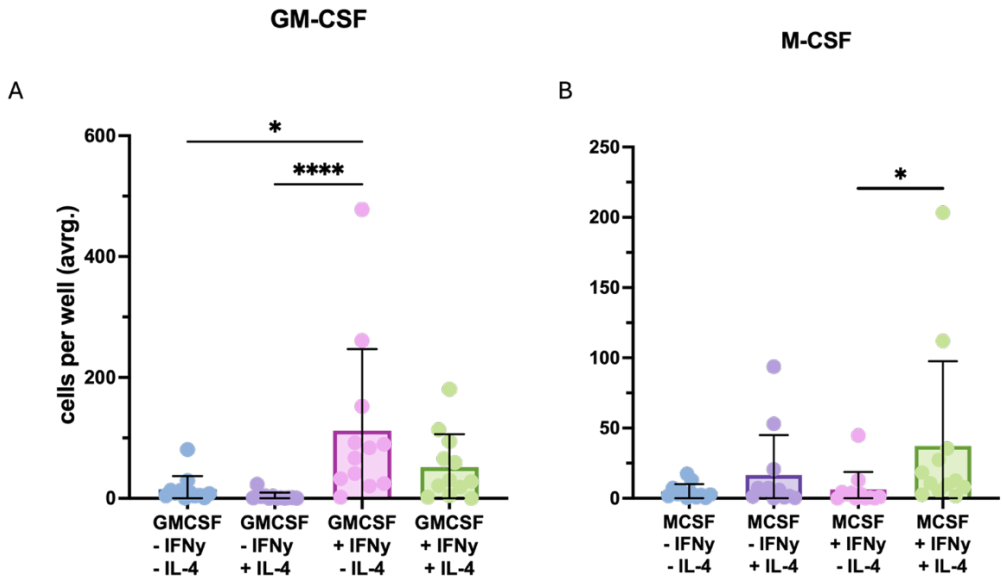

Figure 4.5: Monocytes from GCA patients fuse to form multinucleated giant cells. Monocytes isolated from patient peripheral blood mononuclear cells were plated as previously described and culture for 7 days. After which, cells were stained with the haemacolour staining kit and counted using the ImageJ software. Cells cultured with either IL4 or IFNγ were normalized to the controls (GMCSF (A) or MCSF alone (B)). A Wilcoxon non-parametric analysis was performed to test for statistical significance; **P<0.01, *** P<0.001 (n=12). Error bars represent mean ± SEM

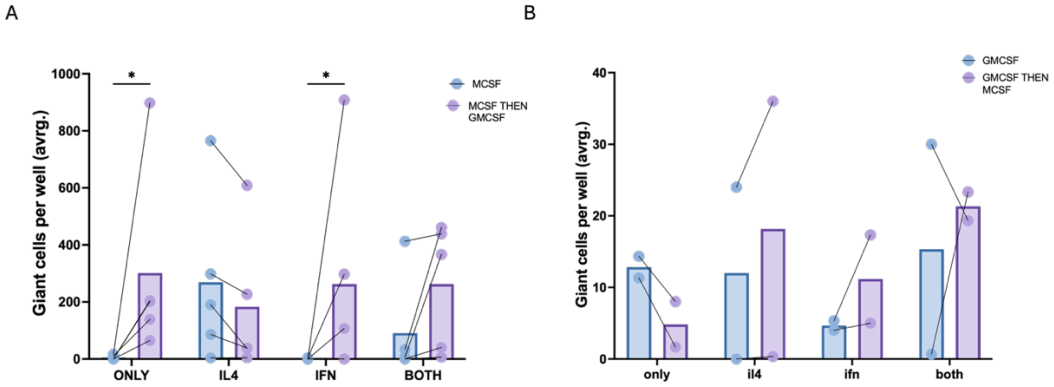

Figure 4.6: Increase in giant cell numbers when cultured with MCSF then GMCSF but not the other way around. Bar graphs showing differences in giant cell numbers in each stimulation condition when (A) MCSF was replaced with GMCSF at 72 hours, N=5 ANOVA, bars represent mean. Lines link donors before and after switch*P< 0.05. (B) GMCSF was replaced with MCSF at 72 hours, N= 2, bars represent mean. Lines link donors before and after switch*P< 0.05.

To verify the similarity of these MGCs in vitro to those observed in GCA tissue, MGCs were stained for selected markers previously described in the spatial transcriptomics analysis (Figure 3.8a). The genes *CTSD* and MMP9 were highly expressed by MGCs and, therefore, were selected as markers to identify GCA MGCs. When in vitro derived macrophages and MGCs were stained for these markers, MMP9 was expressed in both M-CSF and GM-CSF stimulated macrophages (Figure 4.6a). Interestingly, some GM-CSF only stimulated

macrophages stained strongly for MMP9 compared to other monocytes in the same culture condition. Similarly, CTSD was expressed in macrophages stimulated with both GM-CSF and M-CSF (Figure 4.6b) but its staining was weaker in these macrophages than MMP9. Interestingly, while MGCs in both GM-CSF and M-CSF conditions expressed MMP9 *and* CTSD (Figure 4.6c&d), their localisation was different; MGCs generated with M-CSF+IL4 displayed nuclear staining for MMP9 *and* CTSD, whereas those generated with GM-CSF+ IFNγ had cytoplasmic expression suggesting a different mechanism of action for these molecules in MGCs formed from different culture conditions. The nuclear staining observed in these MGCs is unexpected as these molecules are predicted to reside in the cytoplasm or be secreted respectively. This latter, aligned with what was observed in the GCA tissue, where MGCs displayed cytoplasmatic staining for both MMP9 *and* CTSD (Figure 3.6b). This further supports functional differences between M-CSF and GM-CSF derived MGCs as well as the hypothesis that GM-CSF+ IFNγ are the specific factors involved in the formation of MGCs in GCA.

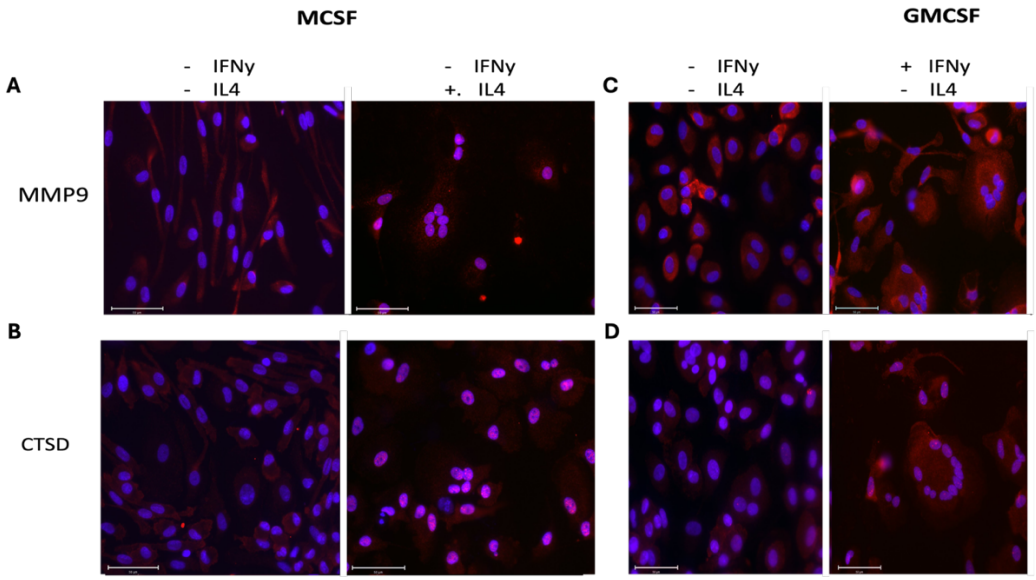

Figure 4.7: GMCSF cultured MGCs express the same markers found in GCA tissue MGCs.

Representative images (20x) of macrophages stimulated with MSCF (A-B) or GMCSF (C-D) stained with anti-MMP9 (A+C)/ anti-CTSD (B+D) with an AF647 secondary (red) and DAPI (blue). Scale bar 50uM.

In addition to MMP9 and CTSD, high expression of *ACP5*, the gene encoding TRAP, was also observed in MGCs present in GCA tissue samples (Figure 4.7). To further verify the similarity of cultured MGCs to those in the tissue, in vitro-derived MGCs were also stained for TRAP. Immunostaining of in vitro cultured MGCs

confirmed TRAP expression within MGCs under both M-CSF and GM-CSF stimulation conditions, indicating that its presence is not restricted to a specific cytokine environment. However, not all MGCs were TRAP-positive, reflecting a heterogeneity that mirrors the variability observed in tissue sections. This partial expression pattern suggests the existence of subpopulations of MGCs with potentially distinct functional roles. Further investigation is required to clarify the regulation and significance of TRAP expression in these different cell states.

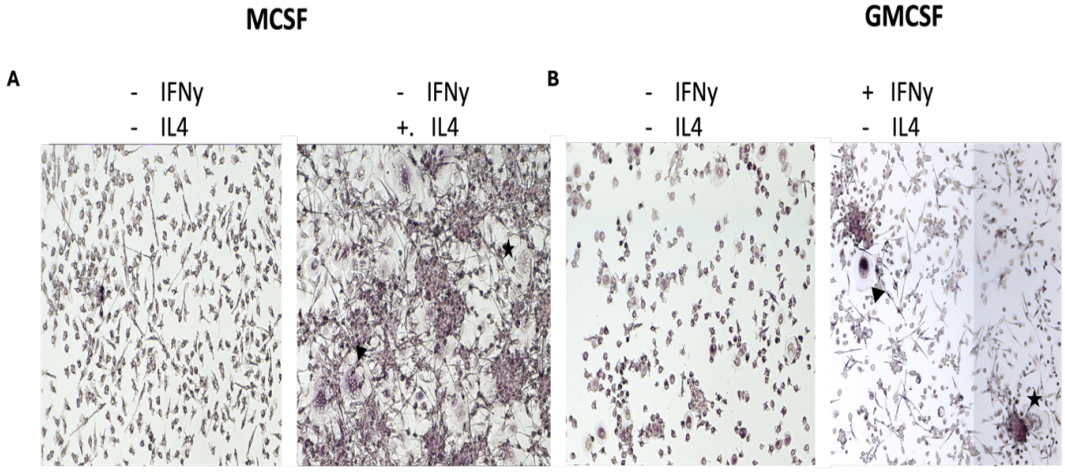

Figure 4.8: TRAP staining of MGCs cultured from GCA monocytes. Representative images (10x) of images of TRAP stained MGCs stimulated with MCSF (A) or GMCSF (B). Black arrows represent TRAP-ve giant cells and black stars represent TRAP +ve giant cells.

Lastly, both FBGCs and LHGCs were observed closely together in GCA TAB tissue (Figure 4.8a), consistent with previous studies (Nordborg *et al.*, 1997). Therefore, whether the same was true for the *in vitro* model of GCA MGCs was also assessed. MGCs were counted based on their morphology in the different stimulation conditions (Figure 4.8b). In GM-CSF+IFNγ and GM-CSF+IFNγ/IL-4 conditions, both LHGCs and FBGCs were present at comparable numbers, 60.7±81 and 51.7±61.6 mean MGCs respectively (Figure 4.9a). Conversely, M-CSF+IL-4 and M-CSF+IL-4/IFNγ conditions yielded significantly more FBGCs than LHGCs (Figure 4.9b). These findings suggest that both MGC types can form under various cytokine environments, and that specific conditions may preferentially bias the morphological outcome. Overall, GM-CSF-derived MGCs were, once again, more closely aligned with the phenotypic characteristic of MGCs found in GCA tissue lesions, where both FBGCs and LHGCs were present. This further supports the hypothesis that GM-CSF and IFNγ are key players in the formation of MGCs in GCA.

Based on these observations in healthy donor-derived cultures, the next step was

to assess whether circulating monocytes from GCA patients exhibited a greater propensity to form MGCs under the same in vitro conditions.

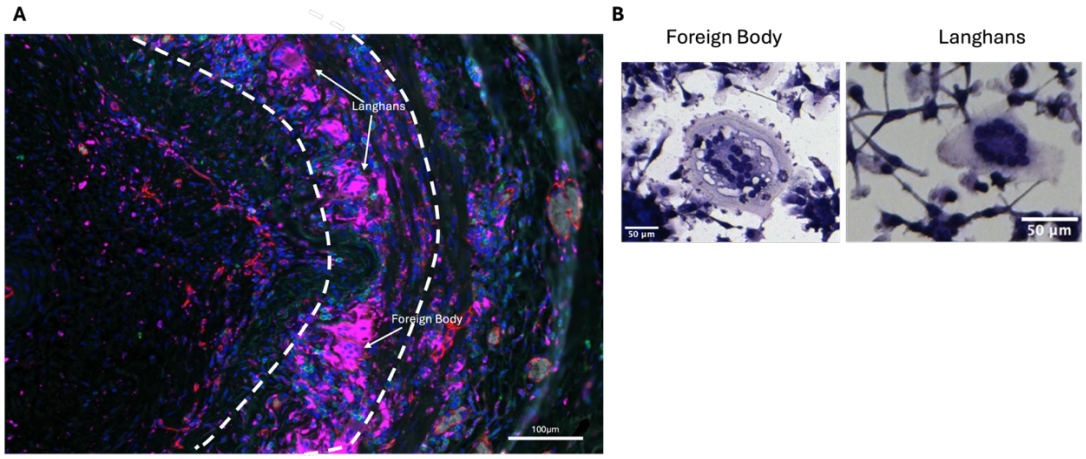

Figure 4.9: Both FBGCs and LHGCs can be seen in GCA tissue and in vitro cultured MGCs. Representative images of Langhans and foreign body giant cells in (A) GCA tissue and (B) in vitro when cultured with GMCSF+ IFNγ. LHGCs have 3-30 nuclei in a semi—annular pattern around the cytoplasm and FBGCs are larger cells with 3-300 nuclei randomly dispersed throughout the cytoplasm.

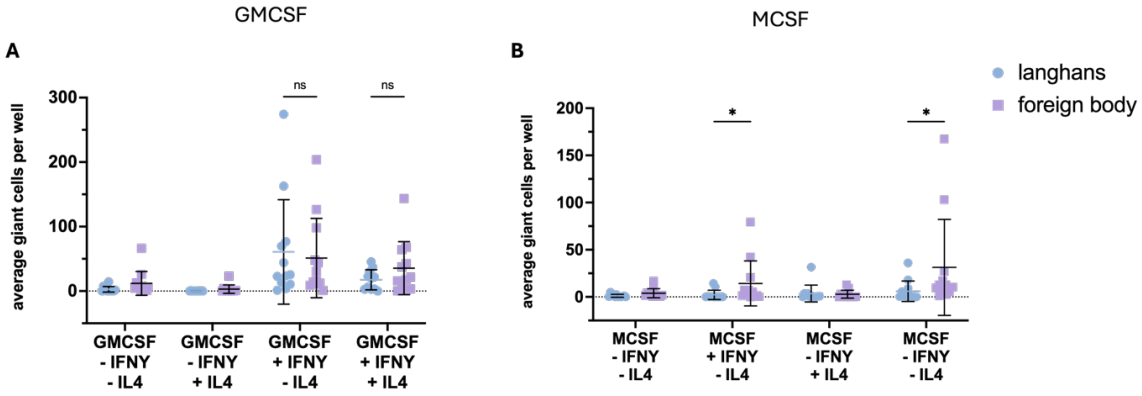

Figure 4.10: Monocytes from GCA patients fuse to form both subsets of MGCs when cultured with GMCSF. Monocytes were cultured for 7 days and MGCs were counted. (A-B) Dot plots showing mean LHGCs (annular nuclei) or FBGCs (>30 nuclei dispersed through the cytoplasm) numbers. A two-way ANOVA was performed using Prism. * Adj. P>0.05. Error bars represent mean ±SD.

4.2.4 Application of the *In Vitro* Model to Compare MGC Formation in GCA and Healthy Controls.

In order to better understand why MGCs form in GCA tissue, a comparative analysis of in vitro derived MGCs between healthy controls and samples from patients with GCA was performed.

When stimulated with GM-CSF+IFNγ, GCA monocyte generated a higher number of MGCs compared to age-matched healthy controls (mean = 120±133.5 *vs* mean=55 ±59.2 cells per well). However, this difference did not reach statistical

significance (Figure 4.10a). This lack of significance could be due to differences in active disease versus those in remission and therefore, this should be investigated further. Furthermore, it is important to note, that due to ethical constraints, no medical history could be acquired from healthy controls, meaning there could be confounding health factors leading to heterogeneity among the data. In contrast, IL-4 stimulation appeared to be more closely associated with MGC formation in healthy donors (Figure 4.10b). This was particularly evident under M-CSF + IL-4 conditions, where healthy controls produced significantly more MGCs than GCA samples (mean = 259±277 *vs* mean= 20±31 cells per well; $p < 0.0001$). These differences confirmed the hypothesis that GM-CSF and IFNγ play a central role in the formation of MGCs in GCA, potentially through mechanisms that reflect an enhanced responsiveness of GCA-derived monocytes to these cytokines compared to those from healthy individuals.

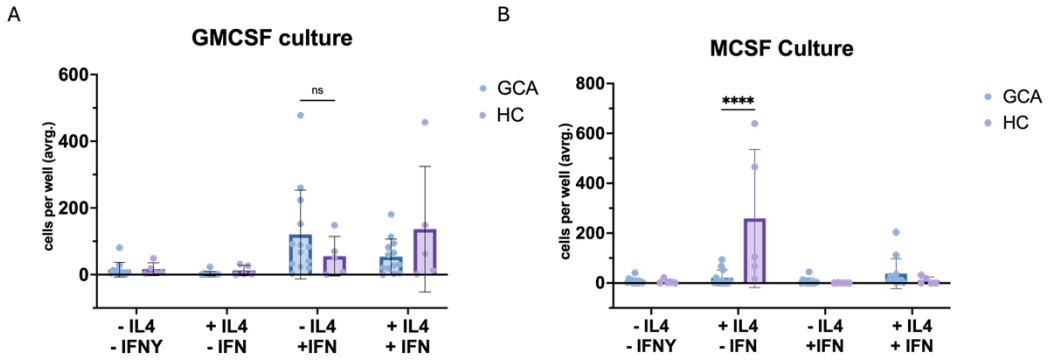

Figure 4.11: MGCs are more likely to fuse under different stimulation between healthy and GCA. Bar graph showing mean MGCs per well when stimulated with (A) GMCSF or (B) MCSF. GCA (N=13) vs healthy (N=5) are shown in blue and purple respectively. Error bars represent mean ±SD. 2-way ANOVA test performed ****Adj. P<0.0001.

Finally, the number of LHGCs and FBGCs between healthy and GCA cultured monocytes were compared. This showed that GCA monocytes were more likely to form both LHGCs and FBGCs when cultured with GM-CSF+IFNγ than healthy control monocytes. (Figure 4.11b). As expected, there was no significant difference in the number of LHGCs when cultured with GM-CSF+IFNγ between GCA and healthy cultures (60±81 mean MGCs compared to 67.3±63.1 mean MGCs respectively). However, a statistically significant increase in FBGCs was observed in the GCA group compared to healthy controls (51±61 mean MGCs vs. 9±16.4 cells per well; $p < 0.05$), suggesting a differential response to this cytokine combination. In contrast, little to no MGC formation, of either subset was

observed in GCA cultures stimulated with M-CSF+IL-4 (Figure 4.11a), while healthy donor macrophages formed both LHGCs and FBGCs under the same conditions. These findings may reflect an underlying pro-inflammatory bias in GCA circulating monocytes, with increased responsiveness to GM-CSF and IFNγ, whereas monocytes from healthy individuals appear more responsive to M-CSF and IL-4 stimulation.

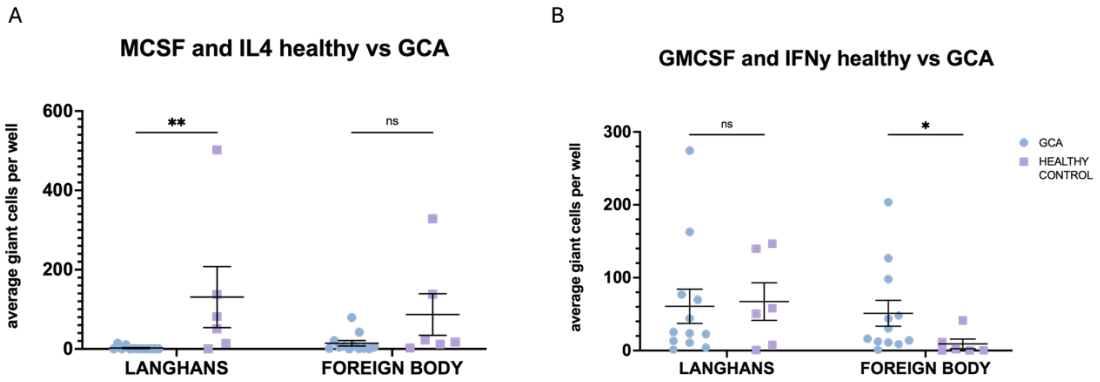

Figure 4.12: GCA MGCs are more likely to form both LHGC and FBGCs than healthy when cultured with GMCSF. Dot plots showing the mean number of each MGC subtype in healthy vs GCA when stimulated with (A) MCSF or (B) GMCSF. Dots represent mean of one donor. Error bars represent mean ±SD. 2-way ANOVA performed in Prism *Adj. P < 0.05 **Adj. P <0.01.

4.3 Discussion.

The previous chapter demonstrated the gene expression of MGCs and the potential role these genes may play in their function in GCA but did not explore the mechanisms involved in MGC formation. Previous studies have used combinations of the cytokines GM-CSF and IFNγ or M-CSF and IL-4 to form MGCs in the context of granulomatous inflammation and foreign body reactions respectively (Takashima *et al.*, 1993; Mcnally and Anderson, 1995; Byrd, 1998; Mizuno, Okamoto and Horio, 2001). Existing models of GCA, such as the ex vivo culture method (Corbera-Bellalta *et al.*, 2014), use pre-established disease with the presence of already formed MGCs, limiting insight into their origin. It was therefore hypothesised that, if MGCs resembling those found in granulomatous conditions can be generated in vitro, they may also be induced by exposing primary GCA-derived monocytes to these cytokines. Accordingly, the aim of this chapter was to develop, optimise, and apply an *in vitro* model to investigate GCA-specific MGC formation.

The data presented in this chapter demonstrates that primary human monocytes can be induced to form MGCs when stimulated with GM-CSF and IFNγ or M-CSF and IL-4, consistent with previous reports (Takashima *et al.*, 1993; Mcnally and Anderson, 1995; Gasser and Möst, 1999). An unexpected finding was the formation of MGCs when monocytes were stimulated with GM-CSF, IFNγ, and IL-4. GM-CSF in combination with IL-4 promotes the differentiation of monocytes toward a dendritic cell phenotype (Chapuis *et al.*, 1997), which typically does not support MGC formation. However, one study showed that immature DCs generated from monocytes with GM-CSF and IL-4 could be redirected toward a macrophage phenotype upon addition of IFNγ (Delneste *et al.*, 2003), suggesting a potential mechanism for MGC formation under this cytokine combination. It is therefore hypothesised that, in this culture system, stimulation with GM-CSF and IL-4, in the presence of IFNγ, may shift monocytes toward a macrophage phenotype, thereby increasing their capacity to fuse into MGCs. Although one study reported that an IL-4 gene polymorphism is connected to GCA (Amoli *et al.*, 2004), one study proposed that elevated IL-9 expression in inflamed arteries reflect the presence of Th9 T cells. Since IL-4 is required for Th9 differentiation (Xue *et al.*, 2019), this suggests that IL-4 may indeed be present in the GCA

microenvironment. This highlights the relevance of evaluating IL-4 as a contributing factor in GCA-associated MGC formation.

Given that MGCs could be generated using primary human monocytes, it was necessary to optimise the culture conditions. The results presented demonstrate that the maximal number of MGCs was reached by day 7, with no significant difference observed between day 7 and 14 following stimulation with M-CSF and IL-4. Interestingly, a substantial but not significant drop of MGC numbers was noted on day 14 in cultures stimulated with GM-CSF and IFNγ. In studies of in vitro osteoclast culture, a similar phenomenon of cell death followed by a resurgence in cell numbers has been observed. Specifically, Akchurin et al. (Akchurin *et al.*, 2008) observed a similar decline in numbers by day 14 followed by a marked resurgence in the numbers of osteoclasts by day 15. Therefore, it would be interesting to culture MGCs for longer than 14 days using long-term live imaging (Wang, Gleeson and Fourriere, 2023) to determine whether this pattern of death and resurgence of MGCs also happens to GCA-derived MGCs. However, this was beyond the scope of the current thesis, and day 7 was selected as the optimal time point for MGC formation.

Furthermore, it is important to note that a considerable variation of MGC numbers among donors was observed. Such variation is common in primary human cell cultures and highlights the need for increased replicate numbers to ensure statistical robustness of the presented results.

In addition to time-course optimisation, the effects of different cytokine concentrations on the formation of MGCs were assessed. Concentrations used in other in vitro studies varied from (2.5 ng/mL) to (100 ng/mL (Takashima *et al.*, 1993, 1993; Mcnally and Anderson, 1995)).

Consistent with the findings in this chapter, a study by Weinberg et al. (Weinberg, Hobbs and Misukonis, 1984) demonstrated that MGC numbers increased with IFNγ concentration up to approximately 100 ng/mL, after which they began to decrease, indicating a dose-dependent response with a plateau effect. Based on this data, the optimal cytokine concentration chosen for future experiments was 40 ng/mL.

Overall, the data presented in this chapter highlight the key role of GM-CSF and IFNγ in the formation of MGCs that closely resemble those found in GCA tissue.

Both of these cytokines have been implicated in the pathogenesis of the disease and are also linked to granulomatous inflammation and associated MGCs (Weyand, Younge and Goronzy, 2011; Corbera-Bellalta *et al.*, 2022). Many effectors of GCA pathogenesis are upregulated by IFNγ, such as IL-6, reactive oxygen species, and TNFα (Jiemy *et al.*, 2025). These are pro-inflammatory markers involved in medial destruction in GCA (McNally and Anderson, 2011b). Furthermore, IFNγ has been implicated in the formation of granulomas in vivo in immunological reactions to pathogens such as M.*tb* (Byrd, 1998). Conversely, IL-4 stimulation is linked to the release of anti-inflammatory cytokines such as IL-10 (McNally and Anderson, 2011b) suggesting that the FBGCs that results from M-CSF and IL-4 stimulation are anti-inflammatory in nature. Supporting this, FBGCS were found to exert a protective role in a mouse model of their formation (Trout and Holian, 2020). Therefore, the presence of both types of MGCs, FBGCs and LHGCs in GCA when cultured with GM-CSF and IFNγ may suggest that MGCs are involved in both media destruction (pro-inflammatory) and intimal hyperplasia (aberrant anti-inflammatory mechanism). To understand the differences between these cells in GCA, future studies could involve laser capture microdissection of both MGC morphologies from GCA tissue and subsequent RNAseq for the whole transcriptomic atlas, as previously reported (Zhang *et al.*, 2022). Alternatively, Single cell spatial transcriptomic platforms, described in the previous chapter (Section 3.3) could be used to explore differences in these MGC subtypes.

It was observed that the sequential stimulation with M-CSF followed by GM-CSF could stimulate monocytes to become MGCs regardless of the additional of IL-4 and/or IFNγ. Interestingly, the same increase in MGC numbers was not observed when cells were first cultured with M-CSF followed by GM-CSF. One study suggests that monocytes and macrophages see both M-CSF and GM-CSF in the GCA vessel (Jiemy *et al.*, 2020). However, this study proposed a model of GM-CSF and M-CSF gradient where GM-CSF is found in the adventitia and M-CSF is found mainly in the media and intima. This is in contrast to the presented data and should be further explored.

However, large variability among donors and a high standard deviation suggest that this experimental technique leads to inconsistent response and donor

numbers need to be increased in future studies to better understand this mechanism in MGC formation.

To further demonstrate that MGCs cultured with GM-CSF and IFNγ are phenotypically similar to MGCs found in GCA tissue, markers which had high transcriptional and protein expression in spatial transcriptomic analysis were assessed in *in vitro* generated MGCs. Both MMP9 and CTSD were expressed in MGCs generated under both GM-CSF+ IFNγ and M-CSF+IL-4. However, the localisation of these markers within the MGCs varied between the two conditions. MGCs cultured with GM-CSF+IFNγ stained strongly for MMP9 and CTSD in their cytoplasm, whereas those stimulated with M-CSF+IL-4 stained stronger in the nucleus. The difference in localisation may indicate differing functions between these two cell types. Cytosolic and extracellular MMP-9 has been widely shown to be involved in the matrix degradation in GCA (Zhu *et al.*, 2007). However, intranuclear MMP9 is thought to be involved in inducing apoptosis in neuronal cells, suggesting M-CSF induced MGCs are primed for apoptosis (Pirici *et al.*, 2012).
Interestingly, this difference in cellular location has been demonstrated in previous literature in macrophages but has not been described in MGCs before. Macrophages have differing MMP9 localisation and function when stimulated with IFNγ compared to IL-4. Stimulation with IFNγ has been shown to increase the extracellular secretion of MMP9 leading to breakdown of extracellular matrix etc. Whereas, IL-4 stimulation increases nuclear translocation of MMP9 and subsequent intracellular proteolysis (Bernaerts *et al.*, 2024). The cytosolic expression of both markers reported in MGCs, within the GCA tissue, further demonstrates the similarity between MGCs generated with GM-CSF+ IFNγ to those within the tissue, rather than those generated with M-CSF+IL-4 (section 3.3.5).

Similar to tissue MGCs, both TRAP positive and negative MGCs were observed in culture. The morphology of the MGCs, classified as LGHC and FBGCs, was not a factor in whether cells stained positively for TRAP or not. One possible explanation for this heterogeneity is the existence of distinct TRAP isoforms. Two isoforms of TRAP are discussed in current literature, form 5a and 5b. Isoform 5b is primarily associated with osteoclast activity and bone matrix

degradation, whereas isoform 5a is linked to inflammatory macrophage function (Janckila *et al.*, 2007). Since conventional histological TRAP staining cannot differentiate between these two isoforms (Barbeck *et al.*, 2022), it is plausible that TRAP-positive MGCs may be expressing the pro-inflammatory isoform TRAP 5a, yet TRAP-negative may represent a different activation stage or lineage. To clarify this, future studies should employ monoclonal antibodies against the specific TRAP isoforms.

The lack of significant difference between GM-CSF+ IFNγ MGC numbers between GCA and healthy controls may be attributed to variation in donors. As previously mentioned, MGCs are present in around 50% of TAB tissues from GCA patients (Weyand and Goronzy, 2023). While this could be attributed to skip lesions meaning MGCs are missed in histological sectioning, it could also be due to a lack of MGCs in certain GCA patients (Albert, Ruchman and Keltner, 1976). This raises questions about what factors lead to the production of MGCs in some GCA patients and not others. These differences between GCA patients may be explained by disease activity. However, this data was not collected and should be implemented in future studies.
One explanation for high numbers of MGC from healthy control monocytes when cultured with GM-CSF+ IFNγ could be age-associated cellular senescence. As GCA is an age-related disease, healthy controls were all over 50 years of age and MGC formation has been linked to an ageing immune system. Ageing cells become senescent, where cells have reversible cell cycle arrest and stop dividing but do not die. This senescence is associated with increased release of pro-inflammatory cytokines known as a Senescence Associated Secretory Phenotype (SASP). These cytokines include, among others, IFNγ and GM-CSF (Kloc *et al.*, 2022).

Despite the usefulness of this model to understand the formation and modulation of MGCs in vitro, it is not without limitations. Firstly, this reductionist approach to a model of MGC formation does not fully depict the physiology of GCA, nor does it address the cellular source(s) of GM-CSF and IFNγ in the progression of the disease. Furthermore, as this model lacks signals from surrounding GCA tissue. As shown in the previous chapter, macrophages display spatial and tissue heterogeneity in disease. Therefore, future studies should aim to build on this

model in order to understand the cellular interactions involved in the formation of MGCs as well as potentially building a model which involves GCA tissue that may lead to polarisation of pathogenic macrophages in this disease.

In conclusion, MGCs that resemble those observed in GCA tissue can be generated in vitro using monocytes enriched from peripheral blood of GCA patients. Stimulation with GM-CSF and IFNγ appears to be the predominant pathway driving the formation of MGCs in this disease-specific context. Whereas monocytes from healthy individuals were more likely to form MGCs when simulated with M-CSF and IL-4.

Furthermore, while both LGHC and FBGC subtypes could be observed in GCA tissue, this morphological diversity was only recapitulated in vitro when GCA patient-derived monocytes were stimulated with GM-CSF and IFNγ. Monocytes from healthy controls did not form both subtypes under the same condition. These findings suggests that GCA monocytes may be intrinsically primed to form both types of MGC in response to GM-CSF and IFNγ. Therefore, the following chapters aimed to answer the question, are GCA monocytes phenotypically and transcriptionally different to those from healthy individuals?

Chapter 5 Investigating the circulating monocyte population.

5.1 Introduction

The previous chapter explored the differences in the ability of healthy and GCA myeloid cells to form MGCs. Monocytes isolated from the peripheral blood of GCA patients were more likely, than healthy control monocytes, to form both LHGCs and FBGCs when stimulated with GM-CSF and IFNγ. The results of these experiments lead to the question of whether circulating monocytes in GCA are pre-primed to become MGCs. To answer this question, the surface expression of cytokine and chemokine receptors was analysed by flow cytometry and the transcriptional and epigenetic profiles of these monocytes by bulk RNA-Seq and CUT&Tag, respectively.

Monocytes are key players in the pathogenesis of GCA. It is thought that circulating monocytes invade the vessels by aberrant production of MMP9 (Watanabe *et al.*, 2018), which degrades the endothelium and paves the way for inflammatory T cells. Thus, initiating the pathogenesis of the disease (see section *introduction section 1.2.1.1.*)
Monocyte-derived macrophages have been shown to be the predominant form of macrophages contributing to vascular immunopathology, in contrast to embryonic progenitor derived tissue resident macrophages (Watanabe and Hashimoto, 2022b). This suggests that circulating monocytes may contain a precursor population, which are already primed to become MGCs, before entering GCA vessels. Furthermore, it was shown in the previous chapter that the cytokines GM-CSF and IFNγ were key players in the formation of MGCs in GCA and therefore, it is important to understand whether circulating monocytes have a greater capacity to respond to these cytokines.
A monocyte precursor population has not yet been described for MGCs found in GCA vessels. However, (Ansalone, Cole, Chilaka, Sunzini, Sood, Robertson, Siebert, Iain B McInnes, *et al.*, 2021) used flow cytometry with epigenetics to determine a specific monocyte precursor population of osteoclasts in RA

patients. While these cells are found in different environmental niches and have different functions, they are closely related MGCs of monocytic origin.

The process of chemotaxis (the movement of cells towards chemokine gradients) is important for the movement of cells in homeostasis. Furthermore, as it is hypothesised that MGCs form from the fusion of macrophages, it can be assumed that chemokines and their receptors are crucial in the process. Monocyte associated chemokine receptors such as CCR2 and CX3CR1 could be observed in GCA TABs in macrophage rich regions (van Sleen, Wang, Kornelis S.M. van der Geest, *et al.*, 2017). Furthermore, previous studies of MGCs in other disease contexts have shown that chemokine receptors such as CCR5 and CCR2 were expressed by FBGCs and osteoclast cells respectively. This shows their importance in this process (Khan *et al.*, 2014).
Therefore, the presence of chemokine receptors thought to be involved in the movement of cells towards the vessel and potentially involved in the fusion of macrophages were investigated.

Additionally, epigenetic mechanisms such as post-translational modifications may play a role in the differences in healthy versus GCA monocytes. Epigenetic modifications influence cell function by modulating expression or repression of genes.
There are a number of epigenetic modifications which can occur due to developmental or environmental factors (Davis and Gallagher, 2019). These include DNA methylation and post-translational histone modifications. DNA methylation has been shown to be highly prevalent on monocytes on GCA specific genes such as CD63, a tetraspanin molecule involved in leukocyte migration and production of VEGF (Estupiñán-Moreno *et al.*, 2022). However, the presence and influence of histone modifications have yet not been analysed in GCA.
Histone post-translational modifications alter chromatin compaction and signalling leading to control of gene expression, i.e. the switching on or off of genes. A number of histone modifications can alter the state of genes, named for the histone, residue and modification type. The modifications focused on in this chapter are H3K4Me3, and H3K27Me3. H3K4Me3 (trimethylation of Histone 3 at Lysine 4) is a modification found at the transcription start sign of genes and

thought to be involved in the activation of genes (Benayoun *et al.*, 2014). Whereas, H3K27Me3 is thought to function as a silencer and repressor of genes (Cai *et al.*, 2021).
Studying the epigenetic profile of GCA circulating monocytes may shed light on monocytes which are primed to become MGCs and, therefore, could lead to the identification of potential drug targets. Furthermore, a better understanding of epigenetic mechanisms, in circulating monocytes could lead to a better understanding of the myeloid compartment in disease as a whole.

To assess the presence and influence of post-translational modifications in GCA, Cleavage Under Targets and Tagmentation (CUT&Tag) analysis was performed. This technique involves the binding of specific chromatin proteins of interest to an antibody. This antibody tethers to a A-Tn5 transposase fusion protein. Activation of this protein fragments the chromatin into libraries which can then be sequenced (Kaya-Okur *et al.*, 2019). This method was used instead of ChIP-seq analysis as it can be run using a much smaller number of cells and give a better signal-to-noise ratio outcome, due to the specificity of the Tn5 integration (Kaya-Okur *et al.*, 2020). As little as 5000 cells can be used to produce high quality data with CUT&Tag, whereas between 1 and 10 million cells are needed for ChIP-seq due to the poor signal to noise ratio (Abbasova *et al.*, 2025).
Finally, RNA-Seq of circulating monocytes was completed simultaneously to further understand differences in monocytes from GCA patients compared to healthy controls.

Therefore, this chapter investigates the surface molecule expression and presence of post-translational histone modifications in GCA through flow-cytometric analysis of surface molecule expression and CUT&Tag analysis of histone modifications. Understanding the circulating monocyte population differences between GCA and healthy controls could help to understand why GCA monocytes are more likely to form MGCs, as described in previous chapters, and, potentially identify novel drug targets.

5.2 Results

5.2.1 GCA monocytes have higher expression of chemokine and growth factor receptors than healthy monocytes.

The previous chapter demonstrated that GCA monocytes were more likely to fuse into MGCs than healthy control monocytes when cultured with IFNγ and GM-CSF. To investigate whether GCA monocytes are pre-primed for MGC formation, flow cytometry was performed to analyse the surface expression of cytokine and chemokine receptors on circulating monocytes from GCA patients and healthy peripheral blood. Patient information is described in the previous chapter (Table 4.1 and Table 4.2 section 4.2.1).

PBMCs were first gated for singlets and live cells using a fixable viability dye. Lineage-positive cells were excluded using a lineage marker cocktail (CD3 for T-cells, CD19 for B cells, CD56 for natural killer cells and CD15 for granulocytes such as neutrophils and eosinophils). HLA-DR expression was used to select antigen presenting cells. Finally, monocytes were subsequently identified based on CD14 and CD16 expression (Figure 5.1a).

To assess surface marker expression, monocytes were stained with antibodies against selected cytokine and chemokine receptors and fluorescence minus one (FMO) controls were used to define positive gates for each receptor (Figure 5.1b and 5.1c).

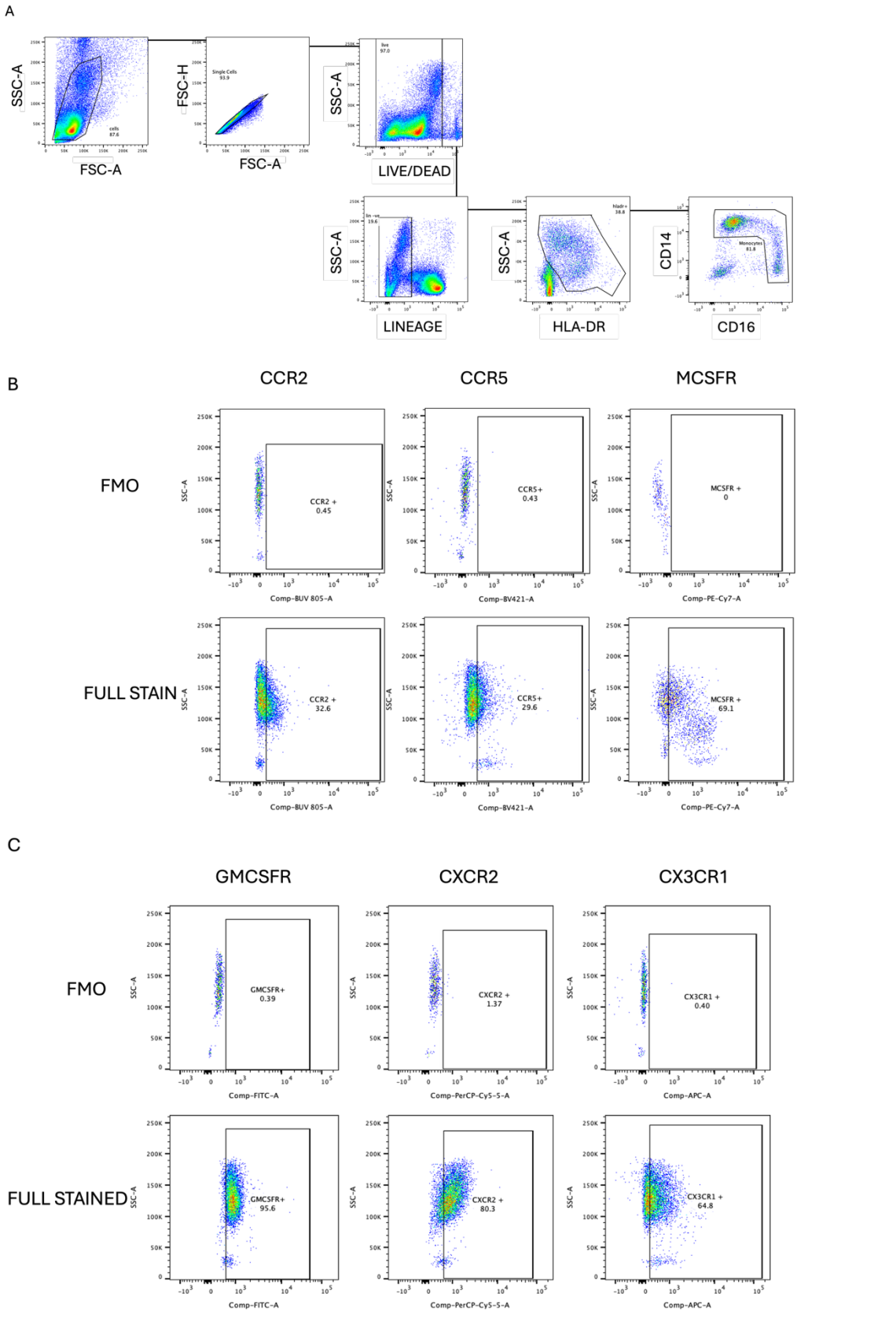

Figure 5.1 : Representative gating strategy of surface marker expression in monocytes. (A) Monocytes were gated from stained PBMCs based on live/dead staining, lack of T and B cell linage markers HLA-DR positivity and the expression of CD14/CD16. For all surface markers of interest, fluorescence minus one (FMO) controls to set the positive gate. Cells were

stained with antibodies for (B) CCR2, CCR5, MCSFR, (C) GMCSFR, CXCR2 and CX3CR1 (see methods section 2.3.1). Percentage of marker expression is shown on each plot.

Analysis of chemokine and cytokine receptors in GCA versus healthy control monocytes showed that GCA monocytes have altered surface receptor expression (Figure 5.2). Some markers did not differ between healthy monocytes and GCA monocytes such as, the M-CSF receptor which was expressed by ~25% of healthy monocytes and around 30% of GCA monocytes. However, both chemokine receptor 5 (CCR5) and GM-CSF receptor showed a significant increase in expression in GCA compared to healthy monocytes. CCR5 was expressed by only 20% of healthy control monocytes but around 50% of GCA monocytes expressed this chemokine receptor (P = 0.014). Interestingly, CCR5 expression on GCA monocytes appeared to be split into two groups: one of high expression (~90-100%); and one of low expression (~20-35%) suggesting variation in expression between GCA patients. Similarly, GM-CSFR was expressed by around 25% of healthy monocytes, whereas around 80% GCA monocytes were positive for GM-CSFR expression (*P* = 0.0001). This difference in GM-CSFR may explain the increase in MGC numbers when GCA monocytes were cultured with GM-CSF. Next, it was important to determine whether receptor expression was altered on different monocyte subsets in GCA versus healthy controls.

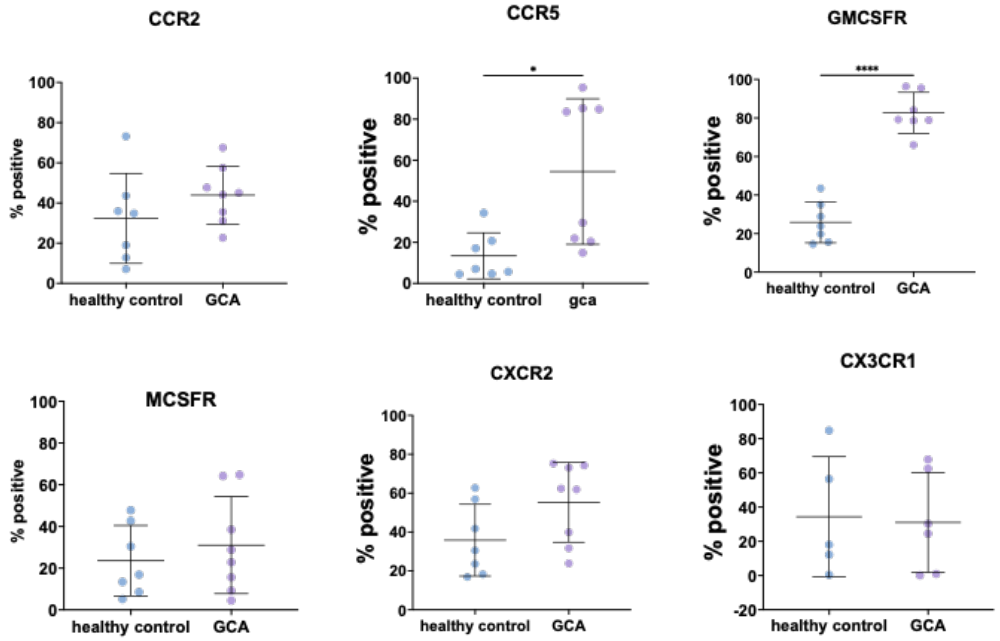

Figure 5.2 : GCA monocytes express different cell surface markers. Quantification of percentage of cells positive for each surface marker in healthy versus GCA monocytes. Points represent individual donors (healthy N=7, GCA N=8). Graphs generated in GraphPad Prism. Error bars represent mean with SD. One-way ANOVA analysis. *P<0.05, ****P<0.0001.

There are three main monocytes subsets based on differing expression of CD14 and CD16 markers. These are: classical ($CD14^{+}CD16^{-}$); intermediate ($CD14^{+}CD16^{+}$); and non-classical ($CD14^{low}CD16^{+}$). In GCA, previous studies have shown an increase in circulating monocyte numbers in GCA compared to healthy peripheral blood, particularly the classical monocyte subset (Reitsema *et al.*, 2023). To determine whether this could be observed in our cohort and whether monocyte subsets have altered receptor expression, monocytes were gated into subsets based on CD14 and CD16 expression (Figure 5.3a). Unexpectedly, analysis of monocyte percentages showed no significant difference in the percentage of classical, intermediate or non-classical monocytes (Figure 5b) between healthy and GCA peripheral blood. However, this means that differences observed in receptor expression between healthy and GCA subsets are not due to differing numbers of each subset.

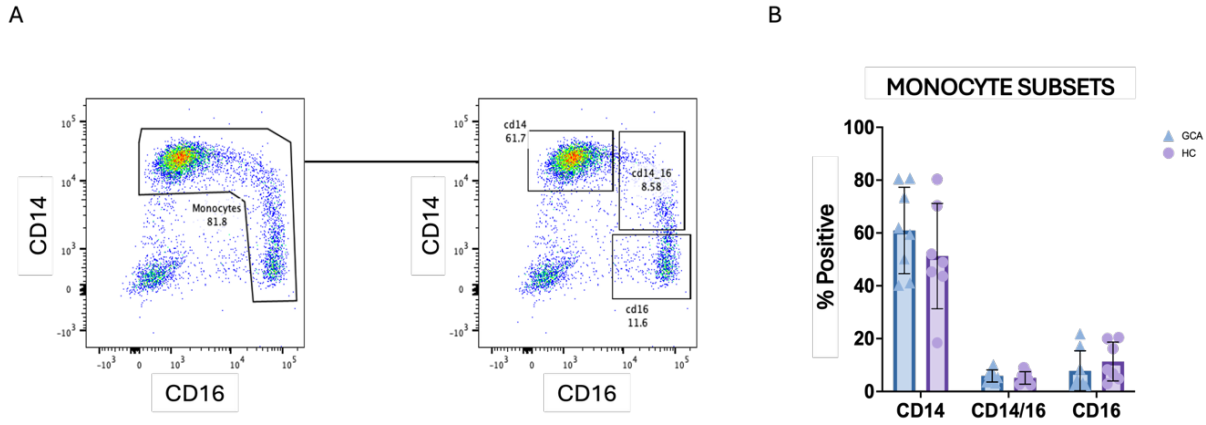

Figure 5.3 : No differences in monocyte subset numbers between GCA and healthy monocytes. Monocytes were gated into classical, Intermediate and non-classical based on expression of CD14 and CD16. ($CD14^{high}CD16^{-}$, $CD14^{high}CD16^{+}$ and $CD14^{Low}CD16^{+}$ respectively (A) Representative image of gating. (B) Quantification of monocyte subsets in healthy versus GCA. Points represent individual donors, bars represent mean. Error bars represent SD. Healthy N=7, GCA N=8. Two-way ANOVA performed in GraphPad Prism.

Next, surface marker expression was analysed on monocyte subsets in both GCA and healthy control blood (Figure 5.4). This analysis showed that expression patterns differed between subsets. CCR5 expression was significantly increased in GCA classical monocytes (20-100% of GCA monocytes compared to < 20% of healthy control monocytes, $P = 0.0001$), as well as on intermediate monocytes (30-90% in GCA *vs* ~30% in healthy controls, $P = 0.0014$). As described in monocytes as a whole, there was wide variation in CCR5 expression across GCA donors in classical monocytes, with low, medium, and high expressor groups observed. Similarly, classical monocytes from GCA patients displayed significant increase of GM-CSFR expression compared to healthy controls: specifically,

almost all classical monocytes in GCA cases expressed GM-CSFR, compared to ~60-80% in healthy controls (*P* = 0.02). This may suggest that increased CCR5 and GM-CSFR leads to an increased responsiveness of these monocytes to their respective ligands, such as CCL3,4,5 and GM-CSF. This increased response may enhance their recruitment to tissue and MGC formation in GCA. Intriguingly, CXCR2 expression, which was not significantly different when monocytes were analysed as a whole, was increased in both classical and intermediate subsets from GCA peripheral blood, but not in healthy controls (*P* = 0.035 and *P*=0.0001, respectively). Upregulation of this chemokine receptor could indicate a role for this chemokine in GCA, but its functional relevance has not yet been established. Taken together, these findings are consistent with a potential role for CCR5 in the recruitment of circulating monocyte, and possibly in MGC formation. Furthermore, increased expression of GM-CSF receptor on classical monocytes in GCA peripheral blood, but not on intermediate and non-classical subsets, may suggest that this population is more responsive to GM-CSF and could explain the increased MGC formation in GM-CSF and IFNγ cultures. The functional significance of these observations will be explored further in this and subsequent chapters.

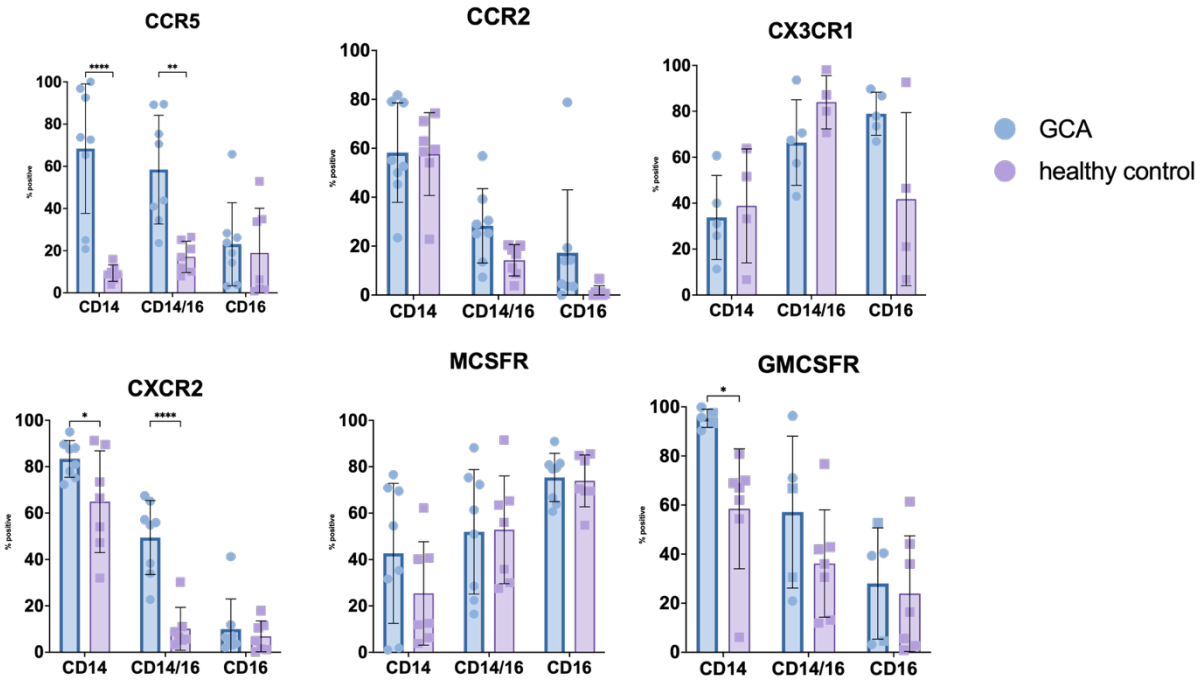

Figure 5.4 : Difference in surface markers is subset dependent.Percentage of marker positive cells were plotted using GraphPad Prism. Points represent individual donors (healthy N= 7, GCA N= 8.) error bars and bars represent mean with SD. One–way ANOVAs were calculated. *P-value= <0.05, **P < 0.01, ****P < 0.0001. Graphs and statistical analysis were performed using GraphPad Prism. N=3.

To build on these findings, transcription and epigenetic modifications in circulating monocytes from GCA patients were next examined. This analysis aimed, not only to validate surface expression observed by flow cytometry, but also to further investigate differences between healthy and GCA monocytes - and to explore why monocytes in GCA may be more prone to forming MGCs.

5.2.2 Patient characteristics of samples used for transcriptomic and epigenetic profiling.

The patient samples used for CUT&Tag and RNA-Seq analysis were collected as part of the TARDIS study (see methods section 2.1.3), with blood collected at the time of diagnosis, six GCA cases were compared to six non-GCA controls (Table 5.1 & 5.2).

Control participants had a mean age of 70.8 years (range 64-88) (Table 5.1), while GCA patients had a mean age of 76 years (range 68-83) years of age (Table 5.2). Steroid exposure is known to influence gene expression and regulation (Barnes, 2006). A key strength of the TARDIS cohort is that both GCA and control samples have received comparable steroid treatment in terms of dose and duration. This ensures that any observed gene expression changes are not attributable to differences in steroid exposure.

Patient	Age	Sex	CRP (mg/l)	ESR (mm/hr)	Pre-biopsy steroids (mg)	Tocilizumab
TARDIS_09	72	F	29	49	440	no
TARDIS_15	65	M	156	55	1200	no
TARDIS_37	70	F	93	92	400	no
TARDIS_33	64	M	21	34	1100	no
TARDIS_21	88	F	31	44	480	no
TARDIS_20	66	M	114	107	660	no

Table 5.1: TARDIS control patient information.M- male, F- female, CRP- C-reactive protein, ESR – erythrocyte sedimentation rate. Prebiopsy steroids, the volume of steroids taken before TAB biopsy and blood samples taken.

Patient	Age	Sex	CRP (mg/l)	ESR (mm/hr)	Pre-biopsy steroids (mg)	Tocilizumab
TARDIS_11	83	M	138	82	920	no
TARDIS_16	68	M	30	37	640	no
TARDIS_02	69	F	176	91	60	no
TARDIS_31	76	F	73	41	920	no
TARDIS_30	79	F	104	69	1200	yes
TARDIS_18	81	F	66	59	660	no

Table 5.2 : TARDIS GCA positive patient information.M- male, F- female, CRP- C-reactive protein, ESR – erythrocyte sedimentation rate. Prebiopsy steroids, the volume of steroids taken before TAB biopsy and blood samples taken.

5.2.3 Expression profile differences between healthy and GCA monocytes.

To investigate potential transcriptional differences, differential gene expression analysis was performed using DESeq2, comparing monocytes from GCA patients and non-GCA controls. Samples TARDIS_21 and TARDIS_31 were not sequenced as not enough cells were purified to run CUT&Tag and RNA-Seq, Furthermore, TARDIS_02 was excluded from the analysis due to an insufficient number of sequenced reads, due to low RNA input. Principal component analysis did not show a clear separation between groups. Two GCA samples clustered closely with the control samples, while the remaining two GCA samples were distinct. (Figure 5.5a). The lack of separation between GCA and control samples in the PCA may reflect shared inflammatory profiles (Table 5.1), the effects of steroid treatment, and the small sample size, which together could limit the ability to detect distinct clustering. However, there was large variation in GCA samples which may indicate heterogeneity among the GCA donors, with one obvious outlier. This outlier was TARDIS_30, the only patient to have received Tocilizumab treatment. Next, the most differentially expressed genes between control and GCA were investigated. Only 8 genes were found to be differentially expressed between GCA and control monocytes. Due to the small sample size and exploratory nature of this analysis, unadjusted *P*-values of <0.05 were used in place of adjusted P-values (P.adj) for differential expression and over-representation analysis (ORA). Therefore, results should be interpreted with caution and future studies should aim to increase the sample size to validate these findings. This showed 130 upregulated (log2Fold >1) genes and 35 down regulated (log2Fold <-1) genes in GCA compared to healthy control. The top 5 most upregulated (red) and downregulated (blue) genes in GCA are labelled (Figure 5.5b). The top 5 most upregulated genes in GCA were CDCA5, PRSS21, TPX2, MELK and ANKRD36BP2. Whereas, the most downregulated genes in GCA were MAP7, CASC8, PTPN13, MUC20 and GPR34. Further analysis of differentially expressed genes showed relatively uniform expression of upregulated genes in the control group but a varied expression of upregulated genes in the GCA group, which further suggests variability between GCA samples (Figure 5.5c). Interestingly, upon further inspection, the GCA sample TARDIS_30, had very high expression of genes (log fold change > 2). This was the only sample to have received Tocilizumab treatment.

Lastly, gene set enrichment pathway analysis was conducted using the most upregulated genes in GCA. This showed 17 significantly enriched pathways (FDR

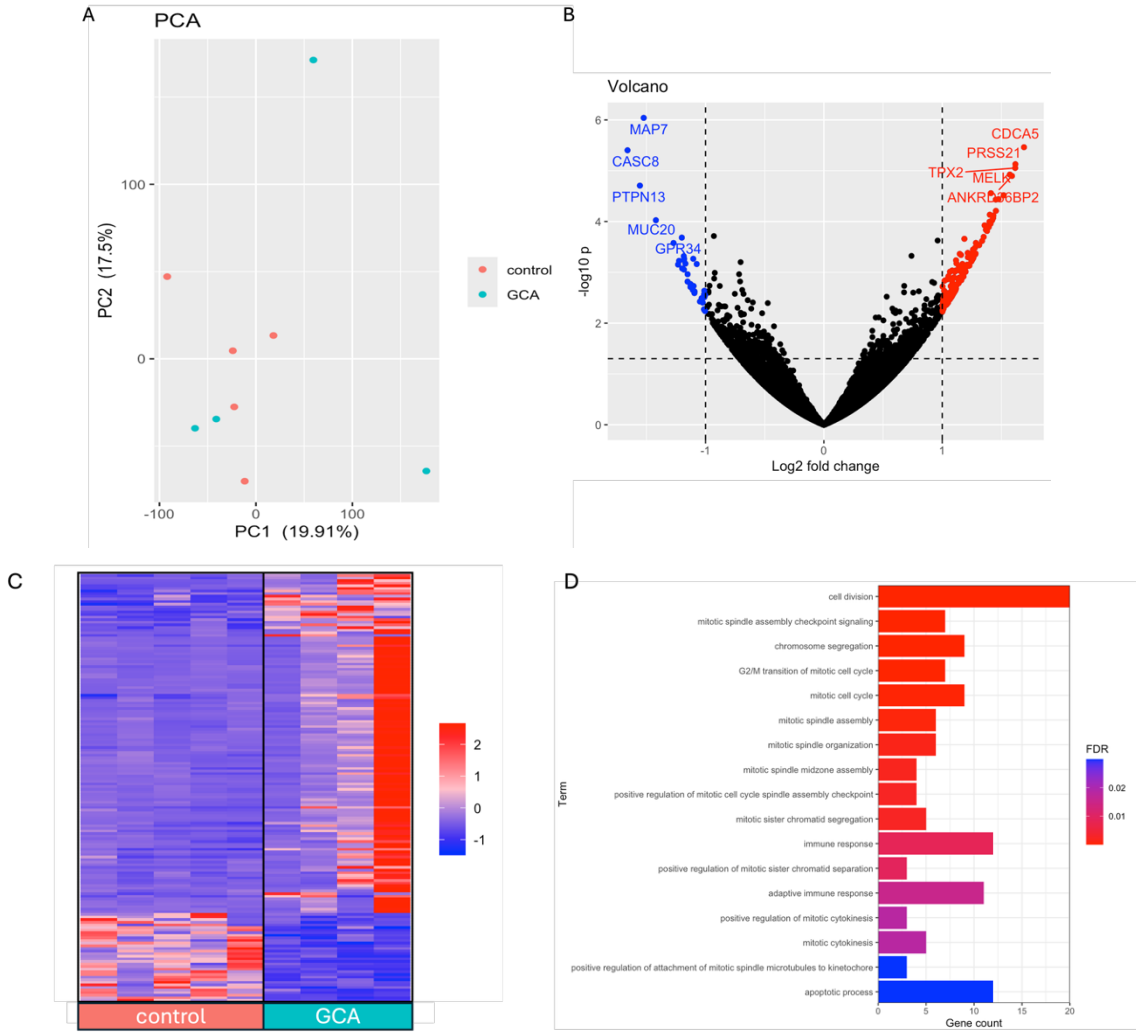

Figure 5.5 : Minimal differences in transcription profiles between GCA and control.RNA-seq data of differential gene expression between control (GCA negative) N – 5 and GCA (GCA positive) N =4. (A) Principal component analysis (PCA) scatter plot of PC1 and PC2 for GCA vs Control. The percentage of total variation explained by each component is given on its axis. Each point represents a donor. (B) Volcano plot of most differentially expressed genes. Dots represent a gene, blue dots = log2fold change < -1 red dots log2fold change > 1. Top 5 most differential genes are labelled. (C) Heatmap of differentially expressed genes in GCA vs Control (P.adj < 0.05). Colours represent log fold change red > 0 blue <0. (D) Over representation analysis (ORA) of differentially expressed genes related to biological function. false discovery rate (FDR) < 0.05.

<0.05). Most enriched pathways concerned cell division processes such as mitotic cell cycle apoptosis and immune response.

To better understand these pathways in GCA and control monocytes, expression of associated genes was analysed (Figure 5.6). This showed significant upregulation of genes associated with these pathways were consistently upregulated in GCA monocytes compared to controls. For example, genes involved in mitotic cytokinesis and cell division such as, CDCA8, BIRC5 and AURKB were ~0.5 fold more expressed in GCA monocytes compared to controls.

Interestingly, a number of immunoglobulin related genes (IGKV3-15, IGKV4-1 and IGHA1) were upregulated in GCA monocytes compared to controls suggesting a role for immunoglobulins in GCA monocytes.

Lastly, transcription of genes of interest from previous flow cytometric studies were investigated in GCA vs control (Figure 5.7). CCR2 and CCR5 were not significantly different in GCA and control despite differences in surface marker expression. In concordance with *in vitro* data generated in the previous chapter, M-CSFR was more expressed in controls than GCA monocytes whereas, GM-CSFR was more expressed in GCA monocytes. However, neither reached statistical significance. Furthermore, flow cytometry data (Figure 1.4) demonstrates that this increase in transcription leads to an increase of GM-CFR expression on the surface of GCA monocytes but not an increase in M-CSFR expression on control monocytes. Interestingly, both CXCR2 and MMP9 were significantly different in GCA versus control. MMP9 has been shown, in previous studies, to be upregulated in GCA monocytes (Estupiñán-Moreno *et al.*, 2022) and an increase in MMP9 protein expression on the cells is thought to cause the media destruction that paves the way for T Cell entry into cranial vessels(Watanabe *et al.*, 2018). However, CXCR2 was upregulated in control monocytes which contradicts the flow cytometry data in section 5.2.1.

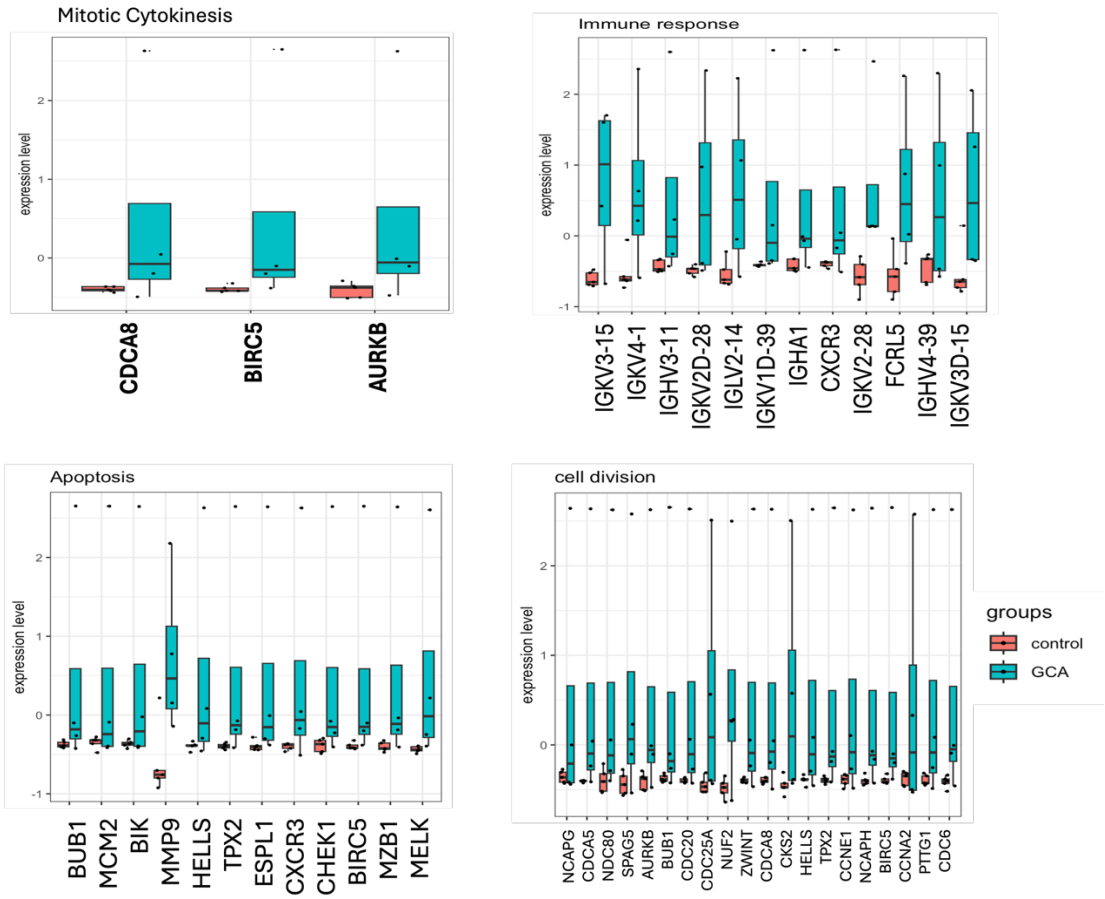

Figure 5.6: Upregulated GCA genes are associated with cell cycle processes. Boxplots showing gene expression in genes associated with enriched biological processes from Over representation analysis (ORA) of differentially expressed genes. Control N = 5, GCA N = 4.

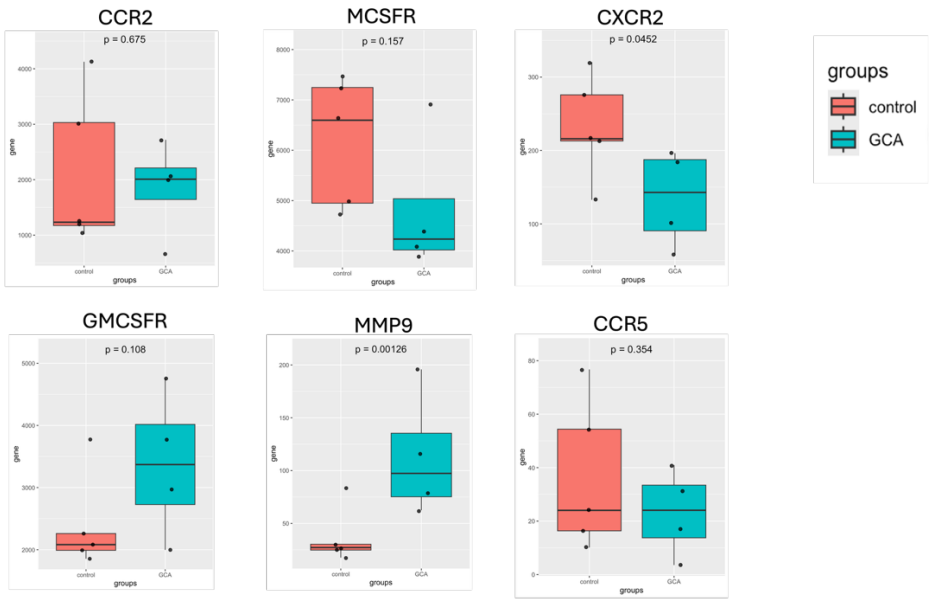

Figure 5.7: Differential expression of genes of interest. Transcription profiles of genes of interest from flow cytometric analysis were investigated in GCA vs Control monocytes. Box plots of gene expression values in control (coral) vs GCA (teal). P-value is shown on the graph. Significance P < 0.05.

5.2.4 Epigenetic modifications in GCA monocytes.

5.2.4.1 CUT&Tag Quality control data.

Finally, to better understand the mechanisms involved in expression differences between GCA and control monocytes, epigenetic changes, known as histone modifications, were investigated in monocytes derived from GCA patients in comparison to non-GCA controls.

Histone modifications were analysed using CUT&Tag sequencing. CUT&Tag analysis was chosen over CHIP-SEQ due to low cell numbers recovered from frozen PBMCs. CUT&Tag is a low-input technique which can be performed with as few as 5000-50000 cells (Kaya-Okur *et al.*, 2019), making it well suited to limited primary cell populations such as patient derived monocytes. To ensure reliability of results, several quality control steps were carried out on sequenced data. To assess quality of CUT&Tag sequencing data, the online tool FastQC was used (Andrews, 2010). Firstly, the mean quality score of each sample per base was plotted by the software (Figure 5.8). Most samples passed this quality check with base calling falling in the 'green' range (corresponding to very good quality). However, samples TARDIS_02 and TARDIS_09 had lower quality calls at higher base pair positions. It is important to note that these samples still fall under the very good quality range and passed the check.

The average number of sequenced reads per sample group, GC percentage, and percentage of duplicate reads for both H3K4Me3 and H3K27Me3 are summarised in table 5.3. The mean number of reads per group for H3K27Me3 ranged from ~25 to 50 million reads, which exceeds the recommended minimum sequencing depth of 2 million reads (Ay-Berthomieu, 2020). Similarly, control samples for H3K4Me3 yielded an average of 12 million reads. However, the GCA group for H3K4Me3 had a substantially lower average read count of only ~940,000 reads, falling below the threshold required for reliable analysis. Due to constraints in sample availability and time, these samples were, nevertheless, included in the analysis, but the results should be interpreted with caution.
The GC content was comparable across all groups, ranging from 45-53%, which meets FastQC quality standards, given that the average human GC content for a

100kb fragment is ~41% (Lander *et al.*, 2001). The percentage of duplicate reads ranged from 8.7-66%. Duplication rate below 20% are generally considered high quality, while rates under 80% are typically deemed acceptable for downstream analysis (Zheng, 2025).

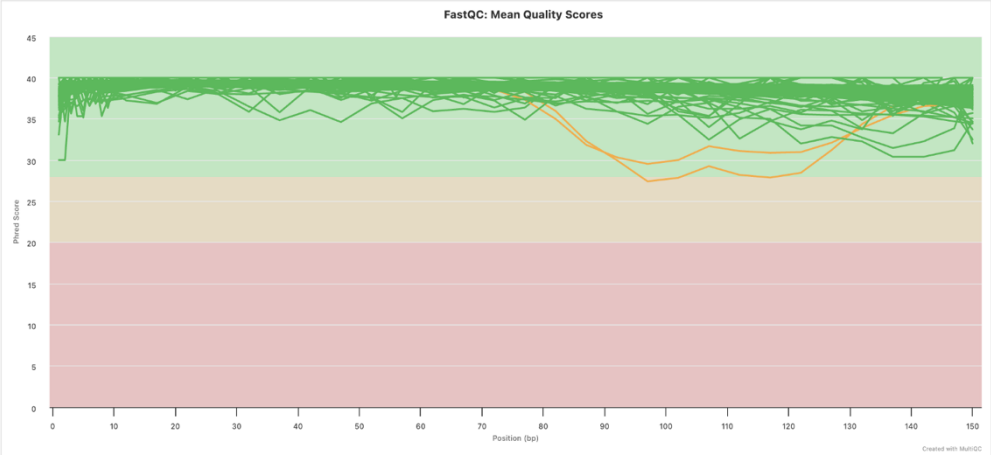

Figure 5.8: CUT&Tag quality control data of H3K4Me3 and H3K27Me3.Quality control analysis was carried out after sequencing. (A) FastQC quality scores of bases called across sequenced fragments. Very good quality (green), reasonable quality (orange) and poor quality (red). Each line represents an individual sample GCA N= 6, control N=6.

Finally, the GoPeaks software was used to call peaks, after reads were aligned to the reference genome. Considerable variability in the numbers of peaks was observed across both sample groups in H3K4Me3 and H3K27Me3 (see Table 5.4 for range). A consensus peak set was, therefore, generated for each sample to assess changes in read distribution. Notably, H3K4Me3 in both GCA and control

sample	group	sequenced reads (millions)	GC Content (%)	Duplicate Reads (%)
H3K4Me3	GCA	0.94	53	44
	Control	12.7	51	66
H3K27Me3	GCA	25.8	51	8.7
	Control	51.7	45	57

Table 5.4: FastQC report summary of reads. Numbers represented as average of each sample.

sample	group	average number of peaks	fraction of reads within peaks (FRiPs)
H3K4Me3	GCA	10473 (2004-16392)	0.04 (0.01-0.06)
	Control	80326 (2433-163779)	0.05 (0.01-0.13)
H3K27Me3	GCA	177957 (56448-8708542)	0.41 (0.29-0.55)
	Control	2222358 (393413-4691721)	0.40177665 (0.3735416-0.4444524)

Table 5.3: Summary of peaks in each sample. Average numbers of peaks and FRiPs in each histone modification and sample group. Range of samples in brackets.

samples had less than 1 million peaks on average, which may have reduced the statistical power of the differential analysis. Fraction of reads within peaks (FRiP) is a quality control metric that shows how many aligned reads fall within the specific called peak regions, where a higher FRiP value indicates a higher signal-to-noise ratio. In this analysis, all FRiPs were above 0.01, this is considered the minimum recommended by ENCODE ChIP-Seq guidelines. There were no differences in FRiP scores between control and GCA sample groups in H3K4Me3 or H3K27me3. However, there was a ~10% difference in FRiP score between H3K4me3 and H3K27Me3. This difference is likely attributable to the distinct genomic distribution of these histone modifications, with H3K4Me3 typically forming narrow peaks at promoter regions and H3K27Me3 forming broader repressive domains. As such, differences in FRiP scores may reflect underlying biological features rather than technical inconsistencies. As all

samples passed initial sequencing QC steps, downstream analysis was carried out accordingly. However, following correction for FRiP scores using ComBat-Seq, some samples were removed, due to extremely low or undetectable read counts. This reduced the overall sample size and might have affected the reliability of subsequent analysis.

In summary, while the data in this chapter meets the minimum criteria for an exploratory analysis, the low sequencing depth of some samples and large variability across groups mean results should be interpreted cautiously. Further analysis with larger cohorts is needed to validate the findings in this thesis.

5.2.4.2 **Altered distribution of H3K27me3 marks in GCA versus control**

DeSeq2 analysis of the H3K27Me3 profile in GCA (n =4) versus control (n=5) showed that the sample groups had a markedly different expression profile, as seen by the separation of the 2 groups in the PCA plot. Control samples displayed high inter-donor variability, whereas GCA samples clustered more closely together. (Figure 5.9a). Comparative analysis identified a number of significantly different peaks in GCA compared to control. Only 430 peaks showed increased signal in GCA, whereas 4634 peaks were decreased in GCA when compared to non-GCA controls (Figure 5.9c). The most significant up- and down-regulated peaks are labelled on the volcano plot (Figure 5.9b). The top upregulated peaks included LINC01619, DENND3, LOC100506472, NPEPL1 and LINCO2087. Conversely, the top five most downregulated peaks were EPYC, RPL23AP87, CCDC4A, DIAPH-AS1 and GPR55. Lastly, heatmap analysis of both control and GCA peaks show some variability among peak expression, with some donors having higher expression than others. This suggests heterogeneity among donors.

To determine whether H3K27Me3 peaks were associated with certain biological pathways in monocytes, over representation analysis (ORA) was conducted on decreased and increased peaks (Figure 5.10a). However, there were no significant (FDR < 0.05) pathways among the increased H3K27Me3 peaks in GCA. Conversely, pathways associated with decreased H3K27Me3 peaks included: cell migration; cell-cell adhesion; and signal transduction (Figure 5.10a). To better understand the involvement of these pathways, the expression of genes associated with them were evaluated (Figure 5.10b). Genes involved in the

positive regulation of gene transcription had increased H3K27Me3 peaks, mostly on control monocytes such as, GPBP1, EBF2, NFATC3 and ACVR1. The only gene to have increased H3K27Me3 on GCA monocytes was NKX2.6. Interestingly the transcription factor CREB1, a transcription factor involved in the activation of the CCR5 gene, was shown to have increased H3K27Me3 on control compared to GCA, suggesting it has reduced gene silencing in GCA. Furthermore, genes associated with cell migration (PDGFRA, CDH8,7 and 6 and TGFBR3) and cell-cell adhesion (ANXA1, ICAM2 and ITGAM1) had increased H3K27Me3 expression on control monocytes compared to GCA monocytes, suggesting GCA monocytes have less repressive marks on these genes, which could indicate increased gene activity.

Finally, to assess whether genes identified in flow cytometry and RNA-Seq analysis of GCA versus control monocytes had altered H3K27me profiles, individual genes such as IFNγ receptor, CCR5 and GM-CSFR were assessed. Analysis of these markers showed that both IFNγ receptor (P=0.0014) and GM-CSF receptor (P=0.04) had significantly increased H3K27me3 peaks in control monocytes compared to GCA monocytes, indicating decreased repression of these genes on GCA monocytes (Figure 5.10a). This may suggest that, transcriptionally, GCA monocytes have less repression in these genes, potentially making them more responsive to stimulation by GM-CSF and IFNγ, consistent with previous *in vitro* data. While CCR5 H3K27me3 peaks were not significantly different between GCA and control (Figure 5.10b), CCR5AS was significantly increased in control (p=0.02). CCR5AS is a long non-coding RNA that is thought to play a role in the stability of CCR5 mRNA, leading to an increase of CCR5 cell surface expression (Kulkarni *et al.*, 2019).

In summary, GCA monocytes have substantial changes in H3K27Me3 profiles compared to control monocytes. These changes correlate with a large decrease in H3K27me3 peaks suggesting a GCA monocytes have less repression of the genes associated with these peaks.

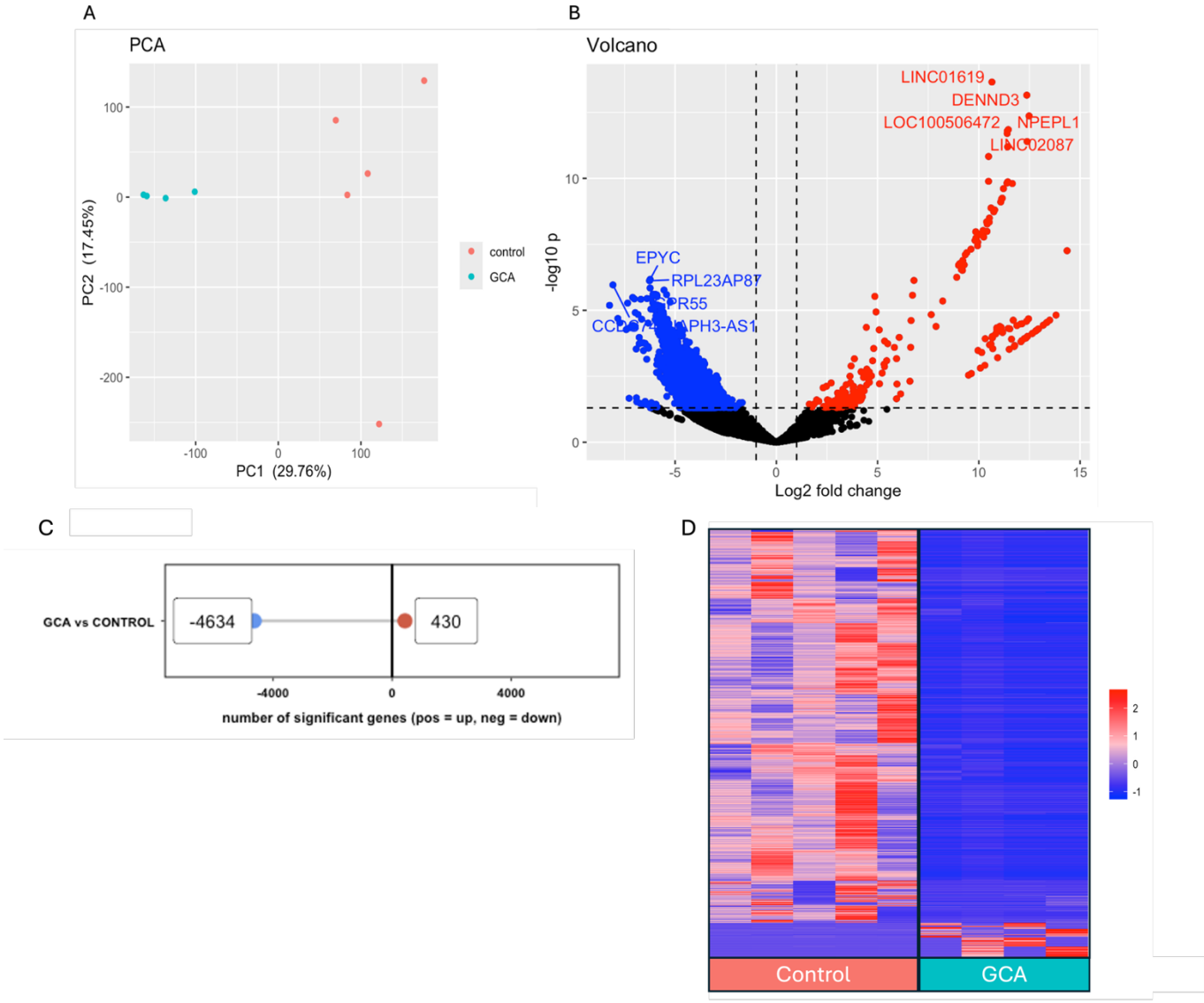

Figure 5.9: Epigenetic changes on the histone H3K27Me3 between control and GCA monocytes.CUT&Tag analysis was conducted using an antibody against H3K27Me3 modification differences between GCA N=4 and control N=5. (A) Principal component analysis (PCA) scatter plot of PC1 and PC2 for GCA vs Control. The percentage of total variation explained by each component is given on its axis. Each point represents a donor. (B) Volcano plot of most differentially expressed genes. Dots represent a gene, blue dots = log2fold change < -1 red dots log2fold change > 1. Top 5 most differential genes are labelled. (C) Lollipop plot showing upregulated in control (represented as downregulated compared to GCA) and upregulated in GCA. (D) Heatmap of differentially expressed genes in GCA vs Control (P.adj < 0.05). Colours represent log fold change red > 1 blue < -1.

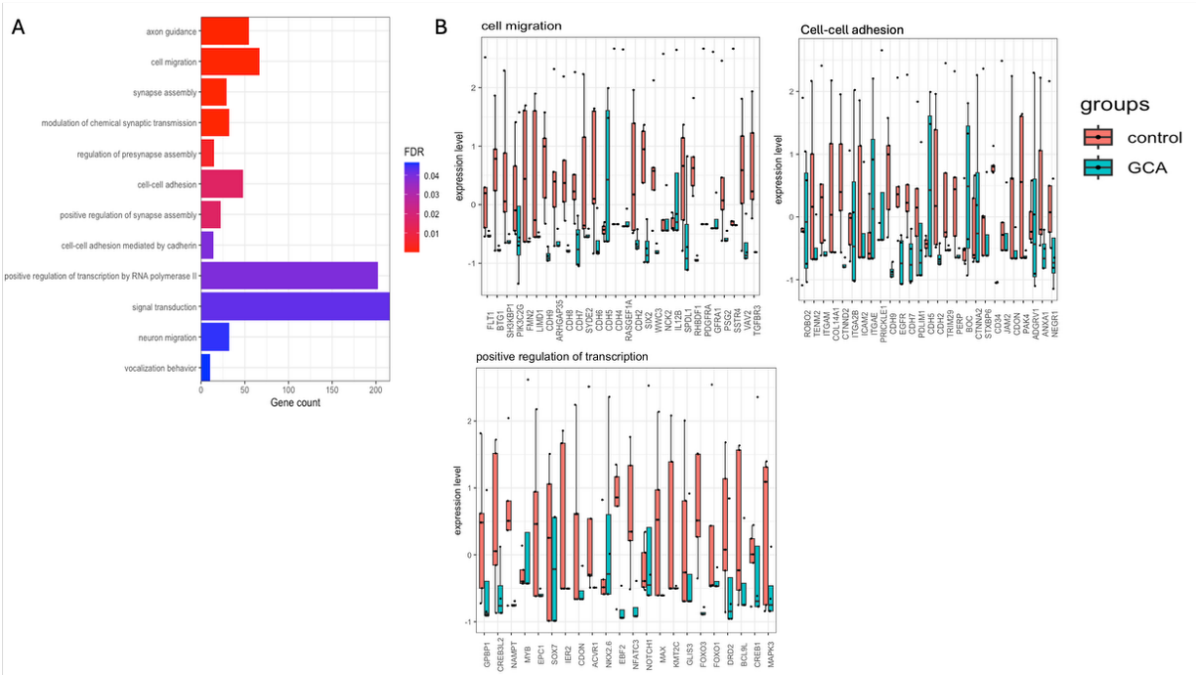

Figure 5.10: Gene set enrichment analysis of H3K27Me3 peaks.(A)Over representation analysis (ORA) of differentially expressed genes related to biological function. False discovery rate (FDR) < 0.05 decreased in GCA. (B) Boxplots showing gene expression in genes associated with enriched biological processes from Over representation analysis (ORA) of differentially expressed genes. Control N = 5, GCA N = 4.

5.2.4.3 Little to no difference in distribution of H3K4me3 marks in GCA versus control.

Differential expression analysis after Combat-Seq correction was carried out on control (n=5) and GCA (n=3) monocytes. This analysis shows that control and GCA samples are mostly different, however, there was slight overlap of one control sample with the GCA sample cluster. Furthermore, the variance of control samples is widespread, suggesting heterogeneity within that group (Figure 5.11a). Due to the small sample size, no peaks reached statistical significance after correcting for multiple testing. Given the exploratory nature of this analysis, a threshold P-value of < 0.05 was used to identify potentially relevant peaks. Therefore, these findings require further validation in future studies. There were less significantly different H3K4Me3 peaks between GCA and control than H3K27Me3 (Figure 5.12b&c), with only 20 significantly decreased peaks in GCA, compared to control and, only 10 increased peaks in GCA. The top 5 most increased peaks include LINC02988, KIAA15490, PPP1R12A-AS1, LOC100507346 and PUDP. Whereas, the top 5 most decreased peaks were HOMEZ, DLEU1-AS1, MIR4275, NGF and MIR4251 (Figure 5.12b).

Heatmap analysis of differentially expressed genes showed large variability in peak expression between both controls and GCA samples, suggesting potential inter-donor heterogeneity in H3k4Me3 profiles (Figure 5.11c). Due to a low number of significantly different genes, ORA and specific gene analysis could not be carried out for H3K4Me3 profiles.

To summarise, relatively few differences in H3K4Me3 peak distributions were observed between GCA and control monocytes although, considerable variability was evident within each group. The majority of differentially marked peaks showed decreased H3K4me3 signal in GCA compared to control, indicating a reduced activation marks in GCA monocytes.

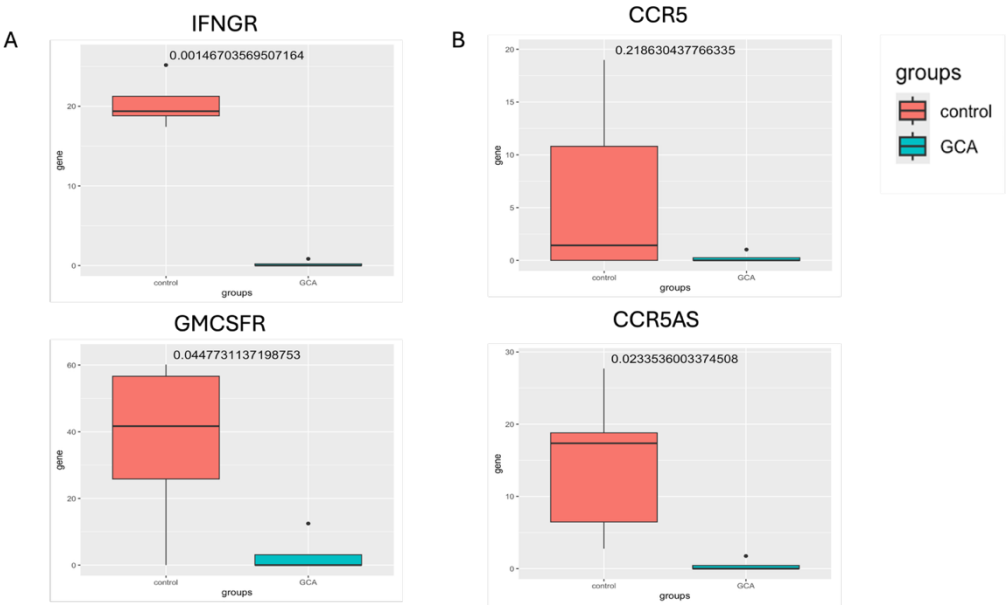

Figure 5.11 Increased repression of MGC related genes in control monocytes.Transcription profiles of genes of interest from flow cytometric analysis were investigated in GCA vs Control monocytes. Box plots of gene expression values in control (coral) vs GCA (teal). P-value is shown on the graph. Significance P < 0.05.

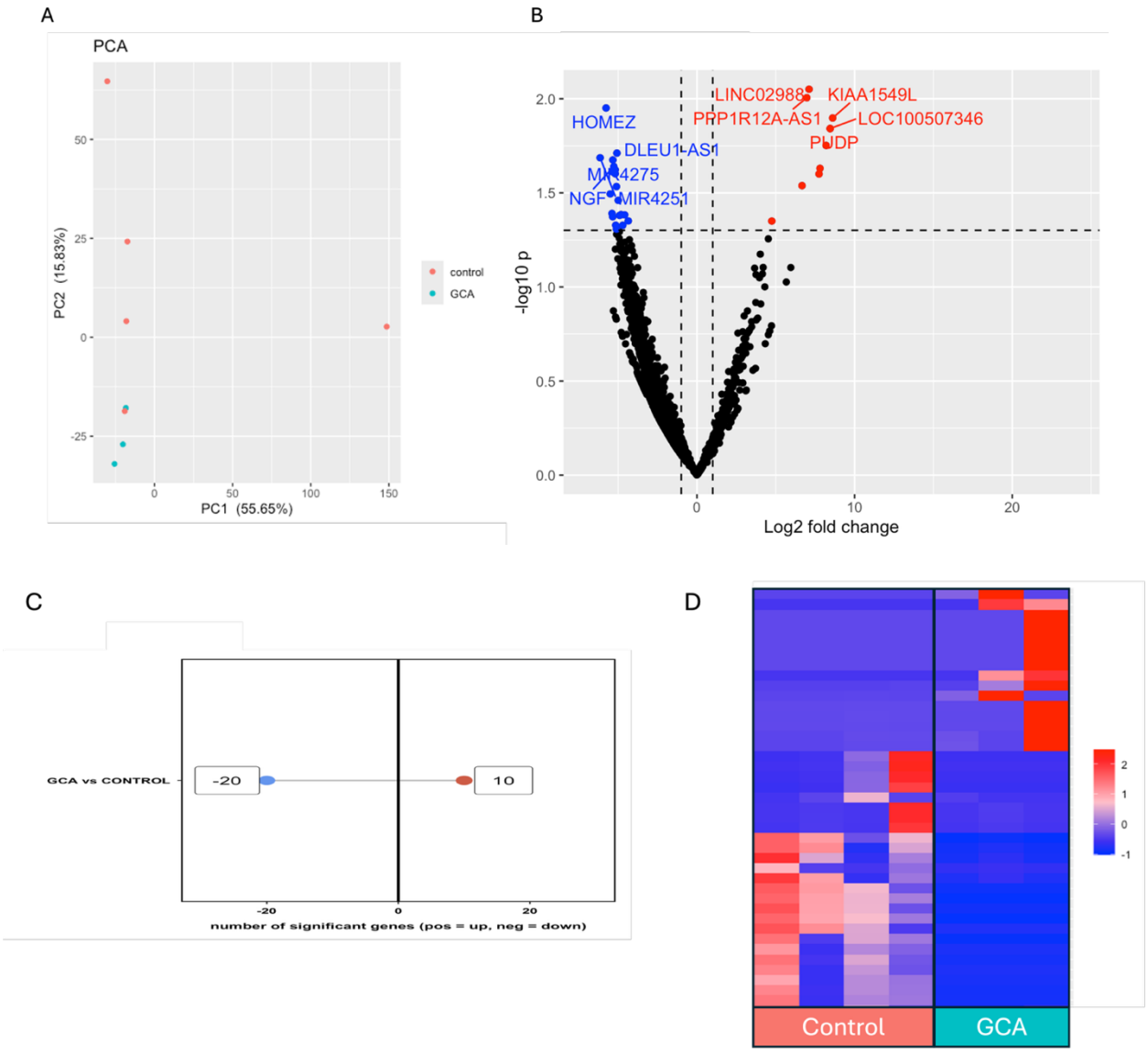

Figure 5.12 Minimal epigenetic changes on the histone H3K4Me3 between control and GCA monocytes.CUT&Tag analysis was conducted using an antibody against H3K4Me3 modification differences between GCA N=4 and control N=5. (A) Principal component analysis (PCA) scatter plot of PC1 and PC2 for GCA vs Control. The percentage of total variation explained by each component is given on its axis. Each point represents a donor. (B) Volcano plot of most differentially expressed genes. Dots represent a gene, blue dots = log2fold change < 0 red dots log2fold change > 0. Top 5 most differential genes are labelled. (C) Lollipop plot showing upregulated in control (represented as downregulated compared to GCA) and upregulated in GCA. Generated using Searchlight2. (D) Heatmap of differentially expressed genes in GCA vs Control (P value < 0.05). Colours represent log fold change red > 0 blue < 0

5.3 Discussion

The previous chapters describe difference in macrophages and MGC formation in GCA compared to healthy controls wherein, GCA monocytes were more likely to form both LHGCs and FBGCs, when stimulated with GM-CSF and IFNγ. Studies have shown that most macrophages in the GCA vessel are of monocytic precursor origin and not embryonic, highlighting a potential role for circulating monocytes in the initiation, progression and the formation of MGCs in GCA. Therefore, this chapter explored the potential surface expression, transcriptomic and epigenetic differences in GCA monocytes compared to control. Furthermore, this chapter aimed to determine whether circulating monocytes from GCA patients are pre-primed to become MGCs when in the vessel.

This chapter employed flow cytometric analysis of monocytes from GCA and healthy controls to determine differences in surface marker expression. Unexpectedly, there were no significant differences between monocyte numbers in GCA and healthy controls as literature suggests (van Sleen, Wang, Kornelis S. M. van der Geest, *et al.*, 2017), however, this may be explained by the highly diverse nature of the cohort. As GCA is a clinical emergency, patients with suspected disease are rapidly treated with high doses of glucocorticoids. Monocyte numbers are reduced to normal levels by glucocorticoid treatment explaining a lack of difference between healthy and GCA (Thompson and van Furth, 1970). Furthermore, this cohort consists of patients with varying disease activity which may account for variability in monocyte numbers. Analysis of total monocytes provided an overview of the global circulating monocyte phenotype in GCA. However, this approach may obscure subset-specific alterations due to the heterogeneous nature of the monocyte compartment. Stratification into classical, intermediate, and non-classical monocytes revealed that several markers became significant only at the subset level, indicating that these changes are driven by specific monocyte populations rather than uniformly expressed across all monocytes. Analysis of monocyte subsets showed that GCA monocytes had significantly higher expression of GM-CSFR, IFNγ, CCR5 and CXCR2. This increase was observed, particularly, in the classical and intermediate monocyte subsets. These findings suggest that circulating GCA monocytes may be more responsive to cytokine and chemokine signals,

potentially enhancing their recruitment to the vessel. Notably, GCA-like MGCs were shown to form from GM-CSF and IFNγ in vitro, therefore, the increased expression of the GM-CSF receptor may reflect an enhanced capacity for these monocytes to contribute to MGC formation in the GCA vascular environment. Studies of osteoclastogenesis in RA have shown that CD14+CD16- monocytes are the main precursor of this multinucleated cell (Xue *et al.*, 2020). However, in the study by Xue et.al, the capacity for intermediate monocytes to form osteoclasts was not observed. It is important to note that osteoclasts are specific MGCs of the bone and only have slight overlaps in function and phenotype with MGCs in GCA (see Section 3.3). Interestingly, a study by (Champion *et al.*, 2018) showed that, while all three monocyte subsets could be stimulated to fuse into multinucleated giant cells, there were distinct differences in the size and morphology of the MGCs produced. This could suggest that the fusion of both classical and intermediate monocytes may be why both types of MGC can be observed in GCA.

Chemokine receptors, such as CXCR2 (also known as IL-8RB) and CCR5, have been implicated in the adhesion and extravasation of monocytes into inflamed vessels in GCA and other vascular pathologies, such as, atherosclerosis (Gerhardt and Ley, 2015). Therefore, it is plausible that elevated expression of these markers on circulating monocytes in GCA reflects their readiness to migrate into the vessels. However, previous studies have suggested that CCR5 is, predominantly, expressed on intermediate (CD14+CD16+) monocytes (Wong *et al.*, 2011), which contradicts the results in this chapter. This may suggest a disease specific shift in receptor expression on GCA monocytes. This observation raises the possibility that CCR5 may be involved not only in monocyte recruitment, but also in in MGC formation. This will be discussed in the following chapter.

Interestingly, when the monocyte population as a whole, and monocyte subsets were assessed by flow cytometry, CCR5 had a distinct expression pattern in GCA monocytes. CCR5 expression appeared to split into three groups (low, medium and high). Steroid dose did not appear to be a factor in CCR5 expression, as one patient receiving a dose of 25mg/day had CCR5 expression on ~97% of classical monocytes. No data on disease activity of the patients assessed by flow cytometry was available for this thesis, so possible parallels between disease

state and CCR5 expression could not be drawn. However, it would be interesting to collect and analyse this data, in future studies, to understand if this difference in CCR5 surface expression is attributable to active versus remission status.

While analysis of surface marker expression is helpful in distinguishing circulating monocytes in GCA and healthy controls, it is not without its limitations, such as, a lack of intracellular staining which means other GCA/MGC related marks, such as, IFNγ were not looked at. Additionally, increased expression of a surface marker does not always correlate with increased function of the protein (Delmonte and Fleisher, 2019).
Furthermore, while many studies observe an increase in monocyte numbers in GCA compared to healthy controls, the data presented in this thesis did not. In the future, it would be interesting to use a method of absolute counting of monocyte numbers to confirm this finding. For example, use of Trucount tubes which contain a known number of fluorescent beads (Hensley *et al.*, 2012). Therefore, to validate surface marker difference and further understand differences between healthy control and GCA circulating monocytes, their transcriptome and epigenetic profiles were investigated. Another limitation of this study was the addition of an Fc block simultaneously with the test antibodies. This may mean that Fc receptors were not adequately blocked and that background staining could be a confounder in this data. Therefore, future studies should aim to ensure the blockade of Fc receptors before the addition of antibodies.

Bulk RNA-Seq analysis was carried out in GCA-positive monocytes and GCA-negative control monocytes. This analysis showed that there was minimal separation between control and GCA samples. This overlap may be due to the nature of the controls used for these experiments. The TARDIS study (outlined in Section 2.1.3) recruited donors who were under investigation for GCA. After clinical and histological evaluation of TABs, patients were defined as GCA positive or controls (GCA negative). By this point, patients had received multiple doses of corticosteroids and also had raised inflammatory markers (Table 5.1). These may have had an impact on gene transcription and, therefore, cause the overlap seen in PCA analysis. Furthermore, cells used in transcriptomic and

epigenetic analyses were isolated from frozen PBMCs. A study by (Stamper *et al.*, 2024) showed that gene transcripts are altered in the process of thawing cells, leading to upregulation of stress and cell death related genes. This may explain the upregulation of genes and pathways associated with apoptosis.

However, RNA-Seq of circulating monocytes did reveal an increase in pathways, such as, cell cycle checkpoints, mitosis and cell division, which could suggest cell cycle dysregulation (Subramanian and Cohen, 2019). This could have implications in the formation of MGCs from GCA monocytes. One study of osteoclastogenesis found a relationship between cell proliferation and osteoclastogenesis (Mizoguchi *et al.*, 2009). Furthermore, (Takegahara *et al.*, 2016b) suggest that incomplete cytokinesis may be involved in the formation of MGCs. Taken together, this data suggests that GCA monocytes have increased expression of MGC formation related genes. Lastly, to validate changes seen in surface expression from flow cytometry, gene expression of these markers was assessed in circulating monocytes.
However, this data was generated with a small number of donors and, therefore, this data should be validated with a more well-powered cohort, and interpretations of this data should be made with caution. In future studies, to further understand circulating monocytes in GCA, the transcriptomic profile of these monocytes could be compared to that of monocytes from other vascular diseases such as ANCA associated vasculitis. This comparison may help to elucidate GCA specific disease mechanisms in monocytes and the extent to which circulating monocytes are pre-programmed in the periphery versus acquiring disease-specific features upon tissue entry.

In order to better understand these transcriptional differences, the epigenetic profiles of circulating monocytes were analysed. Despite passing QC standards, some samples had very few or no peaks after calling with GoPeaks. This peak calling mechanism has high sensitivity for H3K27Me3 peaks and has a higher capability to call specific H3K4Me3 peaks (Yashar *et al.*, 2022). Therefore, it is unlikely that the peak calling mechanism caused this issue.
Analysis of H3K27Me3 peak profiles showed large differences between GCA and control circulating monocytes. Whereas, H3K4Me3 profiles were not as different between the two groups. This suggests that, differences in GCA monocyte

transcription could be due to a lack of gene repression rather than an increase in gene activation. This reduction in H3K27Me3 marks can be observed in Anti-Neutrophil Cytoplasmic Antibody Associated Vasculitis (ANCA), another form of vasculitis. A study by (Renauer, Coit and Sawalha, 2016) showed that this was due to an increase in the H3K27me3 demethylase protein JMJD3. Therefore, it would be interesting to investigate whether there was a high expression of this protein in GCA. Additionally, age related epigenetic modifications were associated with increased H3K27Me3 marks (Wang *et al.*, 2022b). Additionally, the control samples were age matched, suggesting the decrease in H3K27Me3 is a GCA specific mechanism and not due to the age of donors. Furthermore, pathways related to cell migration and cell-cell adhesion and transcription had a reduction in repressive marks in GCA monocytes, compared to healthy. Interestingly, the transcription factors with decreased H3K27Me3 marks included CREB1, ACVR1 and EBF2. CREB1 has been implicated in the transcription of CCR5 (Rutger J Wierda *et al.*, 2012) and both EBF2 and AVCR1 have been shown to be involved in the differentiation of osteoclast pre-cursors to osteoclasts (Kieslinger *et al.*, 2005; Omi, Kaartinen and Mishina, 2019). Therefore, the lack of repression marks on these genes may indicate a difference in chromatin accessibility and, potentially, an upregulation of these mechanisms in GCA.

Furthermore, the H3K27Me3 profile of genes of interest were analysed. This showed significant increase in H3K27Me3 peaks enriched at the IFNγ receptor and GM-CSR loci in control monocytes compared to those from GCA patients. This suggests that the increase of surface expression of GM-CSFR, observed via flow cytometry analysis, in GCA monocytes could be due to a lack of repression of gene activity. Interestingly, the chemokine receptor CCR5 did not have a statistically significant difference in H3K27me3 peak enrichment between GCA and control monocytes. However, a broader distribution of peak values was observed in control samples (ranging from 0-10) compared to a narrower range in GCA (0-1). This variability, coupled with limited sample size, may have contributed to the lack of statistical significance. Repeating the experiment with a larger cohort may help clarify whether differential epigenetic regulation of CCR5 is present in GCA. Intriguingly, H3K27Me3 was significantly increased at the anti-sense RNA CCR5AS locus in control monocytes. This lncRNA has been shown in monocytes to correlate with increased expression of CCR5 on the surface of

cells (Kulkarni *et al.*, 2019). These findings suggest that the elevated CCR5 expression observed in GCA monocytes may not result from direct increase in CCR5 transcription but rather may involve mechanisms mediated by this anti-sense RNA.

To conclude, GCA circulating monocytes exhibit significant differences in surface marker expression, transcriptome, and have different epigenetic profiles compared to that of GCA-negative controls. These cells have significantly increased GMCSR expression on the surface, increased GM-CSFR transcripts and reduced H3K27me3 marks at the GM-CSFR locus. This histone modification is associated with transcriptional repression, suggesting enhanced transcriptional accessibility of this gene in GCA monocytes. This may indicate a CD14+ precursor population that is more susceptible to MGC formation when stimulated by GM-CSF and IFNγ. Furthermore, the relative absence of H3K27Me3 enrichment in GCA monocytes may reflected altered chromatin accessibility which may, in turn, contribute to increased transcriptional activity compared to healthy controls.

Lastly, CCR5 expression on the surface of cells and a lack of CCR5AS repressive histone marks suggests a role for this chemokine receptor in the GCA myeloid compartment. The following chapter explores this hypothesis in more depth with a focus on the contribution of CCR5 to MGC formation.

Chapter 6 The role of CCR5 in MGC formation and GCA.

6.1 Introduction.

In the previous chapter, flow cytometric analysis showed a significant increase in chemokine receptor 5 (CCR5) expression on circulating monocytes in GCA compared to healthy control samples. This prompted investigation into a potential role for CCR5 in the pathogenesis of GCA monocytes, macrophages and MGCs.

The receptor CCR5 is a member of the chemokine receptor family. In homeostasis, this G-protein coupled receptor and its ligands CCL3, 4 and 5 are crucial in the maintenance of homeostasis and induction of immunity, where it regulates the trafficking to sites of infection and effector functions of T cells, macrophages and dendritic cells. This chemokine receptor has been well researched due to its role in HIV entry into cells. HIV research into CCR5 lead to the discovery of a genetic mutation where 32 base pairs are deleted from the CCR5 gene (Galvani and Novembre, 2005). This Δ32 mutation was shown to protect against HIV as it causes a partial (heterozygous WT/D32) or full (homozygous D32/D32) reduction in CCR5 surface expression. Interestingly, CCR5 has been implicated in the pathogenesis of many auto-immune and inflammatory diseases (Jones, Maguire and Davenport, 2011).

In atherosclerosis, an inflammatory vascular pathology with similar immune mediated mechanisms to GCA, CCR5 is thought to play a role in pathogenesis. In a mouse model of atherosclerosis, the interaction of CCR5 and CCL5 was crucial in the migration of monocytes into the vessel (Tacke *et al.*, 2007). Furthermore, many cells in the atherosclerotic plaque (including macrophages) express CCR5. Interestingly, data on the protective nature of the Δ32 mutation against atherosclerosis is conflicting. One study suggests that homozygous Δ32/Δ32 is protective against the development of coronary artery disease (Szalai *et al.*, 2001). However, another study suggested that the Δ32 mutation was not protective against the initiation stages of atherosclerosis (Kuziel *et al.*, 2003). It is important to note, however, that this study was conducted on a mouse model

of atherosclerosis and not human disease. Additionally, CCR5 has been implicated in the pathogenesis of Wegener's Granulomatosis (WG), a form of inflammatory vasculitis affecting the airways and kidneys that can often have MGCs present. In WG, CCR5+ mononuclear leukocytes were enriched in granulomatous inflammation in the lung. Additionally, the CCR5 ligands CCL3 and 4 were expressed by MGCs in the lung tissue. Lastly, the Δ32 mutation was absent on patients who did not have auto-antibodies but was present when these auto-antibodies were also present, suggesting that CCR5 may have a pathogenic role in a form of WG (Zhou *et al.*, 2003).

Notably, CCR5 has been shown to be highly expressed on osteoclast precursors (a cell type closely related to MGCs in terms of lineage and multinucleation). Studies have demonstrated that the use of neutralising antibodies against CCR5 significantly reduced osteoclast numbers, suggesting a possible role in cell fusion, a mechanism that may extend to MGC formation in GCA (Oba *et al.*, 2005). Furthermore, CCR5 inhibition not only decreased osteoclast numbers but also altered their function, indicating that CCR5 contributes to maintaining osteoclast morphology and bone resorption capacity (Lee *et al.*, 2017). Additionally, FBGCs have been shown to express CCR5 and its ligands on their surface (Khan *et al.*, 2014). Therefore, it would be interesting to investigate whether a similar CCR5-dependent pathway is involved in the development and function of MGCs in GCA.

Although CCR5 expression on circulating monocytes was demonstrated in the previous chapter, its presence in GCA tissues has also been reported. CCR5 was found to be highly expressed in infiltrating leukocytes and the adventitia of GCA positive tissues (Brühl *et al.*, 2005). However, the function of CCR5 beyond cell migration, in GCA macrophages and MGCs, has not been explored. Therefore, it was important to determine whether the same could be true in GCA.

Accordingly, this chapter aims to demonstrate the presence of CCR5 and its ligands in the GCA tissue, to determine whether CCR5 is expressed by macrophages and MGCs in the tissue and whether it plays a role the formation and function of these cells. To do this, immunohistochemistry and immunocytochemistry analysis of CCR5 and its ligands was carried out on GCA

positive TAB samples as well as culture macrophages and MGCs for presence of these molecules and potential co-localisation with CD68+ cells. Additionally, modulation of the CCR5 pathway was analysed by the addition of Maraviroc and Leronlimab as well as stimulation in MGCs cultures to determine whether CCR5 plays a role in the formation of MGCs in GCA. Furthermore, as MGCs have been shown to be increased in the TABs of GCA patients who had a relapse of disease, these cells can be implicated in relapse (Restuccia *et al.*, 2016). Therefore, the expression of CCR5 in TARDIS flow cytometry were re-analysed at baseline and at time of relapse to determine whether CCR5 plays a role in disease relapse. Lastly, The UKBiobank GWAS data was used to determine whether CCR5 SNPs correlated with GCA. Understanding the role of CCR5 in the pathogenesis of GCA and formation of MGCs may lead to a compelling case for the repurposing of drugs such as maraviroc and Leronlimab, which have been shown to be safe and effective treatments for HIV etc, for treatment in GCA.

6.2 Results.

6.2.1 Presence of CCR5 in GCA tissue.

The previous results chapter showed that CCR5 expression was significantly higher on GCA circulating monocytes than on those from healthy controls. Therefore, it was important to understand if this high CCR5 expression also occurred in the tissue of GCA patients and, if so, where in the vessel and which cells.

Using spatial transcriptomic data (see section 3.2.1), the presence of CCR5 and its ligands (CCL3, 4 and 5) on CD68+ cells, in various areas of the vessel, was analysed. None of the markers reached statistical significance (Figure 6.1). Notably, CCR5 was similarly expressed across the adventitia, intima and MGC rich areas (Figure 6.1a, P = 0.23). In contrast, CCR5 ligands were differentially expressed in the layers of the vessel. Firstly, CCL4 was the most expressed in MGC rich regions compared to intimal and adventitial macrophages (Figure 6.1b, P = 0.4). Whereas, CCL3 was the most expressed in intimal macrophages and MGC regions but was absent in the adventitia (Figure 6.1c, P = 0.8). Interestingly, this ligand had the highest expression values compared to the others. Lastly, CCL5 was transcriptionally expressed in all three analysed regions (Figure 6.1d, P = 0.66) It was least expressed in the adventitia and higher in the intima and MGC rich regions. These results indicate that intimal macrophages and MGCs have a similar expression profile of CCR5 and its ligands, further supporting the idea that MGCs and intimal macrophages are continuum of the same phenotype and that CCR5 and its ligands, could play a role in MGC formation. It was next important to validate protein expression of CCR5 and its ligands in GCA tissue.

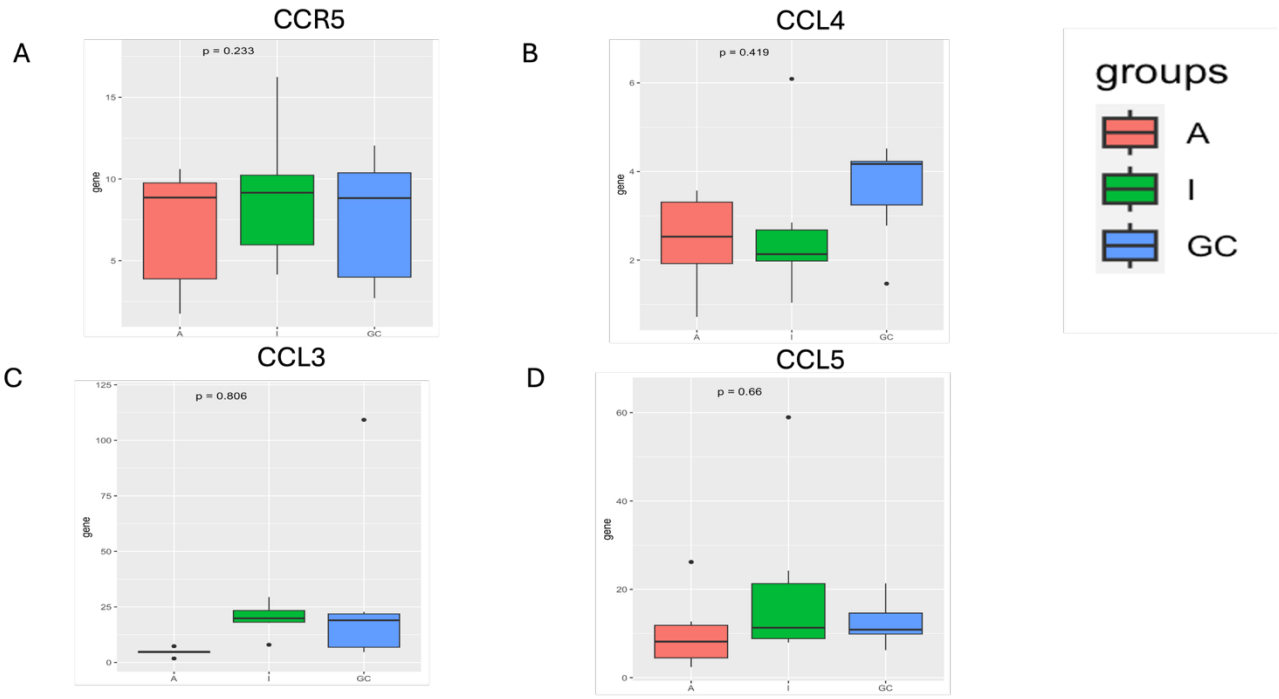

Figure 6.1: Expression of CCR5 and its ligands in TAB tissue.Transcriptional expression of (A) CCR5, (B) CCL4, (C) CCL3 and (D) CCL5 in CD68+ cells of the adventitia A, intima I and giant cell rich regions GC of GCA positive TABs.

To validate protein expression of CCR5 ligands in the tissue, IHC was performed. Among the two ligands stained for, CCL3 exhibited the strongest staining intensity when compared to CCL5. Interestingly, CCL5 was primarily localized within (or on the surface of) multinucleated giant cells, whereas CCL3 was detected in the surrounding cell populations. This suggests that CCL5 may be expressed on the surface of MGCs and affect their function in an autocrine manner, while CCL3 might be secreted either by the giant cells themselves or by the adjacent macrophages and could signal to MGCs in a paracrine manner. However, to determine whether this signalling does occur future co-culture experiments should be performed.

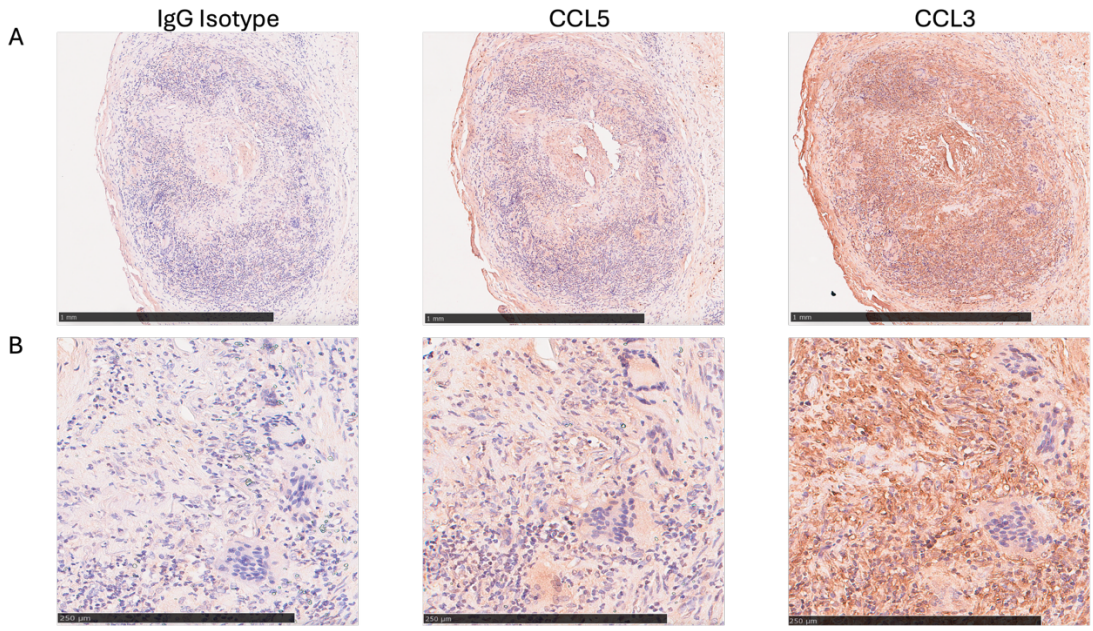

Figure 6.2: CCR5 ligands CCL3 and CCL5 are expressed in GCA tissue. Representative images of immunohistochemistry staining for CCL5 and CCL 3 in GCA positive TABs. Rabbit IgG polyclonal antibody used as an isotype control. (A) Full vessel image scale 1mm. (B) enlarged image showing MGCs (250µm).

To validate CCR5 expression in GCA tissue and to determine whether CCR5 and its ligands are expressed by CD68+ macrophages, multicolour immunofluorescence staining was carried out on GCA TAB tissue. This staining showed high expression of CCR5, CCL3, CCL5 and CD68 in GCA tissue (Figure 6.3a&b). The ligand CCL3 was most expressed in cells surrounding MGCs and closely to CCR5 staining (Figure 6.3a). However, CCL5 could clearly be observed in the cytoplasm of MGCs and co-localised with CD68+. This staining shows that CD68+ve cells in GCA tissue express CCR5 and its ligands, as well as expression by surrounding non-macrophage cells.

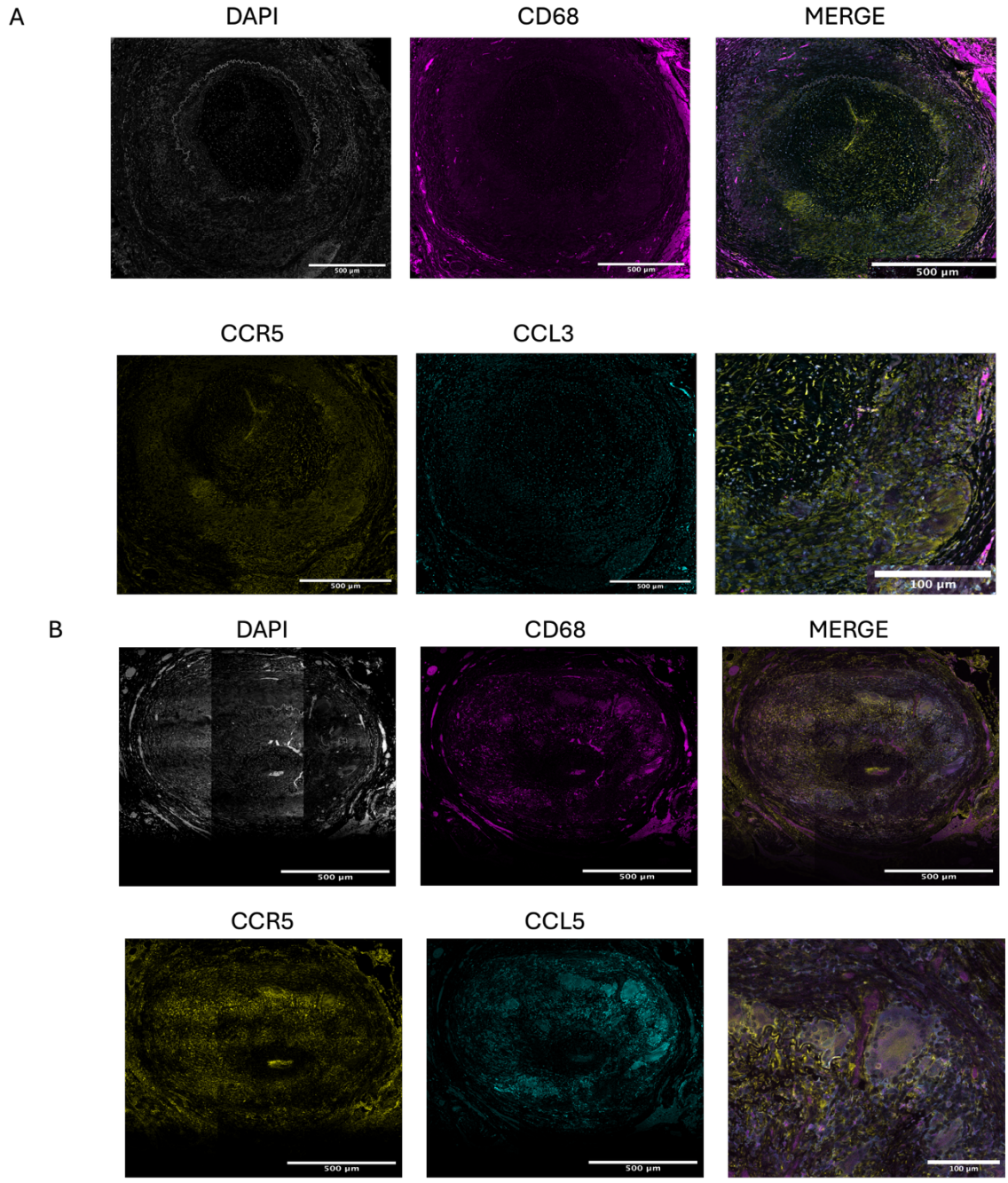

Figure 6.3: CCR5 and its ligands are expressed by CD68+ve cells in the vessel. Representative images of immunofluorescent staining of GCA positive TABs. Nuclei (grey), CD68 (magenta), CCR5 (yellow) and (A) CCL3 (B) CCL5 (Cyan) at 20x magnification. Images of giant cells within TABs are also shown (100µm).

In order to determine whether CCR5 plays a role in the formation of MGCs in GCA, it was first crucial to ensure that MGCs and macrophages generated in the in vitro model (see Section 4.2) were also positive for CCR5 and its ligands. To do this, cultured MGCs were stained with a CCL5 or CCL3 primary antibody, followed by an anti-rabbit fluorescent secondary antibody, together with a fluorescently conjugated CD68 and DAPI for nuclear visualisation.
This showed that CCR5 was highly expressed on both macrophages and MGCs stimulated with GM-CSF+ IFNγ (Figure 6.4). Interestingly, CCL3 was not detected on MGCs or macrophages in culture (Figure 6.4a). This may be due to its secretion by MGCs or surrounding cells, as the washing steps involved in culture and immunofluorescence staining would have removed any secreted CCL3 present in supernatants. CCL5, however, was observed localised at the edges of macrophages and MGCs in culture. An overlap between CCR5 and CCL5 staining was also observed (Figure 6.4b). This could suggest that CCL5 is either being secreted locally or retained on the surface of MGCs.

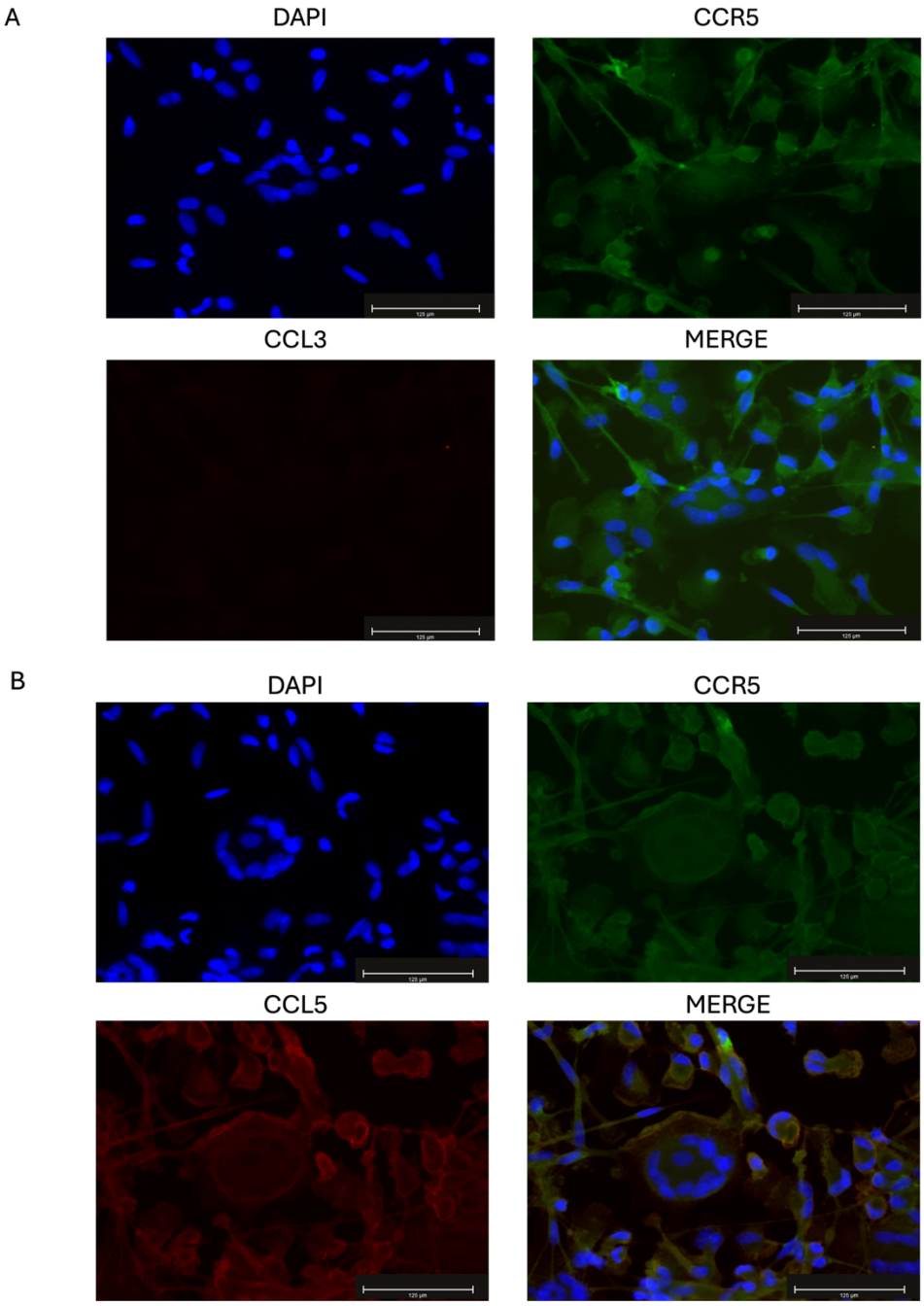

Figure 6.4: CCR5 and its ligands are expressed in cultured

MGCs.Representative images of immunofluorescent staining of GCA positive TABs. Nuclei (blue), CCR5 (green) and (A) CCL3 (B) CCL5 (red) at 20x magnification. Images of giant cells within TABs are also shown (100um).

6.2.2 **CCR5 binding inhibition alters MGC formation.**

Given the expression of CCR5 and its ligands within and around MGCs, its role in the formation of these cells was assessed. In order to do so, a CCR5 antagonist known as Maraviroc was added to the in vitro MGC culture system. Maraviroc is a small molecule inhibitor of CCR5, that binds the receptor in a non-competitive manner. This molecule is already used in clinics to treat HIV as an oral dose. Interestingly, when HIV patients were treated with Maraviroc, they had a reduction in Stroke occurrences compared to placebo controls (Carter and Keating, 2007).

When Maraviroc was added to cells stimulated with GM-CSF+ IFNγ, there were fewer clusters of cells compared to cells cultured without Maraviroc (Figure 6.5a). This suggests that CCR5 signalling is involved in the clustering observed *in vitro*. When MGC numbers were compared between cultures with and without Maraviroc, there were significant differences (Figure 6.5b). When cells were stimulated with GM-CSF+IFNγ, without Maraviroc, an average of 272 (SD = ±368) was observed. Whereas, MGC numbers were significantly reduced to an average of 12 (SD = ±22) MGCs per well ($P < 0.05$). There was a large standard deviation between the 5 donors both with and without Maraviroc suggesting donor variability. Despite this, a consistent reduction of MGC numbers was observed. Alternatively, when M-CSF+IL-4 stimulated cells were treated with Maraviroc, there was no difference in the number of MGCs produced. This suggests that CCR5 is involved in the GM-CSF+ IFNγ pathway but not the pathway involving M-CSF+IL-4.

Lastly, it was important to determine the best concentration of Maraviroc which reduced the most MGC formation. 1 or 10μM of Maraviroc was

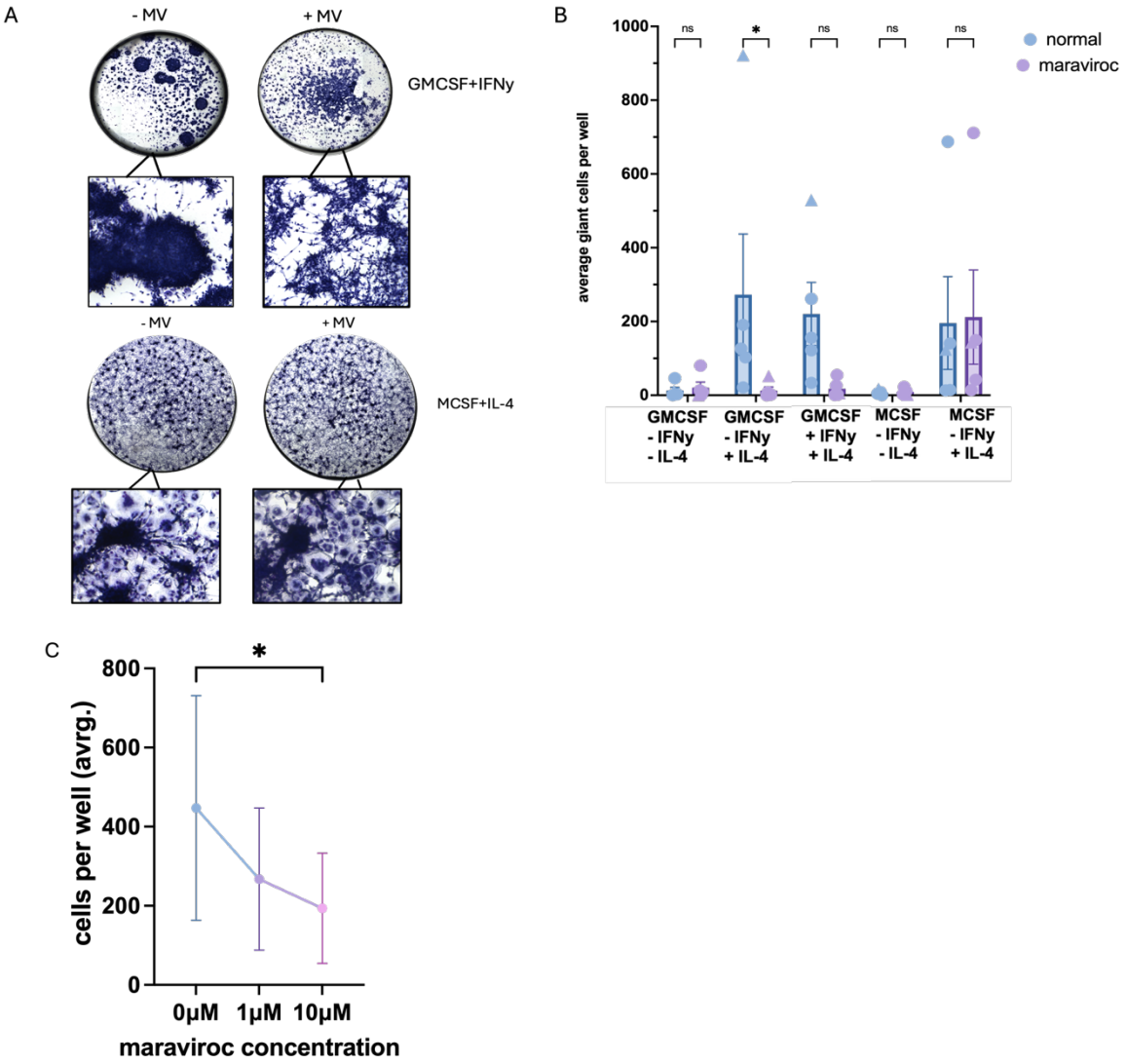

Figure 6.5: Maraviroc treatment significantly reduces MGC formation in healthy macrophage cultures.(A) Bar graph of average MGC per well when leukocyte cones were cultured, as previously described, with and without 10nM of maraviroc. Bars represent mean with standard deviation. One-way ANOVA *P< 0.05 N=5. (B) representative images of cultures with and without maraviroc. (C) Graphs demonstrating reduction of MGCs when CCR5 was inhibited by 1 and 10μM of maraviroc. P <0.05 Non-parametric ANOVA. Points represent average of N=4, error bars represent SD±

added, per well, to GM-CSF+IFNγ stimulated cells. This showed a dose dependant reduction in the number of MGCs produced (Figure 6.5c).

As Maraviroc was shown to reduce MGC formation when healthy monocytes were cultured with GM-CSF+IFNγ but not MCSF+IL-4, it was then important to ensure that the same was true for GCA peripheral blood monocytes.

Surprisingly, there was no significant difference in MGC numbers between GM-CSF+ IFNγ stimulated cells with or without the addition of Maraviroc (Figure 6.6a). With most donors, there did appear to be a non-significant reduction in the number of MGCs in this stimulation, such as one donor which had an average

number of 230 to around 6 MGCs, per well. However, there was one donor which had an increase of MGCs when treated with Maraviroc. Therefore, it would be interesting to gather data on disease states of patients and repeat these experiments.

Furthermore, as previously described, there was no statistically significant difference in MGC numbers between MCSF+IL-4- stimulated cells and those additionally treated with Maraviroc (Figure 6.6b). However, all GCA donors showed a reduction in MGC numbers when Maraviroc was added, which was not observed in experiments with cells from healthy donors. It is important to note the small sample size of this experiment (n=4), due to time and donor availability constraints. An increase in donor numbers may reveal significant differences, similar to those observed in experiments with Maraviroc using monocytes from healthy donors. Additionally, flow cytometry data described in the previous chapter (Section5.2.1, Figure 5.4), showed a difference in CCR5 expression in monocyte subsets. In all previous experiments, the stem cell monocyte enrichment kit, without CD16, depletion was used to isolate monocytes. This kit allows for the isolation of all monocyte subsets. Therefore, it was crucial to determine whether the presence of different monocyte subsets influenced MGC formation outcomes.

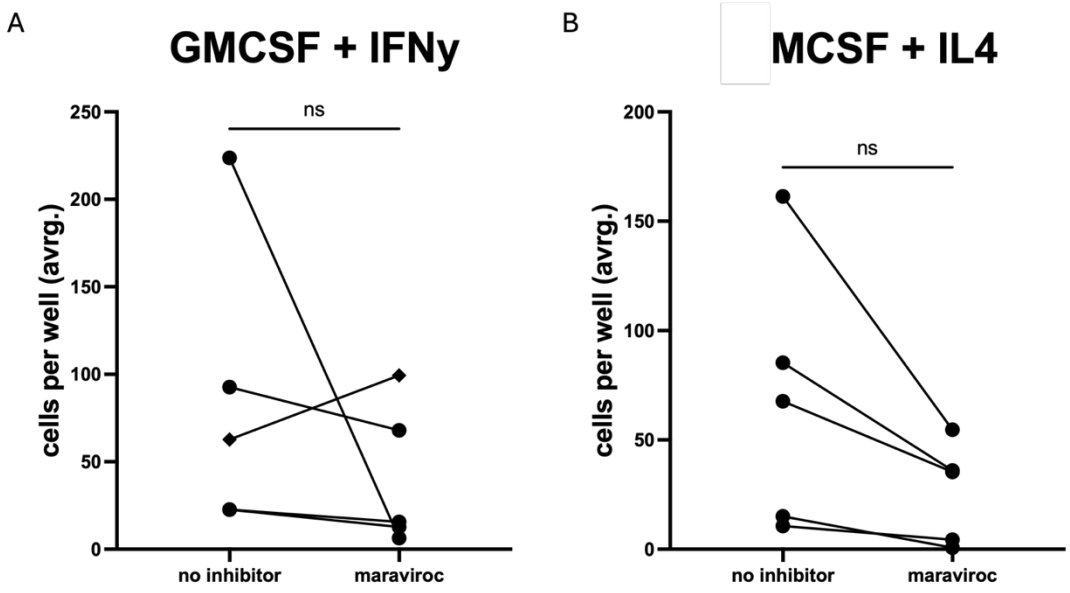

Figure 6.6: In vitro cultured MGCs from GCA peripheral blood do not respond the same to maraviroc.Line graphs represent average MGC numbers with and without CCR5 inhibition by maraviroc in (A) GMCSF+ IFNγ and (B) MCSF+IL-4 stimulation. Points represent one donor (N=5). Paired T-test performed on data.

Studies of other MGC phenotypes, such as osteoclasts, suggest that classical ($CD14^+CD16^-$) monocytes serve as precursors to these cells (Ansalone, Cole, Chilaka, Sunzini, Sood, Robertson, Siebert, Iain B. McInnes, *et al.*, 2021). Therefore, the capacity of different monocyte subsets to form MGCs previously defined stimulation conditions was assessed. To do this, MGC formation resulting from monocytes isolated using an enrichment kit with CD16 depletion (enriching $CD14^+$ $CD16^-$ classical monocytes only) was compared to that of monocytes isolated using an enrichment kit without CD16 depletion (encompassing the tree monocyte population; classical intermediate and non-classical) (Figure 6.7).

Interestingly, when GCA purified classical monocytes were stimulated with GM-CSF+IFNγ, a ~2-fold increase in the number of MGCs produced compared to the total monocyte pool. However, when cells were stimulated with MCSF+IL-4, there was no significant difference in MGC numbers between the monocyte enrichment kits. This implicates the classical monocyte subset as GCA specific precursors and that the presence of CD16+ monocytes may reduce the number of

MGCs in the culture system. Therefore, Maraviroc experiments were then repeated with CD14+ only monocytes from GCA patients.

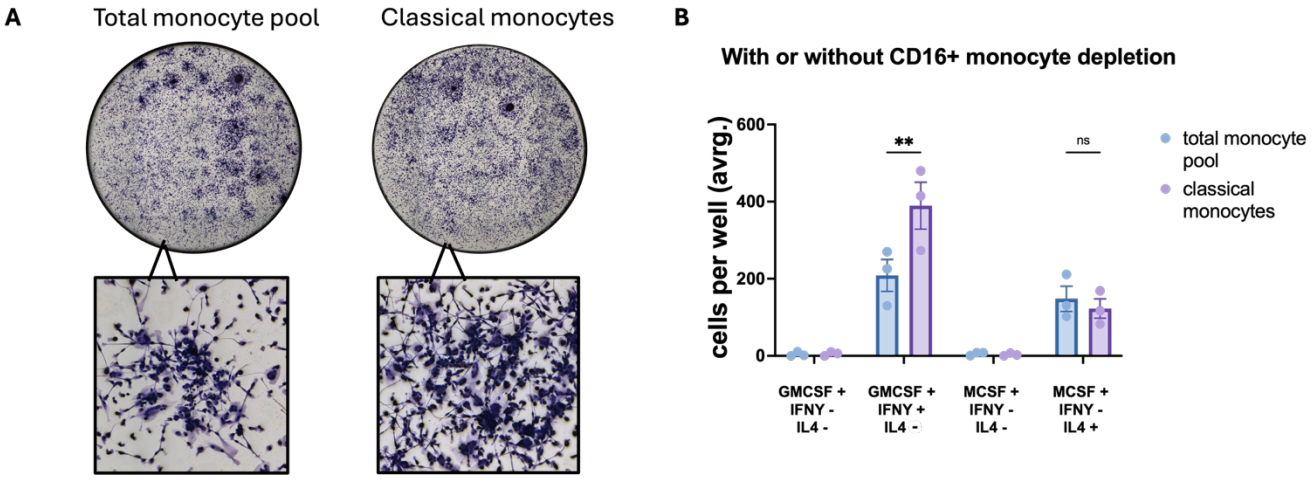

Figure 6.7: Culture of classical monocytes alone leads to more MGC formation than all monocyte subsets together.Representative images of monocytes isolated with the stem cell monocyte isolation kit without CD16 depletion or with cd16 depletion. Monocytes were cultured with 100ng/mL of GM-CSF and 40ng/uL IFNγ (A). After 7 days of culture cells were stained using the haemacolour staining kit from Sigma Aldrich. Wells were imaged using the EVOS and total number of multinucleated giant cells were counted in three donors (B). Dots represent an average of three technical replicates, N=3. A 2-way ANOVA, with multiple comparisons, was performed in GraphPad **adj-P value <0.005.

To determine whether the differences in reduction of MGC numbers by CCR5 inhibition between healthy and GCA was due to the presence of non-classical monocytes in the culture system, previous experiments were repeated with and without CD16 depletion.

These experiments showed that, although there was no significant difference between Maraviroc-treated and untreated cells when monocytes were isolated without CD16 depletion (Figure 6.8a), there was a significant reduction ($P<0.05$) in MGC formation when purified $CD14^{+}CD16^{-}$ cells were stimulated with GM-CSF+IFNγ and treated with Maraviroc (Figure 6.8b). Similarly, when the complete pool of monocytes was stimulated with M-CSF+IL-4, there was a slight but non-significant reduction in the numbers of MGCs following Maraviroc treatment. In contrast, classical monocytes stimulated under the same conditions, showed no difference in the average number of MGCs formed. This data suggests that CD14+

monocytes are likely the main precursors to MGCs when stimulated with GM-CSF+ IFNγ.

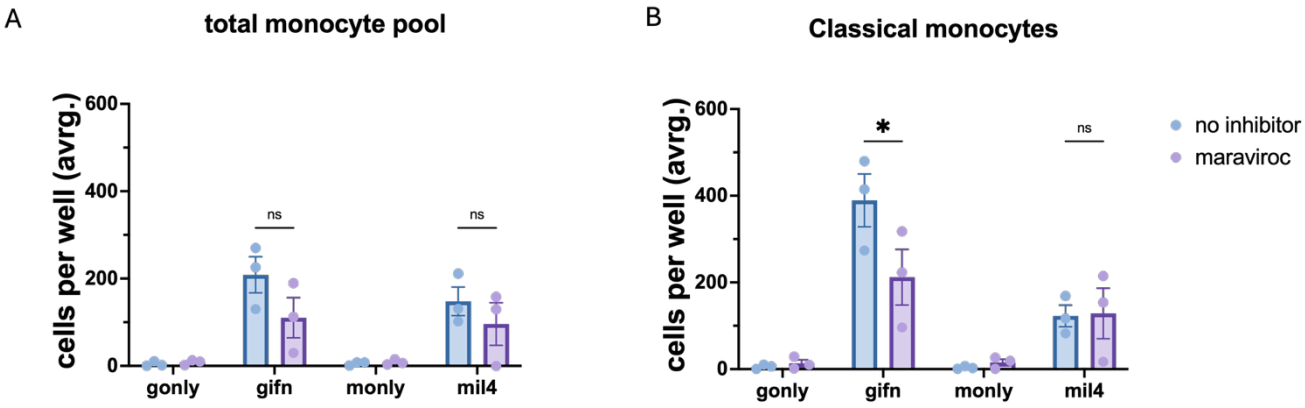

Figure 6.8: Increased inhibition of CD14+ derived MGCs by Maraviroc. Bar graphs showing average MGCs per well when (A) all monocyte subsets or (B) C14+ monocytes alone were cultured with or without maraviroc inhibition of CCR5. Error bars represent mean with SD±. P<0.05 2-way ANOVA performed on Prism.

To validate these findings with an alternative CCR5-modulating approach, the humanised monoclonal antibody, Leronlimab, was used in culture with GCA monocytes.

To do this, 1, 10 and 100nM of Leronlimab was added to cells stimulated with GM-CSF+ IFNγ. Overall, there was a decrease in the number of MGCs formed at all concentrations of Leronlimab. Interestingly, a small increase in MGC numbers was seen when 10nM was added compared to 1nM, although this was not statistically significant (Figure 6.9a). Furthermore, there was an almost 3-fold reduction ($P<0.001$) in the number of MGCs counted per well when 100nM of Leronlimab was added to the culture system (Figure 6.9b). This indicates that high doses of Leronlimab are effective in reducing MGC formation by GM-CSF+ IFNγ stimulation. Intriguingly, this MGC reduction by Leronlimab was greater than Maraviroc (Figure 6.8b), suggesting superior efficacy of Leronlimab in the reduction of MGC formation, warranting further investigation. Given the potential involvement of CCR5 signalling in the formation of MGCs led to questions of which, if any, of its ligands are implicated in this process.

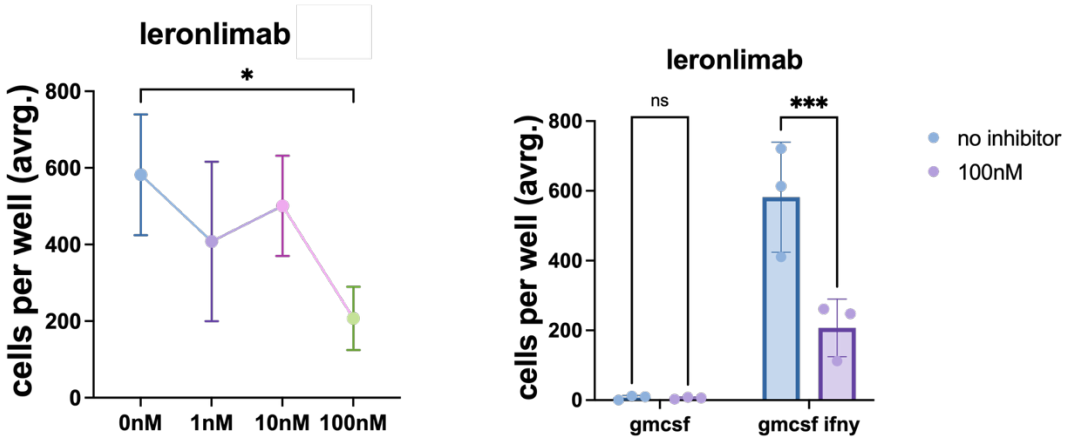

Figure 6.9: Dose dependent reduction of MGCs with Leronlimab.Graphs demonstrating reduction of MGCs when CCR5 was inhibited by 1, 10 and 100nM of Leronlimab. P <0.05 Non-parametric ANOVA. Points represent average of N=3, error bars represent SD± (B) bar graph showing reduction in MGC numbers when CCR5 was inhibited with Leronlimab P<0.001 2-way ANOVA.

CCR5, like many G-protein coupled receptors, is promiscuous and binds many ligands. Two-such ligands known to bind this receptor are CCL3 and CCL5, which were shown previously to be present in GCA-affected vessels, particularly within and around MGCs. To test whether these ligands promote MGC formation, monocyte cultures were stimulated with GM-CSF+/- IFNγ, and CCL3, 5 or both were added on day 0 or day 4 of culture.

The addition of these chemokines with GM-CSF alone was not sufficient to induce MGC formation. However, these chemokines could modulate MGC formation when stimulated with GM-CSF+IFNγ, depending on the time of addition. Unexpectedly, when chemokines were added at the start of the culture (day 0) along with GM-CSF+ IFNγ, there was a decrease in the number of MGCs produced – whether CCL3, CCL5, or both together were added (Figure 6.10a).

In contrast, when CCL3 or both chemokines were added on day 4 (but not CCL5 alone), there was an increase in the number of MGCs formed compared to cultures without chemokine addition. In particular, when CCL3 alone was added there was an increase of ~200 MGCs (Figure 6.10b). Due to time constraints, this experiment was only performed with a single donor (n=1) and statistical analysis could not be performed.

However, when CCL5 was added, there was a noticeable decrease in the number of MGCs compared to GM-CSF+IFNγ alone. This could suggest that MGC formation relies somewhat on the CCL3/CCR5 axis but not CCL5/CCR5 binding, which may induce a separate pathway and actually inhibit the formation of MGCs. Although preliminary, this observation warrants further investigation in a larger donor cohort to assess reproducibility and underlying mechanisms.

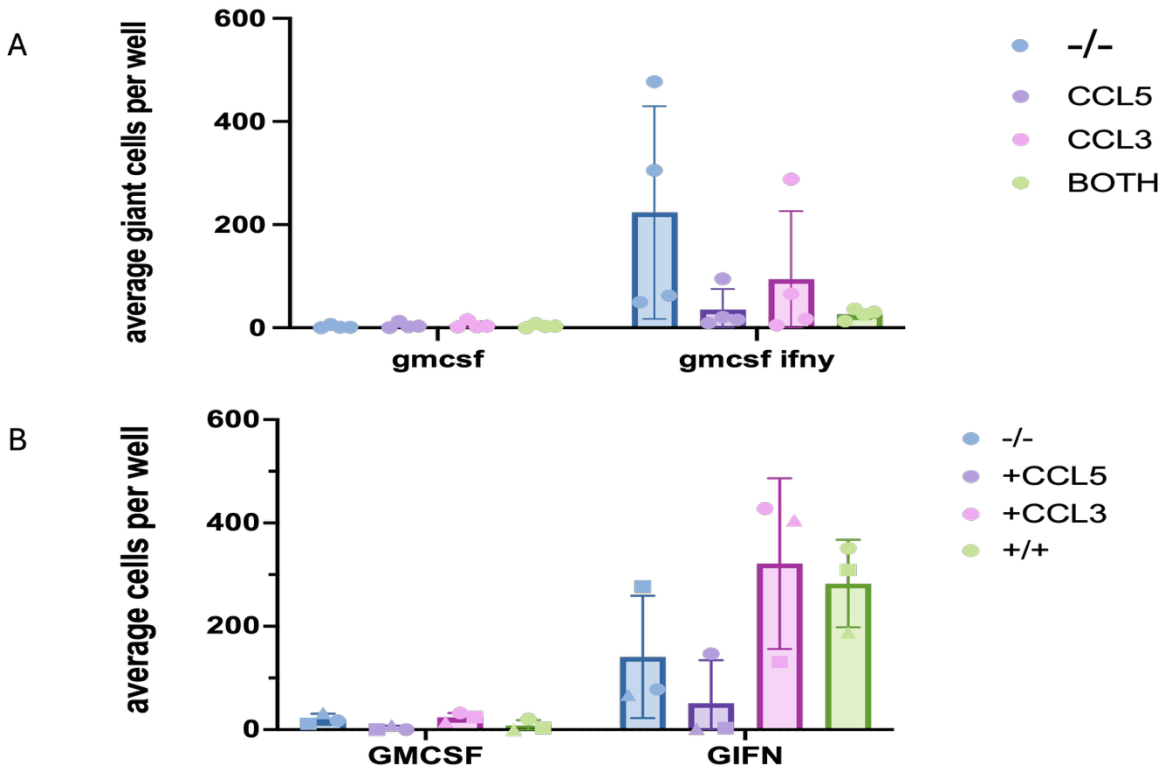

Figure 6.10: CCR5 ligands influence MGC formation in culture.Chemokines CCL3 and CCL5 were added to cultured macrophages on (A) day 0 (N=3) and (B) day 4 (technical replicates of one donor). Bar graph represents average number of MGCs per well. Error bars represent SD±. 2-way ANOVA.

6.2.3 Clinical significance of CCR5 in GCA.

As previously mentioned, it has been hypothesised in a number of GCA studies that MGCs could be linked to relapse of disease (Section 6.1). This chapter describes a potential role for the CCR5 signalling axis in the formation and of MGCs. Therefore, the presence of CCR5 on circulating monocytes before and after the occurrence of a relapse was assessed. This was achieved by flow cytometric analysis of TARDIS patient peripheral blood at the baseline visit and at the time of relapse.

Analysis of CCR5 expression on circulating monocytes revealed several notable findings. While there was no statistically significant difference between CCR5 expression on classical monocytes at baseline and relapse (Figure 6.11a), three out of four donors showed a visible increase in expression. In two donors' expression increased from 80% of monocytes being CCR5+ve to around 100%. It is important to note that this experiment included only four subjects, due to the limited number of TARDIS relapse patients available at the time of analysis. Additionally, there were no observable differences in CCR5 expression on intermediate monocytes at baseline versus relapse (Figure 6.11b). Unexpectedly, there was a significant increase ($P< 0.05$) in the number of non-classical monocytes expressing CCR5 at the time of relapse (Figure 6.11c). This was in contrast to previous data (Figure 5.4), which showed no observable difference in non-classical CCR5 expression. This could suggest a potential role for CCR5 in the relapse of GCA by recruitment or activation of non-classical monocytes.

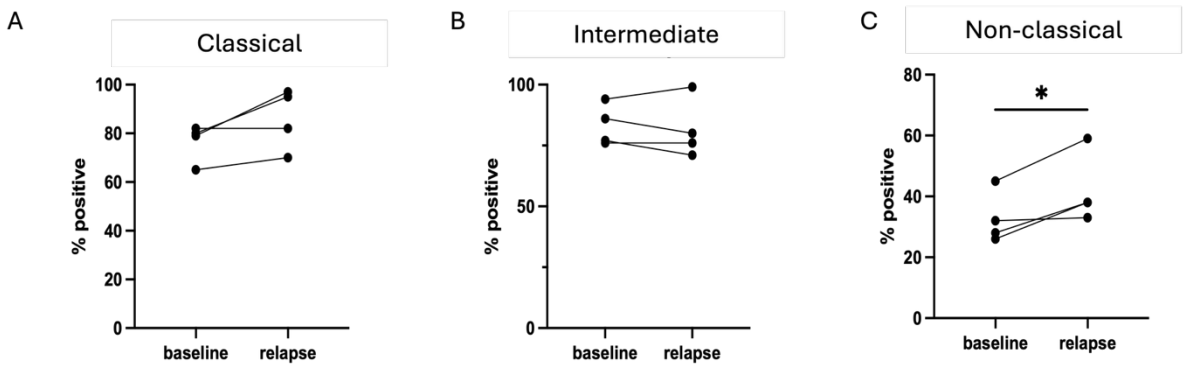

Figure 6.11: CCR5 expression changes between baseline and relapse.Line graphs showing CCR5 expression on (A) classical, (B) intermediate and (C) Non-classical monocyte subsets from TARDIS peripheral blood taken at baseline and at time of relapse. Each point represents a donor (N=4). Paired T-test P<0.05.

Lastly, to further investigate whether CCR5 plays a role in the pathogenesis of GCA, the previously described Δ32 mutation in the CCR5 gene, known to be associated with reduced cardiovascular disease risk and potentially protective in other vasculitides, was assessed. Therefore, to determine whether presence of this mutation could be associated with reduced risk of GCA, a linear regression analysis was carried out to calculate the log-odds of GCA incidence in relation to the presence of the CCR5Δ32 single nucleotide polymorphism (SNP). To do this, the UK Biobank was used (see methods section 2.1.4). Two cohorts were created as outlined in Table 6.1. The median age of the GCA cohort was 64 and the median age of the control cohort was lower at 58. However, it should be noted that these ages represent age at which their data was entered into the UKBiobank and not age at diagnosis. Furthermore, there was a higher proportion of males in the healthy control cohort compared to the GCA cohort. The regression model used accounts for sex and age differences within the cohort.

As the UK Biobank does not include genotyping for the rs333 (CCR5Δ32) mutation, an alternative SNP with high linkage disequilibrium (HLD) rs113010081010081 (a CCRL2 gene mutation) was used as a proxy mutation. HLD genes are genes that are inherited together more often than just chance and therefore, those with the rs113010081010081 mutation are highly likely to have the Δ32 mutation.

A generalised linear model was applied assuming an additive genetic model, whereby, the presence of two minor alleles is expected to have a greater effect than one minor allele. This analysis showed that age and sex highly correlated

with GCA incidence (*P* <0.001), as expected (Table 6.2). Age had a positive estimate of 0.112, suggesting that increasing age is positively correlated with incidence of GCA. Whereas, being male had a negative estimate of -0.7, meaning males were significantly less likely to develop GCA than females. Interestingly, the rs113010081010081 SNP had a negative estimate of -0.15 and a *P*-value of 0.025, indicating that individuals carrying this SNP were significantly less likely to have GCA. Therefore, this data supports the hypothesis that having the delta ∆32 mutation confers a degree of protection against GCA, further implicating the CCR5 axis in the disease pathogenesis.

Variable	GCA (n = 1,233)	Healthy Controls (n = 446,773)
Age (median)	64	58
Sex- male (%)	28.87	45.25
Genetic PCs adjusted for	Yes (1-8)	Yes (1-8)

Table 6.1: UK biobank cohort statistics. GCA defined as having any ICD10 report of M31.5 (GCA with PMR) or M31.6 (other GCA). ICD10 codes excluded from healthy control cohort.

Predictor	estimate	standard error	p-value	significance
age	0.1120214	0.005	<0.001	***
sex- male	−0.7395869	0.06	<0.001	***
SNP	−0.1560377	0.07	0.025	*

Table 6.2: Results from generalized linear model of SNP association with GCA incidence.SNP rs113010081.

6.3 Discussion.

The previous chapter aimed to better understand the differences in the circulating monocyte populations between healthy controls and GCA patients. In doing so, it was observed that up to 100% of GCA circulating monocytes expressed the chemokine receptor CCR5, suggesting a potential role in the pathogenesis of the disease. As CCR5 has been previously indicated in the formation of closely related MGCs, osteoclasts (Lee *et al.*, 2017), this chapter focused on the presence and importance of CCR5 expression on monocytes, macrophages and MGCs in GCA.

This chapter demonstrates that CCR5 and its ligands CCL3, 4, and 5 are expressed throughout GCA effected vessels. Analysis of spatial transcriptomic data showed that the chemokine receptor is universally expressed through all layers of the vessel, while the ligands were most highly expressed in the intimal and MGC rich regions. Large variation of CCR5 expression within the tissue among donors was observed when analysing spatial transcriptomic data. This variation in CCR5 expression was also observed in flow cytometric analysis (Section 5.2.1), suggesting that CCR5 is not expressed universally among all GCA patients. One study by (Estupiñán-Moreno *et al.*, 2022) showed that CCR5 transcription was upregulated in active disease, while it was downregulated in steroid induced remission. Therefore, the variation seen in these experiments could be due to disease activity and steroid treatment.
Furthermore, spatial and CUT&Tag data in previous chapters also demonstrated a potential downstream activation of the CCR5 signalling pathway. For example, in figure 3.6 and 3.7 it was shown that the ERK1/2 pathway and associated genes were enriched in both intima macrophages and MGC and the kinase ERK1 had significantly less H3K27Me3 repressive marks in GCA monocytes compared to healthy controls (figure 5.10). This kinase pathway has been identified as a key downstream pathway in CCR5 signalling (Zeng *et al.*, 2021), further suggesting the role of CCR5 in GCA.

The protein expression of CCR5 and its ligands was assessed by CD68+ cells in GCA tissue was shown by immunofluorescence and immunohistochemical staining. While CCL5 could be detected by IF, CCL3 could not. Conversely, when ligands were assessed by immunohistochemistry, CCL3 and CCL5 could be

observed in GCA tissue. This could be due to increased sensitivity of IHC staining compared to immunofluorescence staining. This increased sensitivity comes from the binding of DAB to HRP when the protein of interest is present meaning low abundance targets can be picked up more efficiently by IHC. Alternatively, The high autofluorescence of red blood cells (Whittington and Wray, 2017) in vascular tissue samples may be dampening a weak CCL3 signal. Therefore, future studies could use an auto-fluorescence quencher such as Trublack. Furthermore, the ligand CCL5 is thought to be produced by de novo synthesis and therefore, the detection of CCL5 by immunofluorescence was unexpected. However, one study in circulating monocytes suggests that these cells store preformed CCL5 intracellularly . However, this study did not include macrophages or monocytes in tissue and therefore, the pre-production of CCL5 in macrophages would need to be confirmed in future studies. Furthermore, CCL5 could be bound, in an autocrine manner to the CCR5 receptor on the surface of cells.

As CCR5, CCL3 and CCL5 were expressed in close proximity to, or within MGCs, the role of this chemokine axis in MGC formation was investigated. This showed that, when CCR5 was inhibited by antagonists, Leronlimab and Maraviroc, MGC formation was greatly reduced. However, there was a greater reduction in MGC numbers when Leronlimab was added to cultures, suggesting Leronlimab is a more potent CCR5 inhibitor than Maraviroc. Interestingly, in vitro HIV studies of CCR5 antagonists as treatment, showed that Maraviroc and Leronlimab acted in a synergistic fashion to inhibit HIV-1 fusion to cells (Murga *et al.*, 2006). It would be interesting, in future studies, to determine whether the same is true in MGC formation and whether simultaneous inhibition by both Leronlimab and Maraviroc would completely inhibit MGC formation in vitro and, therefore, whether these antagonists act on different CCR5 dependent pathways. Furthermore, there were no observable change in MGC numbers when CCR5 inhibitors were added to M-CSF+ IL-4 stimulated cells compared to GM-CSF+IFNγ. It has been shown throughout this thesis that MGCs from GCA patients are more likely to form when stimulated with GM-CSF+IFNγ, suggesting that CCR5 is involved in GCA specific MGC formation. In previous studies, it has been shown that mice deficient in IFNγ or its receptor IFNR2 had reduced expression of both CCL3 and CCL5 (Lin *et al.*, 2009). This demonstrates a potential link between

IFNy, which is a key player in GCA, and CCR5 and its ligands in the formation of MGCs. Surprisingly, when Maraviroc was added to RA osteoclast cultures, the ability of these cells to resorb bone was greatly impaired (Lee *et al.*, 2017). This was shown to be due to impaired podosome belt arrangement. However, the mechanism by which CCR5 inhibition modulates MGCs was not assessed in this chapter. Future studies could investigate how CCR5 inhibition affects the functional capacity of MGCs, for instance by assessing their ability to degrade a Matrigel matrix.

Interestingly, when these CCR5 modulators were added to cultures of GCA patient monocytes, there was no statistically significant difference between MGCs numbers. To determine whether this was due to the presence of non-classical CD16 expressing monocytes, two methods of monocyte enrichment were compared. This showed that classical monocytes cultured alone led to higher numbers of MGCs. Additionally, when Maraviroc was added to classical monocytes, the numbers of MGCs were once again significantly reduced. This indicates that classical monocytes are more likely to be the precursors to MGCs in GCA. This is supported by other MGC studies such as sarcoidosis. It was demonstrated that both FBGCs and LHGCs responded to staining by anti-CD14 antibodies and not anti-CD16 (Okamoto, Mizuno and Horio, 2003b), suggesting these cells are of CD14 monocytic origin. To further investigate this, future studies could employ fluorescent cell sorting to ensure the purity of cultures with each subset of monocyte and the resultant MGC numbers from culture.

When CCR5 ligands CCL3 and CCL5 were added to the culture system, only CCL3 was able to increase the numbers of MGCs produced.
The CCR5/CCL5 axis has been shown to induce anti-apoptotic signals to cells during viral infection (Tyner *et al.*, 2005) and has been linked to tumour cell survival in an autocrine manner in cancer studies (Aldinucci and Colombatti, 2014). Whereas, CCL3 has been shown to be involved in the fusion of osteoclast precursors in Multiple Myeloma (Oba *et al.*, 2005). Additionally, in spatial transcriptomic data and when TAB tissues were stained for ligand expression, CCL3 was shown to be highly expressed in the intimal region of the tissue and on CD68 negative cells. Taken together, this suggests that CCL3 could be sourced from nearby cells leading to cell fusion where as CCL5 could be reducing MGC

cell death. In an Antigen-induced Arthritis (AIA) rat model, addition of CCL3 increased the formation of Osteoclasts (Jordan *et al.*, 2018), supporting its role in the formation of MGCs.

As previously discussed, MGCs could be related to disease relapse (Restuccia *et al.*, 2016). Flow cytometry data, from TARDIS, at baseline and at the time of relapse, showed a slight but not significant increase in the expression of CCR5 on circulating monocytes. In particular, there was a significant increase in the CCR5 expression on $CD14^{low}CD16^{+}$ 'non-classical' monocytes. This preliminary evidence suggests a potential role for CCR5 expression in the incidence of relapse, which should be further investigated in future studies.
Finally, to further shows the importance of CCR5 in GCA pathogenesis a protective role for the SNP rs113010081 against the development of GCA was found in the UK Biobank cohort. However, as the rs333 SNP was not present in this dataset. The rs113010081 was used as a proxy as this mutation is often inherited with the Δ32 mutation While this suggests a high likelihood that the SNPs are inherited together, it is not a guarantee. One study of the role of Δ32 mutations in GCA did not find a significant difference between healthy controls and GCA patients. The rs113010081 mutation corresponds to the gene CCLR2. This 7-transmembrane receptor has been shown to act like an atypical chemokine receptor and has been implicated in the pathogenesis of the vascular pathology, atherosclerosis, whereby the genetic deletion of the CCRL2 gene inhibited macrophage accumulation in the vessels and diminished the formation of the atherosclerotic plaque (Cao *et al.*, 2015). Therefore, to determine whether the protective nature of the SNP is due to a loss of CCR5 function or CCRL2, further studies should be conducted.

In summary, this chapter demonstrated a key role for the chemokine receptor CCR5 in the pathogenesis of GCA. CCR5 and its ligands are universally expressed throughout affected tissue and are closely associated, with not only macrophages, but also MGCs. Modulation of CCR5 can significantly reduce MGC formation in an *in vitro* model of GCA like MGCs but not totally inhibit their formation. Future studies could aim to use higher concentrations of these antagonists to determine whether this would lead to complete inhibition of MGC formation. The ligand involved in this interaction is not yet known. However,

this chapter suggests a role for CCL3 in MGC formation that should be further investigated. Finally, the importance of CCR5 in pathogenesis of GCA was shown by a significantly reduced risk of GCA among those who carry the 32 base pair deletion. To conclude, further studies should be conducted on CCR5, in the context, of GCA to determine its treatment target potential.

Chapter 7 General discussion.

7.1 General discussion.

GCA is the most common form of large-vessel vasculitis in Europe. This granulomatous inflammatory vasculitis can lead to pain, blindness and stroke if not quickly and adequately treated (Farina *et al.*, 2023). The current mainstay treatment is prolonged courses of high-dose steroids, yet many patients will experience a relapse of disease during tapering of steroid doses (Moreel *et al.*, 2023). Furthermore, steroid treatment leads to serious adverse effects, including infection susceptibility and bone loss, which affect the patient's quality of life (Pofi *et al.*, 2023). Therefore, more targeted treatment strategies are urgently needed. A deeper understanding of the basic pathology of GCA, particularly the cellular processes that drive disease, is critical for identifying novel therapeutic targets.

The myeloid compartment, consisting of monocytes, macrophages, and MGCs, is central to GCA pathogenesis (Akiyama, Ohtsuki, Gerald J Berry, *et al.*, 2021) but the mechanisms involved in their formation and function remain poorly defined. To address this gap, spatial transcriptomic profiling was combined with functional assays, and molecular analyses. Specifically, this thesis aimed to provide a better understanding of these cells in GCA pathogenesis by comparing macrophages and MGCs across distinct spatial niches in affected tissue, examining MGC formation in healthy versus GCA monocytes, and assessing differences in circulating monocyte populations using flow cytometry, RNA sequencing, and CUT&Tag epigenetic profiling. Finally, the therapeutic potential of targeting the chemokine receptor CCR5 through inhibition by small-molecules and humanised monoclonal antibodies was explored.

7.2 Multinucleated giant cells as key players in GCA pathology.

MGC presence is a histological hallmark of GCA with ~50% of GCA patients having MGCs present (Johansen *et al.*, 1999; Kaiser *et al.*, 1999; Kloc *et al.*, 2022). However, still very little is known about how these cells form in GCA and

whether they are viable drug targets. This thesis initially investigated the transcriptome of macrophages and MGCs in distinct areas of the GCA vessel using GeoMx spatial profiling (Church *et al.*, 2024). This analysis revealed distinct transcriptional profiles of macrophages in different areas of the vessel. Interestingly, intimal macrophages had an overlapping gene expression profile with MGCs with the only statistically differential gene being the osteoclast marker TRAP. This suggested that intimal macrophages are transcriptionally similar to MGCs. Furthermore, in this analysis, the only differentially expressed gene between these cells was TRAP which could suggest a functional transition from MGC precursors to mature MGCs. This suggests that the local microenvironment at the media–intima may provide the cues required for their formation.

Furthermore, high expression of *FTH1* in MGCs highlights a potential role for iron dysregulation in GCA pathogenesis (Tian *et al.*, 2020). Ferroptosis, an iron-dependent form of cell death, has recently been proposed as a treatment target in other MGC-associated diseases such as RA and OA (Zhao *et al.*, 2023). Interestingly, auto-antibodies against FTH1 have been discovered in GCA, suggesting this axis may warrant further investigation (Baerlecken *et al.*, 2012). However, it remains unclear whether these observations reflect a causal mechanism or represent an epiphenomenon secondary to inflammation. Notably, heterogeneity in *TRAP* expression, with some MGCs positive and others negative, could point to functional diversity or different maturity levels of these cells, reinforcing the notion that MGCs represent a highly plastic cell type, with multifaceted roles in GCA pathology. Additionally, cell deconvolution analysis using the LM22 dataset as a reference, demonstrated that MGCs are transcriptionally most similar to M0 macrophages. These macrophages are thought to be an undifferentiated phenotype with the capacity to become either M1 or M2 polarised (Isali *et al.*, 2022), furthering the theory that MGCs can produce both pro- and anti-inflammatory factors.

While GeoMx spatial transcriptomics provided valuable spatial context, the lack of single-cell resolution introduces some uncertainty in attributing transcripts to specific populations. Therefore, it would be interesting to investigate the macrophages and MGCs, in their spatial niche, using a single cell spatial profiler,

such as, the CosMx platform, to identify differences between MGCs and macrophages and to determine whether intimal macrophages share a similar transcriptional profile to MGCs. Furthermore, it is important to acknowledge that the conventional M1/M2 nomenclature provides only a reductive view of the true plasticity of macrophages (Orekhov *et al.*, 2019). These categories are largely derived from *in vitro* models, which may not accurately reflect the heterogeneity and dynamic states of macrophages *in vivo***.** In this thesis, the LM22 signature matrix was chosen to specifically capture leukocyte-related populations, and the M1/M2 terminology was applied as a starting framework to characterise MGCs within GCA tissues. Future studies could address this limitation by leveraging single-cell sequencing of vascular tissue macrophages to better define the characteristics of healthy macrophages. Generating a reference matrix of vascular macrophages under homeostatic conditions would provide a more physiologically relevant comparator than LM22, which is derived from in vitro–cultured cells and constrained by a simplified M1/M2 polarization framework(Newman *et al.*, 2015a). Such approaches would improve determination of macrophage phenotypes within similar tissue environments and help elucidate the phenotypic characteristics of macrophages in GCA, thereby enabling more accurate and biologically relevant cell deconvolution (cite). For example, reference resources such as MoMAC-VERSE, which integrates macrophage and monocyte profiles across 13 tissues and 41 datasets, could be compared with GCA spatial transcriptomic data to distinguish homeostatic macrophage programs from disease-specific mechanisms (Mulder *et al.*, 2021).

This thesis demonstrates that GM-CSF and IFNγ are critical drivers of MGC formation specific to GCA through a novel model of MGC formation from GCA monocytes (Chapter 4). However, the precise mechanisms by which these cytokines induce multinucleation remain unclear. Importantly, monocytes from GCA patients responded differently to cytokine stimulation compared with healthy controls, highlighting disease-specific alterations in circulating monocytes, the precursors of macrophages within GCA lesions (Watanabe and Hashimoto, 2022b). This finding also emphasises the limitations of previous studies relying on the THP-1 cell line, which may not accurately reflect MGC formation in GCA. The observation that both LHGCs and FBGCs are present in

patient-derived cultures, and within affected vessels, raises the possibility of subtype-specific functions, which may contribute to the transcriptional and functional heterogeneity observed in spatial analyses. One study hypothesised that LHGCs cells represent a precursor state that transitions into FBGCs (van der Rhee, Hillebrands and Th Daems, 1978). This study observed a time-dependent shift from LHGC presence to FBGC presence. It is important to note, however, that this data was generated in a rodent model of induced granulomatous inflammation. Therefore, to verify this in a GCA specific context, future studies could employ laser capture microdissection of MGCs stratified by nuclear number (<30 vs. >30 nuclei), followed by single-cell sequencing, to identify molecular differences between these populations. Collectively, these findings support the hypothesis that circulating monocytes in GCA are intrinsically altered and predisposed to generate pathogenic MGCs.

However, there are some limitations to the *in vitro* model of multinucleation. While this model can be useful for understanding the mechanisms of MGC formation and investigate modulators of their formation, it does not accurately depict the full physiology of this disease, or which other cells of the vessel interact with macrophages to induce multinucleation. Future studies should aim to build on this *in vitro* model to make it more physiological. One such way would be to co-culture GCA monocytes with cells thought to be involved in the pathogenesis of the disease, such as, smooth muscle cells etc. Therefore, it would be beneficial in the understanding of the mechanisms involved in MGC formation in GCA using this method. For example, GCA monocytes could be added in culture with GCA T cells or B cells, as both are known to produce IFNγ (Harris *et al.*, 2005).

Furthermore, emerging technologies, such as, lab-on a-chip culture systems may also provide physiological context to this model. One study showed that human induced pluripotent stem cells could be differentiated to endothelial cells and vascular smooth muscle cells to create a vessel on a chip structure (Orekhov *et al.*, 2019). Therefore, PBMCs from GCA patients could be added to this 3D model, along with GM-CSF and IFNγ, to observe MGC formation in a more physiological context.

7.3 Monocytes in circulation are primed to become MGCs.

Differences in MGC formation between cultured healthy monocytes and GCA monocytes led to the hypothesis that GCA monocytes are primed to respond to GM-CSF and IFNγ to form MGCs. Therefore, this thesis next investigated differences in monocyte populations between GCA patients and healthy controls (Chapter 5). When surface molecule expression was assessed by flow cytometry, GCA monocytes showed an altered expression compared to healthy controls. This included the GM-CSF receptor CD116 (GM-CSFR). Interestingly, the chemokine receptor CCR5 was significantly upregulated in circulating classical and intermediate monocytes, which are thought to be main cells involved in GCA pathogenesis. Increased expression of this chemokine receptor has been associated with many immune mediated diseases such as atherosclerosis, where increased CCR5 is associated with increased accumulation of monocytes within the atherosclerotic plaques (Tacke *et al.*, 2007).

The presence of specific histone modifications can indicate whether a gene is likely to be activated or repressed. An increase in H3K4Me3 is associated with open chromatin and activated gene transcription (Santos-Rosa *et al.*, 2002). On the other hand, increased H3K27Me3 marks are associated with gene repression (Cai *et al.*, 2021). CUT&Tag analysis presented in this thesis suggested that differential gene expression in GCA monocytes was, primarily, due to reduced repression mediated by H3K27 tri-methylation, rather than increased activation via H3K4 tri-methylation. Notably, regulatory regions of GM-CSFR and IFNGR displayed significantly higher levels of H3K27me3 in control monocytes compared with GCA, consistent with reduced repression and greater responsiveness in the disease setting. While CCR5 itself did not show significant epigenetic differences, the antisense transcript CCR5-AS had less repressive marks in GCA monocytes compared to controls. Inhibition of this long non-coding RNA leads to a reduction in CCR5 expression, linking the two (Kulkarni *et al.*, 2019). This prompted further investigation into CCR5 regulation and its role in GCA pathogenesis. Together, these findings demonstrate that monocytes in patients with GCA are epigenetically and phenotypically primed in circulation to differentiate into macrophages and MGCs, providing a mechanistic link between systemic and tissue-level pathology.

Data on epigenetic changes in monocytes and macrophages in disease contexts is very limited as this is an emerging field. However, soluble mediators involved in GCA such as GM-CSF and IFNγ may influence epigenetic changes. One study showed that GM-CSF has been shown in human monocytes to reduce levels of the repressive histone mark H3K27me3 by increasing expression of the histone demethylase JMJD3(Achuthan *et al.*, 2016). In vitro treatment of human monocytes with GM-CSF resulted in elevated JMJD3 mRNA and protein expression, accompanied by a corresponding decrease in H3K27me3 marks. Given that GM-CSF is a key pathogenic molecule in GCA, this mechanism may help explain the reduced H3K27me3 levels observed in GCA monocytes compared with healthy controls. Therefore, future assessment of JMJD3 mRNA and protein expression in GCA tissue and circulating monocytes could provide further insight into potential GM-CSF–driven epigenetic alterations in disease.

However, several limitations in this chapter should be acknowledged. Some control samples were obtained from patients undergoing TAB, due to suspected GCA, raising the possibility of other underlying inflammatory conditions. In addition, most GCA patients had already received corticosteroid treatment, reflecting the clinical reality that treatment-naïve samples are rarely available due to the risk of irreversible visual loss prior to therapy initiation (Le Goueff *et al.*, 2019). Long-term exposure to glucocorticoids has been shown to alter the epigenetic landscape through suppression of demethylases such as JMJD3 leading to an decrease in H3K27Me3 induced gene silencing (Na *et al.*, 2017). Which may be the cause of a reduced H3K27Me3 profile in GCA monocytes. Additionally, emerging studies suggest that sex hormones such as Estrogen have been shown to alter the epigenome (Celestra *et al.*, 2025). As GCA affects women more than men, the differences in the epigenetic profile of GCA monocytes may be due, in part, to these hormones. Nevertheless, both GCA and control groups received comparable doses of steroids prior to sample collection, reducing the confounding nature of this treatment. Sample quality and missing data further reduced the number of replicates, highlighting the need for larger cohorts to validate these findings. Future studies should expand the histone modification analysis to include additional activation marks such as H3K9Ac and H3K27Ac, which are known to regulate inflammatory gene expression. For example, H3K9 acetylation has been shown to activate the IL-6 promoter in macrophages, a key

cytokine implicated in GCA pathogenesis (Hu *et al.*, 2017). Furthermore, IFNγ, shown in this thesis to be a key inducer of MGC formation, has been shown to increase the acetylation of the histone H3K27 (Qiao *et al.*, 2013), implicating it in the process of MGC formation. Such work would provide a more comprehensive understanding of the epigenetic landscape that primes monocytes for differentiation into pathogenic macrophages and MGCs in GCA.

However, it should be noted that macrophages may not be the sole cellular origin of MGCs. Studies of human osteoclastogenesis have demonstrated that dendritic cells can differentiate into osteoclasts and that osteoclasts showed greater transcriptional similarity to DCs than macrophages (Gallois *et al.*, 2010). The same has yet to be shown in GCA. However, one study identified that DCs in both inflamed and non-inflamed arteries were $S100^{+}$ and that some MGCs in GCA vessels were also $S100^{+}$. Suggesting DCs in the vessel can form MGCs(Krupa *et al.*, 2002). Furthermore, this thesis did not investigate the potential role of perivascular macrophages, which reside on the abluminal surface of blood vessels, in MGC formation. In disease states, these cells have been shown to produce pro-inflammatory cytokines and are thought to contribute to lung fibrosis (Lapenna, De Palma and Lewis, 2018). Therefore, future studies should aim to investigate the role of perivascular macrophages and dendritic cells and their potential to form MGCs in GCA.

Lastly, there is evidence that immune cells can be primed within the bone marrow. Hematopoietic stem and progenitor cells (HSPCs) are responsive to soluble inflammatory mediators such as GM-CSF, IFNγ, and other inflammatory signals, which can skew their differentiation toward myelopoiesis at the expense of other immune lineages. This biased myeloid output may contribute to chronic inflammation by establishing a positive feedback loop in which inflammatory cues promote continued myeloid cell production. In atherosclerosis, for example, elevated cholesterol levels are associated with increased GM-CSF signalling, which in turn drives expansion of myeloid cells (cite). Overall, bone marrow priming by soluble mediators such as GM-CSF could prime HSPCs in the bone marrow to become monocytes with the potential to form into MGCs. Therefore, future studies should strive to understand the role of HSPCs in GCA.

7.4 CCR5 is a key molecule in GCA.

Throughout this thesis, CCR5 has emerged as a key molecule defining the difference between healthy monocytes and GCA monocytes. Therefore, the last chapter of this thesis focused on the potential role of this chemokine receptor and its ligands in the pathogenesis of GCA (Chapter 6). Staining by immunohistochemistry and fluorescent antibodies showed that CCR5 was universally expressed throughout the vessel, with a high concentration in MGCs and the surrounding areas. This suggested that CCR5 and its ligands could be a potential mechanism for the formation of MGCs. Blocking CCR5 signalling through Maraviroc and Leronlimab drastically reduced the number of MGCs produced *in vitro*, suggesting a role for the chemokine receptor in this process. However, MGC formation was not fully abrogated, suggesting a redundant mechanism by which MGCs are also formed. Further, adding the CCR5 ligand CCL3 to the culture system induced a greater amount of MGC formation *in vitro*. In Chapter 3, chemokine receptor binding was an enriched molecular function pathway in MGC rich regions with CCL3 being highly expressed in intimal macrophages and MGC rich regions. Therefore, this thesis leads to a hypothesis that CCL3 could be secreted by surrounding cells to macrophages in the intima region which leads to CCR5 signalling and induces MGC formation. Therefore, future studies should aim to investigate the role of CCL3 in MGC formation, in the context of GCA. Interestingly, it has been shown that CCL3 signalling through CCR5 is involved in the formation of osteoclasts, in the context of myeloma, further supporting this hypothesis (Jordan *et al.*, 2018).

The role of CCR5 in GCA pathogenesis was further explored through analysis of CCR5-associated SNPs in relation to disease incidence. Interestingly, the presence of CCR5-associated SNPs correlated with a decreased risk of developing GCA, suggesting that the ∆32 mutation of CCR5 is protective against GCA, further supporting a role for CCR5 in the disease pathogenesis. To add to this, functional analysis revealed that patients who experienced relapse displayed a modest increase in CCR5 expression on circulating monocytes, pointing to a potential role for the CCR5–monocyte axis in disease recurrence. Mechanistically, the CCR5/CCL5 pathway has been implicated in the induction of IL-6 production across multiple inflammatory conditions (Tang, Hsu and Fong, 2010), aligning with the central role of IL-6 in GCA pathogenesis. Furthermore,

CCR5 has been shown to be involved in NF-κB signalling. This signalling can result in the dominance of pro-inflammatory cytokines such as IFNγ, positioning it as a regulator of macrophage activation. This data was acquired in a rat disease model of colitis and, therefore, the correlation of NF-KB and CCR5 should be confirmed in human cells. Epigenetic studies in related diseases, such as inflammatory arthritis, have demonstrated increased H3K27 acetylation at the CCR5 locus (Rutger J. Wierda *et al.*, 2012), supporting the concept that altered chromatin accessibility may enhance CCR5-driven inflammatory responses. Collectively, these results establish CCR5 as a central regulator of GCA pathogenesis, contributing to MGC formation, disease susceptibility, and relapse risk. This identifies CCR5 as a promising therapeutic target that warrants further preclinical and translational investigation.

While this thesis is the first to describe CCR5 as a key molecule involved in the pathogenesis of GCA, in particular the formation of MGCs, it does not propose a mechanism by which this chemokine receptor induces this formation. To better understand the impact of CCR5 inhibition on the GCA vessel as a whole, *ex vivo* studies could be completed on TABs. One study by (Corbera-Bellalta *et al.*, 2014) demonstrate an ex vivo culture model of TABs in Matrigel which can be used to study the effects of therapeutic interventions on the vessel. For example, the anti-CCR5 monoclonal antibody Leronlimab could be added to this culture system to investigate whether it has an effect on pre-existing MGCs and the overall pathogenesis of GCA.

7.5 Summary.

In summary, by investigating MGCs and macrophages in distinct areas of the vessel, a precursor subset of intimal macrophages has been proposed. Furthermore, elucidating the transcriptional profile of these cells has allowed for their distinction as M0-like ‘undifferentiated’ macrophages that can play a role in both media destruction and intimal hyperplasia in the progression of GCA. Additionally, this thesis demonstrates, for the first time, a GCA specific model of multinucleation that can be used to better understand the mechanism of MGC formation in GCA. This in vitro model can be used for further mechanistic studies. Profound differences in surface expression, transcriptional and epigenetic profiles of GCA monocytes compared to healthy monocytes are

shown, indicating that they are primed in circulation to enter the vessel and form MGCs. By integrating spatial, molecular, and functional analyses, this thesis, not only identifies CCR5 as a central driver of monocyte and MGC pathology in GCA but also establishes experimental models that can guide the development of more targeted therapies (Figure 7.1). These insights lay the foundation for future translational approaches aimed at improving outcomes for patients with GCA.

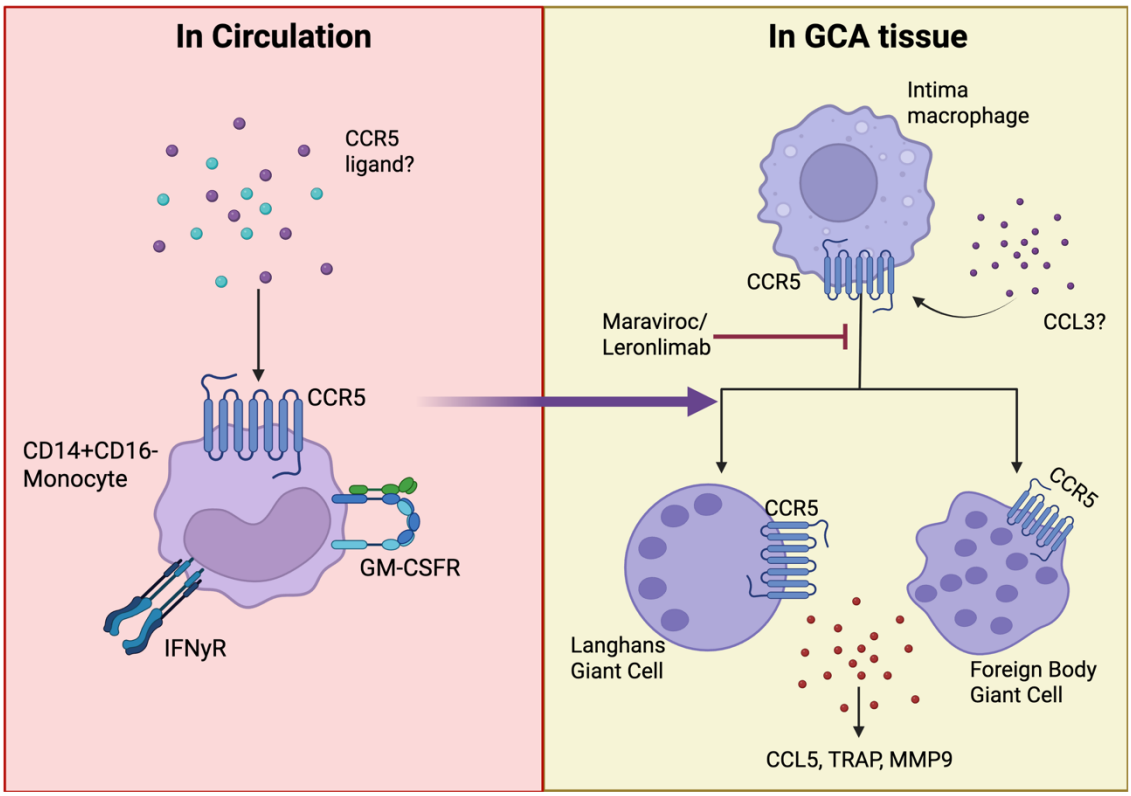

Figure 7.1: Graphical summary of key findings. Summary of monocytes, macrophages and MGC mechanisms in GCA discovered during this thesis. Made using BioRender.

Appendix

Media, buffers and solutions

Complete α-MEM media

- 500ml alpha-mem essential media (Gibco).
- 50ml Heat inactivate fetal bovine serum (FBS, Gibco).
- 5ml Penicillin/Streptomycin (Sigma).
- 5ml L-glutamine (Gibco).

Cell separation buffer

- 500 ml dPBS (PBS; Gibco)
- 1% Heat Inactivated Fetal Bovine Serum (FBS; Gibco)
- 2 mM Ethylenediaminetetraacetic acid (EDTA; Invitrogen)

FACS buffer

- 500 ml PBS
- 2% FBS
- 2 mM EDTA

TRAP fixative solution

- 12.5 ml citrate solution
- 32.5 ml acetone
- 5 ml 37% formaldehyde

166

TRAP staining solution

For 1 ml:

- 900 µL distilled water
- 10 µL Fast Garnet Solution (5 µL Fast Garnet + 5 µL Sodium Nitrite)
- 10 µL Napthol
- 40 µL Acetate
- 50 µL Tartrate (1M - 2.8 g of K-Na Tartrate Tetrahydrate (MW 282.23; $C_4H_4KNaO_6*4H_2O$) in 10 mL H_2O)

TBST

- 1x Tris-buffered saline
- 0.1% Tween

PFA

- 500 ml PBS
- 2% para formaldehyde

2% formaldehyde

- 50 ml dH2O
- 2% methanol-free formaldehyde

0.1% Triton

- PBS
- 0.1% Triton X-100

2% BSA

- 50 ml PBS
- 2% bovine serum albumin

GlasgowMSK
Glasgow Musculoskeletal Diseases Group

University of Glasgow
School of Infection & Immunity

Healthy volunteers over 50 years of age needed please.

Inflammation of blood vessels (vasculitis) is a common occurrence in individuals with rheumatic disorders. To understand this process, we are investigating the levels of numerous molecules in the blood of people with vasculitis. However, to get the complete picture we need to compare these levels to those in healthy volunteers. This will help us to potentially find better treatments for people with this type of condition.

We are looking for male and female volunteers who are **over 50 years of age** to donate a small amount of blood, 40ml, which is equivalent to 8 teaspoons, on one occasion.

If you would like further information on the study or if you would like to participate, please e-mail:

Annie Peacock

GlasgowMSK@glasgow.ac.uk

(PhD student supervisor: Professor Carl Goodyear)

This study received College of MVLS ethical committee approval on 01 November 2022

Reference number: 2012073

Figure 7.2: Healthy donor recruitment poster.

University of Glasgow | College of Medical, Veterinary & Life Sciences

Centre: Glasgow Musculoskeletal Diseases Group
School of Infection & Immunity, MVLS, University of Glasgow

Participant identification number:_____

CONSENT FORM

Title of Project: **Cells and soluble mediators in peripheral blood of normal healthy donors**

Name of Researcher(s):_____

Please initial box

I confirm that I have read and understood the information sheet titled: **Cells and soluble mediators in peripheral blood of normal healthy donors**, dated 25 October 2022, V6.0, for the above study.	☐
I have had the opportunity to think about the information and ask questions, and understand the answers I have been given.	☐
I confirm that I have read and understood the Privacy Notice version 2.0, dated 25 October 2022.	☐
I understand that my participation is voluntary and that I am free to withdraw at any time, without giving any reason, without my legal rights being affected.	☐
I confirm that I agree to the way my data will be collected and processed and that data will be stored for up to 10 years in the University archiving facilities in accordance with relevant Data Protection policies and regulations.	☐
I understand that all data and information I provide will be kept confidential and will be seen only by study researchers and regulators whose job it is to check the work of researchers.	☐
I agree that my name, contact details and data described in the information sheet will be kept for the purposes of this research project	☐
I understand that if I withdraw from the study, my data collected up to that point will be retained and used for the remainder of the study.	☐

Figure 7.3: Healthy donor consent form.

University of Glasgow | College of Medical, Veterinary & Life Sciences

Glasgow Musculoskeletal Diseases Group

1. Study title

Cells and soluble mediators in peripheral blood of normal healthy donors

2. Invitation paragraph

You are being invited to take part in a research study. Before you decide it is important for you to understand why the research is being done and what it will involve. Please take time to read the following information carefully and discuss it with others if you wish. Ask us if there is anything that is not clear or if you would like more information. Take time to decide whether or not you wish to take part. If you decide to take part in this study, you will be given a copy of this Participant Information Sheet and the signed consent form to keep.

3. What is the purpose of the study?

The purpose of the study is to find better treatments for various types of rheumatic diseases.

These disabling diseases affect 700,000 adults aged 20-75 years old in the UK. Little is known about the origin of these diseases or how to effectively prevent their progression. Thus, to find a better treatment for these diseases we need to understand the differences between the people who develop them and the people who do not (you).

4. Why have I been asked to take part?

You have been invited to take part because you are healthy, your age matches with our arthritis patient group, and we would like your blood for a comparison. You will be part of a cohort of approximately 250 healthy people recruited over the period of approximately 5 years.

You can only be in this study if you:

- Healthy and aged 18 years or over.
- You have not donated more than 250ml of blood in the previous month.

5. Do I have to take part?

It is up to you to decide whether or not to take part. You will be given this information sheet and have a suitable amount of time to read it and the opportunity to ask a qualified person about any questions you may have. If you do decide to take part, you will be asked to sign a consent form giving your authorisation to take the blood sample. If you agree to take part, you are still free to withdraw from the study at any time and without giving a reason.

Co-enrolment in 2 studies:

You may be asked to participate in another MVLS ethics committee approved study at the same time as this one (co-enrolment). You will be given the appropriate study information sheet and given a suitable amount of time to read it and the opportunity to ask a qualified person about any questions you may have. You do not have to take part in both studies. If you agree to take part, you are still free to withdraw from the study at any time without giving a reason.

If you are a student at the University of Glasgow or another academic institution your decision to participate or not will not affect your grades in any way.

Figure 7.4: Patient information sheet example.

List of References

Abbasova, L. *et al.* (2025) 'CUT&Tag recovers up to half of ENCODE ChIP-seq histone acetylation peaks', *Nature Communications*, 16(1), p. 2993. Available at: https://doi.org/10.1038/s41467-025-58137-2.

Achuthan, A. *et al.* (2016) 'Granulocyte macrophage colony-stimulating factor induces CCL17 production via IRF4 to mediate inflammation', *The Journal of Clinical Investigation*, 126(9), pp. 3453–3466. Available at: https://doi.org/10.1172/JCI87828.

Agresti, N. *et al.* (2021) 'Disruption of CCR5 signaling to treat COVID-19-associated cytokine storm: Case series of four critically ill patients treated with leronlimab', *Journal of Translational Autoimmunity*, 4, p. 100083. Available at: https://doi.org/10.1016/j.jtauto.2021.100083.

Ahmadzadeh, K. *et al.* (2022) 'Multinucleated Giant Cells: Current Insights in Phenotype, Biological Activities, and Mechanism of Formation', *Frontiers in Cell and Developmental Biology*, 10. Available at: https://doi.org/10.3389/fcell.2022.873226.

Ahmadzadeh, K. *et al.* (2023) 'Multinucleation resets human macrophages for specialized functions at the expense of their identity', *EMBO reports*, 24(3). Available at: https://doi.org/10.15252/embr.202256310.

Akchurin, T. *et al.* (2008) 'Complex dynamics of osteoclast formation and death in long-term cultures', *PLoS ONE*, 3(5). Available at: https://doi.org/10.1371/journal.pone.0002104.

Akiyama, M., Ohtsuki, S., Berry, Gerald J., *et al.* (2021) 'Innate and Adaptive Immunity in Giant Cell Arteritis', *Frontiers in Immunology*, 11, p. 621098. Available at: https://doi.org/10.3389/fimmu.2020.621098.

Akiyama, M., Ohtsuki, S., Berry, Gerald J, *et al.* (2021) 'Innate and Adaptive Immunity in Giant Cell Arteritis', 11(February), pp. 1–17. Available at: https://doi.org/10.3389/fimmu.2020.621098.

Albert, D.M., Ruchman, M.C. and Keltner, J.L. (1976) 'Skip Areas in Temporal Arteritis', *Archives of Ophthalmology*, 94(12), pp. 2072–2077. Available at: https://doi.org/10.1001/archopht.1976.03910040732006.

Aldinucci, D. and Colombatti, A. (2014) 'The Inflammatory Chemokine CCL5 and Cancer Progression', *Mediators of Inflammation*, 2014(1), p. 292376. Available at: https://doi.org/10.1155/2014/292376.

Amoli, M.M. *et al.* (2004) 'Epistatic interactions between HLA-DRB1 and interleukin 4, but not interferon-gamma, increase susceptibility to giant cell arteritis.', *The Journal of Rheumatology*, 31(12), pp. 2413–2417.

An, P. *et al.* (2011) 'Role of Exonic Variation in Chemokine Receptor Genes on AIDS: CCRL2 F167Y Association with Pneumocystis Pneumonia', *PLOS Genetics*, 7(10), p. e1002328. Available at: https://doi.org/10.1371/journal.pgen.1002328.

Anderson, J.M. (2000) 'Multinucleated giant cells', *Current Opinion in Hematology*, 7(1), p. 40.

Andrew J Bannister & Tony Kouzarides (2011) *Regulation of chromatin by histone modifications | Cell Research*. Available at: https://www.nature.com/articles/cr201122 (Accessed: 26 September 2025).

Andrews, S. (2010) *Babraham Bioinformatics - FastQC A Quality Control tool for High Throughput Sequence Data*. Available at: https://www.bioinformatics.babraham.ac.uk/projects/fastqc/ (Accessed: 10 July 2025).

Ansalone, C., Cole, J., Chilaka, S., Sunzini, F., Sood, S., Robertson, J., Siebert, S., McInnes, Iain B, *et al.* (2021) 'TNF is a homoeostatic regulator of distinct epigenetically primed human osteoclast precursors', *Annals of the Rheumatic Diseases*, 80(6), pp. 748–757. Available at: https://doi.org/10.1136/annrheumdis-2020-219262.

Ansalone, C., Cole, J., Chilaka, S., Sunzini, F., Sood, S., Robertson, J., Siebert, S., McInnes, Iain B., *et al.* (2021) 'TNF is a homoeostatic regulator of distinct epigenetically primed human osteoclast precursors', *Annals of the Rheumatic Diseases*, 80(6), pp. 748–757. Available at: https://doi.org/10.1136/annrheumdis-2020-219262.

Ardavín, C. *et al.* (2001) 'Origin and differentiation of dendritic cells', *Trends in Immunology*, 22(12), pp. 691–700. Available at: https://doi.org/10.1016/S1471-4906(01)02059-2.

Aristizábal, B. and González, Á. (2013) 'Innate immune system', in *Autoimmunity: From Bench to Bedside [Internet]*. El Rosario University Press. Available at: https://www.ncbi.nlm.nih.gov/books/NBK459455/ (Accessed: 2 September 2025).

Armstrong, A.T. *et al.* (2008) 'Clinical importance of the presence of giant cells in temporal arteritis', *Journal of Clinical Pathology*, 61(5), pp. 669–671. Available at: https://doi.org/10.1136/jcp.2007.049049.

Arteritis, I.G. *et al.* (2016) 'Description and Validation of Histological Patterns and Proposal of a Dynamic Model of Inflammatory', 95(8), pp. 1–12. Available at: https://doi.org/10.1097/MD.0000000000002368.

Ay-Berthomieu, A.-S. (2020) *Comprehensive Guide to Understanding and Using CUT&Tag Assays*, *Active Motif*. Available at: https://www.activemotif.com/blog-cut-tag (Accessed: 10 July 2025).

Baerlecken, N.T. *et al.* (2012) 'Association of ferritin autoantibodies with giant cell arteritis/polymyalgia rheumatica', *Annals of the Rheumatic Diseases*, 71(6), pp. 943–947. Available at: https://doi.org/10.1136/annrheumdis-2011-200413.

Balistreri, C.R. *et al.* (2007) 'CCR5 Receptor', *Annals of the New York Academy of Sciences*, 1100(1), pp. 162–172. Available at: https://doi.org/10.1196/annals.1395.014.

Barbeck, M. *et al.* (2022) 'Comparison of the Validity of Enzymatic and Immunohistochemical Detection of Tartrate-resistant Acid Phosphatase (TRAP) in the Context of Biocompatibility Analyses of Bone Substitutes', *In Vivo*, 36(5), pp. 2042–2051. Available at: https://doi.org/10.21873/invivo.12930.

Barnes, P.J. (2006) 'Corticosteroid effects on cell signalling', *European Respiratory Journal*, 27(2), pp. 413–426. Available at: https://doi.org/10.1183/09031936.06.00125404.

Benabid, A. and Peduto, L. (2020) ‘Mesenchymal perivascular cells in immunity and disease’, *Current Opinion in Immunology*, 64, pp. 50–55. Available at: https://doi.org/10.1016/j.coi.2020.03.009.

Benayoun, B.A. *et al.* (2014) ‘H3K4me3 breadth is linked to cell identity and transcriptional consistency’, *Cell*, 158(3), pp. 673–688. Available at: https://doi.org/10.1016/j.cell.2014.06.027.

Benhar, L., London, A. and Schwartz, M. (2012) ‘The privileged immunity of immune privileged organs: the case of the eye’, *Frontiers in Immunology*, 3. Available at: https://doi.org/10.3389/fimmu.2012.00296.

Bernaerts, E. *et al.* (2024) ‘Human monocyte-derived macrophages shift subcellular metalloprotease activity depending on their activation state’, *iScience*, 27(11). Available at: https://doi.org/10.1016/j.isci.2024.111171.

Bernardini, G. *et al.* (2003) ‘Analysis of the role of chemokines in angiogenesis’, *Journal of Immunological Methods*, 273(1), pp. 83–101. Available at: https://doi.org/10.1016/S0022-1759(02)00420-9.

Blockmans, D. *et al.* (2025) ‘A Phase 3 Trial of Upadacitinib for Giant-Cell Arteritis’, *New England Journal of Medicine*, 392(20), pp. 2013–2024. Available at: https://doi.org/10.1056/NEJMoa2413449.

Bonilla, F.A. and Oettgen, H.C. (2010) ‘Adaptive immunity’, *Journal of Allergy and Clinical Immunology*, 125(2, Supplement 2), pp. S33–S40. Available at: https://doi.org/10.1016/j.jaci.2009.09.017.

Brooks, P.J., Glogauer, M. and McCulloch, C.A. (2019) ‘An Overview of the Derivation and Function of Multinucleated Giant Cells and Their Role in Pathologic Processes’, *American Journal of Pathology*, 189(6), pp. 1145–1158. Available at: https://doi.org/10.1016/j.ajpath.2019.02.006.

Brühl, H. *et al.* (2005) ‘Expression of DARC, CXCR3 and CCR5 in giant cell arteritis’, *Rheumatology*, 44(3), pp. 309–313. Available at: https://doi.org/10.1093/rheumatology/keh485.

Buchman, A.L. (2001) *Clinical Reviews Therapeutic Recommendations Side Effects of Corticosteroid Therapy*. Available at: http://journals.lww.com/jcge.

Buttgereit, F. *et al.* (2023) ‘Tocilizumab in Giant Cell Arteritis: Better Understanding the Benefits’, *Arthritis and Rheumatology*, 75(4), pp. 489–492. Available at: https://doi.org/10.1002/art.42414.

Byrd, T.F. (1998) ‘Multinucleated Giant Cell Formation Induced by IFN-γ/IL-3 Is Associated with Restriction of Virulent*Mycobacterium tuberculosis*Cell to Cell Invasion in Human Monocyte Monolayers’, *Cellular Immunology*, 188(2), pp. 89–96. Available at: https://doi.org/10.1006/cimm.1998.1352.

Cai, Y. *et al.* (2021) ‘H3K27me3-rich genomic regions can function as silencers to repress gene expression via chromatin interactions’, *Nature Communications*, 12(1), p. 719. Available at: https://doi.org/10.1038/s41467-021-20940-y.

Cao, Y. *et al.* (2015) 'Genetic Deletion of CCRL2 Impairs Macrophage Accumulation in Arterial Intima and Attenuates Atherosclerotic Plaque Development', *Blood*, 126(23), p. 2239. Available at: https://doi.org/10.1182/blood.V126.23.2239.2239.

Carter, N.J. and Keating, G.M. (2007) 'Maraviroc', *Drugs*, 67(15), pp. 2277–2288. Available at: https://doi.org/10.2165/00003495-200767150-00010.

Celestra, D. *et al.* (2025) 'Epigenetic remodeling by sex hormone receptors and implications for gender affirming hormone therapy', *Frontiers in Immunology*, 16, p. 1501959. Available at: https://doi.org/10.3389/fimmu.2025.1501959.

Champion, T.C. *et al.* (2018) 'Monocyte subsets have distinct patterns of tetraspanin expression and different capacities to form multinucleate giant cells', *Frontiers in Immunology*, 9(JUN). Available at: https://doi.org/10.3389/fimmu.2018.01247.

Chapuis, F. *et al.* (1997) 'Differentiation of human dendritic cells from monocytes in vitro', *European Journal of Immunology*, 27(2), pp. 431–441. Available at: https://doi.org/10.1002/eji.1830270213.

Chen, S. *et al.* (2023) 'Macrophages in immunoregulation and therapeutics', *Signal Transduction and Targeted Therapy*, 8(1), p. 207. Available at: https://doi.org/10.1038/s41392-023-01452-1.

Chen, Y. *et al.* (2022) 'Insight into the Molecular Characteristics of Langhans Giant Cell by Combination of Laser Capture Microdissection and RNA Sequencing', *Journal of Inflammation Research*, 15, pp. 621–634. Available at: https://doi.org/10.2147/JIR.S337241.

Chu, C.-Q. (2023) 'Animal models for large vessel vasculitis – The unmet need', *Rheumatology and Immunology Research*, 4(1), pp. 4–10. Available at: https://doi.org/10.2478/rir-2023-0002.

Church, S.E. *et al.* (2024) 'Chapter 47 - Translational and clinical applications of the GeoMx digital spatial profiling platform', in W.B. Coleman and G.J. Tsongalis (eds) *Diagnostic Molecular Pathology (Second Edition)*. Academic Press, pp. 767–783. Available at: https://doi.org/10.1016/B978-0-12-822824-1.00034-1.

Cole, J.J. *et al.* (2021) 'Searchlight: automated bulk RNA-seq exploration and visualisation using dynamically generated R scripts', *BMC Bioinformatics*, 22(1), p. 411. Available at: https://doi.org/10.1186/s12859-021-04321-2.

Constant, S.L. and Bottomly, K. (1997) 'INDUCTION OF TH1 AND TH2 CD4+ T CELL RESPONSES:The Alternative Approaches', *Annual Review of Immunology*, 15(Volume 15, 1997), pp. 297–322. Available at: https://doi.org/10.1146/annurev.immunol.15.1.297.

Cooper, R.J. *et al.* (2008) 'Infection and temporal arteritis: A PCR-based study to detect pathogens in temporal artery biopsy specimens', *Journal of Medical Virology*, 80(3), pp. 501–505. Available at: https://doi.org/10.1002/jmv.21092.

Corbera-Bellalta, M. *et al.* (2014) 'Changes in biomarkers after therapeutic intervention in temporal arteries cultured in Matrigel: A new model for preclinical studies in giant-cell arteritis', *Annals of the Rheumatic Diseases*, 73(3), pp. 616–623. Available at: https://doi.org/10.1136/annrheumdis-2012-202883.

Corbera-Bellalta, M. *et al.* (2022) 'Blocking GM-CSF receptor α with mavrilimumab reduces infiltrating cells, pro-inflammatory markers and neoangiogenesis in ex vivo cultured arteries from patients with giant cell arteritis', *Annals of the rheumatic diseases*, 81(4), pp. 524–536. Available at: https://doi.org/10.1136/annrheumdis-2021-220873.

Cronstein, B.N. and Aune, T.M. (2020) 'Methotrexate and its mechanisms of action in inflammatory arthritis', *Nature Reviews Rheumatology*, 16(3), pp. 145–154. Available at: https://doi.org/10.1038/s41584-020-0373-9.

Davies, L.C. *et al.* (2013) 'Tissue-resident macrophages', *Nature immunology*, 14(10), pp. 986–995. Available at: https://doi.org/10.1038/ni.2705.

Davis, F.M. and Gallagher, K. (2019) 'Epigenetic Mechanisms in Monocyte/Macrophages Regulate Inflammation in Cardiometabolic and Vascular Disease', *Arteriosclerosis, thrombosis, and vascular biology*, 39(4), pp. 623–634. Available at: https://doi.org/10.1161/ATVBAHA.118.312135.

De Smit, E., Palmer, A.J. and Hewitt, A.W. (2015) 'Projected worldwide disease burden from giant cell arteritis by 2050', *Journal of Rheumatology*, 42(1), pp. 119–125. Available at: https://doi.org/10.3899/jrheum.140318.

Delmonte, O.M. and Fleisher, T.A. (2019) 'Flow cytometry: Surface markers and beyond', *Journal of Allergy and Clinical Immunology*, 143(2), pp. 528–537. Available at: https://doi.org/10.1016/j.jaci.2018.08.011.

Delneste, Y. *et al.* (2003) 'Interferon-γ switches monocyte differentiation from dendritic cells to macrophages', *Blood*, 101(1), pp. 143–150. Available at: https://doi.org/10.1182/blood-2002-04-1164.

Deng, J. *et al.* (2010) 'Th17 and Th1 T-Cell Responses in Giant Cell Arteritis', *Circulation*, 121(7), pp. 906–915. Available at: https://doi.org/10.1161/CIRCULATIONAHA.109.872903.

Dobin, A. *et al.* (2013) 'STAR: ultrafast universal RNA-seq aligner', *Bioinformatics*, 29(1), pp. 15–21. Available at: https://doi.org/10.1093/bioinformatics/bts635.

Dorr, P. *et al.* (2005) 'Maraviroc (UK-427,857), a Potent, Orally Bioavailable, and Selective Small-Molecule Inhibitor of Chemokine Receptor CCR5 with Broad-Spectrum Anti-Human Immunodeficiency Virus Type 1 Activity', *Antimicrobial Agents and Chemotherapy*, 49(11), pp. 4721–4732. Available at: https://doi.org/10.1128/aac.49.11.4721-4732.2005.

Esen, I. *et al.* (2021) 'Functionally heterogenous macrophage subsets in the pathogenesis of giant cell arteritis: Novel targets for disease monitoring and treatment', *Journal of Clinical Medicine*, 10(21). Available at: https://doi.org/10.3390/jcm10214958.

Estupiñán-Moreno, E. *et al.* (2022) 'Methylome and transcriptome profiling of giant cell arteritis monocytes reveals novel pathways involved in disease pathogenesis and molecular response to glucocorticoids', *Annals of the Rheumatic Diseases*, 81(9), pp. 1290–1300. Available at: https://doi.org/10.1136/annrheumdis-2022-222156.

Estupiñán-Moreno, E. *et al.* (2024) 'Decoding CD4+ T cell transcriptome in giant cell arteritis: Novel pathways and altered cross-talk with monocytes', *Journal of Autoimmunity*, 146. Available at: https://doi.org/10.1016/j.jaut.2024.103240.

Farina, N. *et al.* (2023) 'Giant cell arteritis: Update on clinical manifestations, diagnosis, and management', *European Journal of Internal Medicine*, 107, pp. 17–26. Available at: https://doi.org/10.1016/j.ejim.2022.10.025.

Gallois, A. *et al.* (2010) 'Genome-wide expression analyses establish dendritic cells as a new osteoclast precursor able to generate bone-resorbing cells more efficiently than monocytes', *Journal of Bone and Mineral Research*, 25(3), pp. 661–672. Available at: https://doi.org/10.1359/jbmr.090829.

Galvani, A.P. and Novembre, J. (2005) 'The evolutionary history of the CCR5-Delta32 HIV-resistance mutation', *Microbes and Infection*, 7(2), pp. 302–309. Available at: https://doi.org/10.1016/j.micinf.2004.12.006.

Gasser, A. and Möst, J. (1999) *Generation of Multinucleated Giant Cells In Vitro by Culture of Human Monocytes with Mycobacterium bovis BCG in Combination with Cytokine-Containing Supernatants*. Available at: https://doi.org/10.1128/iai.67.1.395-402.1999.

Geissmann, F. *et al.* (2010) 'Development of monocytes, macrophages and dendritic cells', *Science (New York, N.Y.)*, 327(5966), pp. 656–661. Available at: https://doi.org/10.1126/science.1178331.

Gerhardt, T. and Ley, K. (2015) 'Monocyte trafficking across the vessel wall', *Cardiovascular Research*, 107(3), pp. 321–330. Available at: https://doi.org/10.1093/cvr/cvv147.

Ginhoux, F. and Guilliams, M. (2016) 'Tissue-Resident Macrophage Ontogeny and Homeostasis', *Immunity*, 44(3), pp. 439–449. Available at: https://doi.org/10.1016/j.immuni.2016.02.024.

Gloor, A.D. *et al.* (2025) 'Precision Over Prednisone: Innovative Treatment Strategies for Giant Cell Arteritis', *Current Treatment Options in Rheumatology*, 11(1), p. 9. Available at: https://doi.org/10.1007/s40674-025-00230-0.

van der Goes, M.C., Jacobs, J.W. and Bijlsma, J.W. (2014) 'The value of glucocorticoid co-therapy in different rheumatic diseases - positive and adverse effects', *Arthritis Research & Therapy*, 16(2), p. S2. Available at: https://doi.org/10.1186/ar4686.

Gonzalez-Gay, M.A. *et al.* (2007) 'Giant Cell Arteritis in Northwestern Spain: A 25-Year Epidemiologic Study', *Medicine*, 86(2), p. 61. Available at: https://doi.org/10.1097/md.0b013e31803d1764.

González-Gay, M.A. *et al.* (2025) 'Revisiting the epidemiology of giant cell arteritis', *Clinical and Experimental Rheumatology* [Preprint].

Graver, J.C. *et al.* (2019) 'Massive B-cell infiltration and organization into artery tertiary lymphoid organs in the aorta of large vessel giant cell arteritis', *Frontiers in Immunology*, 10(JAN). Available at: https://doi.org/10.3389/fimmu.2019.00083.

Guan, F. *et al.* (2025) 'Tissue macrophages: origin, heterogenity, biological functions, diseases and therapeutic targets', *Signal Transduction and Targeted Therapy*, 10(1), p. 93. Available at: https://doi.org/10.1038/s41392-025-02124-y.

Harris, D.P. *et al.* (2005) 'Regulation of IFN-γ Production by B Effector 1 Cells: Essential Roles for T-bet and the IFN-γ Receptor1', *The Journal of Immunology*, 174(11), pp. 6781–6790. Available at: https://doi.org/10.4049/jimmunol.174.11.6781.

Hayman, A.R. (2008) 'Tartrate-resistant acid phosphatase (TRAP) and the osteoclast/immune cell dichotomy', *Autoimmunity*, 41(3), pp. 218–223. Available at: https://doi.org/10.1080/08916930701694667.

Hazra, S. *et al.* (2023) 'Giant cells: multiple cells unite to survive', *Frontiers in Cellular and Infection Microbiology*, 13. Available at: https://doi.org/10.3389/fcimb.2023.1220589.

Head, R. *et al.* (2021) 'Immune checkpoint inhibitor - associated polymyalgia rheumatica / giant cell arteritis occurring in a patient after treatment with Nivolumab : a case report Immune checkpoint inhibitor - associated polymyalgia rheumatica / giant cell arteritis occurring i'.

Hemmatazad, H. and Berger, M.D. (2021) 'CCR5 is a potential therapeutic target for cancer', *Expert Opinion on Therapeutic Targets*, 25. Available at: https://doi.org/10.1080/14728222.2021.1902505.

Henkart, P.A. (1997) 'Introduction: CTL effector functions', *Seminars in Immunology*, 9(2), pp. 85–86. Available at: https://doi.org/10.1006/smim.1997.0064.

Hensley, T.R. *et al.* (2012) 'Enumeration of Major Peripheral Blood Leukocyte Populations for Multicenter Clinical Trials Using a Whole Blood Phenotyping Assay', *Journal of Visualized Experiments : JoVE*, (67), p. 4302. Available at: https://doi.org/10.3791/4302.

Hobeika, M.J. *et al.* (2007) 'Matrix metalloproteinases in peripheral vascular disease', *Journal of Vascular Surgery*, 45(4), pp. 849–857. Available at: https://doi.org/10.1016/j.jvs.2006.09.066.

Holliday, R. (2006) 'Epigenetics: A Historical Overview', *Epigenetics*, 1(2), pp. 76–80. Available at: https://doi.org/10.4161/epi.1.2.2762.

Hu, Lingli *et al.* (2017) 'Epigenetic Regulation of Interleukin 6 by Histone Acetylation in Macrophages and Its Role in Paraquat-Induced Pulmonary Fibrosis', *Frontiers in Immunology*, 7, p. 696. Available at: https://doi.org/10.3389/fimmu.2016.00696.

Huang, W. *et al.* (2022) 'Cellular senescence: the good, the bad and the unknown', *Nature Reviews Nephrology*, 18(10), pp. 611–627. Available at: https://doi.org/10.1038/s41581-022-00601-z.

Isali, I. *et al.* (2022) 'In Vivo Delivery of M0, M1, and M2 Macrophage Subtypes via Genipin-Cross-Linked Collagen Biotextile', *Tissue Engineering. Part A*, 28(15–16), pp. 672–684. Available at: https://doi.org/10.1089/ten.tea.2021.0203.

Isoda, K. *et al.* (2003) 'Deficiency of Interleukin-1 Receptor Antagonist Promotes Neointimal Formation After Injury', *Circulation*, 108(5), pp. 516–518. Available at: https://doi.org/10.1161/01.CIR.0000085567.18648.21.

Janckila, A.J. *et al.* (2007) 'Tartrate-Resistant Acid Phosphatase as an Immunohistochemical Marker for Inflammatory Macrophages', *American Journal of Clinical Pathology*, 127(4), pp. 556–566. Available at: https://doi.org/10.1309/DGEA9BE2VE5VCFYH.

Jiemy, W.F. *et al.* (2020) 'Distinct macrophage phenotypes skewed by local granulocyte macrophage colony-stimulating factor (GM-CSF) and macrophage colony-stimulating factor (M-CSF) are associated with tissue destruction and intimal hyperplasia in giant cell arteritis', *Clinical and Translational Immunology*, 9(9). Available at: https://doi.org/10.1002/cti2.1164.

Jiemy, W.F. *et al.* (2025) 'GM-CSF drives IL-6 production by macrophages in polymyalgia rheumatica', *Annals of the Rheumatic Diseases* [Preprint]. Available at: https://doi.org/10.1016/j.ard.2025.01.004.

Johansen, J.S. *et al.* (1999) 'YKL-40 IN GIANT CELLS AND MACROPHAGES FROM PATIENTS WITH GIANT CELL ARTERITIS', 42(12), pp. 2624–2630.

Jones, K., Maguire, J. and Davenport, A. (2011) 'Chemokine receptor CCR5: from AIDS to atherosclerosis', *British Journal of Pharmacology*, 162(7), pp. 1453–1469. Available at: https://doi.org/10.1111/j.1476-5381.2010.01147.x.

Jordan, L.A. *et al.* (2018) 'Inhibition of CCL3 abrogated precursor cell fusion and bone erosions in human osteoclast cultures and murine collagen-induced arthritis', *Rheumatology (Oxford, England)*, 57(11), pp. 2042–2052. Available at: https://doi.org/10.1093/rheumatology/key196.

Kaiser, M. *et al.* (1999) *Formation of New Vasa Vasorum in Vasculitis Production of Angiogenic Cytokines by Multinucleated Giant Cells*.

Karlmark, K.R., Tacke, F. and Dunay, I.R. (2012) 'Monocytes in health and disease – Minireview', *European Journal of Microbiology & Immunology*, 2(2), pp. 97–102. Available at: https://doi.org/10.1556/EuJMI.2.2012.2.1.

Kaya-Okur, H.S. *et al.* (2019) 'CUT&Tag for efficient epigenomic profiling of small samples and single cells', *Nature Communications*, 10(1), p. 1930. Available at: https://doi.org/10.1038/s41467-019-09982-5.

Kaya-Okur, H.S. *et al.* (2020) 'Efficient low-cost chromatin profiling with CUT&Tag', *Nature Protocols*, 15(10), pp. 3264–3283. Available at: https://doi.org/10.1038/s41596-020-0373-x.

Khan, U.A. *et al.* (2013) 'Foreign body giant cells and osteoclasts are TRAP positive, have podosome-belts and both require OC-STAMP for cell fusion', *Journal of Cellular Biochemistry*, 114(8), pp. 1772–1778. Available at: https://doi.org/10.1002/jcb.24518.

Khan, U.A. *et al.* (2014) 'Differential expression of chemokines, chemokine receptors and proteinases by foreign body giant cells (FBGCs) and osteoclasts', *Journal of Cellular Biochemistry*, 115(7), pp. 1290–1298. Available at: https://doi.org/10.1002/jcb.24781.

Kieslinger, M. *et al.* (2005) 'EBF2 Regulates Osteoblast-Dependent Differentiation of Osteoclasts', *Developmental Cell*, 9(6), pp. 757–767. Available at: https://doi.org/10.1016/j.devcel.2005.10.009.

Kloc, M. *et al.* (2022) 'Giant Multinucleated Cells in Aging and Senescence—An Abridgement', *Biology*, 11(8), p. 1121. Available at: https://doi.org/10.3390/biology11081121.

Krupa, W.M. *et al.* (2002) 'Trapping of Misdirected Dendritic Cells in the Granulomatous Lesions of Giant Cell Arteritis', *The American Journal of Pathology*, 161(5), pp. 1815–1823. Available at: https://doi.org/10.1016/S0002-9440(10)64458-6.

Kular, J. *et al.* (2012) 'An overview of the regulation of bone remodelling at the cellular level', *Clinical Biochemistry*, 45(12), pp. 863–873. Available at: https://doi.org/10.1016/j.clinbiochem.2012.03.021.

Kulkarni, S. *et al.* (2019) 'CCR5AS lncRNA variation differentially regulates CCR5, influencing HIV disease outcome', *Nature immunology*, 20(7), pp. 824–834. Available at: https://doi.org/10.1038/s41590-019-0406-1.

Kuziel, W.A. *et al.* (2003) 'CCR5 deficiency is not protective in the early stages of atherogenesis in apoE knockout mice', *Atherosclerosis*, 167(1), pp. 25–32. Available at: https://doi.org/10.1016/S0021-9150(02)00382-9.

Lakota, K. *et al.* (2011) 'Antibodies against acute phase proteins and their functions in the pathogenesis of disease: A collective profile of 25 different antibodies', *Autoimmunity Reviews*, 10(12), pp. 779–789. Available at: https://doi.org/10.1016/j.autrev.2011.06.001.

Lander, E.S. *et al.* (2001) 'Initial sequencing and analysis of the human genome', *Nature*, 409(6822), pp. 860–921. Available at: https://doi.org/10.1038/35057062.

Langmead, B. and Salzberg, S.L. (2012) 'Fast gapped-read alignment with Bowtie 2', *Nature methods*, 9(4), pp. 357–359. Available at: https://doi.org/10.1038/nmeth.1923.

Lapenna, A., De Palma, M. and Lewis, C.E. (2018) 'Perivascular macrophages in health and disease', *Nature Reviews Immunology*, 18(11), pp. 689–702. Available at: https://doi.org/10.1038/s41577-018-0056-9.

Le Goueff, A. *et al.* (2019) 'Visual loss in giant cell arteritis 3 weeks after steroid initiation', *BMJ Case Reports*, 12(3), p. e228251. Available at: https://doi.org/10.1136/bcr-2018-228251.

Lee, J.W. *et al.* (2017) 'The HIV co-receptor CCR5 regulates osteoclast function', *Nature Communications*, 8(1). Available at: https://doi.org/10.1038/s41467-017-02368-5.

Lemaire, I. *et al.* (1996) *Differential Effects of Macrophage-and Granulocyte-Macrophage Colony-Stimulating Factors on Cytokine Gene Expression During Rat Alveolar Macrophage Differentiation into Multinucleated Giant Cells (MGC) Role For 11-6 in Type 2 MGC Formation'*. Available at: http://www.jimmunol.org/.

Li, H.Y., Xu, J.N. and Shuai, Z.W. (2021) 'Cellular signaling pathways of T cells in giant cell arteritis', *Journal of Geriatric Cardiology*, 18(9), pp. 768–778. Available at: https://doi.org/10.11909/j.issn.1671-5411.2021.09.008.

Li, K.J. *et al.* (2021) 'A meta-analysis of the epidemiology of giant cell arteritis across time and space', *Arthritis Research and Therapy*, 23(1). Available at: https://doi.org/10.1186/s13075-021-02450-w.

Lieveld, M. *et al.* (2014) 'Gene expression profiling of giant cell tumor of bone reveals downregulation of extracellular matrix components decorin and lumican associated with lung metastasis', *Virchows Archiv*, 465(6), pp. 703–713. Available at: https://doi.org/10.1007/s00428-014-1666-7.

Lin, A.A. *et al.* (2009) ‘Gamma interferon signaling in macrophage lineage cells regulates central nervous system inflammation and chemokine production’, *Journal of Virology*, 83(17), pp. 8604–8615. Available at: https://doi.org/10.1128/JVI.02477-08.

Love, M.I., Huber, W. and Anders, S. (2014) ‘Moderated estimation of fold change and dispersion for RNA-seq data with DESeq2’, *Genome Biology*, 15(12), p. 550. Available at: https://doi.org/10.1186/s13059-014-0550-8.

Ly, K.-H. *et al.* (2010) ‘Pathogenesis of giant cell arteritis: More than just an inflammatory condition?’, *Autoimmunity Reviews*, 9(10), pp. 635–645. Available at: https://doi.org/10.1016/j.autrev.2010.05.002.

Maddur, M.S. *et al.* (2012) ‘Th17 Cells: Biology, Pathogenesis of Autoimmune and Inflammatory Diseases, and Therapeutic Strategies’, *The American Journal of Pathology*, 181(1), pp. 8–18. Available at: https://doi.org/10.1016/j.ajpath.2012.03.044.

Maguire, J.J. *et al.* (2014) ‘The CCR5 chemokine receptor mediates vasoconstriction and stimulates intimal hyperplasia in human vessels in vitro’, *Cardiovascular Research*, 101(3), pp. 513–521. Available at: https://doi.org/10.1093/cvr/cvt333.

Ma-Krupa, W. *et al.* (2004) ‘Activation of Arterial Wall Dendritic Cells and Breakdown of Self-tolerance in Giant Cell Arteritis’, *The Journal of Experimental Medicine*, 199(2), pp. 173–183. Available at: https://doi.org/10.1084/jem.20030850.

Maleszewski, J.J. *et al.* (2017) ‘Clinical and pathological evolution of giant cell arteritis: A prospective study of follow-up temporal artery biopsies in 40 treated patients’, *Modern Pathology*, 30(6), pp. 788–796. Available at: https://doi.org/10.1038/modpathol.2017.10.

Maz, M. *et al.* (2021) ‘2021 American College of Rheumatology/Vasculitis Foundation Guideline for the Management of Giant Cell Arteritis and Takayasu Arteritis’, *Arthritis and Rheumatology*, 73(8), pp. 1349–1365. Available at: https://doi.org/10.1002/art.41774.

McDonald, M.M. *et al.* (2021) ‘Osteoclasts recycle via osteomorphs during RANKL-stimulated bone resorption’, *Cell*, 184(5), p. 1330. Available at: https://doi.org/10.1016/j.cell.2021.02.002.

Mcnally, A.K. and Anderson, J.M. (1995) *Interleukin-4 Induces Foreign Body Giant Cells from Human Monocytes/Macrophages Differential Lymphokine Regulation of Macrophage Fusion Leads to Morphological Variants of Multinucleated Giant Cells*, *American Journal of Pathology*.

McNally, A.K. and Anderson, J.M. (2011a) ‘Foreign body-type multinucleated giant cells induced by interleukin-4 express select lymphocyte co-stimulatory molecules and are phenotypically distinct from osteoclasts and dendritic cells’, *Experimental and Molecular Pathology*, 91(3), pp. 673–681. Available at: https://doi.org/10.1016/j.yexmp.2011.06.012.

McNally, A.K. and Anderson, J.M. (2011b) ‘Macrophage fusion and multinucleated giant cells of inflammation’, *Advances in Experimental Medicine and Biology*, 713, pp. 97–111. Available at: https://doi.org/10.1007/978-94-007-0763-4_7.

Mercadante, A.A. and Raja, A. (2025) ‘Anatomy, Arteries’, in *StatPearls*. Treasure Island (FL): StatPearls Publishing. Available at: http://www.ncbi.nlm.nih.gov/books/NBK547743/ (Accessed: 14 September 2025).

Mizoguchi, T. *et al.* (2009) 'Identification of cell cycle–arrested quiescent osteoclast precursors in vivo', *Journal of Cell Biology*, 184(4), pp. 541–554. Available at: https://doi.org/10.1083/jcb.200806139.

Mizuno, K., Okamoto, H. and Horio, T. (2001) 'Muramyl dipeptide and mononuclear cell supernatant induce Langhans-type cells from human monocytes', *Journal of Leukocyte Biology*, 70(3), pp. 386–394. Available at: https://doi.org/10.1189/jlb.70.3.386.

Mohan, S.V. *et al.* (2011) 'Giant cell arteritis: immune and vascular aging as disease risk factors', *Arthritis Research & Therapy*, 13(4), p. 231. Available at: https://doi.org/10.1186/ar3358.

Moreel, L. *et al.* (2023) 'Epidemiology and predictors of relapse in giant cell arteritis: A systematic review and meta-analysis', *Joint Bone Spine*, 90(1). Available at: https://doi.org/10.1016/j.jbspin.2022.105494.

Morrone, C. *et al.* (2021) 'Cathepsin B promotes collagen biosynthesis, which drives bronchiolitis obliterans syndrome', *European Respiratory Journal*, 57(5). Available at: https://doi.org/10.1183/13993003.01416-2020.

Mouchemore, K.A. and Pixley, F.J. (2012) 'CSF-1 signaling in macrophages: pleiotrophy through phosphotyrosine-based signaling pathways', *Critical Reviews in Clinical Laboratory Sciences*, 49(2), pp. 49–61. Available at: https://doi.org/10.3109/10408363.2012.666845.

Mulder, K. *et al.* (2021) 'Cross-tissue single-cell landscape of human monocytes and macrophages in health and disease', *Immunity*, 54(8), pp. 1883-1900.e5. Available at: https://doi.org/10.1016/j.immuni.2021.07.007.

Muratore, F. *et al.* (2016) 'Correlations between histopathological fi ndings and clinical manifestations in biopsy-proven giant cell arteritis Nicol o', 69, pp. 94–101. Available at: https://doi.org/10.1016/j.jaut.2016.03.005.

Murga, J.D. *et al.* (2006) 'Potent Antiviral Synergy between Monoclonal Antibody and Small-Molecule CCR5 Inhibitors of Human Immunodeficiency Virus Type 1', *Antimicrobial Agents and Chemotherapy*, 50(10), pp. 3289–3296. Available at: https://doi.org/10.1128/aac.00699-06.

Murphy, P.M. (2023) '15 - Chemokines and Chemokine Receptors', in R.R. Rich et al. (eds) *Clinical Immunology (Sixth Edition)*. New Delhi: Elsevier, pp. 215–227. Available at: https://doi.org/10.1016/B978-0-7020-8165-1.00015-0.

Na, W. *et al.* (2017) 'Dexamethasone suppresses JMJD3 gene activation via a putative negative glucocorticoid response element and maintains integrity of tight junctions in brain microvascular endothelial cells', *Journal of Cerebral Blood Flow & Metabolism*, 37(12), pp. 3695–3708. Available at: https://doi.org/10.1177/0271678X17701156.

Nandiwada, S.L. (2023) 'Overview of human B-cell development and antibody deficiencies', *Journal of Immunological Methods*, 519, p. 113485. Available at: https://doi.org/10.1016/j.jim.2023.113485.

Narasimhan, P.B. *et al.* (2019) 'Nonclassical Monocytes in Health and Disease', *Annual Review of Immunology*, 37(1), pp. 439–456. Available at: https://doi.org/10.1146/annurev-immunol-042617-053119.

Ness, S., Lin, S. and Gordon, J.R. (2021) 'Regulatory Dendritic Cells, T Cell Tolerance, and Dendritic Cell Therapy for Immunologic Disease', *Frontiers in Immunology*, 12. Available at: https://doi.org/10.3389/fimmu.2021.633436.

Newman, A.M. *et al.* (2015a) 'Robust enumeration of cell subsets from tissue expression profiles', *Nature Methods*, 12(5), pp. 453–457. Available at: https://doi.org/10.1038/nmeth.3337.

Newman, A.M. *et al.* (2015b) 'Robust enumeration of cell subsets from tissue expression profiles', *Nature methods*, 12(5), pp. 453–457. Available at: https://doi.org/10.1038/nmeth.3337.

Ni, K. and O'Neill, H. (1997) 'The role of dendritic cells in T cell activation', *Immunology & Cell Biology*, 75(3), pp. 223–230. Available at: https://doi.org/10.1038/icb.1997.35.

Nordborg, C *et al.* (2001) *Calcification of the internal elastic membrane in temporal arteries: Its relation to age and gender*, *Clinical and Experimental Rheumatology*, pp. 565–568.

Nordborg, C., Nordborg, E. and Petursdottir, V. (2000) 'The pathogenesis of giant cell arteritis: morphological aspects', *Clinical and Experimental Rheumatology*, 18(4 Suppl 20), pp. S18-21.

Nordborg, E. *et al.* (1997) 'Morphological aspects of giant cells in giant cell arteritis: an electron-microscopic and immunocytochemical study', *Clinical and Experimental Rheumatology*, 15(2), pp. 129–134.

Nordborg, E. and Nordborg, C. (2003) 'Giant cell arteritis: epidemiological clues to its pathogenesis and an update on its treatment', *Rheumatology*, 42(3), pp. 413–421. Available at: https://doi.org/10.1093/rheumatology/keg116.

Oba, Y. *et al.* (2005) 'MIP-1α utilizes both CCR1 and CCR5 to induce osteoclast formation and increase adhesion of myeloma cells to marrow stromal cells', *Experimental Hematology*, 33(3), pp. 272–278. Available at: https://doi.org/10.1016/j.exphem.2004.11.015.

Obermajer, N. *et al.* (2008) 'Role of Cysteine Cathepsins in Matrix Degradation and Cell Signalling', *Connective Tissue Research*, 49(3–4), pp. 193–196. Available at: https://doi.org/10.1080/03008200802143158.

Okamoto, H., Mizuno, K. and Horio, T. (2003a) 'Langhans-type and foreign-body-type multinucleated giant cells in cutaneous lesions of sarcoidosis', *Acta Dermato-Venereologica*, 83(3), pp. 171–174. Available at: https://doi.org/10.1080/00015550310007148.

Okamoto, H., Mizuno, K. and Horio, T. (2003b) 'Monocyte-derived multinucleated giant cells and sarcoidosis', *Journal of Dermatological Science*, 31(2), pp. 119–128. Available at: https://doi.org/10.1016/S0923-1811(02)00148-2.

Olga St. Latinovic *et al.* (2009) *(PDF) Pharmacotherapy of HIV-1 Infection: Focus on CCR5 Antagonist Maraviroc*. Available at: https://www.researchgate.net/publication/38096640_Pharmacotherapy_of_HIV-1_Infection_Focus_on_CCR5_Antagonist_Maraviroc (Accessed: 26 September 2025).

Oliphant, C.J., Barlow, J.L. and McKenzie, A.N.J. (2011) 'Insights into the initiation of type 2 immune responses', *Immunology*, 134(4), pp. 378–385. Available at: https://doi.org/10.1111/j.1365-2567.2011.03499.x.

Omi, M., Kaartinen, V. and Mishina, Y. (2019) 'Activin A receptor type 1–mediated BMP signaling regulates RANKL-induced osteoclastogenesis via canonical SMAD-signaling pathway', *The Journal of Biological Chemistry*, 294(47), pp. 17818–17836. Available at: https://doi.org/10.1074/jbc.RA119.009521.

Ong, S.M. *et al.* (2018) 'The pro-inflammatory phenotype of the human non-classical monocyte subset is attributed to senescence article', *Cell Death and Disease*, 9(3). Available at: https://doi.org/10.1038/s41419-018-0327-1.

Oppermann, M. *et al.* (1999) 'Differential Effects of CC Chemokines on CC Chemokine Receptor 5 (CCR5) Phosphorylation and Identification of Phosphorylation Sites on the CCR5 Carboxyl Terminus', *Journal of Biological Chemistry*, 274(13), pp. 8875–8885. Available at: https://doi.org/10.1074/jbc.274.13.8875.

Orekhov, A.N. *et al.* (2019) 'Monocyte differentiation and macrophage polarization', *Vessel Plus*, 3. Available at: https://doi.org/10.20517/2574-1209.2019.04.

Park, J.M. *et al.* (2024) 'Crosstalk between FTH1 and PYCR1 dysregulates proline metabolism and mediates cell growth in KRAS-mutant pancreatic cancer cells', *Experimental & Molecular Medicine*, 56(9), pp. 2065–2081. Available at: https://doi.org/10.1038/s12276-024-01300-4.

Paroli, M., Caccavale, R. and Accapezzato, D. (2024) 'Giant Cell Arteritis: Advances in Understanding Pathogenesis and Implications for Clinical Practice', *Cells*, 13(3). Available at: https://doi.org/10.3390/cells13030267.

Pirici, D. *et al.* (2012) 'Matrix metalloproteinase-9 expression in the nuclear compartment of neurons and glial cells in aging and stroke', *Neuropathology*, 32(5), pp. 492–504. Available at: https://doi.org/10.1111/j.1440-1789.2011.01279.x.

Pofi, R. *et al.* (2023) 'Treating the Side Effects of Exogenous Glucocorticoids; Can We Separate the Good From the Bad?', *Endocrine Reviews*, 44(6), pp. 975–1011. Available at: https://doi.org/10.1210/endrev/bnad016.

Ponte, C. *et al.* (2022) '2022 American College of Rheumatology/EULAR classification criteria for giant cell arteritis', *Annals of the Rheumatic Diseases*, 81(12), pp. 1647–1653. Available at: https://doi.org/10.1136/ard-2022-223480.

Prieto-Peña, D., Castañeda, S., *et al.* (2021) 'Imaging Tests in the Early Diagnosis of Giant Cell Arteritis', *Journal of Clinical Medicine*, 10(16), p. 3704. Available at: https://doi.org/10.3390/jcm10163704.

Prieto-Peña, D., Remuzgo-Martínez, S., *et al.* (2021) 'The presence of both HLA-DRB1[*]04:01 and HLA-B[*]15:01 increases the susceptibility to cranial and extracranial giant cell arteritis', *Clinical and Experimental Rheumatology*, 39(2), pp. 21–26. Available at: https://doi.org/10.55563/clinexprheumatol/nn15lt.

Prieto-Potin, I. *et al.* (2015) 'Characterization of multinucleated giant cells in synovium and subchondral bone in knee osteoarthritis and rheumatoid arthritis', *BMC musculoskeletal disorders*, 16, p. 226. Available at: https://doi.org/10.1186/s12891-015-0664-5.

Proudfoot, A.E.I. (2002) ‘Chemokine receptors: multifaceted therapeutic targets’, *Nature Reviews Immunology*, 2(2), pp. 106–115. Available at: https://doi.org/10.1038/nri722.

Qiao, Y. *et al.* (2013) ‘Synergistic Activation of Inflammatory Cytokine Genes by Interferon-γ-induced Chromatin Remodeling and Toll-like Receptor Signaling’, *Immunity*, 39(3), p. 10.1016/j.immuni.2013.08.009. Available at: https://doi.org/10.1016/j.immuni.2013.08.009.

Régent, A. *et al.* (2017) ‘Autoimmunity Reviews Molecular analysis of vascular smooth muscle cells from patients with giant cell arteritis : Targeting endothelin-1 receptor to control proliferation ☆’, *Autoimmunity Reviews*, 16(4), pp. 398–406. Available at: https://doi.org/10.1016/j.autrev.2017.02.006.

Reitsema, R.D. *et al.* (2023) ‘Aberrant phenotype of circulating antigen presenting cells in giant cell arteritis and polymyalgia rheumatica’, *Frontiers in Immunology*, 14. Available at: https://doi.org/10.3389/fimmu.2023.1201575.

Renauer, P., Coit, P. and Sawalha, A.H. (2016) ‘Epigenetics and Vasculitis: a Comprehensive Review’, *Clinical Reviews in Allergy & Immunology*, 50(3), pp. 357–366. Available at: https://doi.org/10.1007/s12016-015-8495-6.

Restuccia, G. *et al.* (2016) ‘Flares in Biopsy-Proven Giant Cell Arteritis in Northern Italy: Characteristics and Predictors in a Long-Term Follow-Up Study’, *Medicine*, 95(19), p. e3524. Available at: https://doi.org/10.1097/MD.0000000000003524.

van der Rhee, H.J., Hillebrands, W. and Th Daems, W. (1978) *Are Langhans Giant Cells Precursors of Foreign-Body Giant Cells?*, *Arch. Dermatol. Res*, pp. 13–21.

Rittner, H.L. *et al.* (1999) ‘Tissue-Destructive Macrophages in Giant Cell Arteritis’, pp. 1050–1058.

Robinette, M.L., Rao, D.A. and Monach, P.A. (2021) ‘The Immunopathology of Giant Cell Arteritis Across Disease Spectra’, *Frontiers in Immunology*, 12. Available at: https://doi.org/10.3389/fimmu.2021.623716.

Rodríguez-Pla, A. *et al.* (2005) ‘Metalloproteinase-2 and -9 in Giant Cell Arteritis’, *Circulation*, 112(2), pp. 264–269. Available at: https://doi.org/10.1161/CIRCULATIONAHA.104.520114.

Rusconi, S. *et al.* (2022) ‘Leronlimab (PRO 140) *in vitro* activity against 4-class drug resistant HIV-1 from heavily treatment experienced subjects’, *Pharmacological Research*, 176, p. 106064. Available at: https://doi.org/10.1016/j.phrs.2022.106064.

Saade, M. *et al.* (2021) ‘The Role of GPNMB in Inflammation’, *Frontiers in Immunology*, 12, p. 674739. Available at: https://doi.org/10.3389/fimmu.2021.674739.

Sainger, R. *et al.* (2012) ‘Dephosphorylation of circulating human Osteopontin correlates with severe valvular calcification in patients with Calcific Aortic Valve Disease’, *Biomarkers*, 17(2), pp. 111–118. Available at: https://doi.org/10.3109/1354750X.2011.642407.

Samson, M. *et al.* (2017) ‘Recent advances in our understanding of giant cell arteritis pathogenesis’, *Autoimmunity Reviews*, 16(8), pp. 833–844. Available at: https://doi.org/10.1016/j.autrev.2017.05.014.

Santos-Rosa, H. *et al.* (2002) 'Active genes are tri-methylated at K4 of histone H3', *Nature*, 419(6905), pp. 407–411. Available at: https://doi.org/10.1038/nature01080.

Serbina, N.V. and Pamer, E.G. (2006) 'Monocyte emigration from bone marrow during bacterial infection requires signals mediated by chemokine receptor CCR2', *Nature Immunology*, 7(3), pp. 311–317. Available at: https://doi.org/10.1038/ni1309.

Shapouri-Moghaddam, A. *et al.* (2018a) 'Macrophage plasticity, polarization, and function in health and disease', *Journal of Cellular Physiology*, 233(9), pp. 6425–6440. Available at: https://doi.org/10.1002/jcp.26429.

Shapouri-Moghaddam, A. *et al.* (2018b) 'Macrophage plasticity, polarization, and function in health and disease', *Journal of Cellular Physiology*, 233(9), pp. 6425–6440. Available at: https://doi.org/10.1002/jcp.26429.

Shen, G. (2024) 'Vimentin Phosphorylation Stabilization Promotes Multinucleation in Hybrid E/M Carcinoma Cells'. Available at: https://doi.org/10.35248/2157-7633.24.14.643.

Shi, C. and Pamer, E.G. (2011) 'Monocyte recruitment during infection and inflammation', *Nature reviews. Immunology*, 11(11), pp. 762–774. Available at: https://doi.org/10.1038/nri3070.

Shinohara, S. *et al.* (2013) 'Fabrication of in vitro three-dimensional multilayered blood vessel model using human endothelial and smooth muscle cells and high-strength PEG hydrogel', *Journal of Bioscience and Bioengineering*, 116(2), pp. 231–234. Available at: https://doi.org/10.1016/j.jbiosc.2013.02.013.

van Sleen, Y., Wang, Q., van der Geest, Kornelis S.M., *et al.* (2017) 'Involvement of Monocyte Subsets in the Immunopathology of Giant Cell Arteritis', *Scientific Reports*, 7(1). Available at: https://doi.org/10.1038/s41598-017-06826-4.

van Sleen, Y., Wang, Q., van der Geest, Kornelis S. M., *et al.* (2017) 'Involvement of Monocyte Subsets in the Immunopathology of Giant Cell Arteritis', *Scientific Reports*, 7(1), p. 6553. Available at: https://doi.org/10.1038/s41598-017-06826-4.

van Sleen, Y. *et al.* (2019) 'Leukocyte Dynamics Reveal a Persistent Myeloid Dominance in Giant Cell Arteritis and Polymyalgia Rheumatica', *Frontiers in Immunology*, 10, p. 1981. Available at: https://doi.org/10.3389/fimmu.2019.01981.

van Sleen, Y. *et al.* (2021) 'A Distinct Macrophage Subset Mediating Tissue Destruction and Neovascularization in Giant Cell Arteritis: Implication of the YKL-40/Interleukin-13 Receptor α2 Axis', *Arthritis and Rheumatology* [Preprint]. Available at: https://doi.org/10.1002/art.41887.

Stamper, C.T. *et al.* (2024) 'Single-cell RNA sequencing of cells from fresh or frozen tissue reveals a signature of freezing marked by heightened stress and activation', *European Journal of Immunology*, 54(4), p. 2350660. Available at: https://doi.org/10.1002/eji.202350660.

Stone, J.H. *et al.* (2017) 'Trial of Tocilizumab in Giant-Cell Arteritis', *New England Journal of Medicine*, 377(4), pp. 317–328. Available at: https://doi.org/10.1056/NEJMoa1613849.

Strizova, Z. *et al.* (2023) 'M1/M2 macrophages and their overlaps – myth or reality?', *Clinical Science (London, England : 1979)*, 137(15), pp. 1067–1093. Available at: https://doi.org/10.1042/CS20220531.

Subramanian, C. and Cohen, M.S. (2019) 'Over expression of DNA damage and cell cycle dependent proteins are associated with poor survival in patients with adrenocortical carcinoma', *Surgery*, 165(1), pp. 202–210. Available at: https://doi.org/10.1016/j.surg.2018.04.080.

Sun, Y. *et al.* (2025) 'MMP12-dependent myofibroblast formation contributes to nucleus pulposus fibrosis', *JCI Insight*, 10(7), p. e180809. Available at: https://doi.org/10.1172/jci.insight.180809.

Szalai, C. *et al.* (2001) 'Involvement of polymorphisms in the chemokine system in the susceptibility for coronary artery disease (CAD). Coincidence of elevated Lp(a) and MCP-1 −2518 G/G genotype in CAD patients', *Atherosclerosis*, 158(1), pp. 233–239. Available at: https://doi.org/10.1016/S0021-9150(01)00423-3.

Tacke, F. *et al.* (2007) 'Monocyte subsets differentially employ CCR2, CCR5, and CX3CR1 to accumulate within atherosclerotic plaques', *The Journal of Clinical Investigation*, 117(1), pp. 185–194. Available at: https://doi.org/10.1172/JCI28549.

Takashima, T. *et al.* (1993) 'Differential regulation of formation of multinucleated giant cells from concanavalin A-stimulated human blood monocytes by IFN-gamma and IL-4.', *The Journal of Immunology*, 150(7), pp. 3002–3010. Available at: https://doi.org/10.4049/jimmunol.150.7.3002.

Takegahara, N. *et al.* (2016a) 'Involvement of Receptor Activator of Nuclear Factor-κB Ligand (RANKL)-induced Incomplete Cytokinesis in the Polyploidization of Osteoclasts*', *Journal of Biological Chemistry*, 291(7), pp. 3439–3454. Available at: https://doi.org/10.1074/jbc.M115.677427.

Takegahara, N. *et al.* (2016b) 'Involvement of Receptor Activator of Nuclear Factor-κB Ligand (RANKL)-induced Incomplete Cytokinesis in the Polyploidization of Osteoclasts*', *Journal of Biological Chemistry*, 291(7), pp. 3439–3454. Available at: https://doi.org/10.1074/jbc.M115.677427.

Tang, C.-H., Hsu, C.-J. and Fong, Y.-C. (2010) 'The CCL5/CCR5 axis promotes interleukin-6 production in human synovial fibroblasts', *Arthritis & Rheumatism*, 62(12), pp. 3615–3624. Available at: https://doi.org/10.1002/art.27755.

Tang, P. and Wang, J.M. (2018) 'Chemokines: the past, the present and the future', *Cellular & Molecular Immunology*, 15(4), pp. 295–298. Available at: https://doi.org/10.1038/cmi.2018.9.

Tanneberger, A.M. *et al.* (2021) 'Multinucleated giant cells within the in vivo implantation bed of a collagen-based biomaterial determine its degradation pattern', *Clinical Oral Investigations*, 25(3), pp. 859–873. Available at: https://doi.org/10.1007/s00784-020-03373-7.

Teitelbaum, S.L. (2007) 'Osteoclasts: What do they do and how do they do it?', in *American Journal of Pathology*. American Society for Investigative Pathology Inc., pp. 427–435. Available at: https://doi.org/10.2353/ajpath.2007.060834.

Terrier, B. *et al.* (2012) 'Interleukin-21 modulates Th1 and Th17 responses in giant cell arteritis', *Arthritis and Rheumatism*, 64(6), pp. 2001–2011. Available at: https://doi.org/10.1002/art.34327.

Thompson, J. and van Furth, R. (1970) 'THE EFFECT OF GLUCOCORTICOSTEROIDS ON THE KINETICS OF MONONUCLEAR PHAGOCYTES', *The Journal of Experimental Medicine*, 131(3), pp. 429–442. Available at: https://doi.org/10.1084/jem.131.3.429.

Tian, Y. *et al.* (2020) 'FTH1 Inhibits Ferroptosis Through Ferritinophagy in the 6-OHDA Model of Parkinson's Disease', *Neurotherapeutics*, 17(4), pp. 1796–1812. Available at: https://doi.org/10.1007/s13311-020-00929-z.

Timmermans, S., Souffriau, J. and Libert, C. (2019) 'A General Introduction to Glucocorticoid Biology', *Frontiers in Immunology*, 10. Available at: https://doi.org/10.3389/fimmu.2019.01545.

Tomelleri, A. *et al.* (2022) 'Presenting features and outcomes of cranial-limited and large-vessel giant cell arteritis: a retrospective cohort study', *Scandinavian Journal of Rheumatology*, 51(1), pp. 59–66. Available at: https://doi.org/10.1080/03009742.2021.1889025.

Trout, K.L. and Holian, A. (2020) 'Multinucleated giant cell phenotype in response to stimulation', *Immunobiology*, 225(3). Available at: https://doi.org/10.1016/j.imbio.2020.151952.

Trout, K.L., Jessop, F. and Migliaccio, C.T. (2016) 'Macrophage and Multinucleated Giant Cell Classification', in T. Otsuki, Y. Yoshioka, and A. Holian (eds) *Biological Effects of Fibrous and Particulate Substances*. Tokyo: Springer Japan, pp. 1–26. Available at: https://doi.org/10.1007/978-4-431-55732-6_1.

Turvey, S.E. and Broide, D.H. (2010) 'Innate immunity', *Journal of Allergy and Clinical Immunology*, 125(2, Supplement 2), pp. S24–S32. Available at: https://doi.org/10.1016/j.jaci.2009.07.016.

Tyner, J.W. *et al.* (2005) 'CCL5-CCR5 interaction provides antiapoptotic signals for macrophage survival during viral infection', *Nature Medicine*, 11(11), pp. 1180–1187. Available at: https://doi.org/10.1038/nm1303.

Vaiopoulos, A. *et al.* (2023) 'Giant Cell Arteritis: Focusing on Current Aspects From the Clinic to Diagnosis and Treatment', *Angiology*, 74(8), pp. 709–716. Available at: https://doi.org/10.1177/00033197221130564.

Van Sleen, Y. *et al.* (2019) 'Markers of angiogenesis and macrophage products for predicting disease course and monitoring vascular inflammation in giant cell arteritis', *Rheumatology (United Kingdom)*, 58(8), pp. 1383–1392. Available at: https://doi.org/10.1093/rheumatology/kez034.

Veroutis, D. *et al.* (2023) 'Senescent cells in giant cell arteritis display an inflammatory phenotype participating in tissue injury via IL-6-dependent pathways', *Annals of the Rheumatic Diseases* [Preprint]. Available at: https://doi.org/10.1136/ard-2023-224467.

Version, D. and Sleen, V. (2020) 'University of Groningen Monocyte and macrophage heterogeneity in Giant Cell Arteritis and Polymyalgia Rheumatica van Sleen, Yannick'. Available at: https://doi.org/10.33612/diss.113443254.

Vila Cuenca, M. *et al.* (2021) 'Engineered 3D vessel-on-chip using hiPSC-derived endothelial- and vascular smooth muscle cells', *Stem Cell Reports*, 16(9), pp. 2159–2168. Available at: https://doi.org/10.1016/j.stemcr.2021.08.003.

Wang, J., Gleeson, P.A. and Fourriere, L. (2023) 'Long-term live cell imaging during differentiation of human iPSC-derived neurons', *STAR Protocols*, 4(4), p. 102699. Available at: https://doi.org/10.1016/j.xpro.2023.102699.

Wang, K. *et al.* (2022a) 'Epigenetic regulation of aging: implications for interventions of aging and diseases', *Signal Transduction and Targeted Therapy*, 7(1), p. 374. Available at: https://doi.org/10.1038/s41392-022-01211-8.

Wang, K. *et al.* (2022b) 'Epigenetic regulation of aging: implications for interventions of aging and diseases', *Signal Transduction and Targeted Therapy*, 7(1), p. 374. Available at: https://doi.org/10.1038/s41392-022-01211-8.

Wang, Z. *et al.* (2024) 'Targeting tumor-associated macrophage-derived CD74 improves efficacy of neoadjuvant chemotherapy in combination with PD-1 blockade for cervical cancer', *Journal for Immunotherapy of Cancer*, 12(8), p. e009024. Available at: https://doi.org/10.1136/jitc-2024-009024.

Watanabe, R. *et al.* (2017) 'Pro-inflammatory and anti-inflammatory T cells in giant cell arteritis', *Joint Bone Spine*, 84(4), pp. 421–426. Available at: https://doi.org/10.1016/j.jbspin.2016.07.005.

Watanabe, R. *et al.* (2018) 'MMP (matrix metalloprotease)-9-producing monocytes enable T cells to invade the vessel wall and cause vasculitis', *Circulation Research*, 123(6), pp. 700–715. Available at: https://doi.org/10.1161/CIRCRESAHA.118.313206.

Watanabe, R. and Hashimoto, M. (2022a) 'Aging-Related Vascular Inflammation: Giant Cell Arteritis and Neurological Disorders', *Frontiers in Aging Neuroscience*, 14, p. 843305. Available at: https://doi.org/10.3389/fnagi.2022.843305.

Watanabe, R. and Hashimoto, M. (2022b) 'Pathogenic role of monocytes/macrophages in large vessel vasculitis', *Frontiers in Immunology*, 13. Available at: https://doi.org/10.3389/fimmu.2022.859502.

Weinberg, J.B., Hobbs, M.M. and Misukonis, M.A. (1984) 'Recombinant human gamma-interferon induces human monocyte polykaryon formation.', *Proceedings of the National Academy of Sciences of the United States of America*, 81(14), pp. 4554–4557.

Weinberger, T. *et al.* (2020) 'Ontogeny of arterial macrophages defines their functions in homeostasis and inflammation', *Nature Communications*, 11(1), p. 4549. Available at: https://doi.org/10.1038/s41467-020-18287-x.

Wen, Z. *et al.* (2017) *I N F L A M M A T I O N The microvascular niche instructs T cells in large vessel vasculitis via the VEGF-Jagged1-Notch pathway*. Available at: https://www.science.org.

Weyand, C.M. *et al.* (2005) 'Vascular Dendritic Cells in Giant Cell Arteritis', *Annals of the New York Academy of Sciences*, 1062(1), pp. 195–208. Available at: https://doi.org/10.1196/annals.1358.023.

Weyand, C.M. and Goronzy, J.J. (2023) 'Immunology of Giant Cell Arteritis', *Circulation Research*, 132(2), pp. 238–250. Available at: https://doi.org/10.1161/CIRCRESAHA.122.322128.

Weyand, C.M. and Goronzy, Jö.J. (2008) 'Vasculitides', in J.H. Klippel et al. (eds) *Primer on the Rheumatic Diseases*. New York, NY: Springer, pp. 398–409. Available at: https://doi.org/10.1007/978-0-387-68566-3_51.

Weyand, C.M., Younge, B.R. and Goronzy, J.J. (2011) 'IFN-γ and IL-17: The two faces of T-cell pathology in giant cell arteritis', *Current Opinion in Rheumatology*, 23(1), pp. 43–49. Available at: https://doi.org/10.1097/BOR.0b013e32833ee946.

Whittington, N.C. and Wray, S. (2017) 'Suppression of Red Blood Cell Autofluorescence for Immunocytochemistry on Fixed Embryonic Mouse Tissue', *Current protocols in neuroscience*, 81, p. 2.28.1-2.28.12. Available at: https://doi.org/10.1002/cpns.35.

Wierda, Rutger J. *et al.* (2012) 'Epigenetic control of CCR5 transcript levels in immune cells and modulation by small molecules inhibitors', *Journal of Cellular and Molecular Medicine*, 16(8), pp. 1866–1877. Available at: https://doi.org/10.1111/j.1582-4934.2011.01482.x.

Wierda, Rutger J *et al.* (2012) 'Epigenetic control of CCR5 transcript levels in immune cells and modulation by small molecules inhibitors', *Journal of Cellular and Molecular Medicine*, 16(8), pp. 1866–1877. Available at: https://doi.org/10.1111/j.1582-4934.2011.01482.x.

WOLINSKY, H. and GLAGOV, S. (1967) 'Nature of Species Differences in the Medial Distribution of Aortic Vasa Vasorum in Mammals', *Circulation Research*, 20(4), pp. 409–421. Available at: https://doi.org/10.1161/01.RES.20.4.409.

Wong, K.L. *et al.* (2011) 'Gene expression profiling reveals the defining features of the classical, intermediate, and nonclassical human monocyte subsets', *Blood*, 118(5), pp. e16–e31. Available at: https://doi.org/10.1182/blood-2010-12-326355.

Wu, T. *et al.* (2024) *Interfering PTBP1 expression inducing M2 macrophage polarization via miR-124/MAPK pathway*. Available at: https://doi.org/10.21203/rs.3.rs-3874246/v1.

Xue, G. *et al.* (2019) 'IL-4 together with IL-1β induces antitumor Th9 cell differentiation in the absence of TGF-β signaling', *Nature Communications*, 10(1), p. 1376. Available at: https://doi.org/10.1038/s41467-019-09401-9.

Xue, J. *et al.* (2020) 'CD14+CD16− monocytes are the main precursors of osteoclasts in rheumatoid arthritis via expressing Tyro3TK', *Arthritis Research & Therapy*, 22(1), p. 221. Available at: https://doi.org/10.1186/s13075-020-02308-7.

Yáñez, A. *et al.* (2017) 'Granulocyte-monocyte progenitors and monocyte-dendritic cell progenitors independently produce functionally distinct monocytes', *Immunity*, 47(5), pp. 890-902.e4. Available at: https://doi.org/10.1016/j.immuni.2017.10.021.

Yashar, W.M. *et al.* (2022) 'GoPeaks: histone modification peak calling for CUT&Tag', *Genome Biology*, 23(1), p. 144. Available at: https://doi.org/10.1186/s13059-022-02707-w.

Zdrojewicz, Z., Pachura, E. and Pachura, P. (2016) 'The Thymus: A Forgotten, But Very Important Organ', *Advances in Clinical and Experimental Medicine: Official Organ*

Wroclaw Medical University, 25(2), pp. 369–375. Available at: https://doi.org/10.17219/acem/58802.

Zeiner, P.S. *et al.* (2014) 'MIF Receptor CD74 is Restricted to Microglia/Macrophages, Associated with a M1-Polarized Immune Milieu and Prolonged Patient Survival in Gliomas', *Brain Pathology*, 25(4), pp. 491–504. Available at: https://doi.org/10.1111/bpa.12194.

Zeng, Z. *et al.* (2021) 'CCL5/CCR5 axis in human diseases and related treatments', *Genes & Diseases*, 9(1), pp. 12–27. Available at: https://doi.org/10.1016/j.gendis.2021.08.004.

Zhang, X. *et al.* (2022) 'Laser Capture MicrodissectionMicrodissection–Based mRNAMRNA Expression MicroarraysMicroarrays and Single-Cell RNARNA Sequencing in AtherosclerosisAtherosclerosis Research', in D. Ramji (ed.) *Atherosclerosis: Methods and Protocols*. New York, NY: Springer US, pp. 715–726. Available at: https://doi.org/10.1007/978-1-0716-1924-7_43.

Zhao, Hui *et al.* (2023) 'Ferroptosis as an emerging target in rheumatoid arthritis', *Frontiers in Immunology*, 14. Available at: https://doi.org/10.3389/fimmu.2023.1260839.

Zheng, Y. (2025) *Chapter 19 CUT&RUN and CUT&Tag | Choosing Genomics Tools*. Available at: https://hutchdatascience.org/Choosing_Genomics_Tools/cutrun-and-cuttag.html (Accessed: 10 July 2025).

Zhou, Y. *et al.* (2003) 'Relative Importance of CCR5 and Antineutrophil Cytoplasmic Antibodies in Patients with Wegener's Granulomatosis', *The Journal of Rheumatology* [Preprint].

Zhu, X.W. *et al.* (2007) 'Multinucleate Giant Cells Release Functionally Unopposed Matrix Metalloproteinase-9 In Vitro and In Vivo', *The Journal of Infectious Diseases*, 196(7), pp. 1076–1079. Available at: https://doi.org/10.1086/521030.